Bioprospecting of rhizobacteria from the root nodules of *Amphicarpaea bracteata* for enhanced plant growth and salinity stress tolerance of soybean

Gayathri Ilangumaran
Department of Plant Science
McGill University, Montréal

December 2020

A thesis submitted to McGill University in partial fulfillment of the requirements of the degree of PhD in Plant Science

TABLE OF CONTENTS

LIST OF FIGURES

LIST OF TABLES

ABSTRACT

Soybean [*Glycine max* (L.) Merrill] is an important grain legume/oilseed crop grown worldwide. Salinity is a major abiotic stressor that affects plant growth and limits crop productivity. Soybean is a glycophyte and its yield potential can be reduced up to 50% by salinity. Plant growth promoting rhizobacteria (PGPR) are known to enhance plant growth and elicit tolerance to (a)biotic stresses. The goal of this project was to characterize such beneficial bacteria from root nodules of *Amphicarpaea bracteata*, a native relative of cultivated soybean.

In the first study, 15 isolated strains were screened for potential utilization as PGPR of soybean under optimal and salt-stressed conditions. Two of the most promising strains, *Rhizobium* sp. SL42 and *Hydrogenophaga* sp. SL48 were co-inoculated with *Bradyrhizobium japonicum* 532C (*Bj*). The treatment of *Bj*+SL42 resulted in higher shoot biomass than the control, 18% at the vegetative stage, 16% at flowering, 7.5% at pod-filling, and 4.6% at harvest and seed weight was increased by 4.3% under salt stress (EC_e = 7.4 ds/m). Grain yield was raised under optimal conditions by 7.4 and 8.1% with treatments *Bj*+SL48 and *Bj*+SL42+SL48, respectively. Nitrogen assimilation and shoot K^+/Na^+ ratio were also higher in the co-inoculation treatments.

In the second study, proteomic profiling of soybean leaf tissue provided insights into growth and stress response mechanisms elicited by *Rhizobium* sp. SL42 and *Hydrogenophaga* sp. SL48. Several key proteins involved in photosynthesis, respiration and photorespiration were upregulated. These include photosystem I psaK, Rubisco subunits, glyceraldehyde-3-phosphate dehydrogenase, succinate dehydrogenase and glycine decarboxylase. Similarly, stress response proteins such as catalase and glutathione S-transferase (antioxidants), proline-rich precursor protein (osmolyte), and NADP-dependent malic enzyme (linked to ABA signaling) were increased under salt stress.

In the final study, whole genome *de novo* sequencing of the rhizobacterial strains was performed using Illumina and Nanopore sequencers and assembled in MaSuRCA. The genome of *Rhizobium* sp. SL42 consists of one 4.06 Mbp circular chromosome and two plasmids with a GC content of 60%. The genome of *Hydrogenophaga* sp. SL48 consists of a 5.43 Mbp circular chromosome with a GC content of 65%. Genes encoding for various metabolic functions, secretion systems, quorum sensing, and biosynthetic gene clusters were present in their genomes.

Overall, this project determined that (1) *Rhizobium* sp. SL42 and *Hydrogenophaga* sp. SL48 exerted greater beneficial effects on soybean, (2) they regulated the proteome expression of

soybean leaves through multiple signaling pathways, and (3) their genomic features contributed to their function in plant growth promoting activities. The benefits of this project include (1) application of these strains to alleviate stress and advance crop productivity of soybean, (2) molecular basis of the *modus operandi* of plant-microbe interactions at the proteomic level, and (3) understand the functional properties of bacterial genomes that aid plant growth stimulation. This project substantiated that bacteria from an indigenous legume could be applied as bioinoculants to support sustainability and expand the ecological adaptability of soybean.

RÉSUMÉ

Le soya [*Glycine max* (L.) Merrill] est une espèce de plantes légumineuses à grains et oléagineuses cultivée à travers le monde. La salinité est un facteur de stress abiotique qui affecte la croissance des plantes et limite la productivité des cultures. Le soya est un glycophyte et la salinité peut réduire ses rendements jusqu'à 50%. Les rhizobactéries favorisant la croissance des plantes (RFCP) sont reconnues pour leur capacité à améliorer la croissance des plantes ainsi que leur tolérance aux stress (a)biotiques. Le but de ce projet était de caractériser ces bactéries bénéfiques des nodules racinaires de *Amphicarpaea bracteata*, une plante indigène parente au soya cultivé.

Dans la première étude, 15 souches de bactéries isolées ont été examinées pour leur potentiel d'utilisation comme PGPR pour le soya cultivé sous des conditions optimales et de stress salin. Deux des souches les plus prometteuses, *Rhizobium* sp. SL42 et *Hydrogenophaga* sp. SL48, ont été co-inoculées avec *Bradyrhizobium japonicum* 532C (*Bj*). Le traitement *Bj*+SL42 a entrainé l'accumulation de biomasse de tiges la plus élevée comparativement au témoin, par 18% au stade végétatif, 16% à la floraison, 7,5% au remplissage des gousses et 4,6% à la récolte, et a augmenté le poids des grains par 4,3% sous le stress salin (EC_e = 7.4 ds/m). Les rendements en grains étaient supérieurs par 7,4 et 8,1% avec les traitements *Bj*+SL48 et *Bj*+SL42+SL48, respectivement, sous des conditions optimales. L'assimilation d'azote ainsi que le ratio K^+/Na^+ des tiges étaient également supérieurs avec les traitements co-inoculés.

Dans la deuxième étude, le profilage protéomique du tissu foliaire du soya a fourni des aperçus sur les mécanismes de croissance et de réponse au stress suscités par *Rhizobium* sp. SL42 et *Hydrogenophaga* sp. SL48. Plusieurs protéines clés, impliquées dans la photosynthèse, respiration cellulaire et photorespiration, ont été surexprimées incluant photosystème I psaK, les

sous-unités de Rubisco, glycéraldéhyde-3-phosphate déshydrogénase, succinate déshydrogénase et glycine décarboxylase. De même, les protéines de réponse aux stress, telles que les catalases et glutathion S-transférases (antioxydants), précurseurs de protéines riches en proline (osmolyte) et enzymes maliques dépendantes de NADP (liées à la régulation de ABA), étaient plus élevées sous des conditions de stress salin.

Dans la dernière étude, le séquençage *de novo* de l'ensemble du génome des souches de rhizobactéries a été réalisé en utilisant les séquenceurs Illumina et Nanopore et assemblé dans MaSuRCA. Le génome de *Rhizobium* sp. SL42 est composé d'un chromosome circulaire de 4,06 Mbp et de deux plasmides circulaires avec une teneur en guanine-cytosine (GC) de 60%. Le génome de *Hydrogenophaga* sp. SL48 est composé d'un chromosome circulaire de 5,43 Mbp et de deux plasmides circulaires avec une teneur GC de 65%. Des gènes encodant pour différentes fonctions métaboliques, systèmes de sécrétion, détection du quorum et groupes de gènes biosynthétiques étaient présents dans leurs génomes.

En général, ce projet a déterminé que (1) *Rhizobium* sp. SL42 et *Hydrogenophaga* sp. SL48 ont exercé des effets bénéfiques supérieurs sur le soya, (2) ils ont régulé l'expression protéomique des feuilles de soya à travers de multiples voies de signalisation et (3) leurs caractéristiques génomiques ont contribué à leur rôle pour la favorisation de la croissance des plantes. Les bénéfices de ce projet incluent (1) l'application de ces souches pour alléger le stress et pour faire progresser la productivité du soya, (2) base moléculaire du *modus operandi* des interactions plantes-microbes au niveau protéomique et (3) comprendre les propriétés fonctionnelles des génomes de bactéries qui aider à stimuler la croissance des plantes. Ce projet prouve que les bactéries provenant de légumineuses indigènes peuvent être appliquées comme bio inoculant pour supporter la durabilité du soya et accroître son adaptabilité écologique.

ACKNOWLEDGEMENTS

- I express my sincere gratitude to my supervisor Prof. Donald Smith for providing me with an opportunity to conduct graduate research in his lab and encouraging feedback on my thesis.
- I'm grateful to my co-supervisor Prof. Jean-Benoit Charron and my supervisory committee members, Prof. Valérie Gravel and Prof. Sébastien Faucher for their advice, guidance and support throughout my graduate studies.
- I would like to thank the financial support given by the Biomass Canada Cluster. The Biomass Canada Cluster is managed by BioFuelNet Canada and was funded through the Canadian Agricultural Partnership's, Agriscience Program, Agriculture and Agri-Food, Canada.
- My heartfelt thanks to Dr. Sowmylakshmi Subramanian for her valuable inputs on various parts of my project and for teaching me proteomic techniques and data analysis. She has been an incredible colleague and friend, whom I always look up to.
- I sincerely appreciate Dr. Timothy Schwinghamer for helping with statistical analysis and teaching me how to interpret it.
- I'm thankful for the support and motivation given by Dr. Yoko Takishita, Dr. Selvakumari Arunachalam and Dr. Alfred Souleimanov, who always offered their help when in need.
- I would like to thank other members of Smith Lab, particularly Dr. Rachel Backer, Mr. Ateeq Shah and Mr. William Overbeek for their help and suggestions. The help given by Mrs. Saranya Paneerselvam and summer students was indispensable, they were a great assistance in setting up experiments and processing samples. My special thanks to Dr. Dana Praslickova for taking care and cheering me up.
- I sincerely appreciate the help and assistance provided by Mr. Guy Rimmer, Mr. Ian Ritchie, Mr. Drew Anthony, Ms. Melissa LaRiviere of the Department of Plant Science in setting up experiments in the greenhouse and growth chambers. I also thank Ms. Hélène Lalande of the soil chemistry lab, Department of Natural Resources for her assistance with elemental analysis.
- I greatly appreciate the help of Dr. Denis Faubert, Ms. Josée Champgne, Ms. Marguerite Boulos at the Proteomics Discovery Platform, Institut de Recherches Cliniques de Montréal (IRCM) for the proteomics analysis. I extend my thanks to Mr. Shasank, Dr. A. Gandhimathi and others at Genotypic Technology Pvt. Ltd. India for their help with whole genome sequencing and

analysis. I would also like to thank Mr. Pierre Lepage, Mr. Sébastien Brunet and Ms. Sharen Roland at Genome Québec, Montréal for helping with Sanger sequencing.

- I'm thankful to Prof. Sébastien Faucher, Prof. Jacqueline Bede, Prof. Gary Dunphy, Prof. Olivia Wilkins, Prof. Mehran Dastmalchi for giving me an opportunity to work as a teaching assistant for their courses, which inspired and helped me by a lot of means. I would also like to extend my thanks to fellow graduate students and a special mention to Dr. David Meek, whom I worked with as a teaching assistant, for their help, support, and friendship.
- I appreciate the support given by the students and staff in the Department of Plant Science and across-the-board at MacDonald Campus and McGill University, who has touched my life in some way. I greatly cherish the friendships I made during this time
- Last but not least, words can't express how much I owe to my family and friends for their extraordinary affection at all times. Especially to my siblings for their constant adoration, to my mother for keeping me in her thoughts and prayers and to my husband for his unflinching care and unwavering love.

CONTRIBUTION TO ORIGINAL KNOWLEDGE

Chapter 3

This is the first study to report beneficial rhizobacteria isolated from *Amphicarpaea bracteata*, a native legume of Canada (and North America) and their interaction with soybean. Rhizobacteria were isolated from the root nodules and inoculated onto soybean under optimal and salt stress conditions, and promising isolates were identified in the screening experiments. Two isolates, *Rhizobium* sp. SL42 and *Hydrogenophaga* sp. SL48 improved plant growth and salinity tolerance of soybean, along with *Bradyrhizobium japonicum*. This is one of the few studies that monitored the impact of salinity stress and the influence of rhizobacteria on soybean until maturity. The study suggested that these rhizobacterial strains can be effectively utilized as bioinoculants to enhance stress tolerance and promote the growth and yield of soybean.

Chapter 4

Analysis of the soybean leaf proteome revealed a vast network of signaling pathways related to plant growth and stress tolerance mechanisms modulated by the inoculation of SL42 and SL48. The study provided a comprehensive understanding of plant-microbe interactions between soybean, *B. japonicum*, rhizobacterial strains SL42 and SL48 under optimal and salt-stressed growth conditions. Indeed, this is the first time that systemic responses at the proteomic level elicited in the leaves of soybean plants at the vegetative stage due to salinity stress and the roles of rhizobacteria have been reported. This proteomic approach presented insights into the molecular basis of soybean growth and salinity tolerance mechanisms induced by *Rhizobium* sp. SL42 and *Hydrogenophaga* sp. SL48 that could ultimately lead to crop improvement.

Chapter 5

The genome of strains *Rhizobium* sp. SL42 and *Hydrogenophaga* sp. SL48 were sequenced using high-throughput next-generation sequencing technology. Therefore, this contributed to the permanent high-quality whole genome sequence of these two strains, which were submitted to the NCBI database. It also enabled analysis of their systemic function at the genomic level and specific features related to cellular metabolism and production of secondary metabolites that facilitate their ability as plant growth promoting rhizobacteria.

CONTRIBUTION OF AUTHORS

Chapter 1 – The chapter was written entirely by Gayathri Ilangumaran and reviewed by Dr. Smith.

Chapter 2 – Gayathri Ilangumaran gathered literature and prepared the manuscript. Dr. Smith provided feedback and oversaw progression of the manuscript. The chapter was written entirely by Gayathri Ilangumaran.

Chapter 3 – Gayathri Ilangumaran conducted the research, collected data and interpreted results. Dr. Schwinghamer helped with the statistical analysis of the data. Dr. Smith helped Gayathri Ilangumaran in editing the manuscript and providing feedback. The chapter was written entirely by Gayathri Ilangumaran.

Chapter 4 – Gayathri Ilangumaran conducted the research, collected data and interpreted results. Dr. Subramanian helped to analyze the raw LC-MS/MS files and helped with Scaffold and Omicsbox platforms to analyze proteomics data. Dr. Smith reviewed the manuscript and provided feedback. The chapter was written entirely by Gayathri Ilangumaran.

Chapter 5 – Gayathri Ilangumaran conducted genomic data analysis and submitted the sequences to NCBI database. Dr. Subramanian helped with Anti-SMASH analysis. Dr. Smith reviewed the chapter and provided feedback. The chapter was written entirely by Gayathri Ilangumaran.

1 Chapter 1 Introduction

Plants are the major primary producers of the biosphere and mankind has developed the practice of cultivating plants for food, clothing, shelter, livestock and utilities from ancient days and plants have also been continuously harnessed for products to be utilized as medicines and fuels. Nevertheless, the growth and development of a plant are influenced by its ability to withstand a myriad of environmental factors particularly facets of stress. The human population on earth is continuing to expand while the available arable land has been diminishing. Bringing marginal lands under cultivation is greatly needed to meet the demands of global food security.

1.1 Plant growth promoting rhizobacteria

The importance of the rhizosphere microbiome is now being increasingly recognized for its role in plant growth, nutrient uptake and alleviation of environmental stress (Smith et al., 2017). Thus, beneficial microorganisms can be harnessed for their potential in crop management practices, to attain a greater yield, which is usually limited by environmental factors and innate genetic potential. The environmentally safe approach could minimize the use of agricultural chemicals and encourage sustainable management practices.

Interactions between plants and the beneficial soil microbial community are important in crop production, nutrient cycling and environmental resilience (Loreau et al., 2001). Plant growth-promoting rhizobacteria (PGPR) were first defined by Kloepper and Schroth (1979) to describe non-pathogenic beneficial soil bacteria that colonize the roots of plants and that enhance plant growth, assist in nutrient uptake and/or prevent pathogen infection. The rhizosphere of a plant supports large microbial populations capable of engaging in symbiotic relationships. During colonization, PGPR assimilate substances released in root exudates and inturn produce bioactive compounds that promote plant growth or ameliorate stress (Xie et al., 2014). Signal compounds produced by the PGPR stimulate plant growth (Prithiviraj et al., 2003; Lee et al., 2009) and alleviate abiotic stress (Subramanian et al., 2016).

Understanding the characteristics and functions of plant-microbe interactions is imperative for developing technologies that utilize bioinoculants to increase crop productivity, against a challenging backdrop of climate change, increasing demand for food and use for biofuels (Ragauskas et al., 2006). Application of beneficial microbes, such as rhizobia, mycorrhiza and PGPR as biofertilizers and biocontrol agents in crop fields has been in practice and resulted in

higher yields, but often with inconsistent results suggesting that there is much left to understand regarding the influence of environmental conditions on the function and efficacy of microbial inoculants.

1.2 Soybean

The nitrogen-fixing ability of legumes has contributed to their distribution over a range of edaphic conditions and to their diversity with 19,400 species (third largest family in the Angiosperms). A mutualistic relationship exists between the plants of the family Leguminosae and nitrogen-fixing rhizobia that dwell in the root nodules. Cultivated members of this family are incorporated in crop rotations to enrich the soils of fields and pastures with nitrogen. The Leguminosae is the second most important family in agriculture (next to the Graminae) and 41 species have been domesticated, the greatest number for any plant family.

Soybean [*Glycine max* (L.) Merrill] is an economically important grain legume cultivated worldwide; it originated in northeastern China and is mainly cultivated as a rain-fed crop under warm conditions of tropical, subtropical and temperate regions of the world. Soybean grows in a wide range of temperatures and soil types and is moderately tolerant to drought and salinity stresses. It is a glycophyte and salt-affected soils can decrease its yield potential up to 50%. Cultivation of soybean has been documented in North America since the mid-1800s, but it wasn't until after world war II that it gained significance in the Americas (Cloutier, 2017). It is the fourth largest field crop in Canada and production has expanded from coast to coast due to the introduction of early-maturing varieties for higher latitudes with short growing seasons (Dorff, 2007). Soybean exports have steadily increased in the past two decades with commodity soybean (grown for processing) making up the bulk, compared to its food-grade counterpart.

Amphicarpaea bracteata (L.) is native to Canada and the USA, usually found in the woody and shaded areas of wetlands and non-wetlands. It is an herbaceous perennial vine and reproduces annually (PLANTS, 2017). Reproduction occurs through obligate self-fertilization of cleistogamous flowers; populations of *A. bracteata* are highly inbred in their local habitat. The nitrogen-fixing symbiont(s) of this plant are known to be species and subspecies belonging to the genus *Bradyrhizobium*. The edible seeds and roots of the plant are used for food and medicinal purposes by the indigenous communities (Moerman, 1998). *Amphicarpaea bracteata* is the closest native relative to soybean in North America and both genera are classified in the subtribe

Glycininae of the tribe Phaseoleae and the relationship between these two species has been confirmed by molecular studies (Zhu et al., 1995).

At present, the soybean fields in North America have natural populations of *Bradyrhizobium* that can nodulate and fix atmospheric nitrogen in conjunction with soybean, thanks to earlier inoculation programs. The symbiotic bacteria are not transferred through seed from parent to offspring, rather the seedlings have to acquire them from the soil at germination, which means the soil should harbour rhizobial communities. Transfer of genes (horizontal or vertical) between populations of soil bacteria facilitates continuous evolution and localized adaptation, at least to an extent. Micro-evolution has been observed in *Bradyrhizobium* populations from soybean fields in eastern Canada and the strains were associated with *Bradyrhizobium* associated with native legumes (Tang et al., 2012). However, the nodules also contain other plant growth promoting rhizobacteria (PGPR) that presumably exert beneficial effects on their host (Bai et al., 2002). These PGPR of *A. bracteata* might have the potential to improve soybean growth and stress tolerance under short-season and sub-optimal growing conditions prevailing in Canada.

1.3 Soil salinity

Salinity is one of the most prevalent abiotic stresses in agriculture, limiting plant growth and yield. The effects are more prominent in arid and coastal areas where water deficit and influx of seawater make land uncultivable and only tolerant plants (halophytes and xerophytes) can grow (Zhu, 2007). However, other agricultural lands are prone to salinity due to their topography, physiochemical properties of soil, rainfall, irrigation water and groundwater table (Wiebe et al., 2007). Large swaths of land affected by soil salinity have been turned into marginal or non-arable lands and their productivity has decreased sharply. Excessive irrigation and inadequate drainage created salinity have been recognized as a serious problem around the world since salt concentration builds up in the topsoil. The increase in salt concentration at the soil surface is caused by leaching, migration and capillary rise of salts. Because salinity and water are inextricably linked, climate change drives toward extreme consequences in vulnerable regions (Pitman and Lauchli, 2002). Soil salinity has constricted yield on a significant proportion of cultivable lands under irrigation and dryland agriculture. The Canadian prairies are prone to soil salinization, which fluctuates temporally depending on the annual precipitation (Florinsky et al., 2009). It is also a persistent issue in many of the south-, mid-, and north-western states of the USA (NRCS, 2002).

Salinization management has focused on improving irrigation water quality and soil drainage or increasing salt tolerance in plants. Growing salt-tolerant crops has been a prospective strategy for coping with salinity restricted crop production over the history of human civilization. With advances in plant breeding, developing salt-tolerant genotypes has not been very successful due to the complexity of this trait; salt tolerance mechanisms of a plant are complex both at the genetic and physiological levels (Flowers, 2004). Salt stress is largely caused by the uptake of NaCl, the dominant salt in nature; this disrupts both osmotic and ionic balance in plants. The symptoms of osmotic stress overlap symptoms caused by drought and cold stresses. Osmotic stress is caused by reduced water uptake whereas ionic stress is associated with toxicity of Na^+ and Cl^- accumulation in tissues and deficiency of other essential nutrient ions such as K^+ and NO_3^- (Hasegawa et al., 2000; Munns and Tester, 2008). Reactive oxygen species (ROS) are generated in response to stress and disrupt normal physiological functions by damaging cellular components and drives cell death (Van Breusegem and Dat, 2006). Salinity causes growth and yield reduction by decreasing the growth of assimilate-producing source tissues (less shoot biomass) and thereby decreasing the growth of assimilate-consuming sink tissues (flowers, fruits and root biomass).

1.4 Objectives

A comprehensive understanding of the salt stress tolerance in soybean mediated by PGPR is not available and this study attempts to address that gap. The main objectives of the study were:

1. To isolate and screen beneficial rhizobacteria from the nodules of *A. bracteata*, determining their ability to enhance soybean growth and salinity tolerance under greenhouse conditions and to characterize the capability of selected PGPR (*Rhizobium* sp. SL42 and *Hydrogenophaga* sp. SL48) in improving growth and yield of soybean, co-inoculated with *Bradyrhizobium japonicum* 532C.
2. To elucidate the plant growth and salt stress responses elicited by the inoculation of two strains, *Rhizobium* sp. SL42 and *Hydrogenophaga* sp. SL48through proteomic analysis of soybean leaf tissue.
3. To characterize the genome and identify potential genetic elements that enable the strains *Rhizobium* sp. SL42 and *Hydrogenophaga* sp. SL48 to function effectively as PGPR through whole genome sequencing.

2 Chapter 2 Literature Review

Plant Growth Promoting Rhizobacteria in Amelioration of Salinity Stress: A Systems Biology Perspective

Authors: Gayathri Ilangumaran[1] and Donald Lawrence Smith[1]

Affiliations:

[1] Department of Plant Science, McGill University, Macdonald Campus, 21,111 Lakeshore Road, Sainte-Anne-de-Bellevue, QC, Canada.

This manuscript was originally published in Frontiers in Plant Science journal and shared in the thesis via the Creative Commons Attribution 4.0 International Public License.

Ilangumaran, G., and Smith, D.L. (2017). Plant Growth Promoting Rhizobacteria in Amelioration of Salinity Stress: A Systems Biology Perspective. *Front. Plant Sci.* 8, 1768. doi: 10.3389/fpls.2017.01768

2.1 Abstract

Salinity affects plant growth and is a major abiotic stress that limits crop productivity. It is well-understood that environmental adaptations and genetic traits regulate salinity tolerance in plants, but imparting the knowledge gained towards crop improvement remain arduous. Harnessing the potential of beneficial microorganisms present in the rhizosphere is an alternative strategy for improving plant stress tolerance. This review intends to elucidate the understanding of salinity tolerance mechanisms attributed by plant growth promoting rhizobacteria (PGPR). Recent advances in molecular studies have yielded insights into the signaling networks of plant–microbe interactions that contribute to salt tolerance. The beneficial effects of PGPR involve boosting key physiological processes, including water and nutrient uptake, photosynthesis, and source-sink relationships that promote growth and development. The regulation of osmotic balance and ion homeostasis by PGPR are conducted through modulation of phytohormone status, gene expression, protein function, and metabolite synthesis in plants. As a result, improved antioxidant activity, osmolyte accumulation, proton transport machinery, salt compartmentalization, and nutrient status reduce osmotic stress and ion toxicity. Furthermore, in addition to indole-3-acetic acid and 1-aminocyclopropane-1-carboxylic acid deaminase biosynthesis, other extracellular secretions of the rhizobacteria function as signaling molecules and elicit stress responsive

pathways. Application of PGPR inoculants is a promising measure to combat salinity in agricultural fields, thereby increasing global food production.

2.2 Introduction

Climate change has exacerbated the severity of environmental stressors and affects crop production worldwide as part of the present Anthropocene Era. At the same time, there is a need to maintain food security for a growing global population through increases in crop production, while also forging agriculture more sustainable. Going forward, the quality of land and water will be critically pivotal for agriculture. Excess salt concentration in soil and water resources declines agricultural productivity, turns fertile fields to marginal lands, and leads to their abandonment. The Food and Agriculture Organization estimates that salinity has affected more than 6% of land area. Much of this land is not under cultivation but, a substantial proportion of the cultivated land, which constitutes 45 million ha of irrigated land (20% of total) and 32 million ha under dryland agriculture (about 2% of total) has been affected (Munns and Tester, 2008). The proportion of salinized land area might increase owing to climate change conditions conducive for salt accumulation (Othman et al., 2006).

Soluble salts deteriorate the fertility of soil by causing adverse effects on plant growth and development (Munns and Tester, 2008). Osmotic stress is the immediate impact of salinity (occurs within minutes) due to hypertonic conditions and ion toxicity (occurs over several hours to days and weeks) is the result of toxic ions (Na^+ and Cl^-) accumulating in the cells. Perturbed water balance and ion homeostasis affect hormonal status, transpiration, photosynthesis, translocation of nutrients, and other metabolic processes (Munns, 2002a). Beneficial soil microbiota enhance soil-water-plant relations through intricate mechanisms and subtle signaling cues that are not yet well-understood. A widely-proven notion is that the ability of soil microbes to manipulate phytohormonal signaling and trigger several other mechanisms to work in an integrated fashion contribute to enhanced stress tolerance in plants (Dodd and Perez-Alfocea, 2012). Inoculation of crop plants with beneficial microbes is gaining agronomic importance since they facilitate cultivation under saline-prone conditions by improving salt tolerance and hence, restoring yield (Lugtenberg et al., 2013). Bacteria isolated from extreme environments such as deserts and oceans have been shown to induce salt tolerance in crop plants. For example, a *Pseudomonas fluorescens* strain isolated from date-palm rhizosphere in Saharan region promoted root growth in maize (*Zea*

mays) seedlings under salt stress (Zerrouk et al., 2016). Wheat plants (*Triticum aestivum*) inoculated with *Serratia sp.* Sl-12, a halophilic bacterium isolated from a salt lake showed improved salt tolerance and increased shoot biomass (Singh and Jha, 2016).

This review focuses on the evaluation of plant growth promoting rhizobacteria (PGPR) within the context of systems biology approaches for the alleviation of salinity stress with a brief overview of the causes for salinity and courses of plant tolerance. Recent advances in 'omics' technologies deliver a holistic understanding of the regulatory networks of stress responses modulated by the PGPR. Further, the reader may refer to comprehensive reviews on utilization of other beneficial microorganisms including arbuscular mycorrhizal fungi (AMF), endosymbionts, halotolerant, and phyllosphere bacteria to alleviate salinity stress (Yang et al., 2009; Dodd and Perez-Alfocea, 2012; Glick, 2012; Vorholt, 2012; Egamberdieva and Lugtenberg, 2014).

2.3 Salinity

Salinity is one of the major abiotic stressors that undermines plant growth and development (Pitman and Lauchli, 2002). Soil salinization is caused by natural or human activities that increase the concentration of dissolved salts, predominantly sodium chloride in the soil. Primary salinity is caused by natural processes, leading to significant salt accumulation in soil and groundwater over extended periods of time, which result in the formation of salt lakes, salt marshes, marine sediments, and salt scalds in the landscape. Sources of primary salinity may arise from weathering of rocks and minerals that releases soluble salts, precipitation that washes these salts downstream, wind-borne salts from oceans and sand dunes that are deposited inland, and influx of seawater followed by subsequent retreat (Pitman and Lauchli, 2002; Rengasamy, 2002).

Cultivation operations such as land clearing, excessive irrigation, and inadequate drainage are the reasons for secondary salinity. Native vegetation sustains the water table below the subsoil zone with deep roots in semi-arid and arid regions. Replacing perennial species with shallow rooted annual crops and long fallows increases water table leakage and groundwater recharge, which consecutively raises the water table level. Salt is deposited in the topsoil as the water evaporates, resulting in dryland salinity and may eventually form a salt scald. Salinity effects can be more detrimental when the groundwater table is high, as prominent in arid and coastal areas where only salt-tolerant plants (halophytes) grow (Doering and Sandoval, 1981; Rengasamy, 2002). Irrigated lands are more prone to salinity than drylands because irrigation water deposits

salt behind, year after year. Secondary salinization has degenerated vast tracts of irrigated lands to the point that they are no longer economical for cultivation. Plants are often supplied with more water than they can utilize during evapotranspiration. For example, irrigation coupled with instances of heavy rainfall accelerates infiltration and groundwater recharge rates that raise the water table faster than it can drain. As the water table rises, it mobilizes dissolved salts from underground rocks close to the root zone. When the water table is within two meters of the soil surface in clay soils (less than a meter in sandy soils), there is a high probability of salt accumulation in the topsoil and salt stress to plants. Salt is also discharged and redistributed by surface runoff or leached down into soil profile by rainfall and then move laterally to watercourses (Sharma and Prihar, 1973; Pitman and Lauchli, 2002).

Poorly drained soils also suffer from waterlogging in irrigated areas. Clay soil (fine-textured) is less permeable than loam (medium-textured) and sandy soil (coarse-textured) and hence, it has high water holding capacity with low infiltration rate. Water can be stored and used by plants for a long time in clay soil but will not quickly transmit salt away from the root zone. The low porosity of clay soil acts as an impervious layer, causing inadequate drainage (Nassar and Horton, 1999). Inefficient irrigation and drainage systems lead to poor water distribution, resulting in over-irrigated waterlogged areas or under-irrigated water deficit areas, both causing salt accumulation. Waterlogging aggravates salinity stress by limiting aeration and nutrient supply to plants while proper grading and installation of drains to carry excess water and dissolved salts away from water stagnant areas may solve these problems. Groundwater mounds can develop in irrigated areas and force saline groundwater into waterways. Irrigation with salt-rich water increases salt being added to the soil and requires more water to leach out salts to prevent them from accumulating in the topsoil. Leaching reduces salinity levels when there is sufficient drainage and the groundwater table is deep. Conservation farming practices recommend appropriate methods to improve soil structure and irrigation efficiency (Shalhevet, 1994; Bauder and Brock, 2001).

The amount of salt stored in the soil also depends on soil type, with sandy soil having low and high capacity for clay loam minerals due to Na+ bound to negatively charged clay particles. Soil with ECe (electrical conductivity of saturated paste extract) of 4 dS m^{-1} is defined as saline by the USDA salinity laboratory. Most crop species are affected by ECe of less than 4 dS m^{-1} and thus, saline soil inhibits the yield of crops. Salinity caused by irrigation schemes has been

recognized as a serious problem around the world since irrigated land is, on average, twice as productive as rain-fed land and produces about one-third of global food (Munns and Tester, 2008). Because salinity and water are inextricably linked, climate changes drive extreme consequences on agriculture when drought or flooding hit vulnerable regions. Salinization management has focused on improving irrigation water quality and soil drainage to strategically increase salt acclimation in crops (Pitman and Lauchli, 2002).

2.4 Salt tolerance in plants

Salinity tolerance in plants is dependent on its physiological mechanisms, duration of exposure to saline conditions, concentration of salt around roots, local soil–water relations, and microclimate conditions (temperature, humidity, etc.). Salt tolerance is usually quantified over a given period as survival, vegetative growth, or harvestable biomass at different physiological stages of the plant in saline versus non-saline conditions (Munns, 2002b). Crop yield decreases when salt concentration is above the threshold salinity level due to salt affecting the development of reproductive structures or translocation of nutrient reserves. There is a great diversity in salt tolerance between species and each species has a specific threshold salinity. Environmental adaptations and inherent genetic traits regulate salinity tolerance mechanisms in glycophytes and halophytes (Munns, 2002b). The majority of the plants are glycophytes (sensitive to salt) and tend to exclude the salts from roots, delaying salinity stress (Zhu, 2007). Halophytes grow in saline conditions and therefore, possess enhanced tolerance to high salt levels. They accumulate salts, carry through the xylem stream and precipitate them on leaves. Some species have evolved specialized cells called salt glands in shoots to excrete salt on its surface, which is then removed by water or wind. Few attempts have been made to introduce halophyte genes in crop plants and cultivate halophytes for food, forage, or fuel (Flowers et al., 1986; Flowers and Colmer, 2015).

Salinity impairs plant growth by causing osmotic imbalance and ion toxicity. The first osmotic phase occurs immediately when salt concentration increases above a threshold level around the roots. The osmotic stress induces water deficit in roots and shoot growth is arrested within minutes of exposure, but then recovers over several hours to a slow steady rate of growth. The second phase develops with time and is driven by the toxicity of excess Na^+/Cl^- ions that accumulate in the cytoplasm. When the salt concentration exceeds the rate of exclusion by roots or cellular ability to compartmentalize salts in the vacuoles, it builds up in the cytosol and disrupts

cellular structures and functions (Munns, 2002b). Hence, all salinity tolerance in plants is directed towards maintaining osmotic balance and ion homeostasis. Even though the loss of cell turgor after the immediate osmotic shock is transient, reduction of cell elongation and cell division rates in root tips and young leaves over time lead to growth inhibition (Passioura and Munns, 2000). Osmotic stress affects shoot and reproductive development, for instance, younger leaves emerge slowly, lateral buds remain quiescent and flowering starts earlier. The growth regulating mechanisms are speculated to be long-distance signals of hormones and their precursors from roots to shoots. Phytohormone signaling is essential for regulation of cell division and differentiation, thereby controlling plant developmental morphogenesis (Santner and Estelle, 2009). The integrated signaling pathways are crucial in plant protection and adaptation mechanisms during abiotic and biotic stresses. In addition to five classical phytohormones, auxin, gibberellin, cytokinin, abscisic acid, and ethylene, other molecules including salicylic acid, jasmonic acid, nitric oxide, brassinosteroids, and strigolactones have been known to function as plant growth regulators. Phytohormone status is interdependent and both negative feedback and positive stimulation of synthesis have been reported. Many of the proteins including some transcription factors and protein kinases involved in plant hormone signaling have been elucidated. Phytohormone signaling cascades influence osmotic balance and other salt tolerance mechanisms (discussed below) and regulate plant acclimatization to salinity (reviewed in detail by Waśkiewicz et al., 2016). The plant roots encounter salinity first and root elongation rate recovers after initial exposure to salt but root architecture undergoes transition over time and high salt concentration represses formation of lateral roots. The aboveground symptoms of salinity induced osmotic stress overlap to that of drought stress, including leaf senescence and stunted growth (Munns, 2002a).

Osmotic stress affects stomatal conductance instantly due to perturbed water balance and abscisic acid (ABA) synthesis in guard cells, causing stomatal closure. Over the next several hours, transpiration rate is stabilized to a new reduced rate and ABA levels in situ are established (Fricke et al., 2006). Increased osmotic tolerance results in greater leaf expansion and stomatal conductance, which is beneficial only when there is sufficient soil water for transpiration losses (Munns and Tester, 2008). Photosynthesis rate decreases not only because of reduced leaf area and lesser gas exchange but also due to feedback inhibition of unused photosynthates, after exposure to salinity. The growth of sink tissues is constrained and carbohydrates accumulate in plant meristems and storage organs, which otherwise would be used in their proliferation and expansion.

Modulating carbohydrate production in source leaves, phloem transport, and sink utilization downregulate the feedback photoinhibition and boost plant energy metabolism (Paul and Foyer, 2001; Perez-Alfocea et al., 2010). Reactive oxygen species (ROS) are constantly generated by cell organelles as a metabolic by-product and function as signaling molecules but their production is spiked under stressed environments. ROS including hydrogen peroxide, superoxide, and free oxygen radical are profoundly reactive with cellular components and induces programmed cell death. ROS cause chlorophyll degradation and lipid peroxidation that affects photosynthesis and membrane permeability, respectively (Apel and Hirt, 2004).

Plants have developed antioxidant mechanisms involving enzymes (superoxide dismutase, glutathione reductase, catalase, and peroxidases) and molecules (carotenoids, flavonoids, and other phenolics) that prevent tissues from oxidative damages by quenching and detoxifying ROS (Gill and Tuteja, 2010). Upregulation of antioxidant enzyme activity and metabolite synthesis is coordinated by gene networks in response to initial low levels of ROS and other signaling events (Mittler et al., 2004). Antioxidant production and osmolyte accumulation are considered as sensitive physiological markers of salt and other abiotic stresses (Munns, 2002a). A common metabolic change in response to salinity is the synthesis of low molecular weight organic compounds including polyols (sorbitol, mannitol, inositol, or glycerol), amino acids (proline or glutamate), and betaines (glycine betaine) that function as osmolytes. They are compatible solutes and accumulate in the cytosol to maintain osmotic balance both inside and outside the cell. Osmolytes also function as osmoprotectants by preventing desiccation of membranes and stabilize dehydrated enzymes rather playing role in osmoregulation. They facilitate stabilization of subcellular structures and free radical scavenging and protect plants from osmotic stress induced dehydration (Rhodes et al., 2002). Synthesis of osmolytes is an energy-demanding process yet enables the plant to recover from adverse effects of salt stress (Raven, 1985).

Effects of ionic stress are determinant under prolonged exposure to high salinity levels and predominant in salt-sensitive species. Sodium ions are toxic to many plants, so are high concentrations of chlorine, specifically those that are poor excluders of Na^+ (ex: rice and beans) and sensitive to Cl^- (ex: soybean and citrus). The influx of Na^+ from roots is deposited in the xylem, carried through the transpiration stream and accumulated in the leaf blade rather than roots. Excluding Na^+ is a daunting task because a relatively small proportion is recirculated through phloem and most of it remains in the shoot, causing toxicity (Munns, 2002a; Tester and Davenport,

2003). Hence, active efflux of Na^+ from cells and retrieval of Na^+ from xylem is required throughout the plant and achieved by regulatory networks of sodium/proton antiporters and high-affinity potassium transporters (Tester and Davenport, 2003; Davenport et al., 2005). A Na^+/H^+ antiporter SOS1 (salt overly sensitive) localized on the plasma membrane is involved in the transport of Na^+ out of the cell and its activity is dependent on substrate (Na^+) concentration (Qiu et al., 2002). Excess Na^+ ion concentration affects low-affinity potassium uptake system because of the similar chemical nature of Na^+ and K^+ ions thereby, inhibiting K^+ uptake by the roots. Plants activate high-affinity K^+ transporters (HKT) to increase the uptake of K^+ ions over Na^+ ions and K^+ concentration relative to Na^+ in cytoplasm increases salinity tolerance (Rodriguez-Navarro and Rubio, 2006). Salt accumulation in intracellular spaces restrain enzymes involved in photosynthesis and respiration and interfere with vesicular trafficking (Baral et al., 2015; Jacoby et al., 2016). Cytosolic activities are inhibited under a high Na^+/K^+ ratio and cells need to effectively compartmentalize sodium into vacuoles, which further improves osmotic adjustments. Intracellular compartmentation of Na^+ is regulated by Na^+/H^+ antiporters and Na^+/H^+ exchangers (NHX) on the tonoplast, which are driven by a proton gradient (Halfter et al., 2000).

Plants with adequate calcium supply have demonstrated enhanced salt tolerance and supplemental Ca_2^+ stimulates rapid leaf elongation rate (Cramer, 1992). Calcium mediated signaling is important in maintaining Na^+/K^+ ratios by sustaining potassium transporters and suppressing non-selective cation channels and a rise in cytosolic Ca_2^+ levels is the first detectable response to sodium stress (Epstein, 1998). Membrane depolarization activates Ca_2^+ channels in cellular membranes that regulate Ca_2^+ oscillations in the cytosol and generate Ca_2^+ signals under salt stress. The calcium signal sensor, calcineurin B-like protein (CBL4, previously identified as SOS3) forms a complex with a CBL-interacting protein kinase (CIPK24, identified as SOS2) to phosphorylate SOS1, thus enabling its activation (Halfter et al., 2000; Zhu, 2002). Other sensor proteins are calcium dependent protein kinases (CDPKs), SOS3-like calcium binding proteins (SCaBPs), and calmodulins (CaMs) (Chinnusamy et al., 2006). Progressive accumulation of Cl^- is toxic to chloroplasts and mitochondria, and tolerance of high Cl^- concentrations requires compartmentalization and exclusion. The active influx of Cl^- is catalyzed by a $Cl^-/2H^+$ symporter but passive uptake also occurs under saline conditions and efflux takes place through Cl^- permeable channels (Yamashita et al., 1994). Transport of Cl^- to shoots is limited by reduced xylem loading

of Cl^- via anion channels (downregulated by ABA) and Cl^- is actively retrieved from the xylem stream (Gilliham and Tester, 2005).

Biochemical analysis, gene expression and mutant studies conducted to investigate molecular functions of plants in response to salinity revealed that complex signal transduction pathways and gene regulatory networks exist to alleviate stress (Hasegawa et al., 2000). Breeding of salt-tolerant genotypes to improve crop production has been persevered by plant scientists but in spite of the advances, relatively few determinant genetic traits for salt tolerance in crop species have been identified to date (Munns and Tester, 2008). However, the acquired knowledge will lead to the development of tolerant cultivars and implementation of sustainable crop protection measures that are environmentally safe. Conventional breeding practices and genetic engineering techniques could be the most relevant but often time-consuming and cost-intensive strategies. Meanwhile, application of beneficial microbes to increase salt tolerance in plants is a feasible alternative to reclaim salinity prone lands under cultivation (Berg, 2009). A plant, together with its associated microbial community, the phytomicrobiome function as a holobiont. The physiology and metabolism of the host plant are influenced by the phytomicrobiome, facilitating its adaptation to the habitat. Members of the phytomicrobiome, which include PGPR, AMF and other facultative endosymbionts are inoculated as microbial consortia and this strategy has gained interest lately to enhance crop productivity in stressed environments (Smith et al., 2015b).

2.5 Salt tolerance mediated by Plant Growth Promoting Rhizobacteria

During the past century, research has continuously demonstrated numerous beneficial associations between plants and microbes, beginning with the classic legume–rhizobia symbiosis. The plant rhizosphere is enriched with nutrient sources excreted from roots that support the higher abundance of microbial population than the surrounding bulk soil (Lugtenberg and Kamilova, 2009). Free-living beneficial bacteria dwelling in the rhizosphere that exert beneficial activities are known as plant growth promoting rhizobacteria (PGPR). Some of them are facultative endophytes that further invade intercellular spaces of host tissues and thrive as endophytes to establish a mutually beneficial association. PGPR living outside the plant cell are differently associated with plant roots and directly relate to the underlying mechanisms of plant–microbe interactions. The majority of the PGPR colonize the root surface and thrive in spaces between root hairs and rhizodermal layers whereas, some are not physically in contact with the roots (Gray and

Smith, 2005). Root exudates are an integral part of rhizosphere signaling events and regulate communication in beneficial plant–microbe interactions. Phenols, flavonoids, and organic acids secreted by roots have been known to act as chemical signals for bacterial chemotaxis, secretion of exopolysaccharides, quorum sensing and biofilm formation during rhizosphere colonization (Bauer and Mathesius, 2004; Badri et al., 2009; Narula et al., 2009). Isolated from rhizosphere soils, PGPR are screened *in vitro* for plant growth promoting characteristics and tested for beneficial effects in greenhouse and field trials prior to commercialization. PGPR promote plant growth and development through diverse mechanisms such as enhanced nutrient assimilation (biofertilizers) by biological nitrogen fixation, phosphorous solubilisation or iron acquisition (Rodriguez and Fraga, 1999; Steenhoudt and Vanderleyden, 2006; Sharma et al., 2013; Jin et al., 2014; Kuan et al., 2016), control pathogens by antagonism and competition (biocontrol agents) (Compant et al., 2005; Beneduzi et al., 2012; Chowdhury et al., 2015), degrade organic pollutants and reduce metal toxicity of contaminated soils (bioremediation), and facilitate phytoremediation (Divya and Kumar, 2011; Nie et al., 2011; Janssen et al., 2015; Weyens et al., 2015).

Inoculation with PGPR has been known to modulate abiotic stress regulation via direct and indirect mechanisms that induce systemic tolerance (Yang et al., 2009). Many PGPR have been investigated for their role in improving plant-water relations, ion homeostasis and photosynthetic efficiency in plants under salt stress (Figure 2.1); their amelioration mechanisms are intricate and often not well-understood. These mechanisms are regulated by a complex network of signaling events occurring during the plant–microbe interaction and consequently ensuing stress alleviation (Smith et al., 2017). Accumulating evidence using high-throughput techniques implies that understanding the dynamic function of PGPR in relation to stomatal conductance, ion transport, water and nutrient uptake, phytohormonal status, signal transduction proteins, antioxidant enzymes, and carbohydrate metabolism in plants is important for determining the induced systemic tolerance (Figure 2.2).

2.5.1 Osmotic balance

Plant growth promoting rhizobacteria regulate water potential and stomatal opening by affecting hydraulic conductivity and transpiration rate. Maize plants inoculated with *Bacillus megaterium* showed increased root hydraulic conductivity compared to uninoculated plants when exposed to salinity (2.59 dS m-1) and this was correlated with increased expression of two ZmPIP (plasma membrane aquaporin protein) isoforms (Marulanda et al., 2010). PGPR induce osmolyte

accumulation and phytohormone signaling that facilitate plants to overcome initial osmotic shock after salinization. Enhanced proline synthesis in transgenic *Arabidopsis thaliana* with proBA genes derived from *Bacillus subtilis* conferred salt tolerance to the plants (Chen et al., 2007). Inoculation of salt tolerant *Bacillus amyloliquefaciens* SN13 onto rice (*Oryza sativa*) plants exposed to salinity (200 mM NaCl) in hydroponic and soil conditions increased plant salt tolerance and affected expression of 14 genes, of which, four (*SOS1*, ethylene responsive element binding proteins *EREBP*, somatic embryogenesis receptor-like kinase *SERK1* and NADP-malic enzyme *NADP-Me2*) were upregulated and two [glucose insensitive growth *GIG* and (SNF1) serine-threonine protein kinase *SAPK4*] were downregulated under hydroponic conditions whereas, only *MAPK5* (Mitogen activated protein kinase 5) was upregulated under greenhouse conditions. Genes involved in osmotic and ionic stress response mechanisms were modulated by SN13 inoculation (Nautiyal et al., 2013).

Beneficial microorganisms can stimulate carbohydrate metabolism and transport, which directly implicate source-sink relations, photosynthesis, growth rate and biomass reallocation. Seed inoculated *B. aquimaris* strains increased total soluble sugars and reducing sugars in wheat under saline (ECe = 5.2 dS m^{-1}) field conditions and resulted in higher shoot biomass, NPK accumulation, and Na reduction in leaves (Upadhyay and Singh, 2015). Higher plant dry matter accumulation after 36 days in pepper (*Capsicum annuum*) plants inoculated with *Azospirillum brasilense* and *Pantoea dispersa* under salinity was related to enhanced stomatal conductance and photosynthesis, but neither chlorophyll concentration nor photochemical efficiency of photosystem II was affected (del Amor and Cuadra-Crespo, 2012). Microbes exposed to osmolality fluctuations in their surrounding environment accumulate large quantities of osmoprotectants in their cytosol (Kempf and Bremer, 1998). Under such circumstances, biosynthesis of osmolytes including proline, trehalose, and glycine betaines by PGPR is most likely to be quicker than their associated host plants. The compatible solutes absorbed through plant roots aid in maintaining osmotic balance and preventing cellular oxidative damage under saline conditions. Co-inoculation of bean (*Phaseolus vulgaris*) with *Rhizobium tropici* and *Paenibacillus polymyxa* strain modified to overexpress trehalose 6-phosphate gene resulted in increased nodulation, N content and plant growth. A microarray analysis of nodules revealed upregulation of stress tolerance genes suggesting that extracellular trehalose, which functions as an osmoprotectant can induce salinity tolerance (Figueiredo et al., 2008).

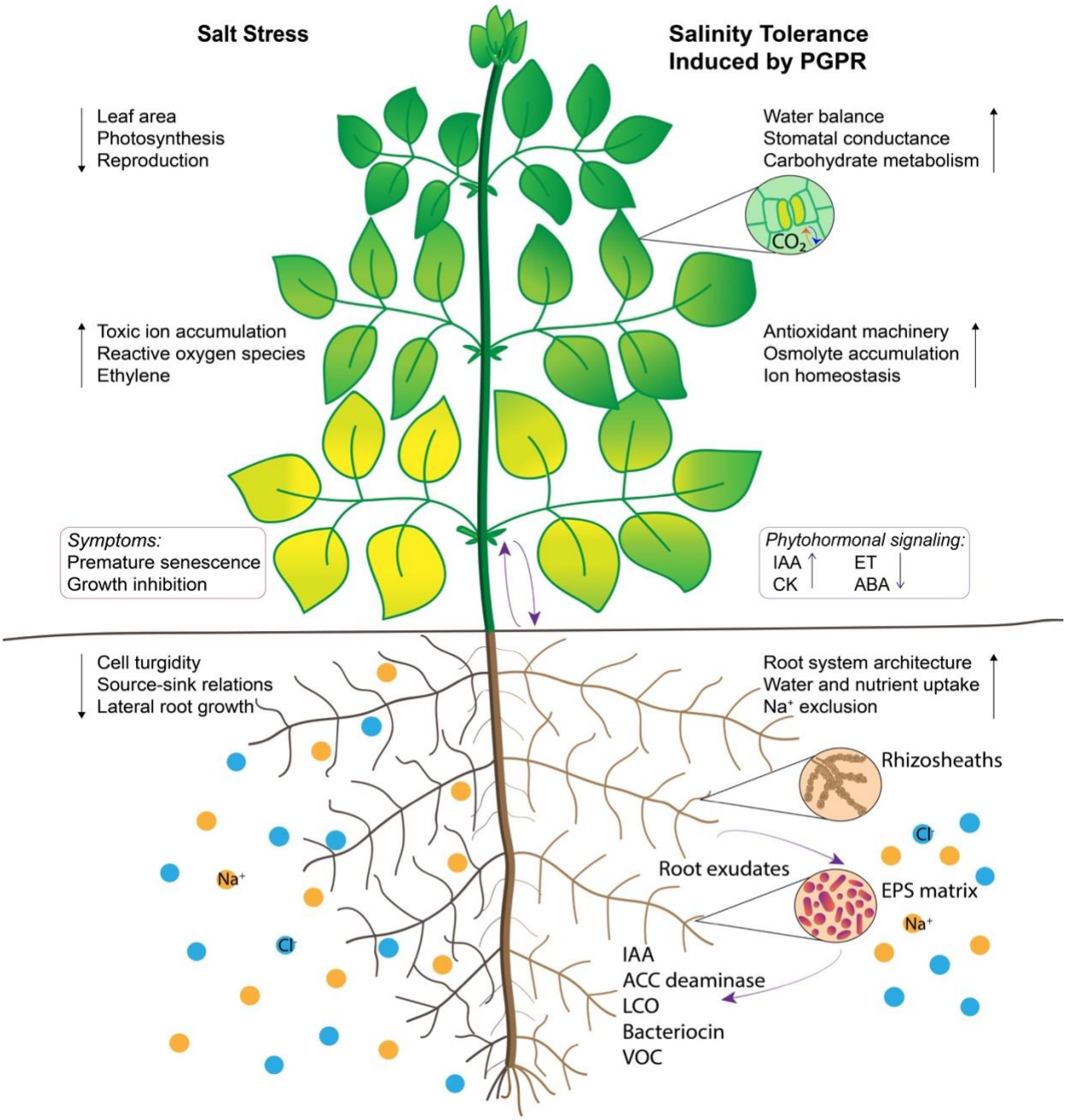

Figure 2.1. Illustration of salt tolerance mechanisms induced by plant growth promoting rhizobacteria (PGPR).
Root surfaces are colonized by PGPR and extracellular polysaccharide matrix acts as a protective barrier against salt stress. Some extracellular molecules function as signaling cues that manipulate phytohormonal status in plants. Enhanced root-to-shoot communication improves water and nutritional balance, source-sink relations and stomatal conductance. Stimulating osmolyte accumulation, carbohydrate metabolism and antioxidant activity delay leaf senescence, which inturn contribute to photosynthesis. Regulation of physiological processes are indicated by black arrows and signaling pathways are indicated by purple arrows.

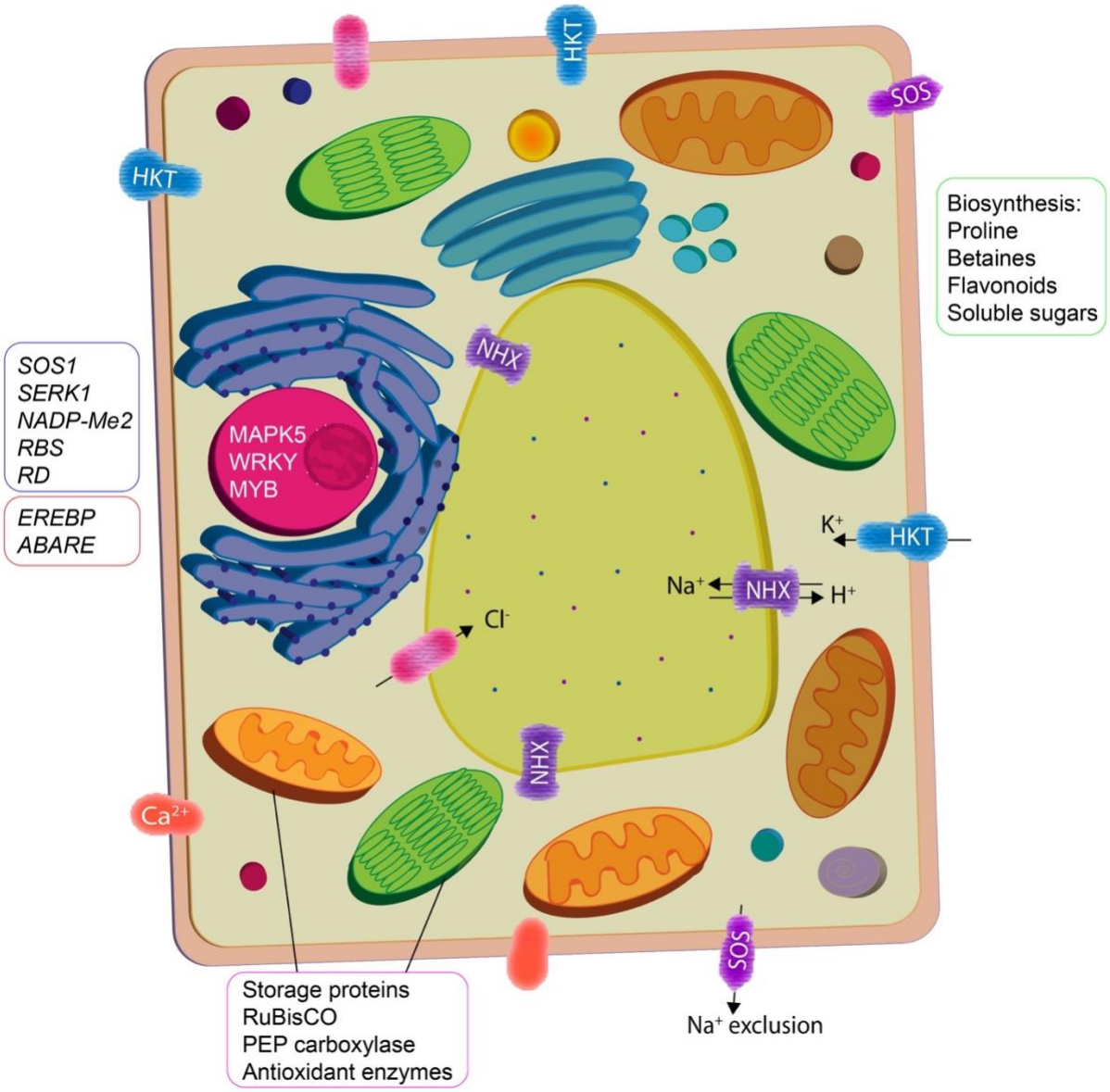

Figure 2.2. Plant growth promoting rhizobacteria interaction mediate cellular activity in plants to ameliorate salinity stress.
Osmotic imbalance and oxidative damage are reduced by enhanced biosynthesis of compatible solutes and antioxidants. Ion homeostasis is maintained by increase in activity of K^+ transporters (HKT) and H^+ exchangers (NHX) that facilitate salt compartmentalization/exclusion. PGPR also upregulate the expression of stress responsive genes (phytohormone signaling) and proteins (vegetative storage, photosynthesis, and antioxidant enzymes).

2.5.2 Ion homeostasis

Bacteria limit plant salt uptake by trapping cations in the exopolysaccharide matrix, altering root structure with extensive rhizosheaths, and regulating expression of ion affinity transporters. PGPR have been known to increase the mineral nutrient exchange of both macro and micronutrients and alleviate nutrient imbalance caused by the high influx of Na^+ and Cl^- ions. Microbial induced nutrient cycling (mineralization), rhizosphere pH changes (organic acids), and metal chelation (siderophores) increase plant nutrient availability (Dodd and Perez-Alfocea, 2012; Lugtenberg et al., 2013). PGPR help maintaining ion homeostasis and high K^+/Na^+ ratios in shoots by reducing Na^+ and Cl^- accumulation in leaves, increasing Na^+ exclusion via roots, and boosting the activity of high-affinity K^+ transporters. Inoculation of *Azotobacter* strains C5 (auxin producing) and C9 in maize plants under salt stress improved K^+ uptake and Na^+ exclusion. Chlorophyll, proline and polyphenol contents in leaves increased and PGPR inoculation enhanced plant stress responses (Rojas-Tapias et al., 2012). In a study conducted with *Arabidopsis thaliana* and *Burkholderia phytofirmans* PsJN to understand the spatiotemporal regulation of short and long-term salt stress, colonized plants exhibited higher tolerance to sustained salt stress. The expressional patterns of genes involved in ion homeostasis (*KT1*, *HKT1*, *NHX2*, and *SOS1*) were altered after stress and rapid molecular changes induced by PsJN may be linked to the observed salt tolerance (Pinedo et al., 2015). A halophyte grass, *Puccinellia tenuiflora* inoculated with *B. subtilis* GB03 showed less Na^+ accumulation and validated by upregulation of *PtHKT1* and *PtSOS1* genes but *PtHKT2* was downregulated in roots under high salt concentrations (200 mM NaCl) (Niu et al., 2016).

2.5.3 Phytohormone signaling

Soil bacteria modulate plant hormone status by releasing exogenous hormones, metabolites, and enzymes that may contribute to increased salt tolerance. Besides, phytohormones and metabolites are synthesized *de novo* in the plants in response signaling events of plant–microbe interactions during stress (Dodd et al., 2010).

2.5.3.1 Auxin

Auxin biosynthesis occurs via multiple pathways in rhizobacteria and one is the utilization of tryptophan present in root exudates and its conversion into indole-3-acetic acid (IAA), which is absorbed by the plant roots. Together with the plant's endogenous IAA pool, an auxin signaling

pathway is triggered and results in stimulation of cell growth and proliferation. IAA produced by PGPR is one of the most common and widely studied bacterial signaling molecules in plant–microbe interactions. The function of exogenous IAA is dependent on the endogenous IAA levels in plants. At optimal IAA concentration, acquisition of bacterial IAA may result in neutral, promotion or inhibition of plant growth (Dodd et al., 2010; Spaepen and Vanderleyden, 2011).

Bacillus amyloliquefaciens SQR9 enhanced salt stress tolerance (100 mM NaCl) of maize seedlings in vitro and bacterial inoculation increased chlorophyll and total soluble sugar contents, improved peroxidase and catalase activity, enhanced glutathione content, and K^+/Na^+ ratio. In addition, salinity induced ABA level was counteracted by SQR9 inoculation, which maintained it at the normal level. These physiological mechanisms to relieve salt stress were confirmed by the upregulation of genes *RBCS*, *RBCL* (encoding RuBisCo subunits), *H(+)-Ppase* (encoding H+ pumping pyrophosphatase), *HKT1*, *NHX1*, *NHX2* and *NHX3*, and also the downregulation of *NCED* expression (encoding 9-cis-epoxycarotenoid dioxygenase) in inoculated seedlings (Chen et al., 2016). *Enterobacter sp.* EJ01 isolated from a halophyte plant, sea china pink (*Dianthus japonicus thunb*) improved plant growth and salt stress tolerance (200 mM) in Arabidopsis and tomato (*Solanum lycopersicum*) plants. Short-term treatment (6 h) with EJ01 increased expression of genes involved in salt stress response such as DRE-binding proteins *DREB2b*, Relative to Desiccation (*RD29A*, *RD29B*), late embryogenesis abundant (*LEA*) genes (*RAB18*), proline biosynthesis (*P5CS1* and *P5CS2*), and stress-inducible priming processes (*MPK3* and *MPK6*) in Arabidopsis seedlings. GFP-tagged EJ01 displayed colonization of the bacteria in the rhizosphere and endosphere of Arabidopsis roots. In addition, ROS scavenging activities including antioxidant enzyme, ascorbate peroxidase were enhanced in inoculated tomato plants under salt stress (Kim et al., 2014).

The role of bacterial cytokinins in salt stress tolerance is largely unknown yet with relatively fewer studies. *Pseudomonas* strains (*P. aurantiaca* TSAU22, *P. extremorientalis* TSAU6 and *P. extremorientalis* TSAU20) enhanced growth up to 52%, compared to control plants and alleviated salinity (100 mM NaCl) induced dormancy of wheat seeds (Egamberdieva, 2009). Cytokinin producing *B. subtilis* inoculated onto lettuce seedlings under water deficit conditions increased accumulation of shoot biomass and shortened roots with only small effect on root biomass. Despite increased shoot cytokinins, the possible role in root-to-shoot signaling was latent seemingly hindered by shoot ABA (Arkhipova et al., 2007).

2.5.3.2 Ethylene

Synthesis of ethylene in response to stress may increase plant tolerance or expedite senescence (Morgan and Drew, 1997). Ethylene regulates plant adaptation to stress at the expense of growth and development. As ethylene levels increase under stress, transcription of auxin response factors is inhibited and it constraints plant growth. PGPR that secrete 1-aminocyclopropane-1-carboxylase (ACC) deaminase restrict ethylene biosynthesis in plants. The enzyme converts ACC, the precursor of ethylene to ammonia and α-ketobutyrate. Many studies have shown enhanced stress tolerance and growth promotion in plants conferred by soil bacteria producing ACC deaminase (Glick et al., 2007). The following examples illustrate some of the salt tolerance mechanisms induced by PGPR producing ACC deaminase.

Pseudomonas putida UW4 inoculated tomato (*Solanum lycopersicum*) seedlings showed increased shoot growth after 6 weeks in saline conditions up to 90 mM NaCl. The expression of Toc GTPase, a gene of the chloroplast protein import apparatus was upregulated, which may facilitate import of proteins involved as a part of stress response (Yan et al., 2014). A nutrient flow study of pea (*Pisum sativum* cv. Alderman) inoculated with *Variovorax paradoxus* 5C-2 under salt stress of 70 and 130 mM NaCl showed increased root to shoot K^+ flow and Na^+ deposition in roots, thereby increasing K^+/Na^+ ratio in shoots. Inoculation with PGPR also increased the photosynthesis rate and electron transport, while decreased stomatal resistance and xylem balancing pressure; overall improved the plant biomass (Wang et al., 2016). *Enterobacter sp.* UPMR18 inoculated okra (*Abelmoschus esculentus*) plants exhibited increase in antioxidant enzyme activities and transcription of ROS pathway genes when grown in 75 mM NaCl and showed enhanced salt tolerance (Habib et al., 2016). ACC deaminase producing strains of *Pseudomonas fluorescens* and *Enterobacter spp.* significantly improved maize yield in salt-affected fields. Higher K^+/Na^+ ratios and NPK uptake were also recorded in inoculated plants under salt stress (Nadeem et al., 2009).

Plant growth promoting rhizobacteria that produce both IAA and ACC deaminase can effectively protect plants from a range of stresses. IAA accumulation induces transcription of ACC synthase genes, which increases ACC concentration, leading to the production of ethylene. PGPR containing ACC deaminase may break down some of the excess ACC and lower plant ethylene levels during an advent of environmental stress and simultaneously allow IAA to promote plant growth (Glick, 2012). Endophytic bacteria (*Arthrobacter sp.* and *Bacillus sp.*) producing ACC

deaminase and IAA increased proline content in sweet pepper (*Capsicum annuum*). The inoculated plants manifested downregulation of stress-inducible genes *CaACCO* (ACC oxidase) and *CaLTPI* (Lipid transfer protein) under mild osmotic stress (Sziderics et al., 2007). *Pantoea dispersa* PSB3 is a native bacterium in chickpea (*Cicer arietinum*) and produces IAA and ACC deaminase. Upon inoculation to chickpea cv. GPF2, it significantly improved plant biomass, pod number, pod weight, seed number, and seed weight in salt (150 mM NaCl) affected plants. The improved salt tolerance was associated with significant reduction of Na^+ uptake and electrolyte leakage and increase of relative leaf water content, chlorophyll content, and K^+ uptake (Panwar et al., 2016).

2.5.3.3 Abscisic acid

There are relatively few studies on determining the role of exogenous ABA in plant–microbe interactions and whether bacterial ABA influences ABA status of plants under salt stress. However, PGPR modulate ABA biosynthesis and ABA-mediated signaling pathways that may contribute to the enhanced growth of salt-stressed plants. Halotolerant *Dietzia natronolimnaea* STR1 induced salinity (150 mM NaCl) tolerance mechanisms in wheat plants via modulation of an ABA-signaling cascade, validated by the upregulation of *TaABARE* (ABA-responsive gene) and *TaOPR1* (12-oxophytodienoate reductase 1) leading to *TaMYB* and *TaWRKY* stimulation, followed by expression of stress response genes including upregulation of *TaST* (a salt stress-induced gene). Expression of SOS pathway related genes and tissue-specific responses of ion transporters were modulated. Gene expression of various antioxidant enzymes and proline content were increased, contributing to enhanced protection against salt stress in PGPR inoculated plants (Bharti et al., 2016). Cucumber (*Cucumis sativus*) plants inoculated with *Burkholderia cepacia* SE4, *Promicromonospora sp.* SE188 and *Acinetobacter calcoaceticus* SE370 had significantly higher biomass under salinity stress (120 mM NaCl). PGPR increased water potential and decreased electrolyte leakage. The inoculated plants showed down-regulation of ABA compared with control plants, while salicylic acid and gibberellin GA4 contents were increased (Kang et al., 2014a). Seed inoculation of cotton (*Gossypium hirsutum*) with *Pseudomonas putida* Rs-198 reduced ABA accumulation and increased plant biomass in salinized soil but the induced salt tolerance can also be attributed to regulated ionic balance and improved endogenous IAA content (Yao et al., 2010). Wheat plants inoculated with PGPR strains *Arthrobacter protophormiae* SA3 and *B. subtilis* LDR2 built up IAA while conflicted the increase of ABA and ACC content under salt stress conditions (100 mM NaCl). The amelioration effect was further validated by the

upregulation of *TaCTR1* (Serine/Threonine protein kinase – ethylene responsive) and *TaDRE2* (drought-responsive element) genes (Barnawal et al., 2017).

2.5.4 Extracellular molecules

The extracellular secretions of PGPR including proteins, hormones, volatiles, polyamines, and other compounds have been determined to manipulate signaling pathways and regulatory functions that positively impact plant defense and development by stimulating growth, inducing disease resistance and eliciting stress tolerance (Barnawal et al., 2013; Kang et al., 2014b; Bhattacharyya et al., 2015; Smith et al., 2015a; Zhou et al., 2016).

2.5.4.1 Exopolysaccharides

Bacteria secrete exopolysaccharides (EPS) which are responsible for attachment, often along with other bacteria, to soil particles and root surfaces. EPS bind soil particles to aggregates, stabilizing soil structures, and increasing water holding capacity and cation exchange capacity (Upadhyay et al., 2011). EPS usually form an enclosed matrix of microcolonies, which confer protection against environmental fluctuations, water and nutrient retention, and epiphytic colonization (Balsanelli et al., 2014). They are also indispensable for mature biofilm formation and functional nodules in legume–rhizobia symbiosis (Stoodley et al., 2002; Skorupska et al., 2006). Inoculation of EPS producing *Pseudomonas mendocina* with an arbuscular mycorrhizal fungus, *Glomus intraradices* onto lettuce (*Lactuca sativa*) resulted in stabilization of soil aggregates under field conditions (Kohler et al., 2006). Inoculation with salt-tolerant *Halomonas variabilis* HT1 and *Planococcus rifietoensis* RT4 increased the growth of chickpea (*Cicer arietinum* var. CM-98) and soil aggregation with roots under high salt concentrations (up to 200 mM NaCl) (Qurashi and Sabri, 2012). Quinoa (*Chenopodium quinoa*) seeds inoculated with *Enterobacter sp.* MN17 and *Bacillus sp.* MN54 improved plant-water relations under saline irrigation conditions of 400 mM NaCl (Yang et al., 2016). EPS production and composition improve bacterial resistance to abiotic stress (Sandhya and Ali, 2015) but the role of EPS in plant salinity tolerance deserves further investigation.

2.5.4.2 Lipo-chitooligosaccharides

Legume–rhizobia symbiosis is affected by salt stress and high levels of salinity inhibit nodule formation and nitrogen fixation (Tu, 1981; Zahran, 1999). Lipo-chitooligosaccharides (LCOs) are secreted by rhizobia as Nod-factors (NFs) in response to flavonoids present in root

exudates and initiate nodule formation. LCOs are conserved at the core but diverge in the N-Acetyl chain length, degree of saturation, and substitutions (glycosylation or sulfation), which are crucial in host specificity (Oldroyd, 2013). Nod-factors also act as stress response signals in legumes and NF synthesis is modulated by other PGPR and abiotic stresses. High salinity (100–200 mM NaCl) inhibited root hair deformation responses to increase in NF concentrations in Soybean (*Glycine max*) – *Bradyrhizobium japonicum* symbiosis (Duzan et al., 2004). Inoculation of IAA producing *Azospirillum brasilense* Cd into the Rhizobium-Bean (*Phaseolus vulgaris* cv. Negro Jamapa) symbiosis increased root branching and flavonoid synthesis under 50 mM NaCl. The co-inoculation also promoted Nod-genes expression in *R. tropici* CIAT899 and *R. etli* ISP42 grown in the presence of root exudates (Dardanelli et al., 2008). Free-living rhizobia are more resistant to salt stress than inside their legume hosts. *R. tropici* CIAT899 is highly tolerant to stress and high salt concentrations enhance Nod-gene expression, Nod-factor synthesis and diversity; 46 different NFs were identified compared to 29 NFs under control with only 15 NFs common to both (Estevez et al., 2009). Inoculation of *B. japonicum* 532C grown in genistein (a flavonoid) induced media significantly enhanced nodulation and growth of soybean under salinity levels (36 and 61 mM NaCl) and such positive effects become more evident with time (Miransari and Smith, 2009) and increased yield up to 21% under salinized field conditions in an earlier study.

2.5.4.3 Bacteriocins

Bacteriocins are small peptides secreted by rhizobacteria that are bactericidal or bacteriostatic against relative bacteria, thus providing a competitive advantage to the producer strain but might also promote microbial diversity in an ecologic niche (Kirkup and Riley, 2004). Application of thuricin 17, isolated from a soybean endosymbiont *Bacillus thuriengenesis* NEB 17 differentially altered the proteome of salt-stressed (250 mM NaCl) Arabidopsis plants. Expression of proteins involved in carbon and energy metabolism pathways were modulated by the bacterial signals. Proteins involved in photosynthesis including PEP carboxylase, RuBisCo-oxygenase large subunit, pyruvate kinase and proteins of photosystems I and II were upregulated along with other stress related proteins (Subramanian et al., 2016b). These bacterial signal compounds also induced similar changes in the proteome of soybean seeds at 48 h under 100 mM NaCl. In addition, isocitrate lyase and antioxidant glutathione-S-transferase were increased. These findings by shotgun proteomics suggested that thuricin 17 positively manipulate plant proteome profile and enhance physiological tolerance to salinity (Subramanian et al., 2016a).

2.5.4.4 Polyamines

Polyamines (PAs) are low molecular weight aliphatic amines with pronounced antioxidant activity that are ubiquitous in all living organisms and modulate ROS homeostasis by scavenging free radicals and stimulating antioxidant enzymes. The most abundant polyamines, spermidine, spermine, and putrescine are implicated in various developmental processes and stress responses in plants (Gupta et al., 2013). Application of exogenous polyamines increase abiotic stress tolerance but PGPR secretion of polyamines is largely unexplored. Spermidine from *Bacillus megaterium* BOFC15 increased cellular polyamine accumulation in Arabidopsis, thereby activating PA-mediated signaling pathways contributing to the osmotic stress tolerance of plants. The bacterial inoculation resulted in greater biomass, elevated photosynthetic capacity and higher antioxidant enzyme activity. Other tolerance mechanisms involved robust root system architecture and ABA dependent stress responses, which maintained water balance and stomatal conductance (Zhou et al., 2016).

2.5.4.5 Volatile compounds

Volatile organic compounds (VOC) released from PGPR are known to stimulate plant growth, resulting in increased shoot biomass, and modulated stress responses. Perception of volatiles by plants and subsequently induced mechanisms require further research (Bailly and Weisskopf, 2012). *B. subtilis* GB03 VOCs mediated tissue specific regulations of Na^+ homeostasis in salt-stressed plants. Arabidopsis under 100 mM NaCl treated with VOCs decreased Na^+ accumulation by concurrently downregulating expression of *HKT1* in roots but upregulating it in shoots. Presumably, the induction of *HKT1* dependent shoot-to-root recirculation resulted in reduced Na^+ accumulation up to ~50% throughout the plant. Treatment with VOCs increased leaf surface area, root mass, and total K^+ content when compared with controls whereas, inoculated *athkt1* mutants showed stunted growth. Exposure to VOCs reduced the total Na^+ level by 18% and enhanced shoot and root growth of *sos3* mutants in 30 mM NaCl (Zhang et al., 2008). A putative VOCs blend released from *Pseudomonas simiae* AU induced salt-tolerance in soybean (*Glycine max*) under 100 mM NaCl by decreasing root Na^+ accumulation and increasing proline and chlorophyll content. Protein expression analysis confirmed upregulation of vegetative storage proteins (Na^+ homeostasis), RuBisCO large chain proteins (photosynthesis) in exposed soybean seedlings (Vaishnav et al., 2015).

Paraburkholderia phytofirmans PsJN VOCs stimulate plant growth and induce salinity tolerance that have been demonstrated both in vitro (150 mM NaCl/15 mM CaCl2) and in soil (200 mM NaCl/20 mM CaCl2). Growth parameters of Arabidopsis plants measured as rosette area, fresh weight, and primary root length were higher than the control plants and exposure to VOCs showed parallel growth promoting effects of direct bacterial inoculation. The emitted compounds were analyzed and the plants were exposed to a blend of 2-undecanone, 7-hexanol, 3-methylbutanol molecules, which mimicked the effect of VOCs (Ledger et al., 2016). Genome wide mapping association of Arabidopsis accession lines revealed 10 genetic loci associated with growth stimulation in response to the presence of *P. simiae* WCS417r *in vitro*, which is partly caused by VOC produced by the bacterium. Even though the study was conducted to select lines for breeding strategies, it is interesting to note that the genotype variation of host plants has different interactions with the associated root microbiome (Wintermans et al., 2016).

2.6 Conclusion

Application of PGPR inoculants as biofertilizers and biocontrol agents is an integral component in organic farming practices (Babalola, 2010). With rising emphasis on sustainable agriculture, environmental protection, and food security, exploitation of beneficial soil microbiota is imperative. Abiotic stresses constraint yield and turn agriculture production systems fragile; in addition, persisting climate change intensify the frequency, degree, and resultant damage of stressful conditions. Plants have evolved complex mechanisms to tolerate abiotic stresses caused by various environmental factors, including salinity. Plant associated bacteria in soil mitigate the adverse effects of these stresses in a more time-sensitive and cost-effective manner, where the development of tolerant cultivars has been somewhat overwhelmed. Research directed towards the application of PGPR in salt-affected fields encourages commercialization of inoculants for salinity tolerance. The systems biology of plant–microbe interactions in response to environmental stimuli such as salinity, opens up new prospects of understanding the regulatory networks of plant salt tolerance modulated by rhizosphere bacteria (Table 2.1). While the induced salt tolerance may be contributed by the release of extracellular compounds that function as chemical signals to the plant, improved soil properties that reduce the impact of salinity is another important benefit yet to be explored. Stress adaptation of plants are induced by associated microbiota and cutting-edge research as discussed above may be successfully applied to improve crop yield in saline prone

regions. The potential application of PGPR to help plants deal with stress in agricultural fields seems vastly large, yet much is left to be utilized.

Table 2.1. Summary of PGPR interaction effects in crop plants under salinity stress from recent studies using systems biology approaches.

	PGPR	Crop species	Beneficial effects	Reference
1.	*Bacillus amyloliquefaciens* SN13	*Oryza sativa*	Upregulation of *SOS1*, *EREBP*, *SERK1*, *NADP-Me2*	Nautiyal et al., 2013
2.	*Bacillus amyloliquefaciens* SQR9	*Zea mays*	Upregulation of *RBCS*, *RBCL, HKT1*, *NHX1*, *NHX2* and *NHX3*	Chen et al., 2016
3.	*Bacillus megaterium*	*Zea mays*	Improved expression of two ZmPIP isoforms	Marulanda et al., 2010
4.	*Bacillus thuriengenesis* NEB17	*Glycine max*	Upregulation of PEP carboxylase, Rubisco-oxygenase large subunit, pyruvate kinase, and proteins of photosystems I and II, isocitrate lyase and antioxidant glutathione-S-transferase	Subramanian et al., 2016a
5.	*Dietzia natronolimnaea*	*Triticum aestivum*	Modulation of ABA signaling cascade, SOS pathway related genes, tissue-specific responses of ion transporters	Bharti et al., 2016
6.	*Enterobacter sp.* UPMR18 (ACC deaminase)	*Abelmoschus esculentus*	Increase antioxidant enzyme activities and upregulation of ROS pathway genes	Habib et al., 2016
7.	*Pseudomonas putida* UW4 (ACC deaminase)	*Solanum lycopersicum*	Increased shoot growth and expression of *Toc GTPase*	Yan et al., 2014
8.	*Pseudomonas simiae* AU	*Glycine max*	Upregulation of vegetative storage proteins, RuBisCO large chain proteins. Decrease in root Na^+ accumulation and increase in proline and chlorophyll content	Vaishnav et al., 2015

2.7 References

1. Apel, K., and Hirt, H. (2004). Reactive oxygen species: metabolism, oxidative stress, and signal transduction. *Annu. Rev. Plant Biol.* 55, 373–399. doi: 10.1146/annurev.arplant.55.031903.141701
2. Arkhipova, T. N., Prinsen, E., Veselov, S. U., Martinenko, E. V., Melentiev, A. I., and Kudoyarova, G. R. (2007). Cytokinin producing bacteria enhance plant growth in drying soil. *Plant Soil* 292, 305–315. doi: 10.1007/s11104-007-9233-5
3. Babalola, O. O. (2010). Beneficial bacteria of agricultural importance. *Biotechnol. Lett.* 32, 1559–1570. doi: 10.1007/s10529-010-0347-0
4. Badri, D. V., Weir, T. L., van der Lelie, D., and Vivanco, J. M. (2009). Rhizosphere chemical dialogues: plant–microbe interactions. *Curr. Opin. Biotechnol.* 20, 642–650. doi: 10.1016/j.copbio.2009.09.014
5. Bailly, A., and Weisskopf, L. (2012). The modulating effect of bacterial volatiles on plant growth: current knowledge and future challenges. *Plant Signal. Behav.* 7, 79–85. doi: 10.4161/psb.7.1.18418
6. Balsanelli, E., de Baura, V. A., Pedrosa, F. D., de Souza, E. M., and Monteiro, R. A. (2014). Exopolysaccharide biosynthesis enables mature biofilm formation on abiotic surfaces by *Herbaspirillum seropedicae. PLOS ONE* 9:e110392. doi: 10.1371/journal.pone.0110392
7. Baral, A., Shruthi, K. S., and Mathew, M. K. (2015). Vesicular trafficking and salinity responses in plants. *IUBMB Life* 67, 677–686. doi: 10.1002/iub.1425
8. Barnawal, D., Bharti, N., Pandey, S. S., Pandey, A., Chanotiya, C. S., and Kalra, A. (2017). Plant growth promoting rhizobacteria enhances wheat salt and drought stress tolerance by altering endogenous phytohormone levels and *TaCTR1/TaDREB2* expression. *Physiol. Plant.* doi: 10.1111/ppl.12614.
9. Barnawal, D., Maji, D., Bharti, N., Chanotiya, C. S., and Kalra, A. (2013). ACC deaminase-containing *Bacillus subtilis* reduces stress ethylene-induced damage and improves mycorrhizal colonization and rhizobial nodulation in *Trigonella foenum-graecum* under drought stress. *J. Plant Growth Regul.* 32, 809–822. doi: 10.1007/s00344-013-9347-3
10. Bauder, J. W., and Brock, T. A. (2001). Irrigation water quality, soil amendment, and crop effects on sodium leaching. *Arid Land Res. Manag.* 15, 101–113. doi: 10.1080/15324980151062724
11. Bauer, W. D., and Mathesius, U. (2004). Plant responses to bacterial quorum sensing signals. *Curr. Opin. Plant Biol.* 7, 429–433. doi: 10.1016/j.pbi.2004.05.008
12. Beneduzi, A., Ambrosini, A., and Passaglia, L. M. P. (2012). Plant growth-promoting rhizobacteria (PGPR): their potential as antagonists and biocontrol agents. *Genet. Mol. Biol.* 35, 1044–1051.
13. Berg, G. (2009). Plant-microbe interactions promoting plant growth and health: perspectives for controlled use of microorganisms in agriculture. *Appl. Microbiol. Biotechnol.* 84, 11–18. doi: 10.1007/s00253-009-2092-7
14. Bharti, N., Pandey, S. S., Barnawal, D., Patel, V. K., and Kalra, A. (2016). Plant growth promoting rhizobacteria *Dietzia natronolimnaea* modulates the expression of stress responsive genes providing protection of wheat from salinity stress. *Sci. Rep.* 6:34768. doi: 10.1038/srep34768
15. Bhattacharyya, D., Garladinne, M., and Lee, Y. H. (2015). Volatile indole produced by rhizobacterium *Proteus vulgaris* JBLS202 stimulates growth of *Arabidopsis thaliana* through

auxin, cytokinin, and brassinosteroid pathways. *J. Plant Growth Regul.* 34, 158–168. doi: 10.1007/s00344-014-9453-x
16. Chen, L., Liu, Y., Wu, G., Veronican Njeri, K., Shen, Q., Zhang, N., et al. (2016). Induced maize salt tolerance by rhizosphere inoculation of *Bacillus amyloliquefaciens* SQR9. *Physiol. Plant.* 158, 34–44. doi: 10.1111/ppl.12441
17. Chen, M., Wei, H., Cao, J., Liu, R., Wang, Y., and Zheng, C. (2007). Expression of *Bacillus subtilis* proBA genes and reduction of feedback inhibition of proline synthesis increases proline production and confers osmotolerance in transgenic Arabidopsis. *J. Biochem. Mol. Biol.* 40, 396–403.
18. Chinnusamy, V., Zhu, J., and Zhu, J. K. (2006). Salt stress signaling and mechanisms of plant salt tolerance. *Genet. Eng. (N Y)* 27, 141–177.
19. Chowdhury, S. P., Hartmann, A., Gao, X. W., and Borriss, R. (2015). Biocontrol mechanism by root-associated *Bacillus amyloliquefaciens* FZB42-a review. *Front. Microbiol.* 6:780. doi: 10.3389/fmicb.2015.00780
20. Compant, S., Duffy, B., Nowak, J., Clement, C., and Barka, E. A. (2005). Use of plant growth-promoting bacteria for biocontrol of plant diseases: principles, mechanisms of action, and future prospects. *Appl. Environ. Microbiol.* 71, 4951–4959. doi: 10.1128/Aem.71.9.4951-4959.2005
21. Cramer, G. R. (1992). Kinetics of maize leaf elongation.2. Responses of a Na-excluding cultivar and a Na-including cultivar to varying Na/Ca salinities. *J. Exp. Bot.* 43, 857–864. doi: 10.1093/jxb/43.6.857
22. Dardanelli, M. S., Fernández de Córdoba, F. J., Espuny, M. R., Rodríguez Carvajal, M. A., Soria Díaz, M. E., Gil Serrano, A. M., et al. (2008). Effect of *Azospirillum brasilense* coinoculated with Rhizobium on *Phaseolus vulgaris* flavonoids and Nod factor production under salt stress. *Soil Biol. Biochem.* 40, 2713–2721.
23. Davenport, R., James, R. A., Zakrisson-Plogander, A., Tester, M., and Munns, R. (2005). Control of sodium transport in durum wheat. *Plant Physiol.* 137, 807–818. doi: 10.1104/pp.104.057307
24. del Amor, F. M., and Cuadra-Crespo, P. (2012). Plant growth-promoting bacteria as a tool to improve salinity tolerance in sweet pepper. *Funct. Plant Biol.* 39, 82–90. doi: 10.1071/Fp11173
25. Divya, B., and Kumar, M. D. (2011). Plant -microbe interaction with enhanced bioremediation. *Res. J. Biotechnol.* 6, 72–79.
26. Dodd, I. C., and Perez-Alfocea, F. (2012). Microbial amelioration of crop salinity stress. *J. Exp. Bot.* 63, 3415–3428. doi: 10.1093/jxb/ers033
27. Dodd, I. C., Zinovkina, N. Y., Safronova, V. I., and Belimov, A. A. (2010). Rhizobacterial mediation of plant hormone status. *Ann. Appl. Biol.* 157, 361–379. doi: 10.1111/j.1744-7348.2010.00439.x
28. Doering, E. J., and Sandoval, F. M. (1981). Chemistry of seep drainage in southwestern north-dakota. *Soil Sci.* 132, 142–149. doi: 10.1097/00010694-198108000-00003
29. Duzan, H. M., Zhou, X., Souleimanov, A., and Smith, D. L. (2004). Perception of *Bradyrhizobium japonicum* Nod factor by soybean [*Glycine max* (L.) Merr.] root hairs under abiotic stress conditions. *J. Exp. Bot.* 55, 2641–2646. doi: 10.1093/jxb/erh265
30. Egamberdieva, D. (2009). Alleviation of salt stress by plant growth regulators and IAA producing bacteria in wheat. *Acta Physiol Plant* 31, 861–864. doi: 10.1007/s11738-009-0297-0

31. Egamberdieva, D., and Lugtenberg, B. (2014). "Use of plant growth-promoting rhizobacteria to alleviate salinity stress in plants," in *Use of Microbes for the Alleviation of Soil Stresses*, Vol. 1, ed. M. Miransari (New York, NY: Springer), 73–96.
32. Epstein, E. (1998). How calcium enhances plant salt tolerance. *Science* 280, 1906–1907.
33. Estevez, J., Soria-Diaz, M. E., de Cordoba, F. F., Moron, B., Manyani, H., Gil, A., et al. (2009). Different and new Nod factors produced by *Rhizobium tropici* CIAT899 following Na+ stress. *FEMS Microbiol. Lett.* 293, 220–231. doi: 10.1111/j.1574-6968.2009.01540.x
34. Figueiredo, M. V. B., Burity, H. A., Martinez, C. R., and Chanway, C. P. (2008). Alleviation of drought stress in the common bean (*Phaseolus vulgaris* L.) by co-inoculation with Paenibacillus polymyxa and *Rhizobium tropici. Appl. Soil Ecol.* 40, 182–188. doi: 10.1016/j.apsoil.2008.04.005
35. Flowers, T. J., and Colmer, T. D. (2015). Plant salt tolerance: adaptations in halophytes. *Ann. Bot.* 115, 327–331. doi: 10.1093/aob/mcu267
36. Flowers, T. J., Hajibagheri, M. A., and Clipson, N. J. W. (1986). Halophytes. *Q. Rev. Biol.* 61, 313–337. doi: 10.1086/415032
37. Fricke, W., Akhiyarova, G., Wei, W. X., Alexandersson, E., Miller, A., Kjellbom, P. O., et al. (2006). The short-term growth response to salt of the developing barley leaf. *J. Exp. Bot.* 57, 1079–1095. doi: 10.1093/jxb/erj095
38. Gill, S. S., and Tuteja, N. (2010). Reactive oxygen species and antioxidant machinery in abiotic stress tolerance in crop plants. *Plant Physiol. Biochem.* 48, 909–930. doi: 10.1016/j.plaphy.2010.08.016
39. Gilliham, M., and Tester, M. (2005). The regulation of anion loading to the maize root xylem. *Plant Physiol.* 137, 819–828. doi: 10.1104/pp.104.054056
40. Glick, B. R. (2012). Plant growth-promoting bacteria: mechanisms and applications. *Scientifica (Cairo)* 2012, 963401. doi: 10.6064/2012/963401
41. Glick, B. R., Cheng, Z., Czarny, J., and Duan, J. (2007). Promotion of plant growth by ACC deaminase-producing soil bacteria. *Eur. J. Plant Pathol.* 119, 329–339. doi: 10.1007/s10658-007-9162-4
42. Gray, E. J., and Smith, D. L. (2005). Intracellular and extracellular PGPR: commonalities and distinctions in the plant-bacterium signaling processes. *Soil Biol. Biochem.* 37, 395–412. doi: 10.1016/j.soilbio.2004.08.030
43. Gupta, K., Dey, A., and Gupta, B. (2013). Plant polyamines in abiotic stress responses. *Acta Physiol. Plant.* 35, 2015–2036. doi: 10.1007/s11738-013-1239-4
44. Habib, S. H., Kausar, H., and Saud, H. M. (2016). Plant growth-promoting rhizobacteria enhance salinity stress tolerance in okra through ROS-scavenging enzymes. *Biomed. Res. Int.* 2016:6284547. doi: 10.1155/2016/6284547
45. Halfter, U., Ishitani, M., and Zhu, J. K. (2000). The Arabidopsis SOS2 protein kinase physically interacts with and is activated by the calcium-binding protein SOS3. *Proc. Natl. Acad. Sci. U.S.A.* 97, 3735–3740. doi: 10.1073/pnas.040577697
46. Hasegawa, P. M., Bressan, R. A., Zhu, J. K., and Bohnert, H. J. (2000). Plant cellular and molecular responses to high salinity. *Annu. Rev. Plant Physiol. Plant Mol. Biol.* 51, 463–499. doi: 10.1146/annurev.arplant.51.1.463
47. Jacoby, R. P., Che-Othman, M. H., Millar, A. H., and Taylor, N. L. (2016). Analysis of the sodium chloride-dependent respiratory kinetics of wheat mitochondria reveals differential effects on phosphorylating and non-phosphorylating electron transport pathways. *Plant Cell Environ.* 39, 823–833. doi: 10.1111/pce.12653

48. Janssen, J., Weyens, N., Croes, S., Beckers, B., Meiresonne, L., Van Peteghem, P., et al. (2015). Phytoremediation of metal contaminated soil using willow: exploiting plant-associated bacteria to improve biomass production and metal uptake. *Int. J. Phytoremediation* 17, 1123–1136. doi: 10.1080/15226514.2015.1045129
49. Jin, C. W., Ye, Y. Q., and Zheng, S. J. (2014). An underground tale: contribution of microbial activity to plant iron acquisition via ecological processes. *Ann. Bot.* 113, 7–18. doi: 10.1093/aob/mct249
50. Kang, S.-M., Khan, A. L., Waqas, M., You, Y.-H., Kim, J.-H., Kim, J.-G., et al. (2014a). Plant growth-promoting rhizobacteria reduce adverse effects of salinity and osmotic stress by regulating phytohormones and antioxidants in *Cucumis sativus*. *J. Plant Interact.* 9, 673–682. doi: 10.1080/17429145.2014.894587
51. Kang, S. M., Radhakrishnan, R., Khan, A. L., Kim, M. J., Park, J. M., Kim, B. R., et al. (2014b). Gibberellin secreting rhizobacterium, *Pseudomonas putida* H-2-3 modulates the hormonal and stress physiology of soybean to improve the plant growth under saline and drought conditions. *Plant Physiol. Biochem.* 84, 115–124. doi: 10.1016/j.plaphy.2014.09.001
52. Kempf, B., and Bremer, E. (1998). Uptake and synthesis of compatible solutes as microbial stress responses to high-osmolality environments. *Arch. Microbiol.* 170, 319–330. doi: 10.1007/s002030050649
53. Kim, K., Jang, Y.-J., Lee, S.-M., Oh, B.-T., Chae, J.-C., and Lee, K.-J. (2014). Alleviation of salt stress by *Enterobacter* sp. *EJ*01 in tomato and Arabidopsis is accompanied by up-regulation of conserved salinity responsive factors in plants. *Mol. Cells* 37, 109–117. doi: 10.14348/molcells.2014.2239
54. Kirkup, B. C., and Riley, M. A. (2004). Antibiotic-mediated antagonism leads to a bacterial game of rock-paper-scissors in vivo. *Nature* 428, 412–414. doi: 10.1038/nature02429
55. Kohler, J., Caravaca, F., Carrasco, L., and Roldan, A. (2006). Contribution of *Pseudomonas* mendocina and Glomus intraradices to aggregate stabilization and promotion of biological fertility in rhizosphere soil of lettuce plants under field conditions. *Soil Use Manage.* 22, 298–304. doi: 10.1111/j.1475-2743.2006.00041.x
56. Kuan, K. B., Othman, R., Abdul Rahim, K., and Shamsuddin, Z. H. (2016). Plant growth-promoting rhizobacteria inoculation to enhance vegetative growth, nitrogen fixation and nitrogen remobilisation of maize under greenhouse conditions. *PLOS ONE* 11:e0152478. doi: 10.1371/journal.pone.0152478
57. Ledger, T., Rojas, S., Timmermann, T., Pinedo, I., Poupin, M. J., Garrido, T., et al. (2016). Volatile-mediated effects predominate in *Paraburkholderia phytofirmans* growth promotion and salt stress tolerance of *Arabidopsis thaliana*. *Front. Microbiol.* 7:1838. doi: 10.3389/fmicb.2016.01838
58. Lugtenberg, B., and Kamilova, F. (2009). Plant-growth-promoting rhizobacteria. *Annu. Rev. Microbiol.* 63, 541–556. doi: 10.1146/annurev.micro.62.081307.162918
59. Lugtenberg, B. J., Malfanova, N., Kamilova, F., and Berg, G. (2013). Plant growth promotion by microbes. *Mol. Microb. Ecol. Rhizosphere* 1-2, 559–573.
60. Marulanda, A., Azcon, R., Chaumont, F., Ruiz-Lozano, J. M., and Aroca, R. (2010). Regulation of plasma membrane aquaporins by inoculation with a *Bacillus megaterium* strain in maize (*Zea mays* L.) plants under unstressed and salt-stressed conditions. *Planta* 232, 533–543. doi: 10.1007/s00425-010-1196-8

61. Miransari, M., and Smith, D. L. (2009). Alleviating salt stress on soybean (*Glycine max* (L.) Merr.) - *Bradyrhizobium japonicum* symbiosis, using signal molecule genistein. *Eur. J. Soil Biol.* 45, 146–152. doi: 10.1016/j.ejsobi.2008.11.002
62. Mittler, R., Vanderauwera, S., Gollery, M., and Van Breusegem, F. (2004). Reactive oxygen gene network of plants. *Trends Plant Sci.* 9, 490–498. doi: 10.1016/j.tplants.2004.08.009
63. Morgan, P. W., and Drew, M. C. (1997). Ethylene and plant responses to stress. *Physiol. Plant.* 100, 620–630. doi: 10.1034/j.1399-3054.1997.1000325.x
64. Munns, R. (2002a). Comparative physiology of salt and water stress. *Plant Cell Environ.* 25, 239–250. doi: 10.1046/j.0016-8025.2001.00808.x
65. Munns, R. (2002b). *Salinity, Growth and Phytohormones.* Berlin: Springer.
66. Munns, R., and Tester, M. (2008). Mechanisms of salinity tolerance. *Annu. Rev. Plant Biol.* 59, 651–681. doi: 10.1146/annurev.arplant.59.032607.092911
67. Nadeem, S. M., Zahir, Z. A., Naveed, M., and Arshad, M. (2009). Rhizobacteria containing ACC-deaminase confer salt tolerance in maize grown on salt-affected fields. *Can. J. Microbiol.* 55, 1302–1309. doi: 10.1139/W09-092
68. Narula, N., Kothe, E., and Behl, R. K. (2009). Role of root exudates in plant-microbe interactions. *J. Appl. Bot. Food Qual. Angewandte Botanik* 82, 122–130.
69. Nassar, I. N., and Horton, R. (1999). Salinity and compaction effects on soil water evaporation and water and solute distributions. *Soil Sci. Soc. Am. J.* 63, 752–758.
70. Nautiyal, C. S., Srivastava, S., Chauhan, P. S., Seem, K., Mishra, A., and Sopory, S. K. (2013). Plant growth-promoting bacteria *Bacillus amyloliquefaciens* NBRISN13 modulates gene expression profile of leaf and rhizosphere community in rice during salt stress. *Plant Physiol. Biochem.* 66, 1–9. doi: 10.1016/j.plaphy.2013.01.020
71. Nie, M., Wang, Y. J., Yu, J. Y., Xiao, M., Jiang, L. F., Yang, J., et al. (2011). Understanding plant-microbe interactions for phytoremediation of petroleum-polluted soil. *PLOS ONE* 6:e17961. doi: 10.1371/journal.pone.0017961
72. Niu, S. Q., Li, H. R., Pare, P. W., Aziz, M., Wang, S. M., Shi, H. Z., et al. (2016). Induced growth promotion and higher salt tolerance in the halophyte grass *Puccinellia tenuiflora* by beneficial rhizobacteria. *Plant Soil* 407, 217–230. doi: 10.1007/s11104-015-2767-z
73. Oldroyd, G. E. (2013). Speak, friend, and enter: signalling systems that promote beneficial symbiotic associations in plants. *Nat. Rev. Microbiol.* 11, 252–263. doi: 10.1038/nrmicro2990
74. Othman, Y., Al-Karaki, G., Al-Tawaha, A., and Al-Horani, A. (2006). Variation in germination and ion uptake in barley genotypes under salinity conditions. *World J. Agric. Sci.* 2, 11–15.
75. Panwar, M., Tewari, R., Gulati, A., and Nayyar, H. (2016). Indigenous salt-tolerant rhizobacterium Pantoea dispersa (PSB3) reduces sodium uptake and mitigates the effects of salt stress on growth and yield of chickpea. *Acta Physiol. Plant.* 38:278. doi: 10.1007/s11738-016-2284-6
76. Passioura, J. B., and Munns, R. (2000). Rapid environmental changes that affect leaf water status induce transient surges or pauses in leaf expansion rate. *Aust. J. Plant Physiol.* 27, 941–948.
77. Paul, M. J., and Foyer, C. H. (2001). Sink regulation of photosynthesis. *J. Exp. Bot.* 52, 1383–1400. doi: 10.1093/jexbot/52.360.1383
78. Perez-Alfocea, F., Albacete, A., Ghanem, M. E., and Dodd, I. C. (2010). Hormonal regulation of source-sink relations to maintain crop productivity under salinity: a case study of root-to-shoot signalling in tomato. *Funct. Plant Biol.* 37, 592–603. doi: 10.1071/Fp10012

79. Pinedo, I., Ledger, T., Greve, M., and Poupin, M. J. (2015). Burkholderia phytofirmans PsJN induces long-term metabolic and transcriptional changes involved in *Arabidopsis thaliana* salt tolerance. *Front. Plant Sci.* 6:466. doi: 10.3389/fpls.2015.00466
80. Pitman, M. G., and Lauchli, A. (2002). "Global impact of salinity and Agricultural ecosystems," in *Salinity: Environment - Plants - Molecules*, eds A. Lauchli and U. Luttage (Amsterdam: Kluwer Academic Publishers), 3–20.
81. Qiu, Q. S., Guo, Y., Dietrich, M. A., Schumaker, K. S., and Zhu, J. K. (2002). Regulation of SOS1, a plasma membrane Na+/H+ exchanger in *Arabidopsis thaliana*, by SOS2 and SOS3. *Proc. Natl. Acad. Sci. U.S.A.* 99, 8436–8441. doi: 10.1073/pnas.122224699
82. Qurashi, A. W., and Sabri, A. N. (2012). Bacterial exopolysaccharide and biofilm formation stimulate chickpea growth and soil aggregation under salt stress. *Braz. J. Microbiol.* 43, 1183–1191. doi: 10.1590/S1517-838220120003000046
83. Raven, J. A. (1985). Regulation of Ph and generation of osmolarity in vascular plants - a cost-benefit analysis in relation to efficiency of use of energy, nitrogen and water. *New Phytol.* 101, 25–77. doi: 10.1111/j.1469-8137.1985.tb02816.x
84. Rengasamy, P. (2002). Transient salinity and subsoil constraints to dryland farming in Australian sodic soils: an overview. *Aust. J. Exp. Agric.* 42, 351–361.
85. Rhodes, D., Nadolska-Orczyk, A., and Rich, P. J. (2002). "Salinity, osmolytes and compatible solutes," in *Salinity: Environment - Plants - Molecules*, eds A. Läuchli and U. Lüttge (Dordrecht: Springer), 181–204.
86. Rodriguez, H., and Fraga, R. (1999). Phosphate solubilizing bacteria and their role in plant growth promotion. *Biotechnol. Adv.* 17, 319–339. doi: 10.1016/S0734-9750(99)00014-2
87. Rodriguez-Navarro, A., and Rubio, F. (2006). High-affinity potassium and sodium transport systems in plants. *J. Exp. Bot.* 57, 1149–1160. doi: 10.1093/jxb/erj068
88. Rojas-Tapias, D., Moreno-Galván, A., Pardo-Díaz, S., Obando, M., Rivera, D., and Bonilla, R. (2012). Effect of inoculation with plant growth-promoting bacteria (PGPB) on amelioration of saline stress in maize (*Zea mays*). *Appl. Soil Ecol.* 61, 264–272.
89. Sandhya, V., and Ali, S. Z. (2015). The production of exopolysaccharide by *Pseudomonas putida* GAP-P45 under various abiotic stress conditions and its role in soil aggregation. *Microbiology* 84, 512–519. doi: 10.1134/S0026261715040153
90. Santner, A., and Estelle, M. (2009). Recent advances and emerging trends in plant hormone signalling. *Nature* 459, 1071–1078. doi: 10.1038/nature08122
91. Shalhevet, J. (1994). Using water of marginal quality for crop production - major issues. *Agric. Water Manage.* 25, 233–269. doi: 10.1016/0378-3774(94)90063-9
92. Sharma, D. R., and Prihar, S. S. (1973). Effect of depth and salinity of groundwater on evaporation and soil salinization. *Indian J. Agric. Sci.* 43, 582–586.
93. Sharma, S. B., Sayyed, R. Z., Trivedi, M. H., and Gobi, T. A. (2013). Phosphate solubilizing microbes: sustainable approach for managing phosphorus deficiency in agricultural soils. *Springerplus* 2:587. doi: 10.1186/2193-1801-2-587
94. Singh, R. P., and Jha, P. N. (2016). Alleviation of salinity-induced damage on wheat plant by an ACC deaminase-producing halophilic bacterium Serratia sp SL-12 isolated from a salt lake. *Symbiosis* 69, 101–111. doi: 10.1007/s13199-016-0387-x
95. Skorupska, A., Janczarek, M., Marczak, M., Mazur, A., and Król, J. (2006). Rhizobial exopolysaccharides: genetic control and symbiotic functions. *Microb. Cell Fact.* 5:7. doi: 10.1186/1475-2859-5-7

96. Smith, D. L., Gravel, V., and Yergeau, E. (2017). Editorial: signaling in the phytomicrobiome. *Front. Plant Sci.* 8:611. doi: 10.3389/fpls.2017.00611
97. Smith, D. L., Praslickova, D., and Ilangumaran, G. (2015a). Inter-organismal signaling and management of the phytomicrobiome. *Front. Plant Sci.* 6:722. doi: 10.3389/fpls.2015.00722
98. Smith, D. L., Subramanian, S., Lamont, J. R., and Bywater-Ekegard, M. (2015b). Signaling in the phytomicrobiome: breadth and potential. *Front. Plant Sci.* 6:709. doi: 10.3389/fpls.2015.00709
99. Spaepen, S., and Vanderleyden, J. (2011). Auxin and plant-microbe interactions. *Cold Spring Harb. Perspect. Biol.* 3:a001438. doi: 10.1101/cshperspect.a001438
100. Steenhoudt, O., and Vanderleyden, J. (2006). Azospirillum, a free-living nitrogen-fixing bacterium closely associated with grasses: genetic, biochemical and ecological aspects. *FEMS Microbiol. Rev.* 24, 487–506. doi: 10.1111/j.1574-6976.2000.tb00552.x
101. Stoodley, P., Sauer, K., Davies, D. G., and Costerton, J. W. (2002). Biofilms as complex differentiated communities. *Annu. Rev. Microbiol.* 56, 187–209. doi: 10.1146/annurev.micro.56.012302.160705
102. Subramanian, S., Ricci, E., Souleimanov, A., and Smith, D. L. (2016a). A proteomic approach to lipo-chitooligosaccharide and thuricin 17 effects on soybean germinationunstressed and salt stress. *PLOS ONE* 11:e0160660. doi: 10.1371/journal.pone.0160660
103. Subramanian, S., Souleimanov, A., and Smith, D. L. (2016b). Proteomic studies on the effects of lipo-chitooligosaccharide and thuricin 17 under unstressed and salt stressed conditions in *Arabidopsis thaliana. Front. Plant Sci.* 7:1314. doi: 10.3389/fpls.2016.01314
104. Sziderics, A. H., Rasche, F., Trognitz, F., Sessitsch, A., and Wilhelm, E. (2007). Bacterial endophytes contribute to abiotic stress adaptation in pepper plants (*Capsicum annuum* L.). *Can. J. Microbiol.* 53, 1195–1202. doi: 10.1139/W07-082
105. Tester, M., and Davenport, R. (2003). Na+ tolerance and Na+ transport in higher plants. *Ann. Bot.* 91, 503–527. doi: 10.1093/aob/mcg058
106. Tu, J. C. (1981). Effect of salinity on rhizobium-root-hair interaction, nodulation and growth of soybean. *Can. J. Plant Sci.* 61, 231–239.
107. Upadhyay, S. K., and Singh, D. P. (2015). Effect of salt-tolerant plant growth-promoting rhizobacteria on wheat plants and soil health in a saline environment. *Plant Biol.* 17, 288–293. doi: 10.1111/plb.12173
108. Upadhyay, S. K., Singh, J. S., and Singh, D. P. (2011). Exopolysaccharide-producing plant growth-promoting rhizobacteria under salinity condition. *Pedosphere* 21, 214–222. doi: 10.1016/S1002-0160(11)60120-3
109. Vaishnav, A., Kumari, S., Jain, S., Varma, A., and Choudhary, D. K. (2015). Putative bacterial volatile-mediated growth in soybean (*Glycine max* L. *Merrill*) and expression of induced proteins under salt stress. *J. Appl. Microbiol.* 119, 539–551. doi: 10.1111/jam.12866
110. Vorholt, J. A. (2012). Microbial life in the phyllosphere. *Nat. Rev. Microbiol.* 10, 828–840. doi: 10.1038/nrmicro2910
111. Wang, Q. Y., Dodd, I. C., Belimov, A. A., and Jiang, F. (2016). Rhizosphere bacteria containing 1-aminocyclopropane-1-carboxylate deaminase increase growth and photosynthesis of pea plants under salt stress by limiting Na+ accumulation. *Funct. Plant Biol.* 43, 161–172. doi: 10.1071/Fp15200
112. Waśkiewicz, A., Gładysz, O., and Goliński, P. (2016). "Participation of phytohormones in adaptation to salt stress," in *Plant Hormones Under Challenging Environmental Factors*, eds G. J. Ahammed and J.-Q. Yu (Dordrecht: Springer), 75–115.

113. Weyens, N., Beckers, B., Schellingen, K., Ceulemans, R., Van der Lelie, D., Newman, L., et al. (2015). The potential of the Ni-resistant TCE-degrading *Pseudomonas putida* W619-TCE to reduce phytotoxicity and improve phytoremediation efficiency of poplar cuttings on A Ni-TCE Co-contamination. *Int. J. Phytoremediation* 17, 40–48. doi: 10.1080/15226514.2013.828016
114. Wintermans, P. C., Bakker, P. A., and Pieterse, C. M. (2016). Natural genetic variation in Arabidopsis for responsiveness to plant growth-promoting rhizobacteria. *Plant Mol. Biol.* 90, 623–634. doi: 10.1007/s11103-016-0442-2
115. Yamashita, K., Kasai, M., Yamamoto, Y., and Matsumoto, H. (1994). Stimulation of plasma-membrane H+-transport activity in barley roots by salt stress - possible role of increase in chloride permeability. *Soil Sci. Plant Nutr.* 40, 555–563.
116. Yan, J. M., Smith, M. D., Glick, B. R., and Liang, Y. (2014). Effects of ACC deaminase containing rhizobacteria on plant growth and expression of Toc GTPases in tomato (*Solanum lycopersicum*) under salt stress. *Botany* 92, 775–781. doi: 10.1139/cjb-2014-0038
117. Yang, A. Z., Akhtar, S. S., Iqbal, S., Amjad, M., Naveed, M., Zahir, Z. A., et al. (2016). Enhancing salt tolerance in quinoa by halotolerant bacterial inoculation. *Funct. Plant Biol.* 43, 632–642. doi: 10.1071/Fp15265
118. Yang, J., Kloepper, J. W., and Ryu, C. M. (2009). Rhizosphere bacteria help plants tolerate abiotic stress. *Trends Plant Sci.* 14, 1–4. doi: 10.1016/j.tplants.2008.10.004
119. Yao, L. X., Wu, Z. S., Zheng, Y. Y., Kaleem, I., and Li, C. (2010). Growth promotion and protection against salt stress by *Pseudomonas putida* Rs-198 on cotton. *Eur. J. Soil Biol.* 46, 49–54. doi: 10.1016/j.ejsobi.2009.11.002
120. Zahran, H. H. (1999). Rhizobium-legume symbiosis and nitrogen fixation under severe conditions and in an arid climate. *Microbiol. Mol. Biol. Rev.* 63, 968–989.
121. Zerrouk, I. Z., Benchabane, M., Khelifi, L., Yokawa, K., Ludwig-Muller, J., and Baluska, F. (2016). A *Pseudomonas* strain isolated from date-palm rhizospheres improves root growth and promotes root formation in maize exposed to salt and aluminum stress. *J. Plant Physiol.* 191, 111–119. doi: 10.1016/j.jplph.2015.12.009
122. Zhang, H., Kim, M. S., Sun, Y., Dowd, S. E., Shi, H., and Paré, P. W. (2008). Soil bacteria confer plant salt tolerance by tissue-specific regulation of the sodium transporter HKT1. *Mol. Plant Microbe Interact.* 21, 737–744. doi: 10.1094/MPMI-21-6-0737
123. Zhou, C., Ma, Z., Zhu, L., Xiao, X., Xie, Y., Zhu, J., et al. (2016). Rhizobacterial strain *Bacillus megaterium* BOFC15 induces cellular polyamine changes that improve plant growth and drought resistance. *Int. J. Mol. Sci.* 17:976. doi: 10.3390/ijms17060976
124. Zhu, J. K. (2002). Salt and drought stress signal transduction in plants. *Annu. Rev. Plant Biol.* 53, 247–273. doi: 10.1146/annurev.arplant.53.091401.143329
125. Zhu, J.-K. (2007). *Plant Salt Stress*. Hoboken, NJ: John Wiley & Sons.

CONNECTING TEXT

The previous section provided an overview of the current understanding around beneficial members of the phytomicrobiome associated with the rhizosphere. Plant growth promoting rhizobacteria (PGPR) hold the potential to improve plant growth and development in a sustainable way. PGPR has been known to modulate abiotic stress regulation via direct and indirect mechanisms that induce systemic tolerance in plants. Phytomicrobiome of the native relatives of cultivated plants could be harnessed to isolate and characterize beneficial PGPR strains that alleviate (a)biotic stress and boost crop productivity. *Amphicarpaea bracteata* is a native legume related to soybean and cross-inoculation of *Bradyrhizobium* symbiont has been studied previously but not the other PGPR associated with the root nodules of this plant. In the present study, we hypothesize that nodule dwelling PGPR strains of *A. bracteata* could be applied to enhance plant growth and stress tolerance of soybean. Based on the background information and literature review, the project described below addresses the following research questions:

1) Does *Amphicarpaea bracteata* harbour beneficial PGPR in its root nodules? Will plant growth and stress tolerance of soybean improve with such strains?
2) What are the mechanisms/pathways in soybean that are elicited by the strains and their role in inducing stress (salt) tolerance and plant growth promotion of soybean?
3) What are the genomic characteristics of the strains that might contribute to their function as PGPR?

3 Chapter 3 Rhizobacteria From Root Nodules of an Indigenous Legume Enhance Salinity Stress Tolerance in Soybean

Authors: Gayathri Ilangumaran[1], Timothy Damian Schwinghamer [2] and Donald Lawrence Smith[1]

Affiliations:

[1] Department of Plant Science, McGill University, Macdonald Campus, 21,111 Lakeshore Road, Sainte-Anne-de-Bellevue, QC, Canada.

[2] Lethbridge Research and Development Centre, Agriculture and Agri-Food Canada, Lethbridge, AB, Canada.

This manuscript was originally published in Frontiers in Sustainable Food Systems journal and shared in the thesis via the Creative Commons Attribution 4.0 International Public License.

Ilangumaran, G., Schwinghamer, T. D., and Smith, D.L. (2021). Rhizobacteria From Root Nodules of an Indigenous Legume Enhance Salinity Stress Tolerance in Soybean. *Front. Sustain. Food Syst.* 4, 308. doi: 10.3389/fsufs.2020.617978

3.1 Abstract

Soybean is the most widely grown legume worldwide, but it is a glycophyte and salinity stress can decrease its yield potential up to 50%. Plant growth promoting rhizobacteria (PGPR) are known to enhance growth and induce tolerance to abiotic stresses including salinity. The aim of this study was to isolate such PGPR from the root nodules of *Amphicarpaea bracteata*, a North American relative of soybean. Isolated strains were identified, and 15 strains were screened for potential utilization as PGPR of soybean through a series of greenhouse trials. Four isolates that greatly improved shoot and root growth were further selected and screened under a range of salt concentrations. Two of the most promising strains, *Rhizobium sp*. SL42 and *Hydrogenophaga sp*. SL48 were ascertained to exert the greatest beneficial effects on soybean growth and salinity tolerance. They were co-inoculated with *Bradyrhizobium japonicum* 532C (*Bj*) and the plants were grown up to the harvest stage. The treatment of *Bj*+SL42 resulted in higher shoot biomass than the control, 18% at the vegetative stage, 16% at flowering, 7.5% at pod-filling, and 4.6% at harvest and seed weight was increased by 4.3% under salt stress (EC_e = 7.4 ds/m). Grain yield was raised under optimal conditions by 7.4 and 8.1% with treatments *Bj*+SL48 and *Bj*+SL42+SL48, respectively. Nitrogen assimilation and shoot K^+/Na^+ ratio were also higher in the co-inoculation treatments. This study suggested that inoculation with bacteria from an indigenous legume can

induce stress tolerance, improve growth and yield to support sustainability, and encourage ecological adaptability of soybean.

3.2 Introduction

Salinity is a major threat to agricultural sustainability and undermining the crop productivity on arable lands worldwide of which more than 50% is predicted to be affected by 2050 (Ashraf, 1994). It is anticipated that climate changes may hasten the aridisation of the Great Plains of North America during this century, leading to deficits in groundwater level and increased salinization of soil and water resources (Florinsky et al., 2009). The Canadian Prairies are susceptible to salinity, due to their soil type, moisture loss, high evapotranspiration rates and mineral salts in groundwater (Wiebe et al., 2007). The temporal fluctuation of soil salinity in this region is controlled by groundwater depth, which in turn is related to annual precipitation (Florinsky et al., 2009). Excessive use of road salts during winter may risk contamination of water sources and groundwater table in regions above 40°N (EnvironmentCanada, 2001). Soil salinity is also a pressing problem in many states of the USA on both irrigated and rainfed agricultural lands (NRCS, 2002). Salinity stress is mainly caused by uptake of NaCl, the dominant salt in nature, which creates both osmotic and ionic imbalances in plants. These lead to physiological dysfunctions that inhibit plant growth and development, thereby declining crop yield (Munns and Tester, 2008). Soil salinization has caused an estimated annual loss of $257 million CAD to Canadian farmers in 1998. Even though salinization risk has been lowered in the Prairies through better land-soil-water management practices, it persists to be a localized issue (AAFC, 2020).

Soybean [*Glycine max* (L.) Merrill] is an agriculturally important grain legume and oilseed crop worldwide. Due to the abundant protein (36%) and oil (19%) reserves in its seed, soybean has found uses as food for human consumption, animal feed, edible oil and industrial products (Thoenes, 2004). Soybean is capable of fixing atmospheric nitrogen through its symbiotic association with species of *Bradyrhizobium (B. japonicum, B. elkani, B. liaoningense, and B. yuanmingense)* in root nodules. Hence, it is an ideal rotation crop with corn, wheat, cotton and other arable crops, to increase soil nitrogen content and reduce production costs. Cultivation of soybean has gained significance in North America after world war II (Cloutier, 2017). Now, Canada and the USA are prominent global suppliers and consumers with the USA ranking first (60% of soybean trade). Soybean production has been steadily on the rise in Canada during recent

years (Supplementary Table 3.1) and cultivation has expanded in the southern regions, bolstered by the introduction of early-maturing varieties (Dorff, 2007).

However, sub-optimal growing conditions are met with environmental challenges other than just low temperatures. Soybean is basically a short-day plant (development is influenced by daylength), relatively resistant to temperature fluctuations (more extreme temperatures affect flowering and pod-setting), grown in a wide range of soils (except very sandy), sensitive to waterlogging and moderately tolerant to drought and salinity (FAO, 2002). According to the FAO crop database, "yield decrease due to soil salinity is: 0% at EC_e 5 mmhos/cm, 10% at 5.5, 25% at 6.2, 50% at 7.5 and 100% at EC_e 10 mmhos/cm." Salinity stress may cause physiological and biochemical disorders in soybean that inhibit seed germination and plant growth, aggravate leaf chlorosis and bleaching, decrease biomass accumulation, restrain nodulation and nitrogen fixation, and reduce yield and seed quality (Phang et al., 2008). Salinity has significantly reduced the germination percentage, plant height and shoot dry weight of 45 day-old plants of three soybean cultivars. There was also an increase in sodium and chloride levels in the leaf tissues (Essa, 2002). In soybean cv. Williams, seedling growth declined to 5% at 220 mmolal NaCl and no growth was recorded at 330 mmolal NaCl (Hosseini et al., 2002). Association mapping of soybean seed germination revealed 1,142 single nucleotide polymorphisms associated with salt tolerance. Salinity tolerance is influenced by numerous genetic and environmental factors and a complex trait, such that molecular breeding for salt-tolerant soybean cultivars has been challenging (Kan et al., 2015).

When commercial cultivation of soybean began in North America (early twentieth century), seeds were inoculated with the *Bradyrhizobium* strains capable of nodulating soybean to facilitate nitrogen fixation because they were not existing in the soil. Thus, populations of bradyrhizobia have become established in soils that had no prior soybean cropping history as a result of selective enrichment over the years by the host plant (Weaver et al., 1972). Subsequently, there has been research interest in exploring the symbiotic associations of native legumes and their relationships with soybean. *Amphicarpaea bracteata* (American hog peanut) is an annual plant of the family Leguminosae, native to eastern North America, found in a variety of partially shaded, wet habitats (Parker, 1994). *A. bracteata* is closely related to soybean, confirmed by molecular studies and both genera are classified in the subtribe Glycininae of the tribe Phaseoleae (Zhu et al., 1995). Symbiotic specificity and nodule formation with rhizobia strains are genetically controlled

by nodulation restriction alleles in the host legume (Devine et al., 1990; Wilkinson et al., 1996). The inoculation of soybean plants with 10 *Bradyrhizobium* strains from *A. bracteata* resulted in nodule formation but no nitrogen fixation (Marr et al., 1997). Micro-evolution was observed within *Bradyrhizobium* populations from the soils of soybean field sites in eastern Canada and the isolated strains were clustered with isolates from the native legumes (Tang et al., 2012). In a later study by Bromfield et al. (2017), inoculation of soybean with root-zone soils of native legumes including *A. bracteata* resulted in nodulation. Upon isolation, bacteria of the *Bradyrhizobium* genus and closely related taxa were inoculated onto soybean, and some of the bacteria containing *nodC* and *nifH* gene sequences effectively fixed nitrogen, while the others were ineffective.

Symbiotic association with rhizobia has been the primary focus of plant-microbe interaction research on legumes, and more particularly soybean, but there are also other beneficial plant growth promoting rhizobacteria (PGPR) associated with them. Endophytic bacteria were isolated from soybean nodules and co-inoculation of *Bacillus subtilis* NEB4, *B. subtilis* NEB5 and *B. thuringiensis* NEB17 with *B. japonicum* increased soybean growth and plant dry weight (Bai et al., 2002a). PGPR influence plant growth through direct and indirect mechanisms such as nitrogen fixation, nutrient assimilation, and secretion of exopolysaccharides and signaling molecules (Hynes et al., 2008; Adesemoye and Kloepper, 2009). Distinct genera of PGPR have been known to act as elicitors of induced systemic tolerance to abiotic stress (Yang et al., 2009). Many studies have reported on the beneficial role of PGPR co-inoculated with *Bradyrhizobium* on growth, yield and stress tolerance of soybean. Co-inoculation with *Serratia proteamaculans* 1–102 and *S. liquefaciens* 2–68 increased plant dry weight and nodule number in soybean under sub-optimal root-zone temperatures in a soil-less media (Bai et al., 2002b). In a field study, seed co-inoculation with *Azospirillum brasilense* increased soybean yield by 14.1% (Hungria et al., 2013). Co-inoculation with *Pseudomonas putida* TSAU1 improved plant growth, root architecture, nitrogen and phosphorous content of soybean under salt stress in a hydroponic experiment (Egamberdieva et al., 2017).

Diverse PGPR may be associated within the nodules of *A. bracteata* and they may confer better adaptation of soybean plants to the soil and environmental conditions prevailing in Canada and benefit co-inoculation with *B. japonicum* for nitrogen fixation. The current study had two objectives. First, bacteria isolated from the root nodules of *A. bracteata* were screened for their ability to enhance plant growth and salt stress tolerance of soybean by evaluating seed germination

and growth parameters in a greenhouse environment. Successive screening was then performed at a range of salt concentrations to determine the threshold salinity tolerance of soybean, inoculated with selected isolates. Second, two of the most promising bacteria were co-inoculated with *Bradyrhizobium japonicum* 532C, to validate their role as PGPR able to induce salinity tolerance, improve nutrient assimilation and increase growth and yield of soybean plants.

3.3 Materials and Methods

3.3.1 Isolation of bacteria from root nodules

Plants of *Amphicarpaea bracteata* were collected along the shore of Lac St. Louis on the Macdonald Campus of McGill University, located in Sainte-Anne-de-Bellevue, Quebec, Canada. The nodules present on the roots of *A. bracteata* were relatively smaller and fewer than those of cultivated soybean plants (Supplementary Figure 3.1). The nodules were separated from the roots, washed and surface sterilized using 70% (v/v) ethanol for two min. They were crushed using micro pestles and the suspension was serially diluted in sterile water. The dilutions (from 10^{-2} to 10^{-7}) were plated on Kings B and yeast extract mannitol (YEM) agar plates. The plates were incubated at 25 °C for 24–96 h. Single colonies of bacteria (excluding mold or actinomycetes) that were morphologically different from one another were re-isolated on new agar plates to obtain pure colonies (Supplementary Figure 3.2). The individual colonies of 15 isolates were grown in liquid broth for culture maintenance and stored in glycerol stocks at −80°C.

3.3.2 Preparation of bacterial culture

The bacteria were grown in Kings B or YEM broth for 48 h, incubated at 25°C and 150 rpm. The cultures were harvested by centrifugation at 5,000 × g for 10 min, room temperature (Awel^{TM} MF 48-R, NuAire, USA) and the supernatant was discarded. The pellet was suspended in 10 mM $MgSO_4$ and the optical density was adjusted to 0.1 at A_{600nm} (Ultraspec 4300 pro UV/Visible Spectrophotometer, Biochrom). The prepared suspension was used in downstream experiments.

3.3.3 Identification of nodule bacteria

The identification of the isolated bacteria was done by Sanger di-deoxy nucleotide sequencing (Genome Quebec, Montreal, Canada) of the 16S rRNA gene. Briefly, the samples were diluted 1:10 with water and the PCR mix was prepared with Taq DNA polymerase (Roche

FastStart High Fidelity PCR system 2500 U), 27F (5′-AGAGTTTGATCMTGGCTCAG-3′), and 1492R (3′-TACGGYTACCTTGTTACGACTT-5′) primers and run in the PCR cycler (Eppendorf Mastercycler® ProS) for 40 cycles. The amplified product was sequenced on Applied Biosystems™ 3730XL DNA Analyzer platform. The assembled sequences (in FASTA format) were queried for similarity using the BLAST tool to find reference prokaryotic type strains (https://blast.ncbi.nlm.nih.gov/). Based on the score and percent identity, the isolated strains were classified into specific genus and species and the assembled sequences were then submitted to GenBank, NCBI (https://submit.ncbi.nlm.nih.gov/subs/genbank/). A phylogenetic analysis was performed with EMBL-EBI webservices API tools: multiple sequence alignment was generated using the interface for Clustal Omega program (https://www.ebi.ac.uk/Tools/msa/clustalo/). The output was used to generate a phylogenetic tree with the Simple Phylogeny tool (https://www.ebi.ac.uk/Tools/phylogeny/simple_phylogeny/) using the ClustalW2 program. The phylogeny tree was constructed using iTOL (Interactive Tree of Life https://itol.embl.de/) interface (Letunic and Bork, 2019) with the Phylogenetic tree file.

3.3.4 Screening for salinity tolerance of the isolates

The isolates were tested for their tolerance capacity of salt stress at 100, 250, and 500 mM NaCl solution. The initial culture was adjusted to 0.01 OD and added to the growth media with added salt in a 96-well plate. The plate was incubated in Cytation5™ reader (BioTek Instruments Inc.,) at 25 °C and the growth curve was measured at A_{600nm} for up to 48 h. The isolates were also screened for PGP activities including biofilm formation, nitrogen fixation, phosphorous solubilization, production of 1-aminocyclopropane-1-carboxylate (ACC) deaminase, indole-3-acetic acid (IAA) and siderophores following standard protocols (Jensen et al., 1960; Schwyn and Neilands, 1987; Bric et al., 1991; Penrose and Glick, 2003; O'Toole, 2011; Goswami et al., 2014).

3.3.5 Screening of bacterial isolates for inducing salinity tolerance in soybean

3.3.5.1 Seed germination assay I

Soybean seeds (Absolute RR) were soaked in the bacterial cell suspension (at a rate of 100 µL per seed) or 10 mM $MgSO_4$ (control) for 30 min. The seeds were then placed on Petri dishes (10 seeds per plate) lined with P8 filter paper containing 5 mL of sterile water or 100 mM NaCl solution (EC = 9.8 ds m^{-1}). The plates were sealed with parafilm, incubated at 25 °C in the dark inside a growth chamber and germination was counted at 24, 36, and 48 h periods.

3.3.5.2 Greenhouse trial I

Seeds were bacterized with the inoculum at a rate of 500 µL per seed. Bacterized and control seeds (5 seeds per pot) were placed in 15.25 cm (diameter) pots filled with vermiculite (Perlite Canada Inc.) treated with 300 mL water or 100 mM NaCl solution (EC_e = 5 ds m^{-1}). The pots were placed in a greenhouse room maintained at 25 ± 2°C and 50% relative humidity (Supplementary Figure 3.3). Seedling emergence was counted on 7th and 8th DAP (days after planting) and the plants were thinned to one seedling per pot. The plants were irrigated with 50 mL water thrice a week and fertilized with 1212 strength Hoagland's solution once a week and sampled at 28th DAP. Plant growth variables including plant height, leaf area, shoot dry weight, and root dry weight were measured. Roots were scanned (EPSON Expression 11000XL) and analyzed using WinRHIZO™ (Regent Instruments Inc.) image analysis platform to measure root volume, length, and surface area.

3.3.5.3 Seed germination assay II

Based on the previous experiments, four bacterial isolates were selected and tested further for their ability to induce salt stress tolerance in soybean. A seed germination experiment as described above was conducted at different levels of salinity (0, 100, 125, 150, 175, and 200 mM NaCl solution) and at two cell densities (1×10^8 and 1×10^{10} cfu mL^{-1}).

3.3.5.4 Greenhouse trial II

A pot experiment with the different salinity levels and four bacterial isolates at 1×10^8 cfu mL^{-1} was set in a greenhouse to test the salinity tolerance threshold of soybean. A procedure similar to that described above was followed and the plants were sampled at 28th DAP. All experiments were repeated twice with six replications for each treatment.

3.3.6 Plant growth and development of soybean under salt stress

Two bacterial isolates were selected and co-inoculated with *Bradyrhizobium japonicum* 532C (all strains at 1×10^8 cfu mL^{-1}) on soybean seeds (seed bacterization). The seeds were then placed in 25.5 cm (diameter) pots filled with vermiculite and each pot received 1 L water or 150 mM NaCl solution (EC_e = 7.4 ds m^{-1}). The pots were placed in a greenhouse room maintained at 25 ± 2°C and 50% relative humidity. Irrigation was set at 50 mL (+25 mL, if light intensity during the day was >1,000 lux) per pot per day during the vegetative stage and increased to 100 mL (+25 mL) during flowering and pod-filling stages and then reduced to 75 mL (+25 mL) during the

harvest stage. The plants were given 1 g of water-soluble fertilizer in 1 L water (6-11-31, Hydroponic, Plant Prod, Canada) and 2 g of triple superphosphate per pot, at 2 weeks after seeding and then regularly at every growth stage after sampling the previous growth stage. The plants were sampled at mid-vegetative (~30 DAP), mid-flowering (~60 DAP), mid-pod-filling (~90 DAP) and harvest (~110 DAP) stages, and growth variables were measured (Supplementary Figures 3.4 and 3.5). The experiment was repeated twice with 12 replications for each treatment. Dried tissue samples were ground for elemental analysis, measured as mg g^{-1} dry weight of the plant tissue. N and P were measured on a flow injection analyzer (FIA) (Lachat QuickChem 8000, Hach® USA) and K, Ca and Na were measured after dilutions and appropriate modifier addition on an atomic absorption spectrophotometer (AAS) (Varian 220FS). Seed composition was analyzed at SGS Agrifood laboratories, SGS Canada Inc., Guelph, Canada. Nodules were collected from soybean plants after harvest; bacteria were grown on YEM agar plates similar to the isolation procedure described above and colonies were observed after 48 h of incubation.

3.3.7 Statistical analysis

Data were analyzed using a generalized linear mixed model that was performed using the GLIMMIX procedure in SAS (v 9.4, SAS Inc., Cary, NC). The SAS PROC GLIMMIX models were "mixed" due to the inclusion of fixed (treatment, salinity, and treatment × salinity) and random (RANDOM Rep) effects. The normal distribution was not assumed for the response (i.e., the observed variables) and therefore the models were "generalized." Distributions were specified using the "DIST =" option in the MODEL statement and selected from the exponential family of distributions based on model fit statistics, that is, the Bayesian Information Criterion (BIC) that is part of the PROC GLIMMIX output (IC = Q was specified in the PROC GLIMMIX statement). Variance homogeneity was not assumed, and the structure of variance heterogeneity was specified using a "RANDOM _RESIDUAL_/GROUP =" statement and selected based on the BIC. Multiple comparisons were adjusted according to Scheffe's method (i.e., the ADJUST = SCHEFFE option in the LSMEANS statement). Effect slice tables were produced using SLICE and SLICEDIFF in the LSMEANS statement. The data for soybean growth and yield were broken into subsets based on the observed stages of plant development, and data from the respective subsets were analyzed separately using PROC GLIMMIX.

3.4 Results

3.4.1 Nodule bacteria of *Amphicarpaea bracteata*

Bacterial colonies from *A. bracteata* nodules were obtained from 10^{-3}, 10^{-4}, and 10^{-5} dilutions. Since *Bradyrhizobium* takes nearly a week to grow on YEM plates, colonies that grew on the agar were selected after 24 to 96 h incubations. These non-*Bradyrhizobium* colonies of endophytic bacteria were re-isolated and 15 such pure cultures were grown and maintained on Kings B and YEM. One of the strains, SL45, was difficult to culture further and not used in downstream experiments. Of these putative PGPR isolates, there were at least 10 morphologically distinct colonies and they were arbitrarily labeled for identification purposes.

The bacteria identified using partial sequencing of the 16S rRNA gene showed the presence of diverse genera thriving in the nodules of *A. bracteata* (Supplementary Table 3.2) that could be isolated successfully. Five strains were belonging to *Pseudomonas*, two belonging to each of the genera *Hydrogenophaga* and *Variovorax*. The isolates SL36 and SL53 could not be identified using Sanger sequencing because of poor quality PCR product. One *Rhizobium* species was isolated, which is presumed to be one of the associated symbionts of *A. bracteata* for biological nitrogen fixation. A neighbor-joining phylogenetic tree file was constructed using the 16S rRNA gene sequences (Figure 3.1). The phylogenetic tree revealed that *Hydrogenophaga* and *Variovorax* genera are in the same cluster whereas the *Bacillus subtilis, Gemmobacter sp., Flavobacterium sp., Rhizobium sp*., and *Devosia sp*., are in the subsequent nodes of divergence, distant from one another.

The isolates differed from each other in their growth patterns when grown under salt conditions (Supplementary Figure 3.6). There was a gradual decrease in growth of strain SL31 with increasing salt concentrations, but it still reached ~1 OD in 500 mM NaCl at 48 h, which is the highest level of growth among all the isolates. Steady growth was observed in strain SL42 up to 250 mM NaCl, but growth was almost negligible at 500 mM NaCl. The salt concentration of 100 mM NaCl increased the growth of strains SL47 and SL48 when compared to 0 mM NaCl, but growth decreased at higher salt concentrations. Growth declined for strain SL52 but progressed for strain SL53 with increasing salt concentrations. Growth was either reduced or inhibited under salt for the other isolates and markedly lower than the isolates mentioned above. Many of the isolates exhibited PGPR characteristics of ACC deaminase and IAA production (Table 3.1 and Supplementary Figure 3.7). *Rhizobium sp.* SL42 and *Hydrogenophaga sp.* SL48 showed a strong

affinity for nitrogen fixation, ACC deaminase activity and biofilm formation. Moreover, *Hydrogenophaga sp.* SL48 also exhibited profuse IAA synthesis from L-tryptophan.

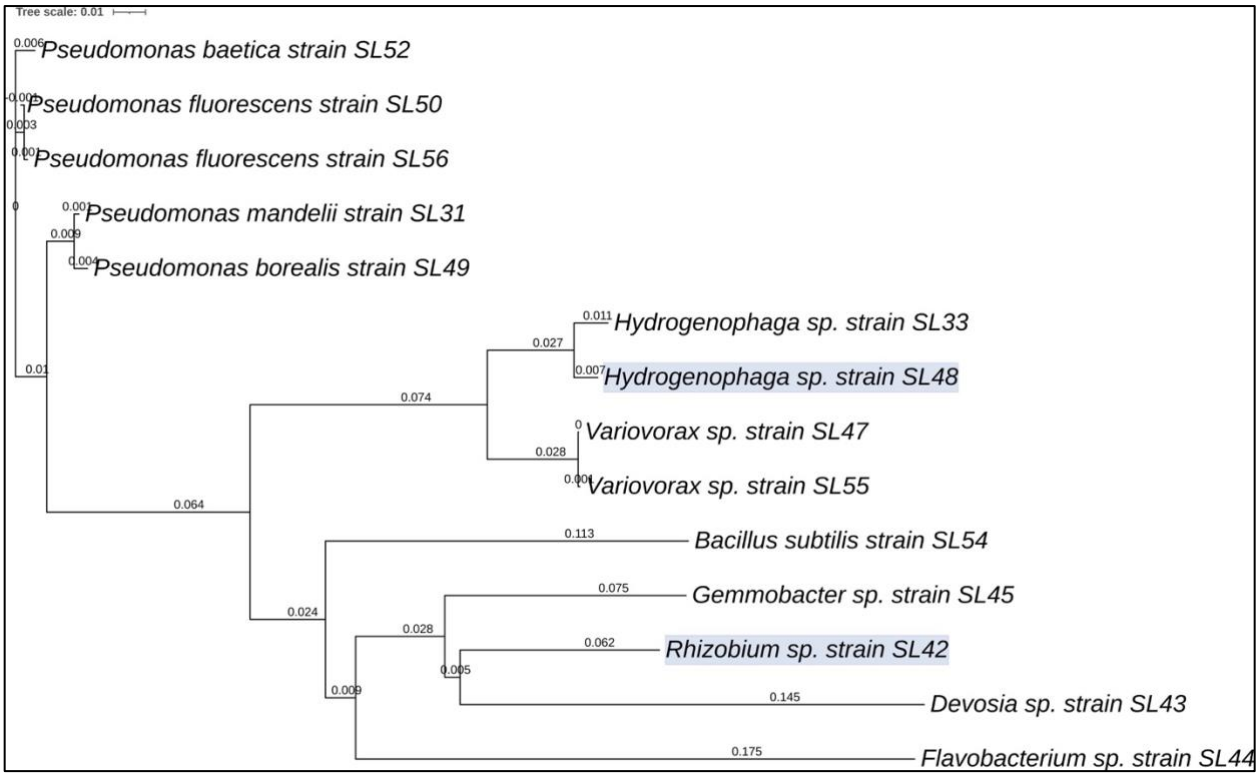

Figure 3.1. Phylogenetic relationships between 14 bacterial strains isolated from the nodules of *A. bracteata* based on the 16S rRNA gene sequences.
Phylogram was generated using iTOL based on the tree file from CLUSTALW2. Values on the lines indicate branch length from the node (tree: Newick/PHYLIP; kimura—false; tossgaps—off; Clustering—Neighbor joining; percent identity matrix—false).

Table 3.1. PGPR characteristics of the isolated strains characterized using biochemical assays.

	Strain	N – fixation	P– solubilization	IAA	ACC deaminase	Biofilm
1.	SL31	-	-	-	++	-
2.	SL33	-	-	+	-	++
3.	SL36	++	-	-	++	+++
4.	SL42	+++	-	+	++	++++
5.	SL43	-	-	-	-	-
6.	SL44	-	-	-	-	-
7.	SL47	-	-	+++	+++	++++
8.	SL48	+++	-	++++	++	+++
9.	SL49	-	-	+++	++	-
10.	SL50	-	-	++	+++	-
11.	SL52	-	-	+	+++	-
12.	SL53	+++		+	++	++
13.	SL54	+++	-	-	++	+
14.	SL55	-	-	++	+++	-
15.	SL56	-	-	++	+++	-

Qualitative assessment: - indicates absence of the trait, + indicates presence of the trait, and additional + indicates the intensity of the trait exhibited by the isolates

3.4.2 Isolated bacteria induce salinity tolerance in soybean

Seed germination was counted when radicle emergence was observed (Supplementary Figure 3.8). There were significant differences between optimal and salt stress conditions at various time points and also among treatments ($P = 0.002$). Under optimal conditions, inoculation with strains SL43, SL47, SL48, and SL49 had significantly increased ($P = 0.0001$) germination rates at 36 and 48 h (~80 %) compared to the control treatment (60%). Under 100 mM NaCl, the germination rate was negligible at 24 h with 0% for control treatment and <5% for the isolates. Germination rate at 36 h was higher ($P = 0.004$) for the treatments SL42, SL47, SL48, SL49, and SL53 (~40%) than the control (30%). There was a greater increase ($P = 0.0031$) in germination rate at 48 h for treatments SL42 and SL48 (65%) than the control (40%) (Figure 3.2) and treatments with other isolates SL36, SL43, SL47, SL49, SL52, SL53, and SL55 were also higher (50–55%) (Supplementary Figure 3.9).

Seedling emergence under optimal conditions was not significantly higher for treatments when compared to the control (Supplementary Figure 3.10). However, under salt stress of 100 mM NaCl emergence rate was significantly increased ($P = 0.0002$) for all but SL31 of the bacterial treatments at 8th DAP. Growth variables of soybean plants were measured at 28th DAP (Supplementary Figure 3.11). Significant increases ($P < 0.0001$) were observed in plant height for treatments SL42, SL43, SL47, SL48, and SL49 compared to the control under optimal conditions. Treatments with SL47 and SL48 showed significant increases ($P < 0.0001$) under salt stress and slight increases in plant height were also observed for treatments SL42 and SL49. Leaf area was significantly higher ($P < 0.0001$) for treatments with SL42, SL47, SL48, and SL49 than the control under both optimal and salt stress conditions. A parallel outcome was observed in shoot biomass, with treatments SL42, SL43, SL47, SL49, and SL50 showing significant increases ($P < 0.0001$) under optimal conditions and treatments SL42, SL44, SL47, SL48, SL49, and SL55 showing significant increases ($P < 0.0001$) under salt stress. Root dry weight was significantly higher for treatments SL36 and SL43 under optimal conditions ($P < 0.0001$) and for the treatments SL33, SL36, SL43, SL50, SL55, and SL56 under salt stress ($P = 0.0004$). However, root volume was significantly increased ($P = 0.0003$) for treatments SL31, SL33, SL36, SL42, SL48, SL49, SL50, SL55, and SL56 compared to the control treatment under salt stress. Results of the most beneficial strains, SL42 and SL48 are shown in Figure 3.3. Yet only treatments SL42 and SL50 showed significant increases ($P = 0.04$) in root length, and SL31 and SL42 showed significant increases ($P = 0.01$) in root surface area under salt stress (Supplementary Figure 3.12).

3.4.3 Soybean growth under different salt concentrations

Based on the results of the first screening, four isolates, *Rhizobium sp*. SL42, *Hydrogenophaga sp*. SL48, *Pseudomonas borealis* SL49, and *Variovorax sp*. SL55 were selected for the next trial. Seed germination of soybean was differentially affected under a range of salt concentrations (Figure 3.4). All bacterial treatments resulted in increases over the control treatment. The germination rate was 65% for SL42, 80% for SL48, 60% for SL49, and 70% for SL55 at 0 mM NaCl after 72 h compared to the 45% germination rate in control treatment. At 100 and 125 mM NaCl, the germination rate was around 60% for the bacterial treatments and 42% for the control treatment. The germination rate at 1×10^8 cfu mL^{-1} was 58% for SL42, 55% for SL48, 60% for SL49, and 43% for SL55 at 150 mM, while the control reached about 40%. The germination rate was considerably lower at higher salt concentrations of 175 and 200 mM NaCl.

For SL55, no significant increase in germination rate was observed except at 175 mM NaCl (Supplementary Figures 3.13 and 3.14). The germination rates for the two inoculums, 1×10^8 and 1×10^{10} cfu mL^{-1} were mostly parallel to each other but slight variations were present in a few cases and 1×10^8 cfu mL^{-1} was selected as the inoculum density for successive experiments.

Seedling emergence rate at 8th DAP was significantly higher for the treatment SL42 at all the salt concentrations from 100 (*P = 0.0326*) to 200 mM (*P = 0.0153*) NaCl than the control treatment. It was also increased by treatments SL48, SL49, and SL55 at different salt levels but the statistical significance varied. Growth variables of soybean treated with the four isolates, grown under a range of salt concentrations were measured at 28th DAP (Supplementary Figure 3.15) and plant growth was greatly reduced at 175 and 200 mM NaCl. Leaf area was significantly increased by the treatments with SL48 at 0, 125, and 150 mM NaCl (*P = 0.01*) and SL42 at 100 (*P = 0.022*) and 125 mM NaCl compared to control treatments. This corresponded to the increase in shoot biomass, which was significantly higher than the control for treatments SL42 at 125, 150 (*P = 0.0016*), 175, and 200 mM NaCl and SL48 at 150 (*P < 0.0001*) and 175 mM NaCl. Shoot dry weight was improved by SL48 and SL42 at other NaCl concentrations as well, albeit not significantly. Treatment with SL49 has significantly increased shoot biomass at 150 (*P = 0.02*) and 175 mM NaCl. Root dry weight was significantly higher at 0 mM NaCl for the treatments SL48 (*P = 0.001*) and SL49 and at 150 mM for the treatments SL42 (*P = 0.0015*), SL48 (*P = 0.0011*), and SL55 (*P = 0.002*). The root dry weight was also increased by the bacterial treatments at higher salt concentrations (175 and 200 mM NaCl). The results indicated that the strains SL42 and SL48 have greatly improved soybean growth under a range of salt stress conditions (Figure 3.5). Though salt stress of 100-150 mM NaCl had significant differences between the control and bacterial treatments, 150 mM NaCl provided a much clearer distinction related to salinity stress in the shoot (*P = 0.0004)* and root biomass (*P = 0.0036)*.

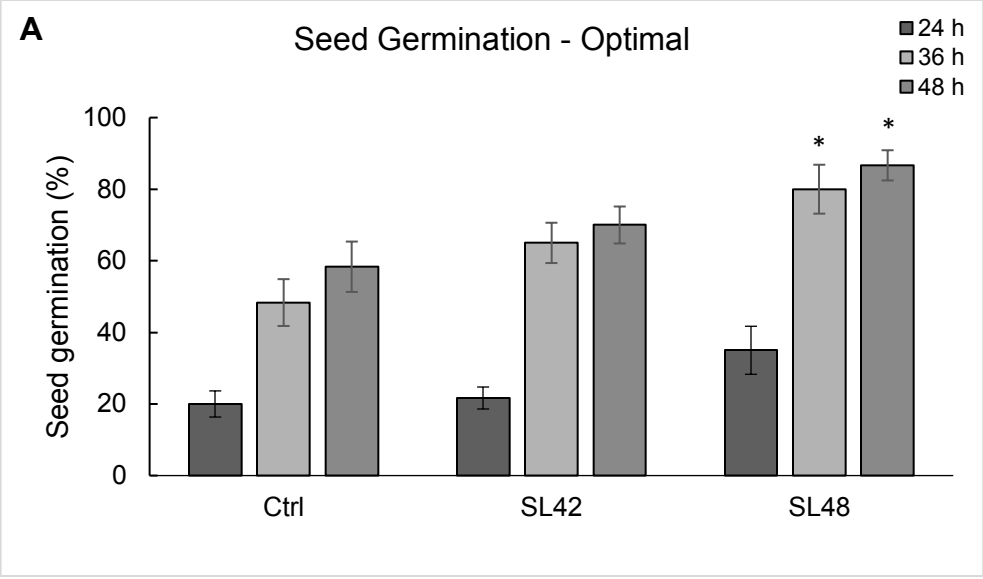

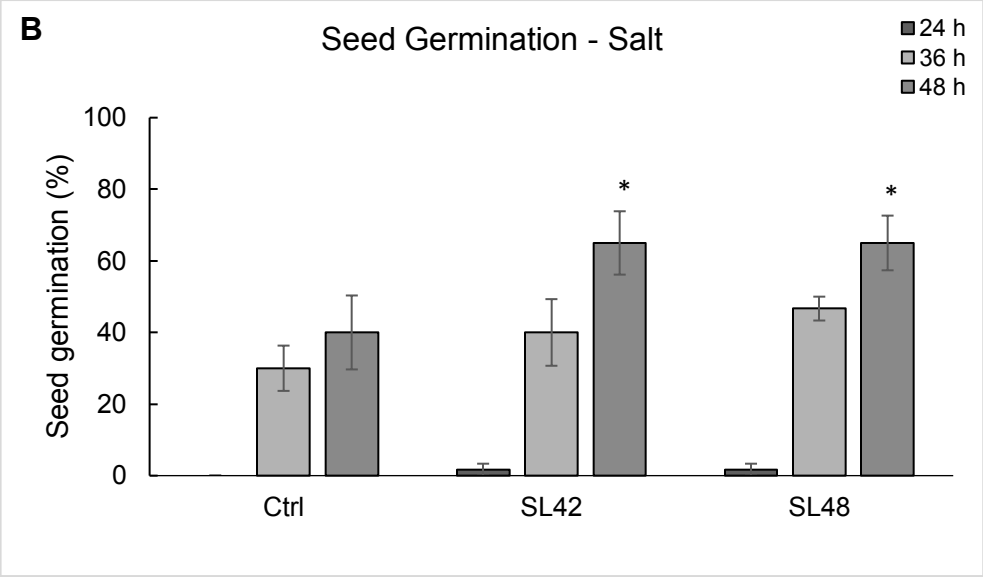

Figure 3.2. Seed germination rate of soybean at 24, 36, and 48 h under **(A)** optimal (water) and **(B)** salt (100 mM NaCl) conditions.
The seeds were treated with 10 mM $MgSO_4$ as control or bacterized with strains SL42 and SL48. Values represent mean ± SE (n = 6[10]). Significant differences (increase) between the bacterial treatments and the respective control treatments (optimal or salt) are indicated by asterisk above the data points, *$p \leq 0.05$ ($\alpha = 0.05$).

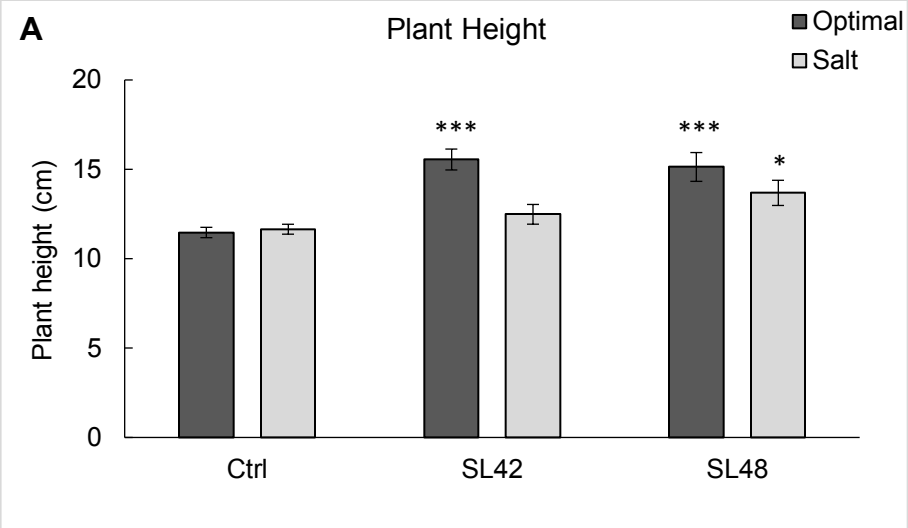
A
Plant Height
Optimal
Salt
Plant height (cm)
20
15
10
5
0
***
***
*
Ctrl
SL42
SL48

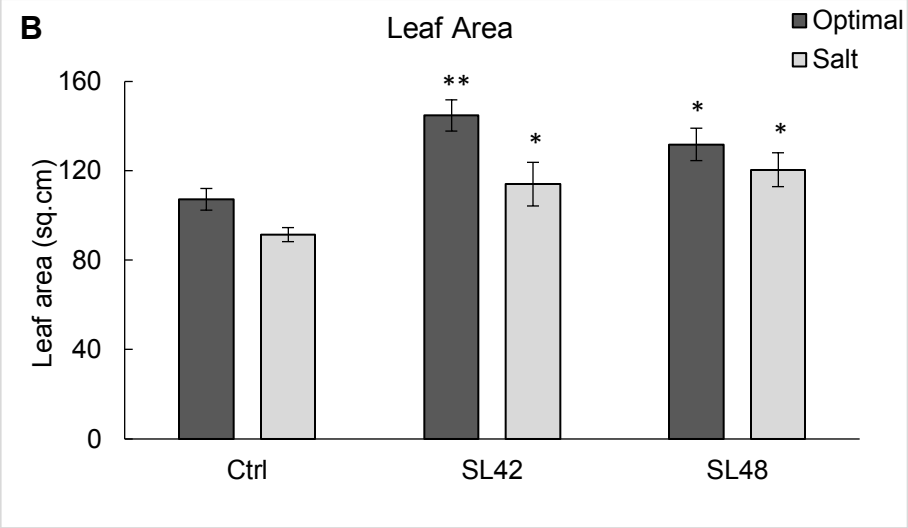
B
Leaf Area
Optimal
Salt
Leaf area (sq.cm)
160
120
80
40
0
**
*
*
*
Ctrl
SL42
SL48

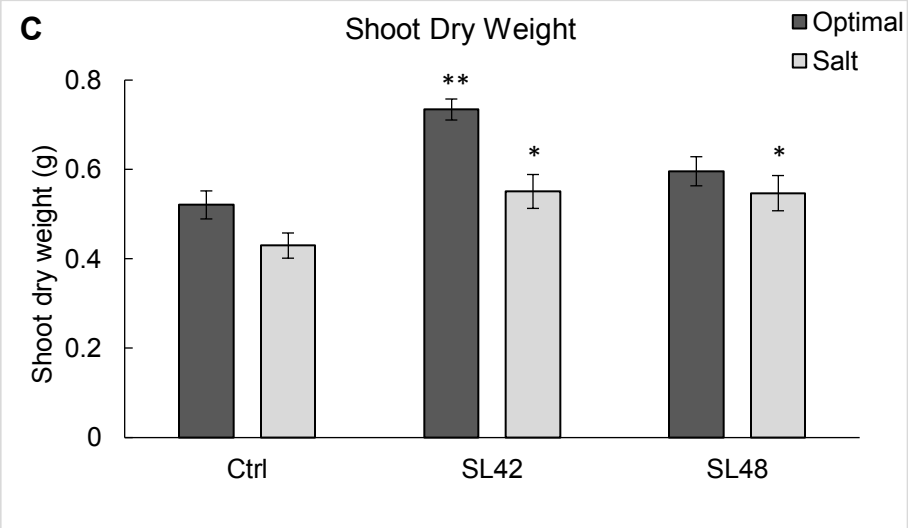
C
Shoot Dry Weight
Optimal
Salt
Shoot dry weight (g)
0.8
0.6
0.4
0.2
0
**
*
*
Ctrl
SL42
SL48

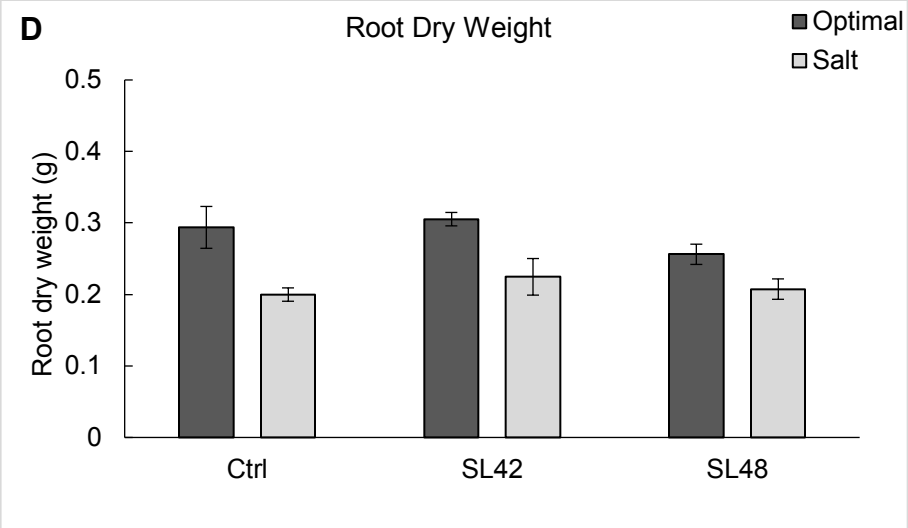
D
Root Dry Weight
Optimal
Salt
Root dry weight (g)
0.5
0.4
0.3
0.2
0.1
0
Ctrl
SL42
SL48

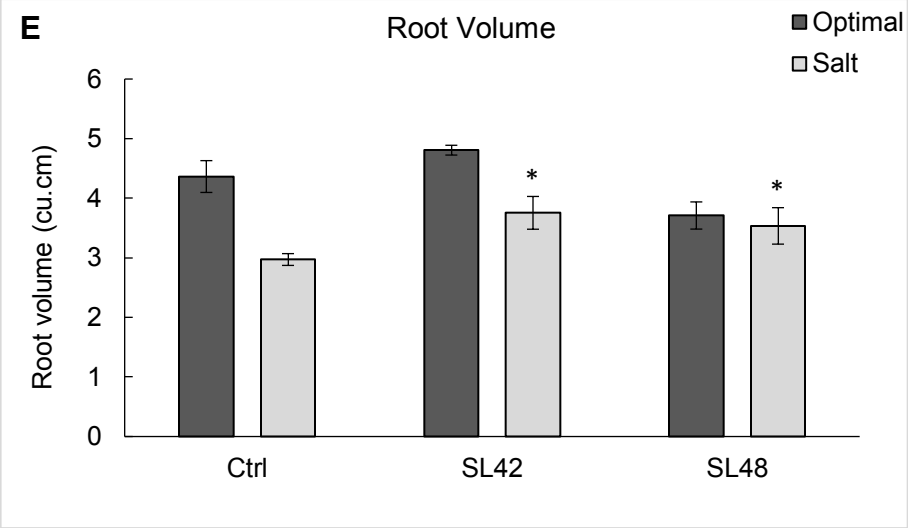
E
Root Volume
Optimal
Salt
Root volume (cu.cm)
6
5
4
3
2
1
0
*
*
Ctrl
SL42
SL48

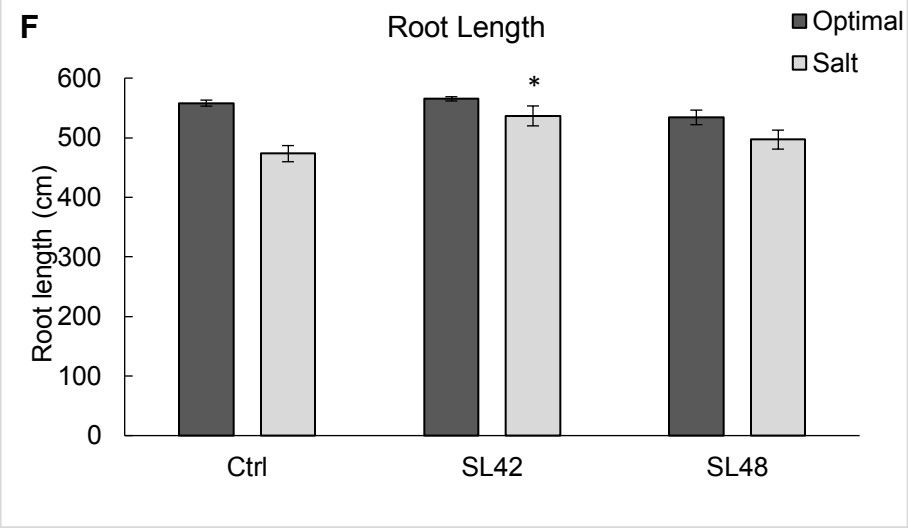
F
Root Length
Optimal
Salt
Root length (cm)
600
500
400
300
200
100
0
*
Ctrl
SL42
SL48

Figure 3.3. Growth variables of soybean, **(A)** Plant height, **(B)** Leaf area index, **(C)** Shoot dry weight, **(D)** Root dry weight, **(E)** Root volume, and **(F)** Root length measured at 28th DAP under optimal (water) and salt (100 mM NaCl) conditions.
The seeds were treated with 10 mM $MgSO_4$ as control or bacterized with strains SL42 and SL48. Values represent mean ± SE (n = 6). Significant differences (increase) between the bacterial treatments and the respective control treatments (optimal or salt) are indicated by asterisk above the data points, *$p \leq 0.05$, **$p \leq 0.001$, ***$p \leq 0.0001$ ($\alpha = 0.05$).

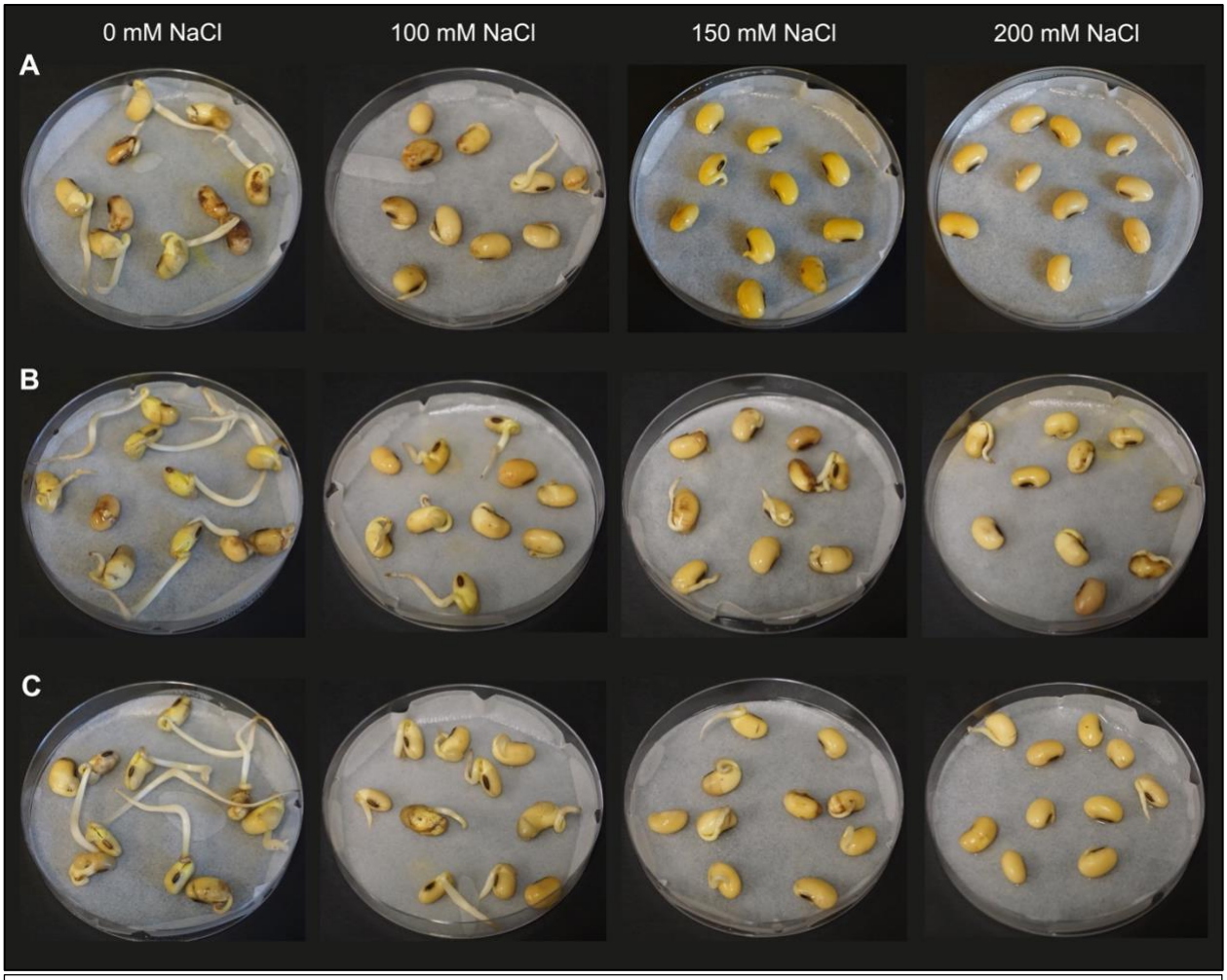

Figure 3.4. Seed germination of soybean at 72 h under increasing salt concentrations (0, 100, 150, and 200 mM NaCl). The seeds were treated with **(A)** 10 mM MgSO4 as control or bacterized with strains **(B)** SL42 and **(C)** SL48.

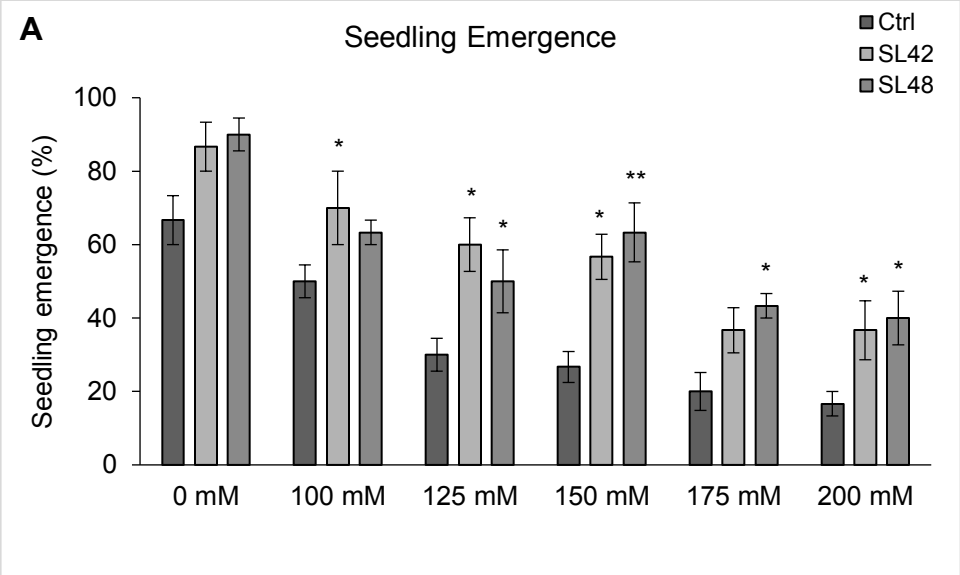
A
Seedling Emergence
Ctrl
SL42
SL48
Seedling emergence (%)
100
80
60
40
20
0
0 mM
100 mM
125 mM
150 mM
175 mM
200 mM

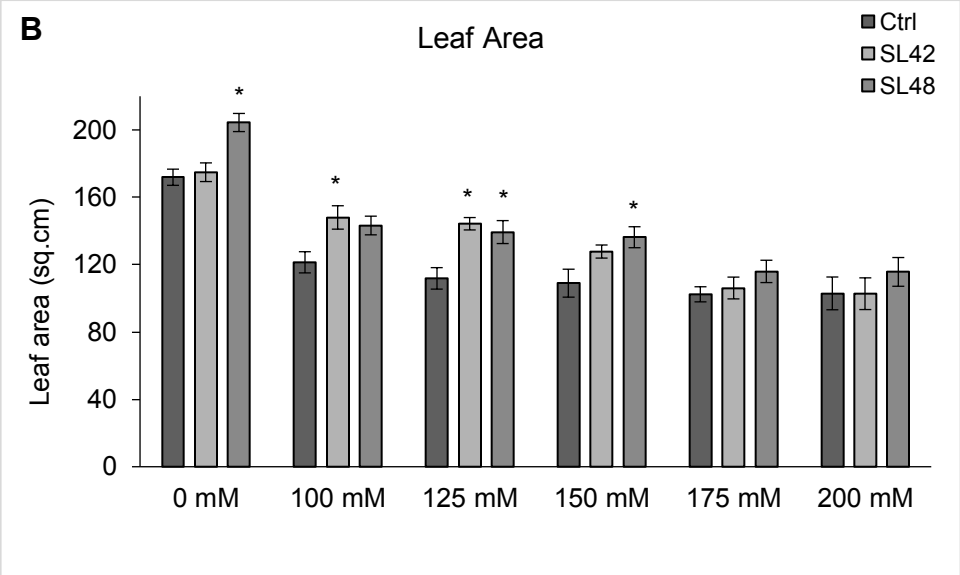
B
Leaf Area
Ctrl
SL42
SL48
Leaf area (sq.cm)
200
160
120
80
40
0
0 mM
100 mM
125 mM
150 mM
175 mM
200 mM

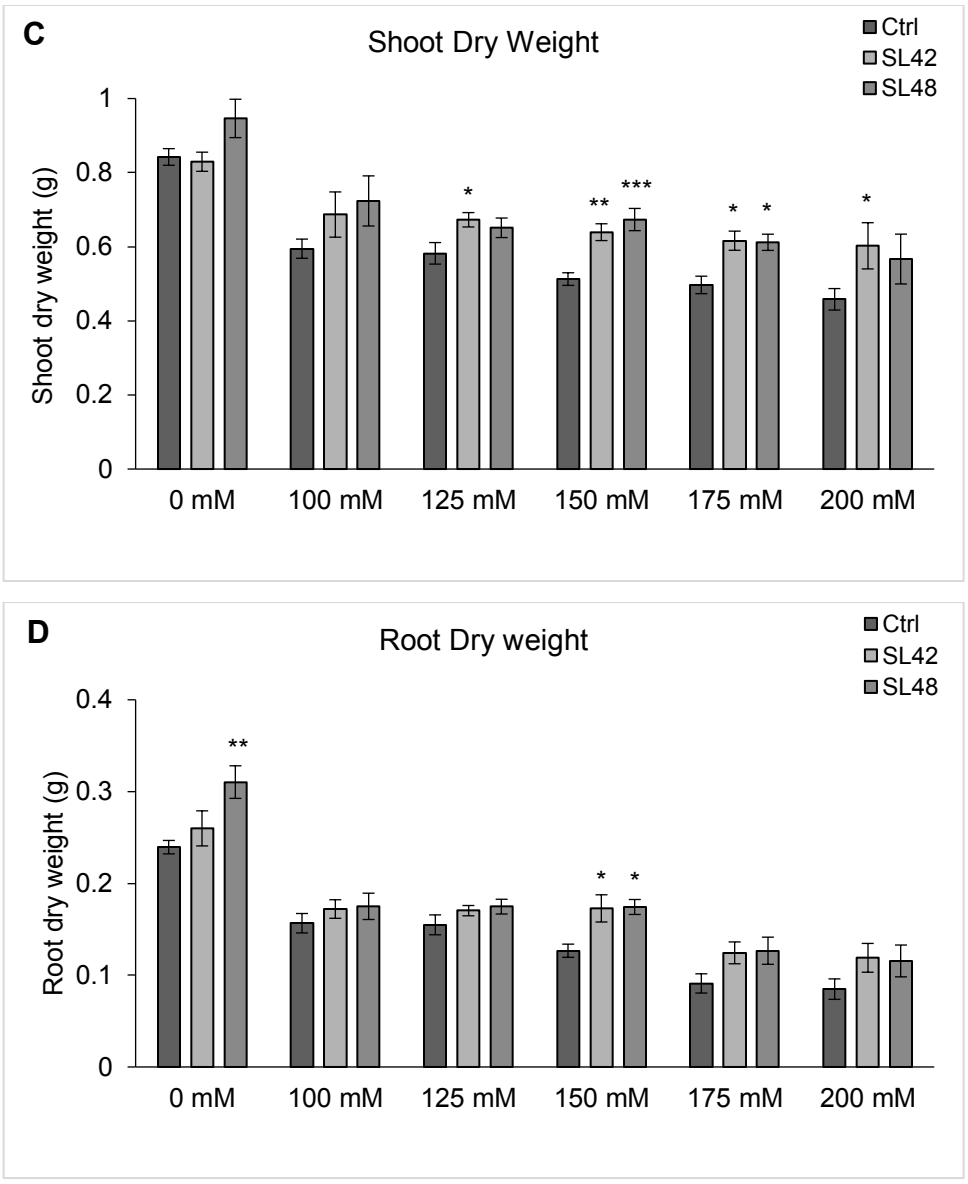

Figure 3.5. Growth variables of soybean, **(A)** Seedling emergence rate measured on 8th DAP and growth variables of soybean **(B)** Leaf area, **(C)** Shoot dry weight, and **(D)** Root dry weight measured at 28th DAP under increasing salt concentrations (0, 100, 125, 150, 175, and 200 mM NaCl).

The seeds were treated with 10 mM $MgSO_4$ as control or bacterized with strains SL42 and SL48. Values represent mean ± SE (n = 6). Significant differences (increase) between the bacterial treatments and the respective control treatments of a particular salt concentration are indicated by asterisk above the data points, *$p \leq 0.05$, **$p \leq 0.001$, ***$p \leq 0.0001$ ($\alpha = 0.05$).

3.4.4 Co-inoculation of nodule isolates improves the growth and development of soybean

Two of the bacterial isolates, *Rhizobium sp*. SL42 and *Hydrogenophaga sp*. SL48 were co-inoculated with *Bradyrhizobium japonicum* 532C and the soybean plants were grown under optimal or 150 mM NaCl conditions. Inoculation with *B. japonicum* alone served as the control as it is the standard N_2-fixing symbiont of soybean. Even though growth variables under optimal conditions were insignificantly different for plants inoculated with *B. japonicum* because of the uninhibited nitrogen fixation, co-inoculation with SL42 and SL48 enhanced plant growth in most cases. However, under salt stress, there were substantial differences between the co-inoculation treatments and the *B. japonicum* control and the co-inoculation treatments resulted in higher growth than the control in all respects.

During the vegetative and flowering stages, the growth variables were all significantly different ($P < 0.0001$) between the optimal and salt stress conditions. At the vegetative stage, plant height ($P = 0.0001$), shoot biomass ($P = 0.2764$), and root dry weight ($P = 0.0935$) were increased by the *B. japonicum*+SL42 treatment compared to the control, *B. japonicum* (*Bj*) under salt stress. Shoot biomass was also increased by the *B. japonicum*+SL42+SL48 treatment under both optimal and salt stress conditions. During the flowering stage, plant height ($P = 0.1934$), leaf area ($P = 0.1562$) (Figure 3.7), shoot biomass ($P = 0.0872$), and root dry weight ($P = 0.1766$) were all higher for the *B. japonicum*+SL42+SL48 treatment, and also for the other co-inoculation treatments than the *B. japonicum* control under salt stress. The treatment of *B. japonicum*+SL42+SL48 was also the highest under optimal conditions (except for plant height), although the difference was more notable under salt stress. At the pod-filling stage, shoot biomass was increased by the treatments of *B. japonicum*+SL42 ($P = 0.1001$) and *B. japonicum*+SL42+ SL48 ($P = 0.3866$), as was the case with other growth variables, compared to the *B. japonicum* control under salt stress. The treatment of *B. japonicum*+SL42 also improved plant growth under optimal conditions (except for leaf area index). Plant height (Figure 3.6) and leaf area (Figure 3.7) of soybean increased exponentially up to the pod-filling stage and vegetative growth was stationary as the plants reached maturity. During the harvest stage, the shoot biomass was considerably reduced due to the senescence of leaves and not much of a difference among the treatments were observed. Overall, the co-inoculation treatments have resulted in increased shoot dry weight by 1.6 and 18.3% at vegetative, 11.9 and 27% at flowering, 7.1 and 7.5% at pod-filling, 7.5 and 4.6% at harvest under optimal and salt stress conditions, respectively (Figure 3.8). The

root dry weight under salt stress was particularly increased by the treatment of *B. japonicum*+SL42, by 28% at vegetative, 16% at flowering, 9% at pod-filling, and 24.5% at harvest stages (Figure 3.9).

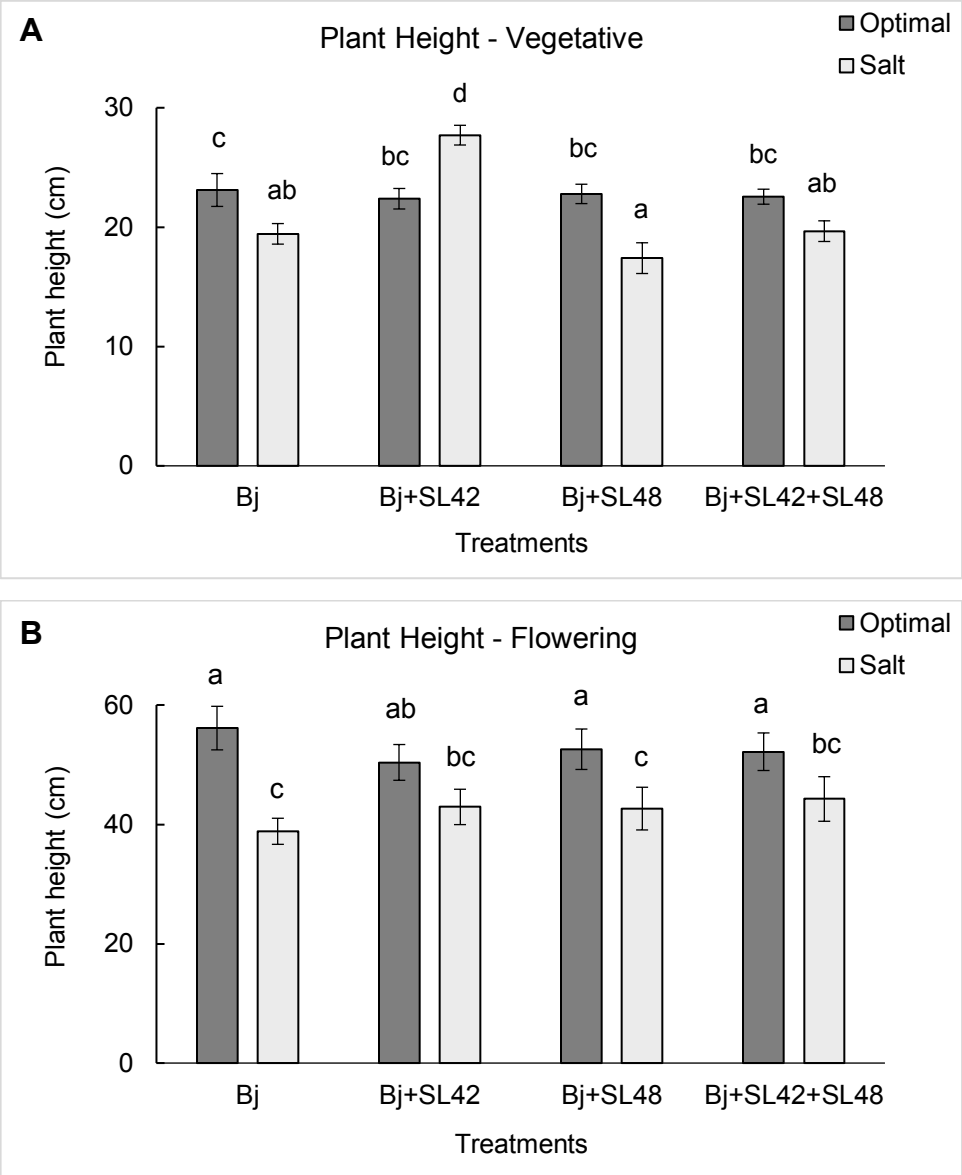

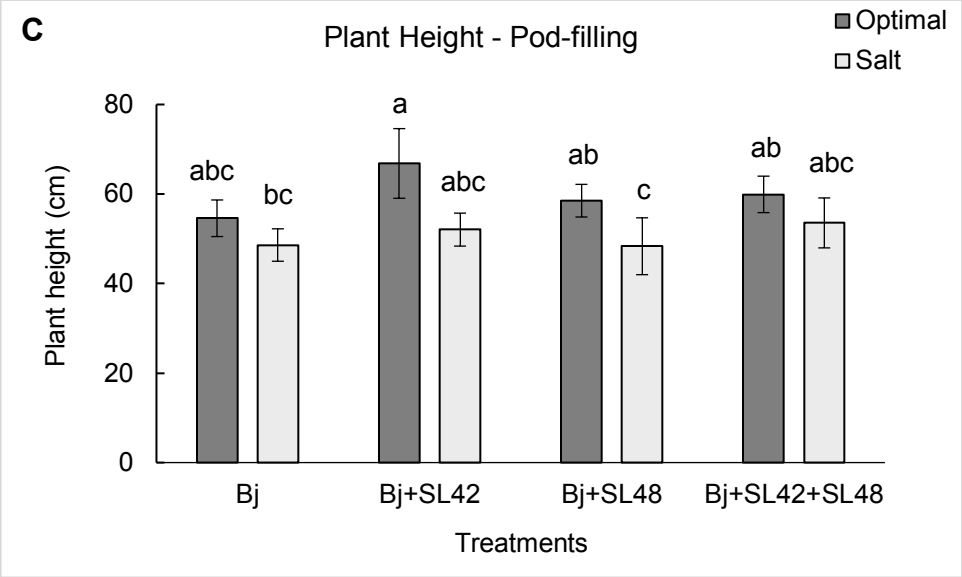

Figure 3.6. Height of soybean plants measured at **(A)** mid-vegetative, **(B)** mid-flowering, and **(C)** mid-pod-filling stages under optimal (water) and salt (150 mM NaCl) conditions. The seeds were bacterized with *Bradyrhizobium japonicum* (Bj), Bj+SL42, Bj+SL48 and Bj+SL42+SL48. Values represent mean ± SE (n=12). Scheffe grouping for least square means was used for multiple means comparison and means with the same letter(s) are not significantly different ($\alpha = 0.05$).

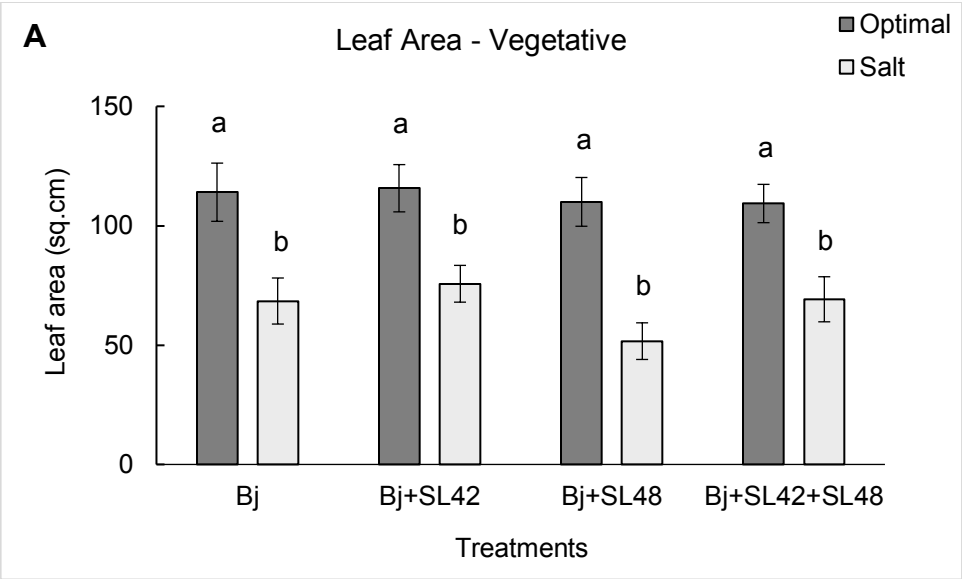

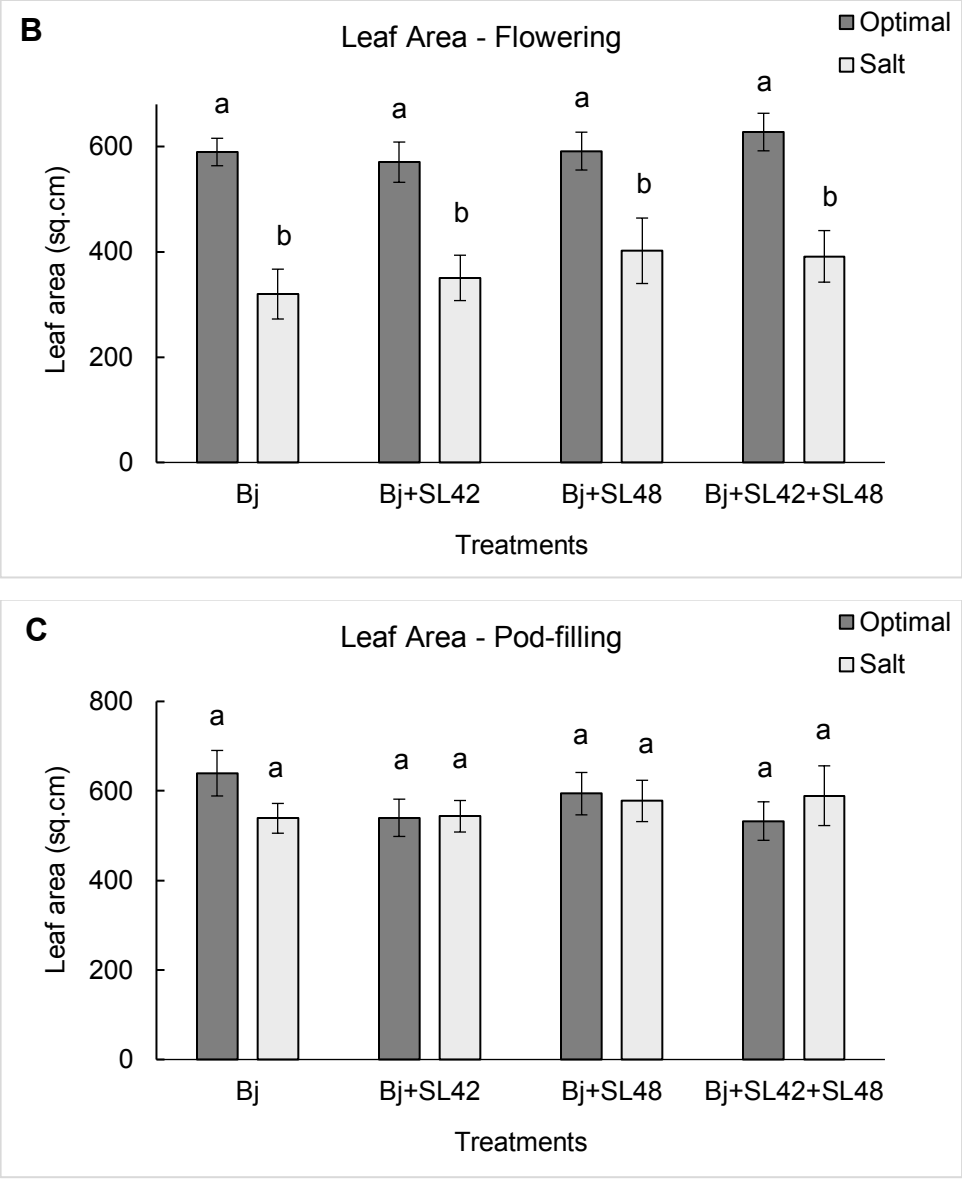

Figure 3.7. Leaf area of soybean plants measured at **(A)** mid-vegetative, **(B)** mid-flowering, and **(C)** mid-pod-filling stages under optimal (water) and salt (150 mM NaCl) conditions. The seeds were bacterized with *Bradyrhizobium japonicum* (Bj), Bj+SL42, Bj+SL48 and Bj+SL42+SL48. Values represent mean ± SE (n = 12). Scheffe grouping for least square means was used for multiple means comparison and means with the same letter(s) are not significantly different ($\alpha = 0.05$).

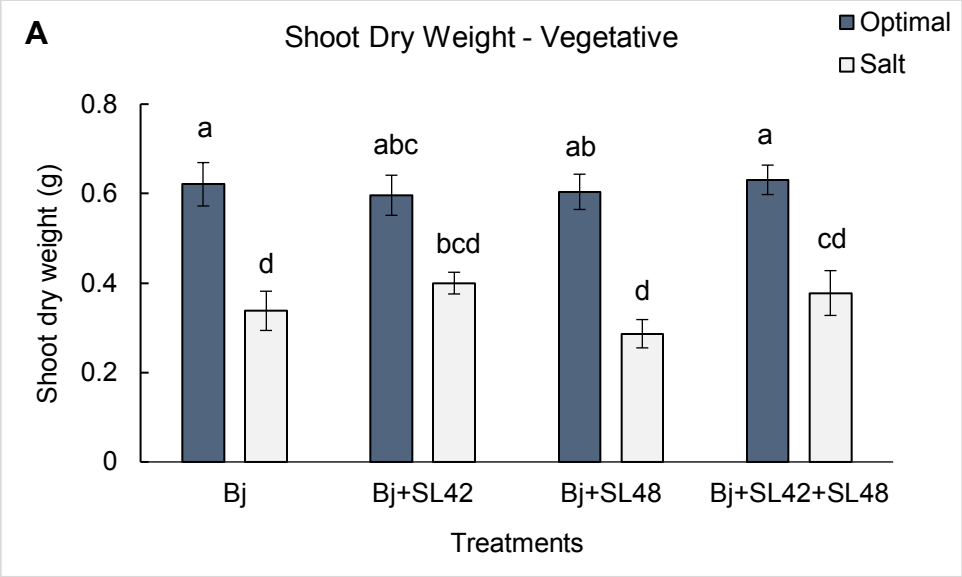
A
Shoot Dry Weight - Vegetative
Optimal
Salt
Shoot dry weight (g)
0.8
0.6
0.4
0.2
0
a
d
abc
bcd
ab
d
a
cd
Bj
Bj+SL42
Bj+SL48
Bj+SL42+SL48
Treatments

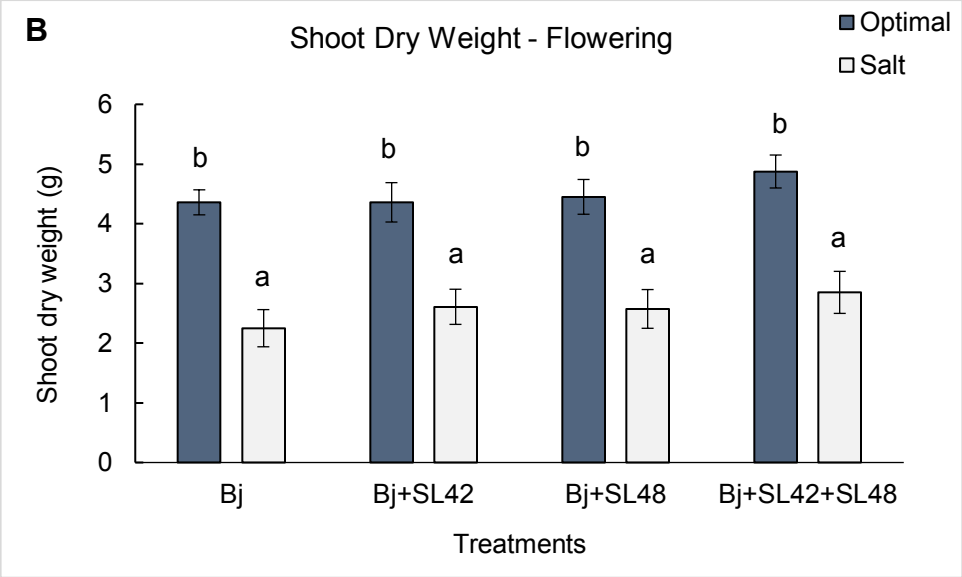
B
Shoot Dry Weight - Flowering
Optimal
Salt
Shoot dry weight (g)
6
5
4
3
2
1
0
b
a
b
a
b
a
b
a
Bj
Bj+SL42
Bj+SL48
Bj+SL42+SL48
Treatments

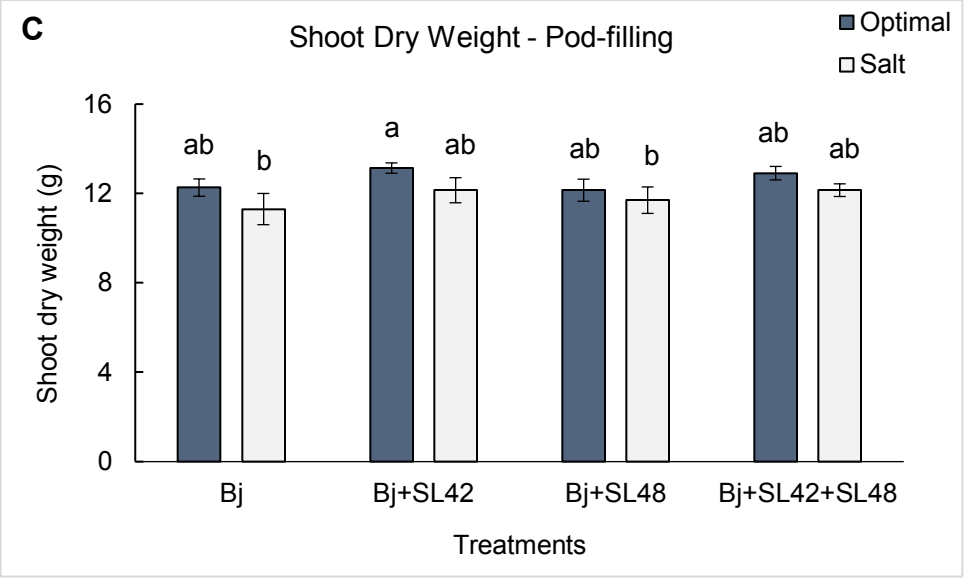

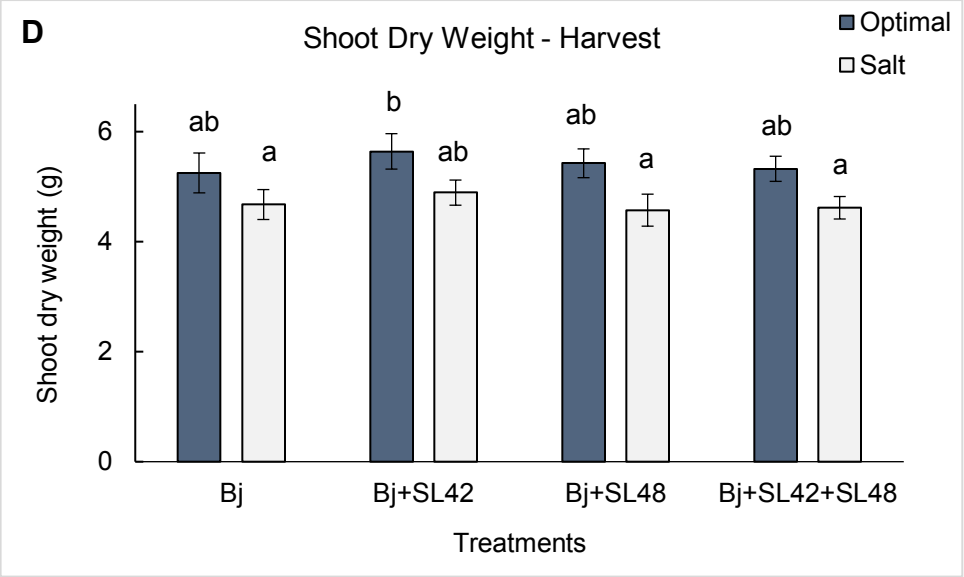

Figure 3.8. Shoot biomass of soybean plants measured at **(A)** mid-vegetative, **(B)** mid-flowering, **(C)** mid-pod-filling, and **(D)** harvest stages under optimal (water) and salt (150 mM NaCl) conditions.
The seeds were bacterized with *Bradyrhizobium japonicum* (Bj), Bj+SL42, Bj+SL48, and Bj+SL42+SL48. Values represent mean ± SE (n = 12). Scheffe grouping for least square means was used for multiple means comparison and means with the same letter(s) are not significantly different ($\alpha = 0.05$).

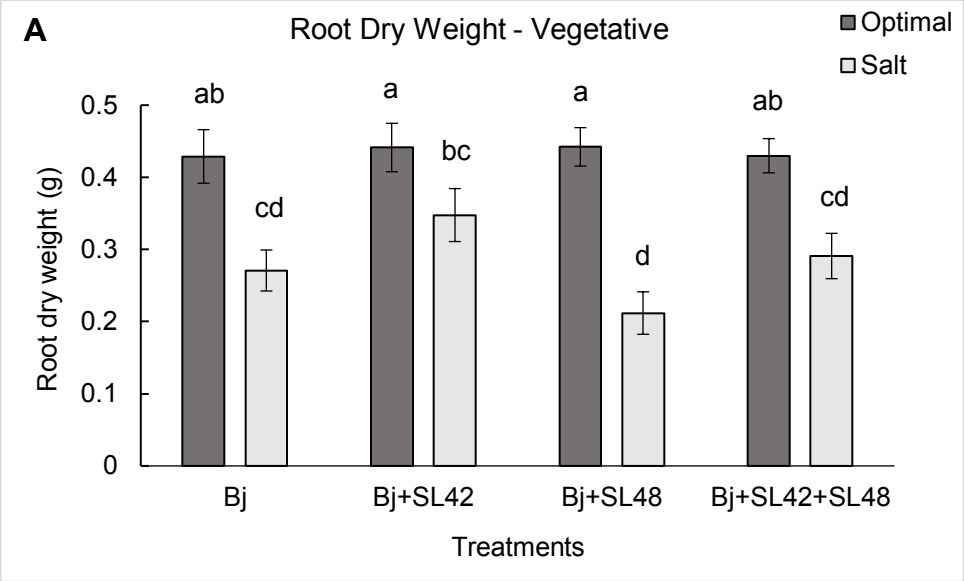
A
Root Dry Weight - Vegetative
Optimal
Salt
Root dry weight (g)
0.5
0.4
0.3
0.2
0.1
0
ab
cd
a
bc
a
d
ab
cd
Bj
Bj+SL42
Bj+SL48
Bj+SL42+SL48
Treatments

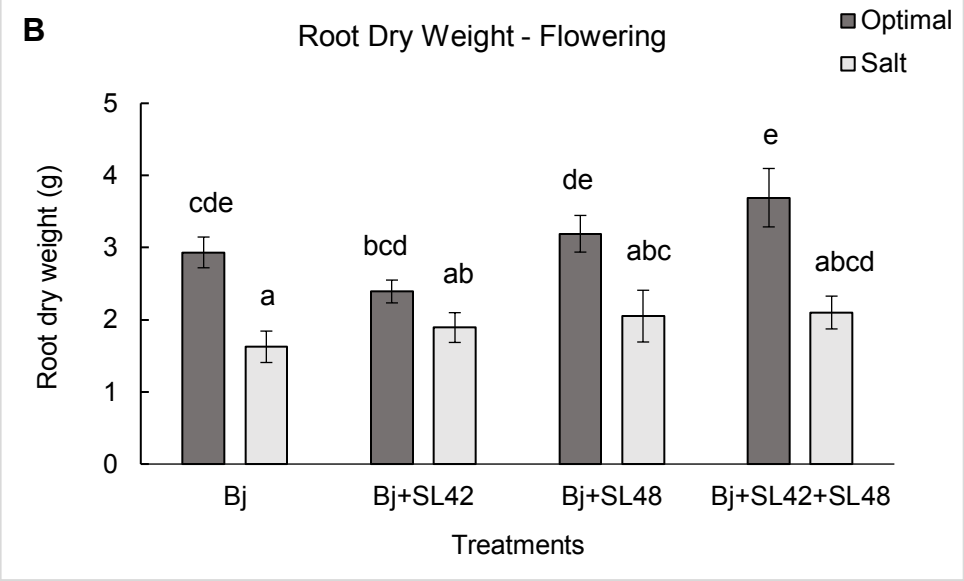
B
Root Dry Weight - Flowering
Optimal
Salt
Root dry weight (g)
5
4
3
2
1
0
cde
a
bcd
ab
de
abc
e
abcd
Bj
Bj+SL42
Bj+SL48
Bj+SL42+SL48
Treatments

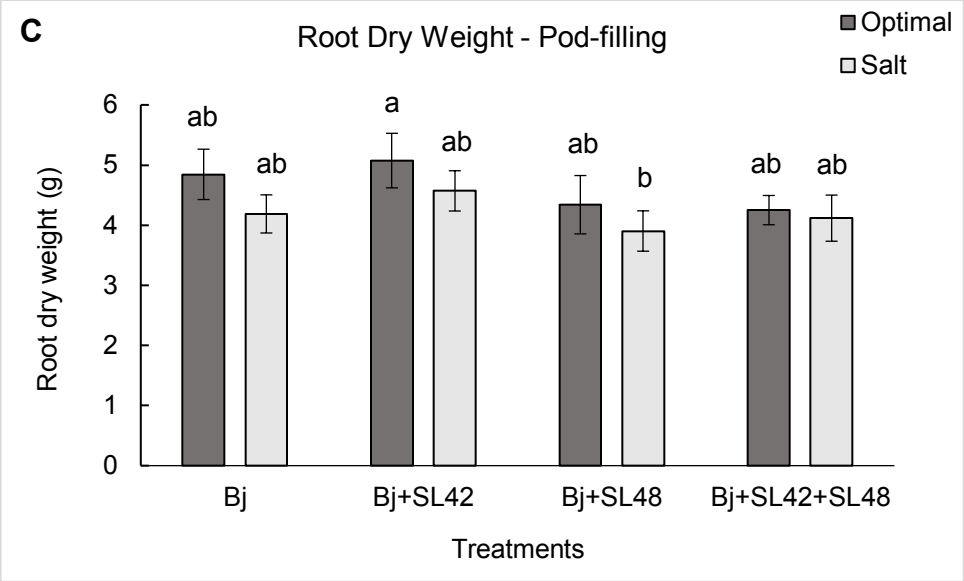

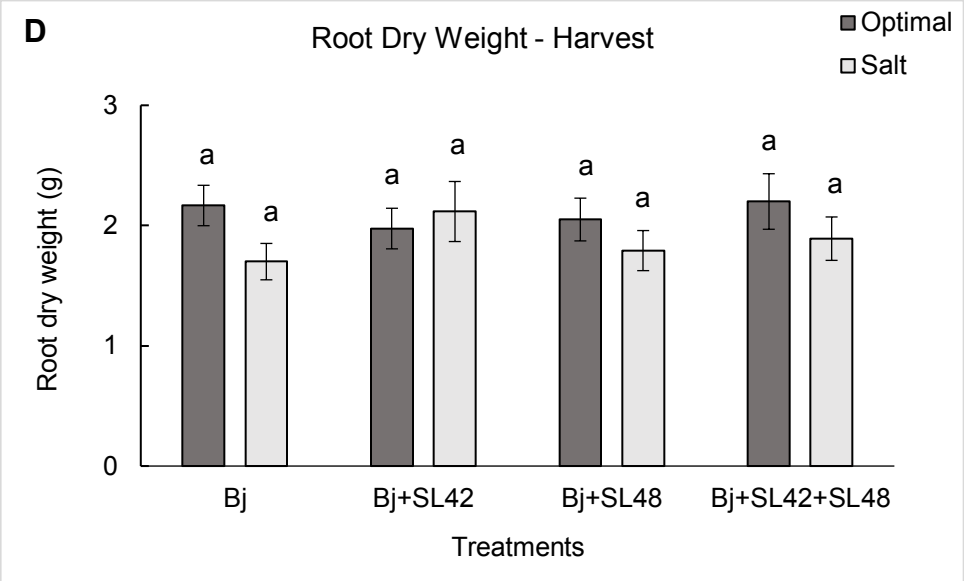

Figure 3.9. Root dry weight of soybean plants measured at **(A)** mid-vegetative, **(B)** mid-flowering, **(C)** mid-pod-filling, and **(D)** harvest stages under optimal (water) and salt (150 mM NaCl) conditions.
The seeds were bacterized with *Bradyrhizobium japonicum* (Bj), Bj+SL42, Bj+SL48, and Bj+SL42+SL48. Values represent mean ± SE (n = 12). Scheffe grouping for least square means was used for multiple means comparison and means with the same letter(s) are not significantly different ($\alpha = 0.05$).

The yield variables, seed weight and seed number were increased by all three co-inoculation treatments compared to *B. japonicum* alone under both optimal and salt stress conditions (Figure 3.10). The treatment of *B. japonicum*+SL42 increased seed weight by 4.3% (*P = 0.7207*) and seed number by 10.5% (*P = 0.2788*) under salt stress. The other treatments, *B. japonicum*+SL48 and *B. japonicum*+SL42+SL48 increased seed weight by 7.4% (*P = 0.449*) and 8.1% (*P = 0.3347*), under optimal conditions and 3.6% (*P = 0.7145*) and 3.1% (*P = 0.8686*) under salt stress, respectively. Even though seed weight and seed number were less in salt stress than the optimal conditions, the difference between the corresponding treatments was small. The harvest index is the proportion of seed dry weight to the aboveground biomass and the treatments with *B. japonicum*+SL48 and *B. japonicum*+SL42+SL48 had higher harvest indices (*P = 0.1621*) than that of the treatments with *B. japonicum* and *B. japonicum*+SL42, under both optimal and salt stress conditions.

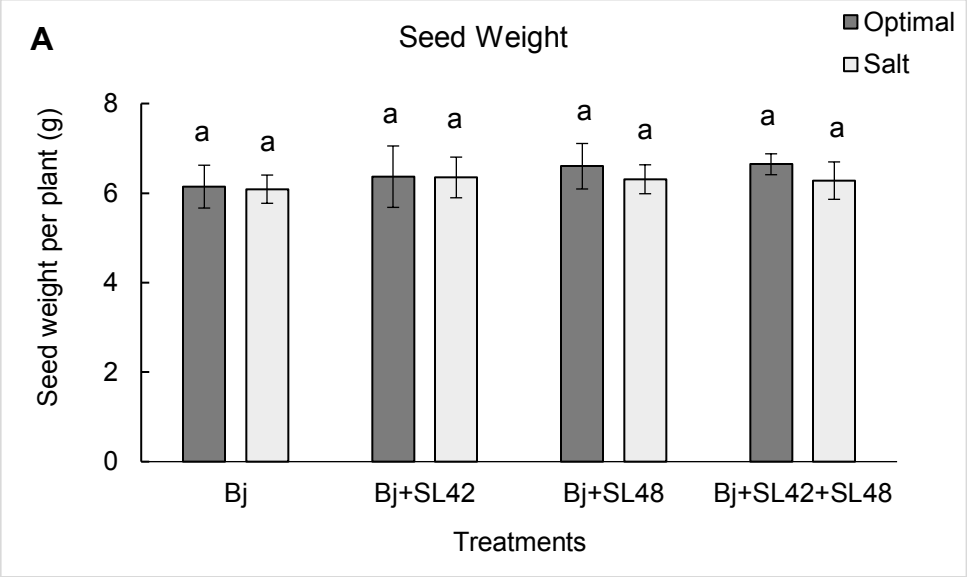

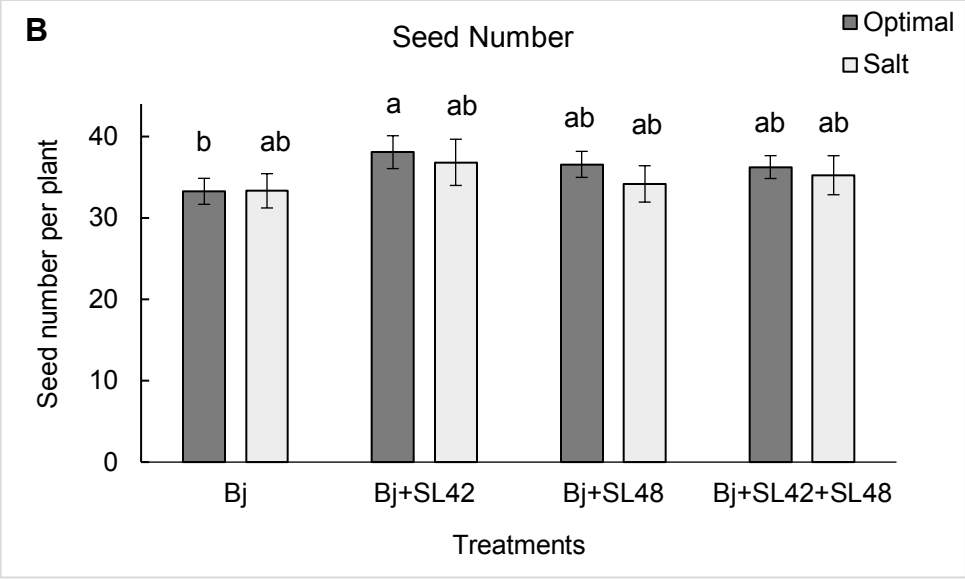

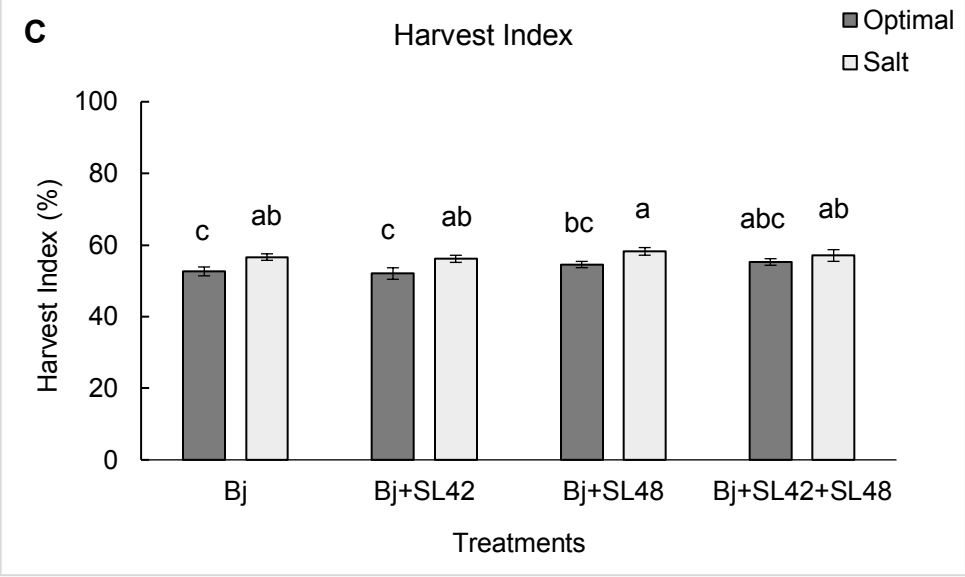

Figure 3.10. Yield variables of soybean plants measured after harvest **(A)** seed weight, **(B)** seed number, and **(C)** harvest index under optimal (water) and salt (150 mM NaCl) conditions.
The seeds were bacterized with *Bradyrhizobium japonicum* (Bj), Bj+SL42, Bj+SL48, and Bj+SL42+SL48. Values represent mean ± SE (n = 12). Scheffe grouping for least square means was used for multiple means comparison and means with the same letter(s) are not significantly different ($\alpha = 0.05$).

3.4.4.1 Nutrient composition analysis of plant tissues and seeds

The nutrient analysis provided an interesting perspective on how the nutrients were translocated between various plant tissues throughout the developmental stages. Nitrogen concentration was largely unvarying in the vegetative and flowering stages, except that shoot N concentration was greater than that of roots. No significant difference was observed in nitrogen concentration between the treatments since all of them were inoculated with *B. japonicum*. At pod-filling, N concentration under salt stress was lower than optimal in leaves, shoot, and roots but almost equal in the pods and at harvest, it was less in the shoot and pods but more or less equal in the roots (Supplementary Table 3.3). This is reflected in the seed quality where the protein concentration was lower under salt stress (34%) than optimal (37%) conditions. Nitrogen assimilation was calculated as a ratio of total N concentration in the tissues to the dry weight, and it was significantly reduced ($P < 0.0001$) with the salt stress at all the developmental stages. At the vegetative stage, N assimilation did not vary among treatments and was corresponding to the amount of fertilizer applied under optimal conditions (60 mg per plant) since the nodules will be still developing at this stage and not fully functional yet. As the plants developed, biological nitrogen fixation was actively occurring, evident by the high N assimilation. During the flowering stage, treatment of *B. japonicum*+SL42+SL48 had increased N assimilation under optimal and salt conditions. At the pod-filling stage, inoculation with *B. japonicum*+SL42 showed higher N assimilation under optimal conditions, yet the treatment of *B. japonicum*+SL42+SL48 resulted in the highest N assimilation under salt stress. At the harvest stage, N assimilation was relatively higher for the *B. japonicum*+SL42 treatment under both optimal and salt-stressed conditions (Table 3.2).

Phosphorous concentration was higher under salt stress than optimal conditions at the flowering and pod-filling stages, but more or less equal at the vegetative and harvest stages (Supplementary Table 3.4). The treatment of *B. japonicum*+SL42+SL48 had the lowest P concentration in the shoot and pods at the harvest stage but highest in the seeds under salt stress. Potassium concentration under salt stress was lower and sodium concentration was higher than optimal conditions at the vegetative stage (Supplementary Tables 3.5, 3.6). The plants at this stage had higher salt accumulation relative to their biomass and hence, the K^+/Na^+ ratio (Table 3.3) was lower. The treatment of *B. japonicum*+SL42 had higher K concentration and lower Na concentration in the shoot than the *B. japonicum* control, and so, the shoot K^+/Na^+ ratio was

significantly higher ($P = 0.006$) under salt stress. Potassium concentration under salt stress was higher in the leaves, shoot, and pods but lower in the roots at flowering, pod-filling, and harvest stages than optimal conditions. Sodium concentration was relatively higher under salt stress and much of the Na was accumulated in the roots, as compared to the shoot and leaves. This explains the low K^+/Na^+ ratio in roots versus the high K^+/Na^+ ratio in the shoot and leaves. The treatment of *B. japonicum*+SL48 had lower Na concentration in the leaves and significantly higher ($P < 0.0001$) K^+/Na^+ ratio than the *B. japonicum* control under salt stress at the flowering stage. The K^+/Na^+ ratio was significantly increased ($P < 0.01$) by the *B. japonicum*+SL42 treatment under salt stress in the leaves during the pod-filling stage. Treatment with *B. japonicum*+SL48 increased K concentration and decreased Na concentration in the shoot and pods, which resulted in higher K^+/Na^+ ratios at the harvest stage. Calcium concentration in the shoot and roots were relatively higher under salt stress than optimal conditions at the flowering, pod-filling and harvest stages, indicating that the plants were also utilizing Ca^{2+} to maintain ionic balance under salinity stress (Supplementary Table 3.7).

Table 3.2. Total Nitrogen assimilation in shoot and root tissues of soybean through the developmental stages.

Treatments	**Optimal**	**Salt**	**Optimal**	**Salt**
	Vegetative stage		**Flowering stage**	
	P = 0.542	*P = 0.3922*	*P = 0.3499*	*P = 0.7125*
Bj	55.62 ±6.36	35.31 ±5.26	572.77 ±24.96	322.98 ±21.40
Bj+SL42	60.52 ±1.04	39.64 ±7.44	561.20 ±48.26	360.97 ±18.38
Bj+SL48	60.80 ±5.50	21.92 ±2.44	613.69 ±63.51	357.90 ±18.52
Bj+SL42+SL48	58.58 ±6.51	32.71 ±3.31	679.05 ±57.68	360.59 ±45.72
	Pod-filling stage		**Harvest stage**	
	P = 0.4104	*P = 0.3142*	*P = 0.5496*	*P = 0.622*
Bj	1795.54 ±73.41	1407.42 ±60.49	285.99 ±37.43	213.10 ±12.95
Bj+SL42	1849.71 ±91.22	1497.74 ±86.39	294.78 ±27.36	225.96 ±20.87
Bj+SL48	1728.23 ±41.03	1455.76 ±57.62	259.59 ±32.88	196.21 ±5.92
Bj+SL42+SL48	1778.99 ±96.30	1551.74 ±70.02	293.55 ±25.86	202.31 ±12.76

Values represent mean ± SE (n=12).

Table 3.3. Distribution of K^+/Na^+ in different plant tissues through the developmental stages of soybean.

Treatments	Optimal	Salt	Optimal	Salt
	Vegetative: Shoot		**Flowering**: Shoot	
	P = 0.5220	*P = 0.0065*	*P = 0.4234*	*P = 0.6128*
Bj	254.51 ±68.90	47.66 ±9.70	665.28 ±224.79	142.83 ±25.72
Bj+SL42	197.71 ±35.67	76.11 ±19.68	783.88 ±215.66	185.02 ±40.09
Bj+SL48	159.00 ±30.97	29.46 ±3.33	872.86 ±171.62	194.68 ±55.18
Bj+SL42+SL48	219.71 ±56.53	54.47 ±13.11	1184.70 ±425.62	231.78 ±62.76
	Vegetative: Root		**Flowering**: Root	
	P = 0.4619	*P = 0.8506*	*P = 0.2347*	*P = 0.8806*
Bj	3.30 ±0.40	1.82 ±0.10	4.75 ±0.34	2.16 ±0.23
Bj+SL42	3.19 ±0.10	1.69 ±0.24	4.56 ±0.35	2.24 ±0.13
Bj+SL48	2.86 ±0.18	1.88 ±0.07	5.23 ±0.34	2.15 ±0.33
Bj+SL42+SL48	3.11 ±0.15	1.97 ±0.42	5.51 ±0.40	2.27 ±0.35
	Pod-filling: Leaves		**Flowering**: Leaves	
	P = 0.0072	*P = 0.0088*	*P = 0.6510*	*P <.0001*
Bj	215.98 ±62.23	232.97 ±26.94	425.80 ±27.13	317.67 ±21.29
Bj+SL42	272.06 ±3.14	599.77 ±176.51	365.97 ±43.21	357.96 ±91.51
Bj+SL48	431.80 ±99.21	219.03 ±42.57	502.20 ±69.57	515.35 ±142.80
Bj+SL42+SL48	686.93 ±90.96	331.00 ±102.04	373.02 ±75.04	445.21 ±194.94
	Pod-filling: Shoot		**Harvest**: Shoot	
	P = 0.5937	*P = 0.1282*	*P = 0.0906*	*P = 0.404*
Bj	786.69 ±226.81	92.10 ±36.67	40.71 ±7.08	1.83 ±0.57
Bj+SL42	523.81 ±139.14	38.31 ±5.75	77.01 ±20.80	1.26 ±0.38
Bj+SL48	499.56 ±113.14	68.86 ±10.89	60.02 ±12.82	2.31 ±0.69
Bj+SL42+SL48	645.64 ±97.23	61.80 ±20.85	67.53 ±12.35	2.35 ±0.54
	Pod-filling: Pods		**Harvest**: Pods	
	P = 0.4089	*P = 0.1799*	*P = 0.257*	*P = 0.2863*
Bj	1029.94 ±130.26	366.12 ±84.35	393.44 ±113.12	63.94 ±14.32
Bj+SL42	821.22 ±137.93	689.29 ±101.93	609.17 ±191.17	38.03 ±13.11
Bj+SL48	1032.80 ±440.95	436.10 ±48.10	387.16 ±71.89	86.54 ±20.10
Bj+SL42+SL48	602.90 ±159.18	664.29 ±176.20	384.78 ±64.55	58.60 ±12.43
	Pod-filling: Root		**Harvest**: Root	
	P = 0.0184	*P = 0.2422*	*P = 0.9461*	*P = 0.088*
Bj	4.66 ±0.41	1.24 ±0.10	2.40 ±0.27	0.59 ±0.05
Bj+SL42	3.99 ±0.30	1.43 ±0.15	2.48 ±0.11	1.22 ±0.50
Bj+SL48	5.41 ±0.45	1.44 ±0.10	2.78 ±0.51	0.52 ±0.08
Bj+SL42+SL48	5.63 ±0.46	1.19 ±0.09	2.82 ±0.86	0.44 ±0.03

Values represent mean ± SE (n=12).

Seed nutritional composition analysis showed that the moisture, protein, and fiber concentrations decreased, and fat, ash, and potassium concentrations increased under salt stress conditions. Sodium concentration was also significantly higher under salt stress ($P = 0.0079$). The treatment of *B. japonicum*+SL42+SL48 had the highest protein, fiber, phosphorus, potassium, calcium, sodium, and magnesium concentrations and the lowest moisture, fat, and ash concentrations under salt stress (Supplementary Table 3.8). Diversity in the nodule bacteria of soybean was observed at 10^{-4} and 10^{-5} dilutions and the colonies were disparate between optimal and salt-stressed plants (Supplementary Figure 3.16). Colonies similar to the morphology of SL42 and SL48 were prominent in the co-inoculation treatments, specifically, the *B. japonicum*+SL42 treatment had predominantly SL42 colonies under salt stress. Also, the bacterial population was higher in the *B. japonicum*+SL42+SL48 treatment than the control, *B. japonicum*.

3.5 Discussion

Rhizobia and legumes have established their mutualistic association over 100 million years of coevolution and the association between different lineages of both the rhizobia and the legume has diverged to be species-specific and spatially-specific (Parker, 1999). This mutualistic specificity also holds true for the host relationship with other members of the phytomicrobiome, including other bacteria in the nodules. The nodules of *Amphicarpaea bracteata* have endophytic bacteria other than its *Bardyrhizobium* symbiont. The vastness in the diversity of these bacteria suggests that they might be effectively functioning as plant growth promoting rhizobacteria (PGPR) in their host. The tested isolates do not coexist with *B. japonicum* in nature (or at least not known yet) and in this study, they were introduced to a related host intended to exert beneficial effects. Co-inoculation of PGPR with rhizobia was reported in various legume plants and proposed to be used as inoculants (Bai et al., 2002a).

Seed germination is the initiation of plant growth and favorable conditions are necessary for successful germination and subsequent seedling emergence. The rate of germination and the time to seedling emergence are important in terms of crop establishment at the beginning of the growing season. Seedling emergence and younger seedlings are more prone to risk from salinity since root development occurs in the topsoil, which generally has higher accumulation of soluble salts (Almansouri et al., 2001). Salt was pre-applied to vermiculite before planting the soybean seeds in the greenhouse, so as to mimic the salinity stress under field conditions where salt is

already present in the topsoil and the seeds have to undergo the process of germination and development in the presence of salt. The seedling stage of the soybean plant is considered to be more sensitive than seed germination (Hosseini et al., 2002) and that is why the effect of salinity stress was acute and precise in the screening experiments where the plants were grown up to the mid-vegetative stage. Salinity stress inhibited seed germination, affected seedling growth, reduced biomass accumulation and decreased seed weight of soybean (Essa, 2002). The plants exhibited symptoms of salinity stress, the seedling emergence was slower, and the growth was less compared to the optimal conditions. The mechanisms underlying the inhibition of soybean seed germination and growth by salinity stress are only partially understood (Zhang et al., 2014). Salt stress leads to the up-regulation of ABA and ethylene biosynthesis and down-regulation of GA during seed germination and auxin and cytokinin during plant growth (Shu et al., 2017). The PGPR are reported to modulate phytohormone signaling involved in salinity stress; a rhizobacterium *Sphingomonas sp*. LK11, known to secrete phytohormones (auxins and gibberellins) and trehalose had significantly increased plant growth under drought-induced osmotic stress in soybean (Asaf et al., 2017). Another rhizobacterium, *Arthrobacter woluwensis* AK1 was shown to ameliorate salinity stress by decreasing ABA content, regulating antioxidant activities and salt tolerance genes and reduced sodium uptake in soybean (Khan et al., 2019). Several isolates, including SL42, SL48, and SL49 have significantly improved seed germination and shoot biomass under salt stress and similar results were observed in the consecutive greenhouse trial as well. The isolates also produced IAA and ACC deaminase, which at least partly explains the observed plant growth promotion and stress tolerance.

Since the bacteria were isolated from the nodules of *A. bracteata* that has *Bradyrhizobium sp*. as the symbiont, they have co-existed in the nodules. Hence, the behavior of nodule bacteria was speculated to be potentially complementary when co-inoculated with a related symbiont in soybean. The plants were grown up to the harvest stage and samples were collected at every growth stage to discern the effect of the isolates on the salinity response of soybean. Soybean has varying water requirements throughout its growing season and rapid root and shoot growth are noted from mid-vegetative to mid-pod-filling stages when the water requirements are also the highest. Though the plant is moderately tolerant and able to withstand short periods of drought and salinity stress, they affect development and crop yield and the plant is most susceptible to the stressors during the vegetative and flowering stages (FAO, 2002). Shoot dry weight of soybean was more affected by

salt stress than root dry weight, as reported previously (Essa, 2002) and above-ground plant growth was significantly reduced ($P < 0.0001$) by salinity during the vegetative and flowering stages when the plant was suffering from chronic salt stress. At the later development stages (pod-filling and harvest) this difference was seldom noticed because the plants would have developed tolerance mechanisms and acclimatized to the stress with time (Munns and Tester, 2008). The degree of salt tolerance in soybean differs among developmental stages (Phang et al., 2008). The plant is sensitive to salinity at early growth stages, but this doesn't necessarily mean it will also be sensitive at later growth stages. The results would probably vary if the plants were exposed to another surge of salinity stress at the later growth stages. For soybean, both flowering and pod-filling stages are responsive to water availability and significant yield loss occurred when the plants were exposed to drought at these developmental stages (Westgate and Peterson, 1993). Soluble salts are usually localized in the sub-surface layers and the concentration of these salts reduces water availability and the roots may be exposed to salt-contaminated soil water table (Rengasamy, 2002). Nevertheless, it is interesting to note that the salt stress is contained in a closed system in the greenhouse and salt volume was applied proportionately to the field capacity of the pot volume. Under field conditions, the intensity of the stress fluctuates depending on other environmental factors such as precipitation or evapotranspiration.

The plants were supplied with a low N fertilizer and the nitrogen fixation was predominantly carried out by *Bradyrhizobium japonicum*. The decrease in nitrogen accumulation under salinity stress was due to the inhibition of root nodulation and biological nitrogen fixation. The number of root nodules and root hair curling were constrained by salt stress (Tu, 1981). The N content of the pods dramatically decreased from the pod-filling to harvest stages indicating the translocation of N to the pods and then to the seeds. The protein content of the seeds was reduced under salinity stress whereas, the oil content was increased. Despite the decline in photosynthesis, translocation of assimilates to the sink tissues were largely maintained in soybean under drought stress (Huber et al., 1984). Phytohormone signaling coordinates partitioning of the assimilates between source and sink, and thereby maintains growth, development and function (Perez-Alfocea et al., 2010). The co-inoculation treatments resulted in higher seed weight and seed number than the control under salt stress and allowed the plants to at least partially overcome the effects of stress on reproduction. The isolates might regulate signaling events in the plants during the initial osmotic phase but later shift towards balancing ionic stress under salinity. Potassium is a key

nutrient in maintaining ion homeostasis under salinity and the ratio of K^+ to Na^+ is determined by the rate of K^+ assimilation. The high cytosolic K^+/Na^+ ratio is critical for plant salinity tolerance and the function of K^+ transporters is regulated by osmolytes and calcium signaling. Ionic homeostasis is maintained by excluding Na^+ and Cl^- and restricting their accumulation in plant tissues and compartmentalizing the toxic ions in vacuoles (Shabala and Cuin, 2008). The ability of the plants treated with isolates SL42 and SL48 to maintain a high K^+/Na^+ ratio through various growth stages is indeed an indication of induced salinity tolerance. Follow-up studies are in progress to understand the mode of action of the isolates and the adaptive mechanisms elicited in the plants. The primary reason for using vermiculite as the sole potting medium is that it is inert, ruling out the possibility of interference by organic matter (including microflora) usually present in the soil or peat-based potting medium. This has proved to be an effective testing tool for salt stress mitigation by the bacterial inoculation and plant nutrient uptake from the added fertilizer. The observations of nodule bacterial colonies indicated that SL42 and SL48 predominantly inhabited the nodules of soybean and also supported the resident nodule phytomicrobiome population. Indigenous microbial communities influence the survival of inoculated bacteria and vice-versa (Trabelsi and Mhamdi, 2013). However, the tested strains are a part of the native habitat, so that the potential concern for altering the ecosystem function of soil microbial communities is diminished. They have a competitive advantage over the resident soil microbiota since they provide a synergistic plant-microbe interaction with soybean. Considering that many other factors are at play under a field condition, extensive field trials are needed to determine the beneficial effects of these microbes on soybean growth and yield in local agriculture production systems.

3.6 Conclusions

Soybean cultivation has reached its northern hemisphere limit and expansion/extension of cultivation both spatially and temporally will be possible when the plants can further acclimatize to the native conditions. Co-inoculation with native nodule bacterial strains can help in the adaptation and expression of particular traits such as salt/drought tolerance or cold acclimatization induced by the bacteria can benefit the associated plant. Early plant response mechanisms to these stresses overlap each other, which means inoculation with these bacteria can be an asset to sustainable soybean production under the Canadian agricultural scenario. Moreover, such growth promoting technology as this might invigorate native soil properties (both abiotic and biotic),

create synergy with the native soil microflora, assist in the reduction of chemical inputs and advance crop productivity. However, multiple field trials are required to demonstrate the potential of these isolates to boost yield by growth promotion and stress alleviation. Even though adaptation to salinity stress depends on various factors including the plant's innate potential and the environmental conditions, implementing a cost-effective strategy of PGPR inoculation to enhance stress tolerance will be fruitful and helpful to meet the rising demands for global food production.

3.7 References

1. AAFC (2020). *Soil Salinization Indicator. Agriculture and Agri-Food Canada*. Available online at: https://www.agr.gc.ca/eng/agriculture-and-climate/agricultural-practices/soil-and-land/soil-salinization-indicator/?id=1462912470880 (accessed April 12, 2020).
2. Adesemoye, A. O., and Kloepper, J. W. (2009). Plant-microbes interactions in enhanced fertilizer-use efficiency. *Appl. Microbiol. Biotechnol.* 85, 1–12. doi: 10.1007/s00253-009-2196-0
3. Almansouri, M., Kinet, J. M., and Lutts, S. (2001). Effect of salt and osmotic stresses on germination in durum wheat (*Triticum durum* Desf.). *Plant Soil* 231, 243–254. doi: 10.1023/A:1010378409663
4. Asaf, S., Khan, A. L., Khan, M. A., Imran, Q. M., Yun, B. W., and Lee, I. J. (2017). Osmoprotective functions conferred to soybean plants via inoculation with *Sphingomonas* sp LK11 and exogenous trehalose. *Microbiol. Res.* 205, 135–145. doi: 10.1016/j.micres.2017.08.009
5. Ashraf, M. (1994). Breeding for salinity tolerance in plants. *Crit. Rev. Plant Sci.* 13, 17–42. doi: 10.1080/07352689409701906
6. Bai, Y. M., D'Aoust, F., Smith, D. L., and Driscoll, B. T. (2002a). Isolation of plant-growth-promoting *Bacillus* strains from soybean root nodules. *Can. J. Microbiol.* 48, 230–238. doi: 10.1139/w02-014
7. Bai, Y. M., Pan, B., Charles, T. C., and Smith, D. L. (2002b). Co-inoculation dose and root zone temperature for plant growth promoting rhizobacteria on soybean [*Glycine max* (L.) Merr] grown in soil-less media. *Soil Biol. Biochem.* 34, 1953–1957. doi: 10.1016/S0038-0717(02)00173-6
8. Bric, J. M., Bostock, R. M., and Silverstone, S. E. (1991). Rapid *in situ* assay for indoleacetic-acid production by bacteria immobilized on a nitrocellulose membrane. *Appl. Environ. Microbiol.* 57, 535–538. doi: 10.1128/AEM.57.2.535-538.1991
9. Bromfield, E. S. P., Cloutier, S., Tambong, J. T., and Thi, T. V. T. (2017). Soybeans inoculated with root zone soils of Canadian native legumes harbour diverse and novel *Bradyrhizobium* spp. that possess agricultural potential (vol 40, pg 440, 2017). *Syst. Appl. Microbiol*. 40:517. doi: 10.1016/j.syapm.2017.10.003
10. Cloutier, J. (2017). *Soy Story: A Short History of Glycine max in Canada. Statistics Canada*. Available online at: https://www150.statcan.gc.ca/n1/pub/21-004-x/2017001/article/14779-eng.htm (accessed April 12, 2020).
11. Devine, T. E., Kuykendall, L. D., and Oneill, J. J. (1990). The Rj4 allele in soybean represses nodulation by chlorosis-inducing bradyrhizobia classified as DNA homology group-ii by antibiotic-resistance profiles. *Theor. Appl. Genet.* 80, 33–37. doi: 10.1007/BF00224012

12. Dorff, E. (2007). *The Soybean, Agriculture's Jack-of-all-Trades, Is Gaining Ground Across Canada. Statistics Canada*. Available online at: https://www150.statcan.gc.ca/n1/en/pub/96-325-x/2007000/article/10369-eng.pdf?st=6wd-Sqjq (accessed April 12, 2020).
13. Egamberdieva, D., Wirth, S., Jabborova, D., Rasanen, L. A., and Liao, H. (2017). Coordination between *Bradyrhizobium* and *Pseudomonas* alleviates salt stress in soybean through altering root system architecture. *J. Plant Interact.* 12, 100–107. doi: 10.1080/17429145.2017.1294212
14. EnvironmentCanada (2001). *Priority Substances List Assessment Report for Road Salts. EnvironmentCanada*. Available online at: https://www.canada.ca/en/health-canada/services/environmental-workplace-health/reports-publications/environmental-contaminants/canadian-environmental-protection-act-1999-priority-substances-list-assessment-report-road-salts.html#a342 (accessed April 12, 2020).
15. Essa, T. A. (2002). Effect of salinity stress on growth and nutrient composition of three soybean (*Glycine max* L. Merrill) cultivars. *J. Agron. Crop Sci.* 188, 86–93. doi: 10.1046/j.1439-037X.2002.00537.x
16. FAO (2002). *Soybean. Food and Agriculture Organization of the United Nations*. Available online at: http://www.fao.org/land-water/databases-and-software/crop-information/soybean/en/ (accessed April 12, 2020).
17. Florinsky, I. V., Eilers, R. G., Wiebe, B. H., and Fitzgerald, M. M. (2009). Dynamics of soil salinity in the Canadian prairies: application of singular spectrum analysis. *Environ. Model Softw.* 24, 1182–1195. doi: 10.1016/j.envsoft.2009.03.011
18. Goswami, D., Dhandhukia, P., Patel, P., and Thakker, J. N. (2014). Screening of PGPR from saline desert of Kutch: growth promotion in Arachis hypogea by *Bacillus licheniformis* A2. *Microbiol. Res.* 169, 66–75. doi: 10.1016/j.micres.2013.07.004
19. Hosseini, M. K., Powell, A. A., and Bingham, I. J. (2002). Comparison of the seed germination and early seedling growth of soybean in saline conditions. *Seed Sci. Res.* 12, 165–172. doi: 10.1079/SSR2002108
20. Huber, S. C., Rogers, H. H., and Mowry, F. L. (1984). Effects of water-stress on photosynthesis and carbon partitioning in soybean (*Glycine-max* [L] Merr) plants grown in the field at different CO_2 levels. *Plant Physiol.* 76, 244–249. doi: 10.1104/pp.76.1.244
21. Hungria, M., Nogueira, M. A., and Araujo, R. S. (2013). Co-inoculation of soybeans and common beans with rhizobia and azospirilla: strategies to improve sustainability. *Biol. Fertil. Soils* 49, 791–801. doi: 10.1007/s00374-012-0771-5
22. Hynes, R. K., Leung, G. C., Hirkala, D. L., and Nelson, L. M. (2008). Isolation, selection, and characterization of beneficial rhizobacteria from pea, lentil, and chickpea grown in western Canada. *Can. J. Microbiol.* 54, 248–258. doi: 10.1139/W08-008
23. Jensen, H. L., Petersen, E. J., De, P. K., and Bhattacharya, R. (1960). A new nitrogen-fixing bacterium - *Derxia gummosa* nov-gen-nov-spec. *Arch. Mikrobiol.* 36, 182–195. doi: 10.1007/BF00412286
24. Kan, G. Z., Zhang, W., Yang, W. M., Ma, D. Y., Zhang, D., Hao, D. R., et al. (2015). Association mapping of soybean seed germination under salt stress. *Mol. Genet. Genomics* 290, 2147–2162. doi: 10.1007/s00438-015-1066-y
25. Khan, M. A., Asaf, S., Khan, A. L., Jan, R., Kang, S. M., Kim, K. M., et al. (2019). Rhizobacteria AK1 remediates the toxic effects of salinity stress via regulation of endogenous phytohormones and gene expression in soybean. *Biochem. J.* 476, 2393–2409. doi: 10.1042/BCJ20190435

26. Letunic, I., and Bork, P. (2019). Interactive Tree Of Life (iTOL) v4: recent updates and new developments. *Nucleic Acids Res.* 47, W256–W259. doi: 10.1093/nar/gkz239
27. Marr, D. L., Devine, T. E., and Parker, M. A. (1997). Nodulation restrictive genotypes of *Glycine* and *Amphicarpaea*: a comparative analysis. *Plant Soil* 189, 181–188. doi: 10.1023/A:1004203018770
28. Munns, R., and Tester, M. (2008). Mechanisms of salinity tolerance. *Annu. Rev. Plant Biol.* 59, 651–681. doi: 10.1146/annurev.arplant.59.032607.092911
29. NRCS (2002). *Salinity in Agriculture. Natural Resources Conservation Service, United States Department of Agriculture*. Available online at: https://www.nrcs.usda.gov/wps/portal/nrcs/detailfull/national/water/quality/tr/?cid=nrcs143_010914 (accessed April 12, 2020).
30. O'Toole, G. A. (2011). Microtiter dish biofilm formation assay. *J. Vis. Exp.* 47:2437. doi: 10.3791/2437
31. Parker, M. A. (1994). Evolution in natural and experimental populations of *Amphicarpaea-bracteata*. *J. Evol. Biol.* 7, 567–579. doi: 10.1046/j.1420-9101.1994.7050567.x
32. Parker, M. A. (1999). Mutualism in metapopulations of legumes and rhizobia. *Am. Nat.* 153, S48–S60. doi: 10.1086/303211
33. Penrose, D. M., and Glick, B. R. (2003). Methods for isolating and characterizing ACC deaminase-containing plant growth-promoting rhizobacteria. *Physiol. Plant* 118, 10–15. doi: 10.1034/j.1399-3054.2003.00086.x
34. Perez-Alfocea, F., Albacete, A., Ghanem, M. E., and Dodd, I. C. (2010). Hormonal regulation of source-sink relations to maintain crop productivity under salinity: a case study of root-to-shoot signalling in tomato. *Funct. Plant Biol.* 37, 592–603. doi: 10.1071/FP10012
35. Phang, T. H., Shao, G. H., and Lam, H. M. (2008). Salt tolerance in soybean. *J. Integr. Plant Biol.* 50, 1196–1212. doi: 10.1111/j.1744-7909.2008.00760.x
36. Rengasamy, P. (2002). Transient salinity and subsoil constraints to dryland farming in Australian sodic soils: an overview. *Aust. J. Exp. Agric.* 42, 351–361. doi: 10.1071/EA01111
37. Schwyn, B., and Neilands, J. B. (1987). Universal chemical-assay for the detection and determination of siderophores. *Anal. Biochem.* 160, 47–56. doi: 10.1016/0003-2697(87)90612-9
38. Shabala, S., and Cuin, T. A. (2008). Potassium transport and plant salt tolerance. *Physiol. Plant* 133, 651–669. doi: 10.1111/j.1399-3054.2007.01008.x
39. Shu, K., Qi, Y., Chen, F., Meng, Y. J., Luo, X. F., Shuai, H. W., et al. (2017). Salt stress represses soybean seed germination by negatively regulating GA biosynthesis while positively mediating ABA biosynthesis. *Front. Plant Sci.* 8:1372. doi: 10.3389/fpls.2017.01372
40. Tang, J., Bromfield, E. S. P., Rodrigue, N., Cloutier, S., and Tambong, J. T. (2012). Microevolution of symbiotic *Bradyrhizobium* populations associated with soybeans in east North America. *Ecol. Evol.* 2, 2943–2961. doi: 10.1002/ece3.404
41. Thoenes, P. (2004). "The role of soybean in fighting world hunger," in *VIIth World Soybean Research Conference* (Foz do Iguassu: Food and Agriculture Organization of the United Nations).
42. Trabelsi, D., and Mhamdi, R. (2013). Microbial inoculants and their impact on soil microbial communities: a review. *Biomed Res. Int.* 2013:863240. doi: 10.1155/2013/863240
43. Tu, J. C. (1981). Effect of salinity on rhizobium-root-hair interaction, nodulation and growth of soybean. *Can. J. Plant Sci.* 61, 231–239. doi: 10.4141/cjps81-035

44. Weaver, R. W., Dumenil, L. C., and Frederic, LR (1972). Effect of soybean cropping and soil properties on numbers of *Rhizobium-japonicum* in Iowa soils. *Soil Sci.* 114:137. doi: 10.1097/00010694-197208000-00009
45. Westgate, M. E., and Peterson, C. M. (1993). Flower and pod development in water-deficient soybeans (*Glycine-max* L Merr). *J. Exp. Bot.* 44, 109–117. doi: 10.1093/jxb/44.1.109
46. Wiebe, B. H., Eilers, R. G., Eilers, W. D., and Brierley, J. A. (2007). Application of a risk indicator for assessing trends in dryland salinization risk on the Canadian Prairies. *Can. J. Soil Sci.* 87, 213–224. doi: 10.4141/S06-068
47. Wilkinson, H. H., Spoerke, J. M., and Parker, M. A. (1996). Divergence in symbiotic compatibility in a legume-*Bradyrhizobium* mutualism. *Evolution* 50, 1470–1477. doi: 10.1111/j.1558-5646.1996.tb03920.x
48. Yang, J., Kloepper, J. W., and Ryu, C. M. (2009). Rhizosphere bacteria help plants tolerate abiotic stress. *Trends Plant Sci.* 14, 1–4. doi: 10.1016/j.tplants.2008.10.004
49. Zhang, W. J., Niu, Y., Bu, S. H., Li, M., Feng, J. Y., Zhang, J., et al. (2014). Epistatic association mapping for alkaline and salinity tolerance traits in the soybean germination stage. *PLoS ONE* 9:e84750. doi: 10.1371/journal.pone.0084750
50. Zhu, T., Shi, L., Doyle, J. J., and Keim, P. (1995). A single nuclear locus phylogeny of soybean based on DNA-sequence. *Theor. Appl. Genet.* 90, 991–999. doi: 10.1007/BF00222912

A NOTE ON STATISTICAL INTERPRETATION

In the "Results" section of Chapter 3, if the text indicates "significant difference" this means that the treatment has a significant effect on the variable measured, compared to the appropriate control, the difference being statistically significant at $P \leq 0.05$. If it only indicates "increase" or "decrease", this means that the treatment has no significant effect on the variable measured, compared to the control, that is, the numerical difference was not statistically significant ($P \geq 0.05$). But, the treatment did result in a numerical (percent) increase or decrease in the variable measured relative to the control treatment. The respective P-values of the treatment versus control comparisons are always mentioned in parentheses, whether significant or not. This clarity is necessary to interpret the results, particularly in experiments where plants were co-inoculated with the rhizobacterial strains and *Bradyrhizobium* under greenhouse conditions. The results were non-significant in the absence of salt stress yet, even under this condition, numerical increases with the treatments were observed, and they did occur consistently across a wide range of variables. Some of the results were non-significant in the presence of salt stress but, the numerical increases were much higher with the treatments and they can neither be ignored and nor considered to have no effect. In any case, the differences between the PGPR inoculated treatments and the *Bradyrhizobium* control under growth chamber conditions in Chapter 4 were almost always statistically significant in the presence of salt stress.

CONNECTING TEXT

In Chapter 3, two strains isolated from root nodules of *Amphicarpaea bracteata*, *Rhizobium* sp. SL42 and *Hydrogenophaga* sp. SL48, co-inoculated with *Bradyrhizobium japonicum* 532C were shown to increase plant growth and development under optimal and salt-stressed conditions in a greenhouse setting. However, the mode of action through which the strains enhance plant growth and salinity stress tolerance was uninvestigated; this was explored here, in order to understand the *modus operandi* of plant-microbe interactions. In Chapter 4, a proteomic approach was used to analyze growth and stress response mechanisms elicited in soybean leaf tissue by bacterial inoculation under both optimal and salt-stressed conditions. This was useful to determine the beneficial effects of SL42 and SL48 and how they assist the plant in adapting to the stress and sustaining growth under these adverse conditions.

4 Chapter 4 Soybean Leaf Proteomic Profile Influenced by Rhizobacteria Under Optimal and Salt Stress Conditions

Authors: Gayathri Ilangumaran[1], Sowmyalakshmi Subramanian[1] and Donald Lawrence Smith[1]

Affiliations:

[1] Department of Plant Science, McGill University, Macdonald Campus, 21,111 Lakeshore Road, Sainte-Anne-de-Bellevue, QC, Canada.

This manuscript is in preparation for submission to Molecular Plant Microbe Interactions (MPMI).

4.1 Abstract

Soil salinity is a major abiotic stressor inhibiting plant growth and development by affecting a range of physiological processes. Plant growth promoting rhizobacteria (PGPR) are considered a sustainable option for alleviation of stress and enhancement of plant growth, yet their mode of action is complex and largely unexplored. In this study, an untargeted proteomic approach provided insights into growth and stress response mechanisms elicited in soybean plants by *Rhizobium* sp. SL42 and *Hydrogenophaga* sp. SL48. The plants were grown under optimal and salt-stressed conditions up to their mid-vegetative stage; shoot growth variables were increased in the bacteria-treated plants. Shotgun proteomics of soybean leaf tissue revealed that a number of proteins related to plant growth and stress tolerance were modulated in the bacterial inoculation treatments. Several key proteins involved in major metabolic pathways of photosynthesis, respiration and photorespiration were upregulated. These include photosystem I psaK, Rubisco subunits, glyceraldehyde-3-phosphate dehydrogenase, succinate dehydrogenase and glycine decarboxylase. Similarly, stress response proteins such as catalase and glutathione S-transferase (antioxidants), proline-rich precursor protein (osmolyte), and NADP-dependent malic enzyme (linked to ABA signaling) were increased under salt stress. The functions of proteins related to plant growth and stress adaptation led to an expanded understanding of plant-microbe interactions. These findings suggest that the PGPR strains regulated proteome expression in soybean leaves through multiple signaling pathways, thereby inducing salinity tolerance and improving plant growth in the presence of this abiotic stress challenge. They play a crucial role in the development of soybean plants under stressful conditions and therefore could potentially be utilized as biostimulants to mitigate stress effects and boost crop productivity.

4.2 Introduction

Salinity is one of the major abiotic stressors, causing detrimental effects on plant growth and development. Soil salinity declines crop productivity and eventually leads to the deterioration of cultivable land and desertification (Abrol et al., 1988; Zorb et al., 2019). Plant growth is affected when the salt concentration in its root zone is above the stress-induction threshold and it is caused by an initial osmotic phase (water imbalance) and a later ionic phase (ion toxicity). Although roots are the first point of contact in salinity stress, the onset of stress triggers root-to-shoot communication. The responses include stomatal closure, photosynthesis inhibition, oxidative damage and toxic ion accumulation in the tissues. As a result, leaf area and shoot growth are reduced, and leaf chlorosis and premature senescence are accelerated (Munns and Tester, 2008). Plant salinity tolerance is regulated by a plethora of mechanisms at the molecular, cellular and physiological levels, throughout the plant's developmental stages and is reflected in growth rate. These mechanisms have evolved diversely in the plant kingdom so that the degree of salinity tolerance in plants varies among species and genotypes (Chinnusamy et al., 2006).

Soybean [*Glycine max* (L.) Merrill] is an important legume-oilseed crop due to its high protein and oil contents. It is a major source of edible oil, protein and livestock feed and is cultivated globally. In 2019-20, Brazil (124 million tonnes) and the USA (96.8 million tonnes) were the leading producers, and Canada was the 7th largest producer (6 million tonnes) (SoyStats, 2020). The plant establishes a symbiotic association with *Bradyrhizobium* that dwell in the root nodules and fix atmospheric nitrogen. Soybean enriches soil nitrogen content in agricultural production systems and thus, is included in crop rotations with other arable crops (Zhang and Li, 2003). Expanding soybean cultivation and increasing soybean yield, particularly under stress, has been the major focus of soybean research over the years. Soybean is a glycophyte, and is moderately tolerant to salinity stress; seed germination is delayed when exposed to salt and growth traits including seedling emergence, plant height, leaf area, shoot dry weight, nodulation, number of pods, weight per 100 seeds and seed quality are affected by salinity stress (Phang et al., 2008).

Plant-microbe interactions have crucial functions in plant growth and ecosystem function. Beneficial plant growth promoting rhizobacteria (PGPR) are widely studied and have been shown to elicit tolerance mechanisms that mitigate abiotic stress effects. Inoculation with PGPR modulates plant signaling events involving phytohormones, stress-responses, photosynthesis rate, chlorophyll content, osmolyte accumulation, antioxidant activity, root system architecture, and

shoot growth and developmental regulation (Gray and Smith, 2005; Kang et al., 2014). A number of studies have reported the influence of PGPR on growth promotion and stress alleviation in soybean with respect to these mechanisms. Soybean seedlings exposed to *Pseudomonas simiae* AU showed significant upregulation of the vegetative storage protein (VSP), gamma-glutamyl hydrolase (GGH) and RuBisCO large chain proteins under salt stress (100 mM NaCl). The plants also had higher proline and chlorophyll contents (Vaishnav et al., 2015). Inoculation with *Bacillus firmus* SW5 resulted in higher chlorophyll, proline, glycine betaine, phenolic and flavonoid contents and antioxidant enzyme activities in soybean plants under salt stress levels of 40 and 80 mM NaCl. Expression of antioxidant enzyme genes, *APX*, *CAT*, *POD*, and Fe-*SOD* (ascorbate peroxidase, catalase, peroxidase, superoxide dismutase) and salt-response genes, GmVSP, *GmPHD2* (plant-homeo-domain gene of DNA binding ability), *GmbZIP62* (transcription factor involved in ABA and stress signaling), *GmWRKY54* (salt and drought stress tolerance), GmOLPb (osmotin-like protein b isoform gene encoding a neutral PR-5 protein), and *CHS* (chalcone synthase involved in the flavonoid biosynthetic pathway) were upregulated in the salt-stressed plants (El-Esawi et al., 2018).

Soybean plants inoculated with *B. thuringiensis* showed greater stomatal conductance and transpiration rates than the control plants under drought stress. Further, the plants, along with those inoculated with *B. subtilis* and *B. cereus*, showed differential expression of the stress-responsive genes *GmDREB1D* (dehydration-responsive element binding), *GmEREB* (ethylene-responsive element binding), *GmP5CS* (Δ^1-pyrroline-5-carboxylase synthetase) and *GmGOLS* (galactinol synthase) (Martins et al., 2018). Halotolerant PGPR strains inoculated onto soybean resulted in higher antioxidant enzyme activity, K^+ uptake, chlorophyll content, and plant growth but decreased ABA level under 200 mM NaCl. The expression of *GmST1* (salt-tolerance 1) and *GmLAX3* (auxin resistant 3) were upregulated in the inoculated seedlings (Khan et al., 2019a). One of the PGPR, *Arthrobacter woluwensis* AK1 increased antioxidant activities and decreased Na^+ uptake in soybean plants grown under 100 and 200 mM NaCl. Further, the inoculated plants showed upregulation of *GmLAX1* (auxin resistant 1), *GmAKT2* (potassium channel), *GmST1* and *GmSALT3* (salt tolerance-associated gene on chromosome 3) and downregulation of *GmNHX1* (Na^+/H^+ antiporter) and *GmCLC1* (chloride channel) (Khan et al., 2019b). It is unsurprising that many of these studies used soybean leaf tissue to elucidate the mechanisms of plant salinity tolerance elicited by PGPR as leaves exhibit clear symptoms of stress and stress responses.

Amphicarpaea bracteata (hog peanut) is a legume, native to North America and the closest relative of soybean in eastern North America (Marr et al., 1997). In the earlier study (Chapter 3), bacteria were isolated from the root nodules of *A. bracteata* and inoculated onto soybean and screened based on their ability to improve plant growth and salinity tolerance. Two isolates, *Rhizobium* sp. SL42 and *Hydrogenophaga* sp. SL48 were co-inoculated with *Bradyrhizobium japonicum* 532C were shown to increase plant growth and development under optimal and salt-stressed conditions in a greenhouse setting. The bacteria are currently evaluated for their capacity to enhance soybean growth under field conditions, to be potentially applied as inoculants in soybean crop production systems. However, it is imperative to understand the plant mechanisms regulated by the strains and the function of plant-microbe interactions causing enhanced growth and stress tolerance of soybean. In this present study, we used a proteomic approach to analyze growth and stress related responses elicited in the leaf tissue of soybean plants at their mid-vegetative stage, grown in a controlled environment under both optimal and salt-stressed conditions.

4.3 Materials and Methods

4.3.1 Bacteria culture propagation and inoculation

The bacteria *Rhizobium* sp. SL42, *Hydrogenophaga* sp. SL48 and *B. japonicum* 532 C were grown in YEM broth for 48 h, incubated at 25 °C and 150 rpm. The cultures were harvested by centrifugation at 5,000 × g for 10 min, room temperature (Awel^{TM} MF 48-R, NuAire, USA) and the supernatant was discarded. The pellet was suspended in 10 mM $MgSO_4$ and the optical density was adjusted to 0.1 at A_{600nm} (Ultraspec 4300 pro UV/Visible Spectrophotometer, Biochrom). Soybean seeds (Absolute RR) were soaked in the bacterial cell suspension at a rate of 500 µL per seed or 10 mM $MgSO_4$ (control) for 30 min.

4.3.2 Soybean growth conditions and sample collection

Bacterized and control seeds (5 seeds per pot) were placed in 15.25 cm pots filled with vermiculite (Perlite Canada Inc.) treated with 300 mL water or 150 mM NaCl. The pots were placed in a growth chamber (Conviron®, Canada) and maintained at 25 ± 2 °C and 50% relative humidity. Seedling emergence was counted on 7th DAP (days after planting) and the plants were thinned to one seedling per pot. The plants were irrigated with 300 mL water twice a week (every

3-4 days) and fertilized with ½ strength Hoagland's solution once a week and sampled at 28th DAP. Above ground plant growth variables including plant height, leaf area, shoot fresh weight and dry weight were measured. Dried tissue samples were ground for elemental analysis, N and P were measured on a flow injection analyzer (FIA) (Lachat QuickChem 8000, Hach® USA) and K, Ca and Na were measured after dilutions and appropriate modifier addition on an atomic absorption spectrophotometer (AAS) (Varian 220FS). The experiment was repeated four times with eight treatments and six replications for each treatment under optimal and salt-stressed conditions. Three replications were allocated for measuring growth variables and three replications were allocated for protein extraction, excluding the first repetition.

4.3.3 Shotgun Proteomics

For protein extraction, soybean leaves were harvested, flash-frozen in liquid nitrogen and stored at -80 °C. The samples collected were pooled to form a single biological replicate; each treatment comprised 3 independent biological replications. The protein was extracted using a plant total protein extraction kit (Sigma-Aldrich, St. Louis, MO, USA).

4.3.3.1 Protein extraction

Briefly, samples were finely ground in liquid nitrogen and ~100 mg of sample was transferred to a sterile Eppendorf tube. It was incubated with 1 mL of 80% ice-cold methanol-protease inhibitor cocktail for 20 min in -20 °C and centrifuged at 12,000 rpm for 10 min at 4 °C. The supernatant was discarded, and the procedure was repeated thrice. The sample was then incubated in acetone and washed twice following a similar procedure to remove pigments and other secondary metabolites. The RW4 (Protein extraction Reagent Type 4) solution was added to the pellet, vortexed for 30s and incubated for 10 min at room temperature (22 °C). After centrifugation at room temperature, the supernatant was collected in a new tube. The protein content was quantified using the Lowry method and samples of 20 μg of protein in 20 μL of 1M urea. The samples were subjected to shotgun proteomic analysis at the Institut de recherches cliniques de Montréal (IRCM).

4.3.3.2 Proteome profiling

Total protein was tryptic digested prior to being subjected to LC-MS/MS using a Velos Orbitrap instrument (Thermo Fisher, MA, USA). Tandem mass spectra were extracted; charge state deconvolution and deisotoping were not performed. MS/MS samples were analyzed using

Mascot (Matrix Science, London, UK; Mascot in Proteome Discoverer 2.4.0.305). Mascot was set up to search the Refseq database Glycine_max (86,460 entries), assuming the digestion enzyme trypsin. Mascot was searched with a fragment ion mass tolerance of 0.020 Da and a parent ion tolerance of 10.0 PPM. Carbamidomethyl of cysteine (+57 on C) was specified in Mascot as a fixed modification. Oxidation of methionine (+16 on M) was specified in Mascot as a variable modification.

4.3.3.3 Criteria for protein identification

Scaffold (version Scaffold_4.11.1, Proteome Software Inc., Portland, OR) was used to validate MS/MS based peptide and protein identifications. Peptide identifications were accepted if they could be established at greater than 95.0% probability by the Peptide Prophet algorithm (Keller et al., 2002) with Scaffold delta-mass correction. Protein identifications were accepted if they could be established at greater than 99.0% probability and contained at least 2 identified peptides. Protein probabilities were assigned by the Protein Prophet algorithm (Nesvizhskii et al., 2003). Proteins that contained similar peptides and could not be differentiated based on MS/MS analysis alone were grouped to satisfy the principles of parsimony. Proteins sharing significant peptide sequence similarity were grouped into clusters.

4.3.4 Statistical analysis

The experiment was established following a completely randomized design. The data were analyzed using the SAS statistical package v.9.4 (SAS Institute Inc., Cary, NC, USA) with Proc Mixed model at a 95% confidence interval and multiple means comparison was by Tukey's HSD (honest significant difference) at $\alpha = 0.05$.

Proteomics data were analyzed using Scaffold v.4 (Proteome software, Inc.) for Fisher's exact test and fold change of identified/known proteins between two sample categories after normalization (embedded) of the quantitative spectral count. The FASTA files generated were analyzed using OmicsBOX (BioBam, Bioinformatics Solutions) and the integrated Blast2GO-Pro and InterProScan web services were used for functional annotation of the proteins and to classify the proteins based on functional domains, enzyme codes (EC), biological processes (BP), molecular functions (MF) and cellular components (CC). Scaffold was also used to generate FASTA, Peaklist, and mzldentML files. The LC-MSMS proteomics data is in the process of being

submitted to the to the ProteomeXchange Consortium via the PRIDE partner repository (http://proteomecentral.proteomexchange.org).

4.4 Results

4.4.1 Plant growth and elemental analysis

Seedling emergence at 7th DAP was considerably lower under salt stress than optimal conditions (Table 4.1). It was significantly improved by bacterial inoculation and treatment with SL42 (*P = 0.0308*) and SL42+SL48 (*P = 0.147*) had higher emergence rates than the control under optimal conditions, while treatment with SL48 had the highest emergence rate (*P = 0.226*) under salt stress. On the other hand, *B. japonicum*+SL42 increased the emergence rate under both optimal and salt-stressed conditions.

Table 4.1. Seedling emergence rate (%) of soybean at 7th DAP under optimal and salt stress conditions.

Treatments	Optimal	Salt	Treatments	Optimal	Salt
	P = 0.0004			*P = 0.0999*	
Ctrl	71.67 ^{bc} ±5.75	63.33 ^{c} ±5.95	Bj	76.67 ^{ab} ±6.44	70.00 ^{ab} ±3.89
SL42	86.67 ^{a} ±2.84	65.00 ^{c} ±5.00	Bj+SL42	81.67 ^{a} ±4.58	75.00 ^{ab} ±3.59
SL48	76.67 ^{abc} ±3.33	71.67 ^{bc} ±3.86	Bj+SL48	71.67 ^{ab} ±5.75	73.33 ^{ab} ±6.20
SL42+SL48	81.67 ^{ab} ±4.58	66.67 ^{c} ±6.20	Bj+SL42+SL48	78.33 ^{ab} ±4.58	65.00 ^{b} ±6.57

Values represent mean ± SE (n=12). Bj – *Bradyrhizobium japonicum* 532C, SL42 – *Rhizobium* sp. SL42, SL48 – *Hydrogenophaga* sp. SL48

The growth variables of soybean plants were measured at 28th DAP (Figure 4.1). Plant height was significantly increased by treatment with SL42 (*P = 0.0446*) under optimal conditions and for the plants inoculated with SL48 (*P = 0.0316*) and SL42+SL48 (*P = 0.0098*) under salt stress (Figure 4.2). Plants inoculated with *B. japonicum* were tallest under optimal conditions but under salt stress, all three co-inoculation treatments *B. japonicum*+SL42 (P = 0.0277), *B. japonicum*+SL48 (*P = 0.0551*) and *B. japonicum*+SL42+SL48 (*P = 0.4846*) resulted in greater plant height than *B. japonicum* alone. Leaf area was higher for bacterial treatments with SL42 and SL48 than the control under optimal conditions and treatments of SL48 and SL42+SL48 under salt-stressed conditions, albeit not significant (Figure 4.3). When co-inoculated, *B. japonicum* +SL42 (*P = 0.3312*) and *B. japonicum*+SL42+SL48 (*P = 0.3471*) resulted in higher leaf area than *B. japonicum* under optimal conditions. Similarly, *B. japonicum*+SL42 (*P = 0.0464*), *B. japonicum*

+SL48 (*P = 0.2547*) and *B. japonicum*+SL42+SL48 (*P = 0.3157*) had higher leaf area than the *B. japonicum* alone under salt stress.

Shoot fresh weight was significantly increased by treatment with SL42 (*P = 0.0293*) and SL48 (*P = 0.0496*) under optimal conditions and treatment with SL42+SL48 (*P = 0.2091*) under salt stress than the control (Figure 4.4). Co-inoculation treatment of *B. japonicum*+SL42+SL48 increased shoot fresh weight under optimal (*P = 0.2356*) and salt stress (*P = 0.363*) conditions. However, *B. japonicum*+SL42 had significantly higher (*P = 0.0227*) shoot fresh weight under salt stress than the *B. japonicum* alone. Shoot dry weight was greater for bacterial treatments with SL42 and SL48 than the control under optimal and salt-stressed conditions (Figure 4.5). Treatment with SL42+SL48 significantly increased (*P = 0.0144*) shoot dry weight compared to the control under salt stress. The co-inoculation treatments, *B. japonicum*+SL42 (*P=0.1209*) and *B. japonicum* +SL42+SL48 (*P = 0.0631*) resulted in higher shoot dry weight than *B. japonicum* under optimal conditions. The treatment of *B. japonicum*+SL48 had significantly increased (*P = 0.039*) shoot dry weight and other co-inoculation treatments, *B. japonicum*+SL42 (*P=0.1128*) and *B. japonicum* +SL42+SL48 (*P = 0.1958*), also increased shoot dry weight compared to the *B. japonicum* alone under salt stress.

Overall, under optimal conditions, SL42 and SL48 bacterial treatments improved plant growth, whereas under salt stress co-inoculation with SL42+SL48 significantly increased plant growth compared to the control treatment. Growth variables were higher in the *B. japonicum* inoculated treatments than those that had no *B. japonicum*, because of biological nitrogen fixation, which increased shoot N content and boosted vegetative growth. Plant growth was increased by the co-inoculation of *B. japonicum* with SL42 and SL48 compared to *B. japonicum* by itself. Although differences between the co-inoculation treatments were not statistically significant under optimal conditions, they were significant under salt stress.

Figure 4.1. Soybean plants at 28th DAP grown in controlled environment under optimal and salt-stressed conditions.
The treatments are **(A)** control **(B)** SL42 **(C)** SL48 **(D)** SL42+SL48 **(E)** Bj **(F)** Bj+SL42 **(G)** Bj+SL48 **(H)** Bj+SL42+SL48. The seeds were treated with 10 mM $MgSO_4$ or bacterized with the *Rhizobium* sp. SL42, *Hydrogenophaga* sp. SL48 or co-inoculated and (B) Seeds were bacterized with *Bradyrhizobium japonicum* (Bj) as control or the strains were co-inoculated with Bj.

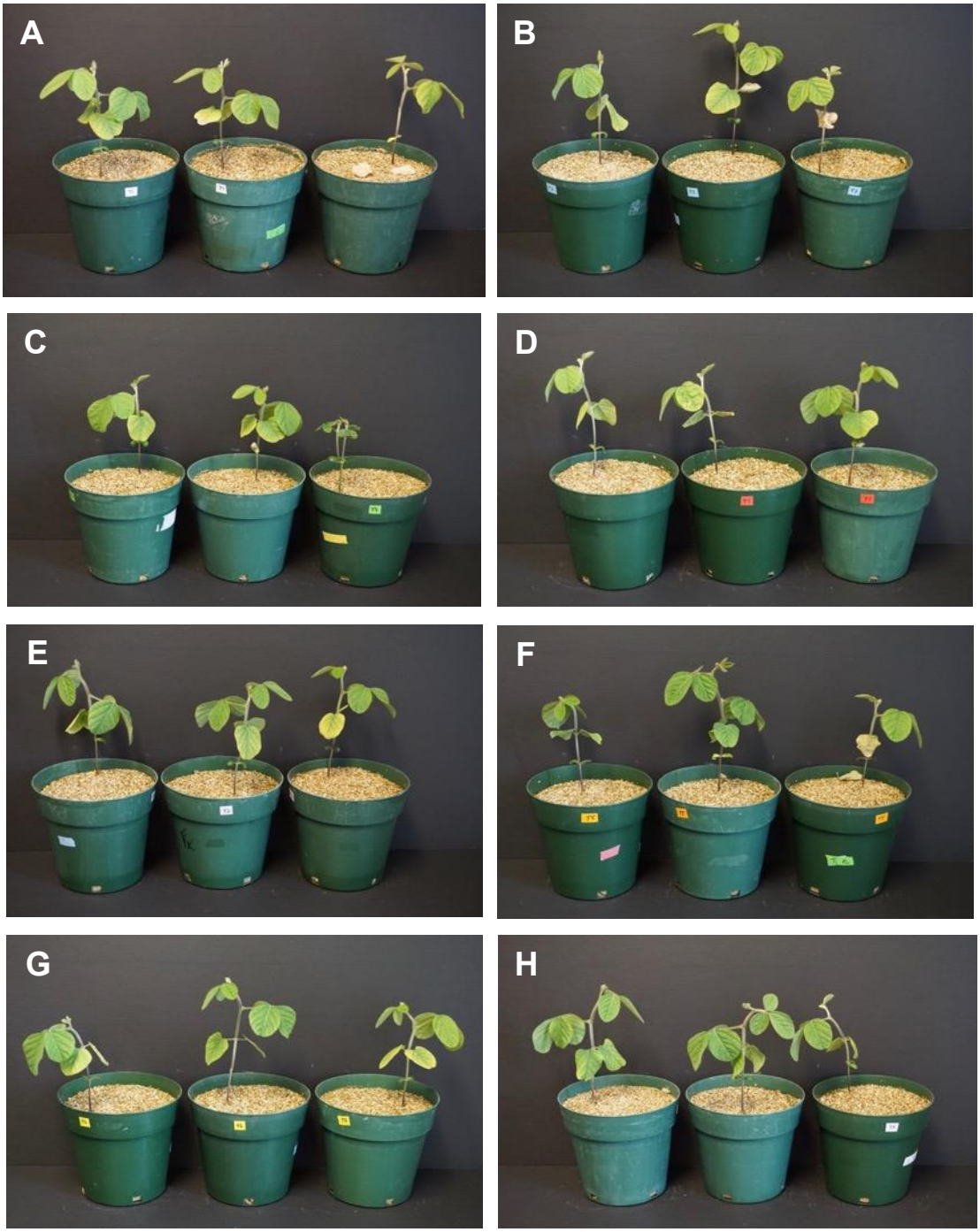

Figure 4.1. (cont.) Soybean plants at 28th DAP grown in controlled environment under optimal and salt-stressed conditions. The treatments are **(A)** control **(B)** SL42 **(C)** SL48 **(D)** SL42+SL48 **(E)** Bj **(F)** Bj+SL42 **(G)** Bj+SL48 **(H)** Bj+SL42+SL48. The seeds were treated with 10 mM $MgSO_4$ or bacterized with the *Rhizobium* sp. SL42, *Hydrogenophaga* sp. SL48 or co-inoculated and (B) Seeds were bacterized with *Bradyrhizobium japonicum* (Bj) as control or the strains were co-inoculated with Bj.

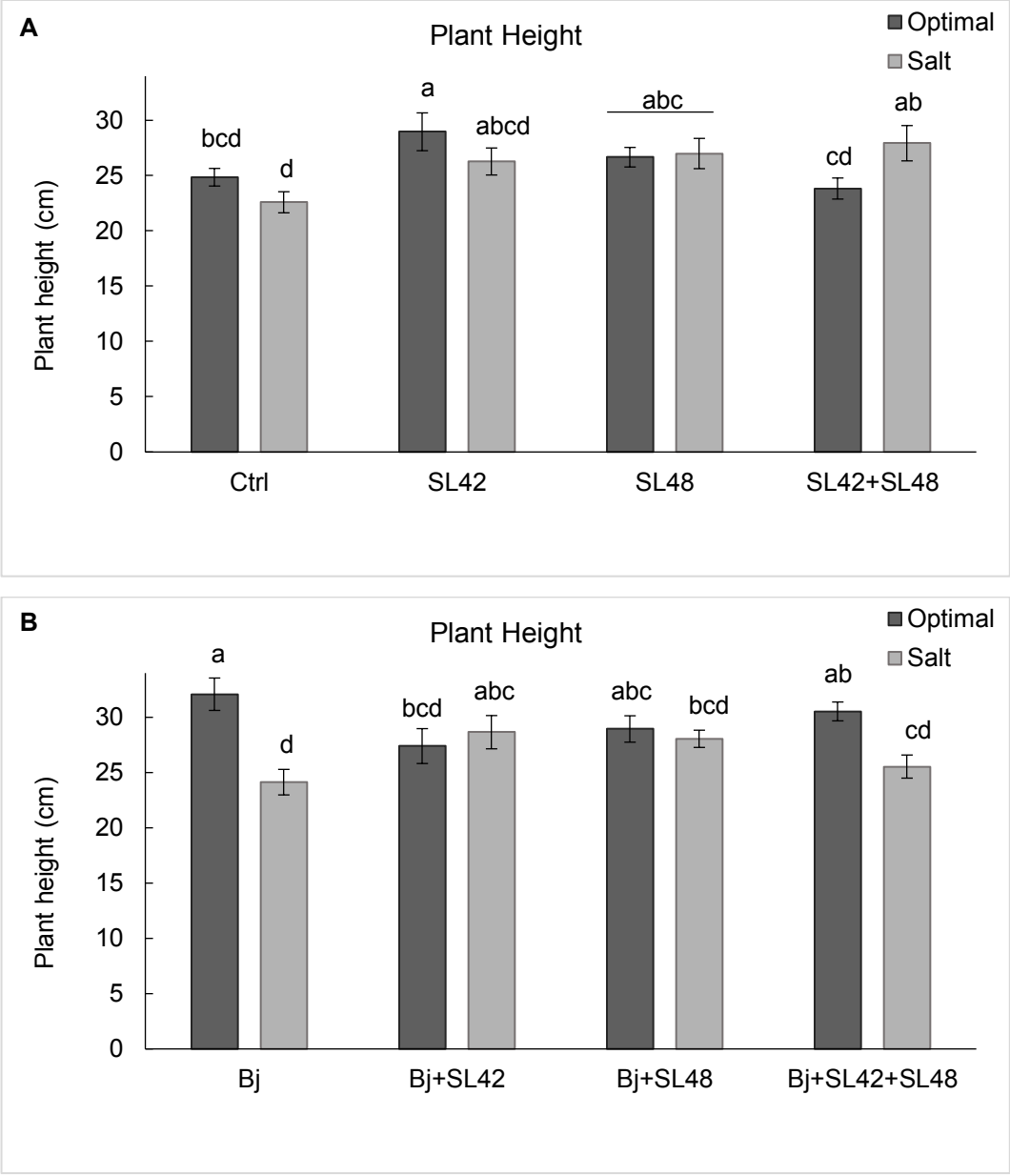

Figure 4.2. Height of soybean plants measured at 28th DAP under optimal and salt stress conditions.
(A) The seeds were treated with 10 mM $MgSO_4$ or bacterized with the *Rhizobium* sp. SL42, *Hydrogenophaga* sp. SL48 or co-inoculated and **(B)** Seeds were bacterized with *Bradyrhizobium japonicum* (Bj) as control or the strains were co-inoculated with Bj. Values represent mean ± SE (n=12).

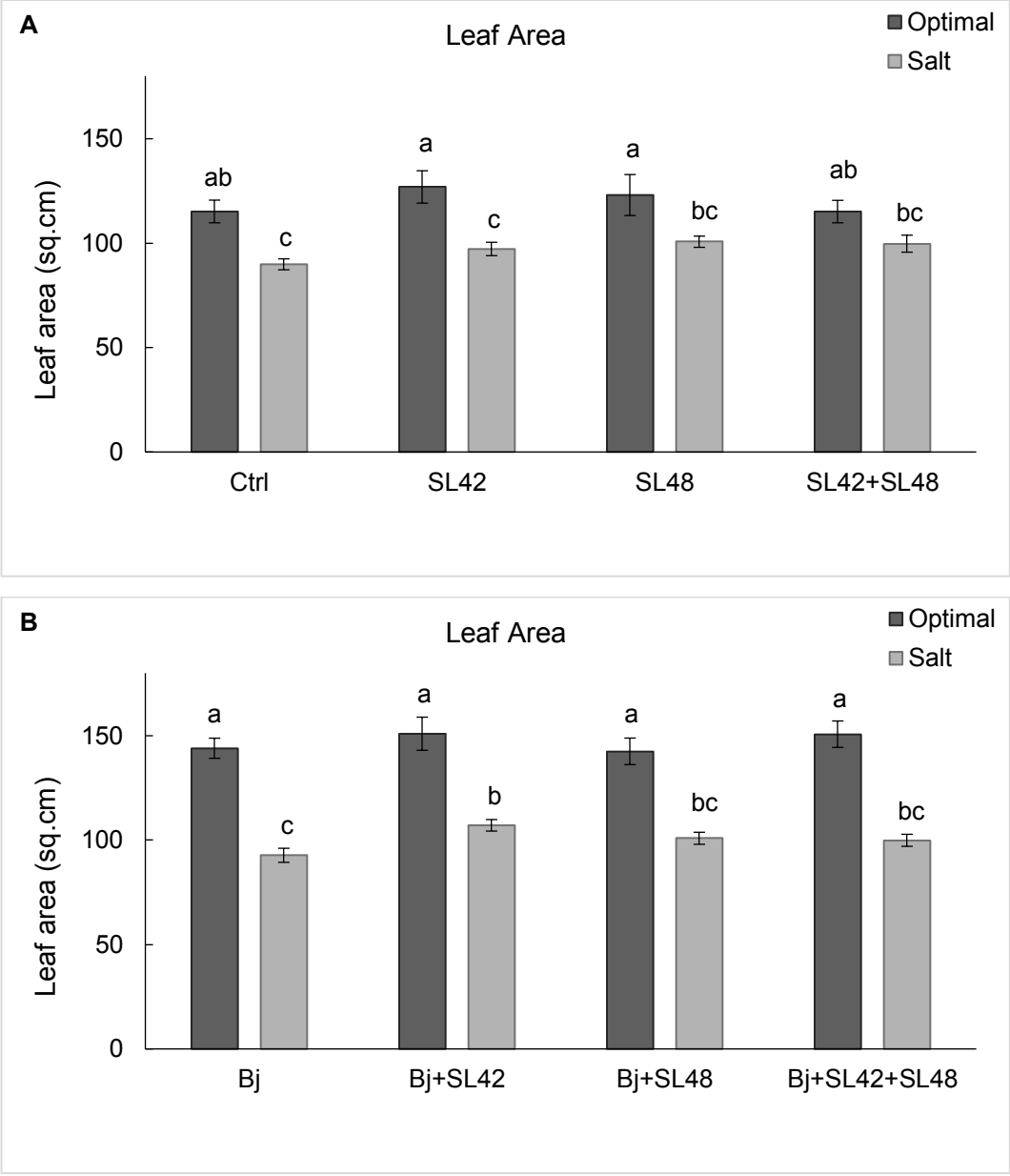

Figure 4.3. Leaf area of soybean plants measured at 28th DAP under optimal and salt stress conditions.
(A) The seeds were treated with 10 mM $MgSO_4$ or bacterized with the *Rhizobium* sp. SL42, *Hydrogenophaga* sp. SL48 or co-inoculated and **(B)** Seeds were bacterized with *Bradyrhizobium japonicum* (Bj) as control or the strains were co-inoculated with Bj. Values represent mean ± SE (n=12).

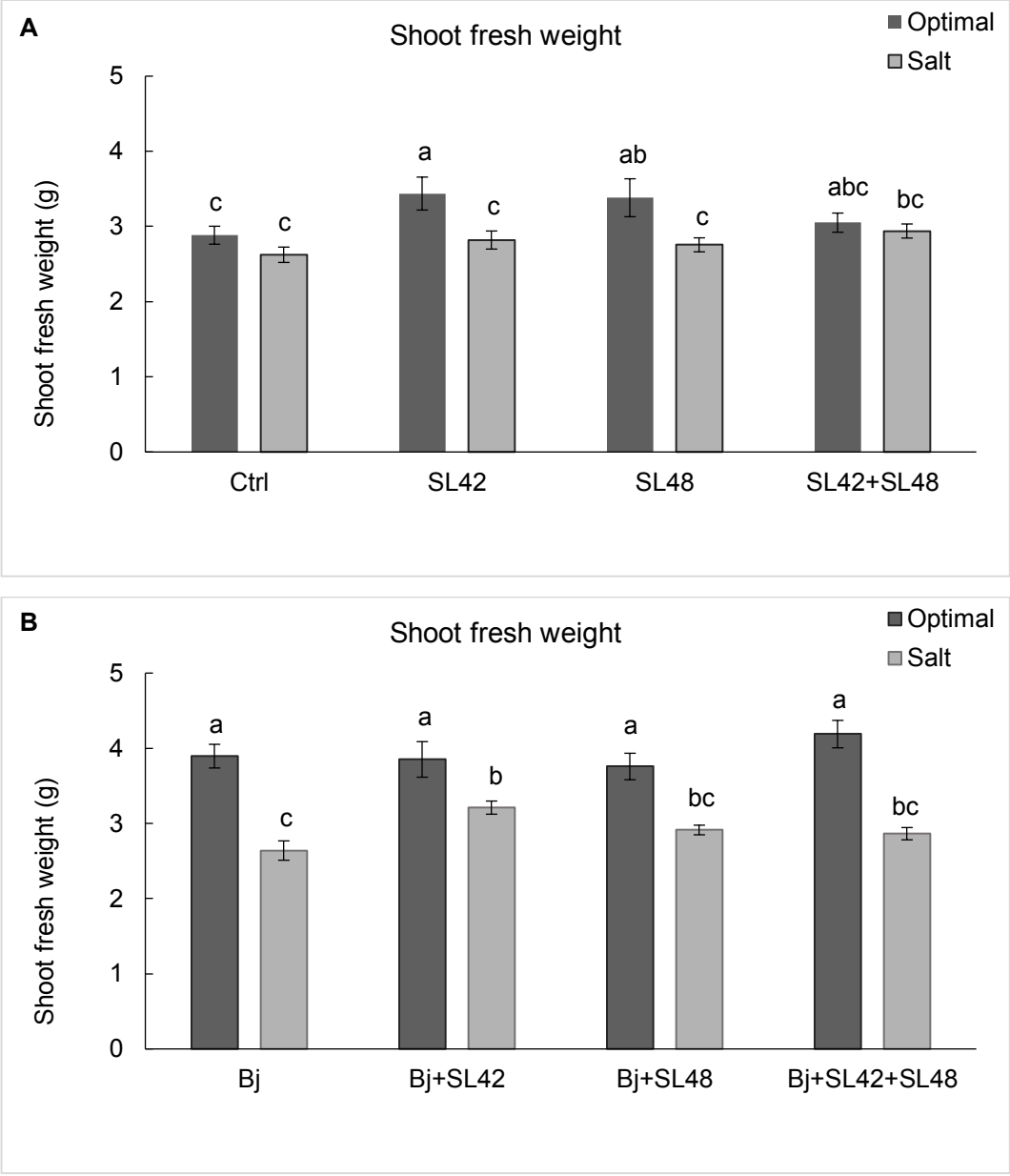

Figure 4.4. Shoot fresh weight of soybean plants measured at 28th DAP under optimal and salt stress conditions.
(A) The seeds were treated with 10 mM $MgSO_4$ or bacterized with the *Rhizobium* sp. SL42, *Hydrogenophaga* sp. SL48 or co-inoculated and **(B)** Seeds were bacterized with *Bradyrhizobium japonicum* (Bj) as control or the strains were co-inoculated with Bj. Values represent mean ± SE (n=12).

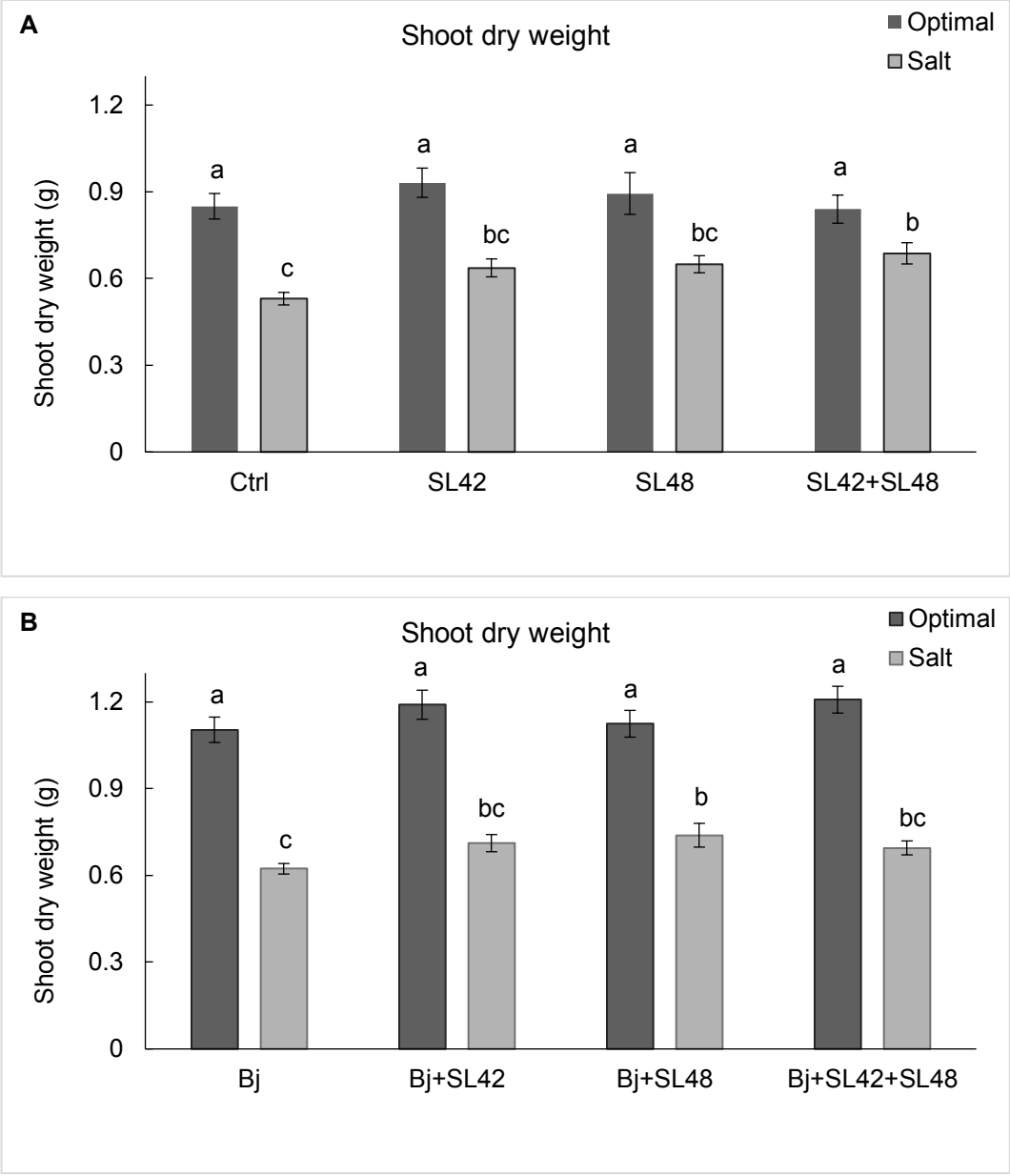

Figure 4.5. Shoot dry weight of soybean plants measured at 28th DAP under optimal and salt stress conditions.
(A) The seeds were treated with 10 mM $MgSO_4$ or bacterized with the *Rhizobium* sp. SL42, *Hydrogenophaga* sp. SL48 or co-inoculated and **(B)** Seeds were bacterized with *Bradyrhizobium japonicum* (Bj) as control or the strains were co-inoculated with Bj. Values represent mean ± SE (n=12).

Elemental analysis revealed the nutrient composition of the soybean leaf tissues (Table 4.2). Salt-stressed plants had slightly higher N concentrations and markedly higher concentrations of P, K and Na, but lower Ca concentration than the optimally grown plants. The difference between treatments in nutrient elemental concentrations under optimal or salt stress conditions was generally slight. Treatment with SL42 resulted in higher P concentration under optimal conditions. Calcium concentration was lesser in the treatments with *B. japonicum* and SL42 than in the other treatments under optimal conditions. Potassium concentration was increased with bacterial inoculation under optimal and salt stress conditions. Due to high Na^+ concentration, the K^+/Na^+ ratio was lower under salt stress, even though K concentration was higher. Treatments of SL42 and *B. japonicum* +SL42 had lower Na^+ content under salt stress and a higher K^+/Na^+ ratio.

Table 4.2. Elemental analysis of major nutrients of soybean shoot tissue at 28th DAP under optimal and salt stress conditions.

Treatments	Nitrogen (mg. g^{-1})		Phosphorous (mg. g^{-1})		Calcium (mg. g^{-1})	
	Optimal	Salt	Optimal	Salt	Optimal	Salt
Ctrl	15.43 ±2.44	18.29 ±0.86	0.95 ±0.09	1.48 ±0.17	7.23 ±0.24	4.84 ±0.36
SL42	17.33 ±2.32	18.48 ±1.56	1.21 ±0.23	1.55 ±0.16	6.65 ±0.89	4.94 ±0.37
SL48	15.62 ±2.62	17.87 ±1.42	0.99 ±0.07	1.56 ±0.15	7.68 ±0.59	4.89 ±0.18
SL42+SL48	17.86 ±2.48	17.56 ±1.35	0.98 ±0.09	1.48 ±0.12	7.11 ±0.15	4.54 ±0.39
Bj	20.06 ±1.02	20.42 ±0.80	0.83 ±0.09	1.40 ±0.12	6.56 ±0.38	4.76 ±0.21
Bj+SL42	21.46 ±0.95	21.99 ±1.58	0.87 ±0.08	1.49 ±0.17	6.66 ±0.54	4.57 ±0.23
Bj+SL48	21.37 ±0.64	22.07 ±1.16	0.94 ±0.11	1.51 ±0.20	6.55 ±0.40	4.64 ±0.20
Bj+SL42+ SL48	21.22 ±0.83	21.73 ±0.73	0.86 ±0.06	1.40 ±0.15	6.88 ±0.32	4.62 ±0.16
Treatments	Potassium (mg. g^{-1})		Sodium (mg. g^{-1})		K:Na	
	Optimal	Salt	Optimal	Salt	Optimal	Salt
Ctrl	10.48 ±1.59	21.31 ±1.63	0.05 ±0.03	0.31 ±0.04	213.42	68.89
SL42	11.37 ±1.26	23.22 ±2.40	0.06 ±0.01	0.27 ±0.02	203.52	85.63
SL48	11.31 ±1.03	23.51 ±1.69	0.06 ±0.02	0.29 ±0.02	186.71	81.62
SL42+SL48	10.59 ±1.38	21.41 ±1.17	0.04 ±0.02	0.26 ±0.07	246.65	82.20
Bj	9.81 ±1.25	22.51 ±2.81	0.08 ±0.05	0.39 ±0.05	116.98	57.96
Bj+SL42	10.11 ±1.05	20.13 ±1.36	0.07 ±0.02	0.32 ±0.06	151.88	63.27
Bj+SL48	10.69 ±1.13	22.45 ±2.41	0.06 ±0.03	0.42 ±0.07	187.87	53.77
Bj+SL42+ SL48	10.09 ±1.12	20.93 ±1.61	0.05 ±0.03	0.35 ±0.02	199.81	59.83

Values represent mean ± SE (n=4). Bj – *Bradyrhizobium japonicum* 532C, SL42 – *Rhizobium* sp. SL42, SL48 – *Hydrogenophaga* sp. SL48

4.4.2 Proteomic analysis

4.4.2.1 Quantitative spectra of soybean leaf proteome

To understand the role of the inoculated bacteria on the metabolism and physiology of optimal and salt-stressed soybean plants, a LC-MS/MS based proteome profiling of the total leaf protein extracted was performed. Based on the quantitative value of the identified spectra, the treatment contrasts were analyzed for fold-change after normalization (≥ 1.2) and Fisher-exact test ($P \leq 0.05$) to narrow down proteins that were relatively up- or down-regulated. Some of the key proteins might be missed from the analysis due to the very stringent criteria but this allowed for focusing on the proteins that were differentially expressed. Also, for ease of functional interpretation, proteins that were different between the control and the other treatments were analyzed instead of all possible contrasts. The number of identified proteins was higher under salt-stressed than under optimum plant growth conditions and they were classified into known, predicted, probable and uncharacterized proteins.

A number of proteins that play an important role in plant growth, development and stress tolerance were significantly upregulated by the bacterial treatments compared to the control (Tables 4.3-4.6). The commonly upregulated proteins related to cellular function and metabolism included ATP synthases, chlorophyll a-b binding proteins, glyceraldehyde-3-phosphate dehydrogenase A subunit, PSI subunit psaK, RubisCO small and large chains, thioredoxins in the chloroplast, glycine dehydrogenase, NADH dehydrogenases, succinate dehydrogenases in the mitochondria, chaperonins, cytoskeleton proteins (actin and tubulin), peroxisomal enzymes, ribosomal subunits and proteosome regulatory subunits. The upregulated proteins involved in phytohormone signaling and stress-responses comprised aconitate hydratase, aquaporins, catalases, glutathione S-transferases, heat shock proteins, lipoxygenases, multicystatin, superoxide dismutases and transketolases. Proteins that were participating in the biosynthesis of alkaloids, carotenes, flavonoids, isoflavonoids, soyasaponins and other secondary metabolites were also upregulated. Interestingly, when the strains were co-inoculated with *B. japonicum* under salt stress, specific proteins were upregulated commonly across the treatments relative to the *B. japonicum* control including PSII protein H, Calvin cycle CP12-2, cucumisin, gibberellin-regulated protein 6 precursor, heme binding 2 and topless-related proteins.

Proteins involved in amino acids, nucleic acids, sugars and starch biosynthesis, nutrient assimilation and mobilization and regulation of plant growth and developmental processes such as

ABC transporters, alpha-amylase inhibitor/lipid transfer/seed storage family protein precursor, arginosuccinate lyase, asparagine synthetase, carbamoyl-phosphate synthases, ferredoxins, ferritins, glucose-6-phosphate 1-dehydrogenase, glutamate synthetase, kunitz-type trypsin inhibitor KTI1-like, peroxisomal citrate synthase, polyadenylate-binding proteins, PEP carboxylase, phosphoglycerate kinase, pyruvate kinases and subtilisin-like proteases were upregulated (Tables 4.7-4.10). A comparison of quantitative spectra of major proteins (photosynthesis, antioxidants, and phytohormonal) among treatments under optimal and salt-stressed conditions is given in Table 4.11. Moreover, there were unique proteins that were only expressed in the bacterial treatments and not in the controls, such as carboxyl esterase 8, inactive PAP, linoleate 9S-lipoxygenase-2 and 5, lipid transfer protein EARLI 1-like, lysM domain-containing protein, starch synthase enolase, and stress-induced SAM22 (Appendix B, Supplementary Tables 4.1-4.12). The fold change of significantly downregulated proteins was ≤ 1.0 and so, these were not considered.

Table 4.3. Fold change of selected proteins that were commonly upregulated by the treatments SL42, SL48 and SL42+SL48 relative to control under optimal condition.

	Protein	SL42	SL48	SL42+ SL48
1	Cluster of asparagine synthetase 2	4.5	13	9.5
2	Cluster of glucose-6-phosphate dehydrogenase	3.3		3.3
3	Cluster of PREDICTED: glutathione S-transferase GST 9 isoform X1	1.4	1.4	1.4
4	Cluster of S-formylglutathione hydrolase		3.2	2.6
5	NADH dehydrogenase subunit 7 (chloroplast)	1.5		1.5
6	PREDICTED: thioredoxin H1	1.3	1.3	
7	PREDICTED: UDP-glucose flavonoid 3-O-glucosyltransferase 7-like		1.7	1.9
8	prolyl endopeptidase	1.4	1.5	1.8
9	ribulose bisphosphate carboxylase small chain 4	1.2	1.1	1.3
10	soyasaponin III rhamnosyltransferase		1.3	1.5

Values represent fold change of quantitative spectra relative to control ($P \leq 0.05$; n=3).
SL42 – *Rhizobium* sp. SL42, SL48 – *Hydrogenophaga* sp. SL48

Table 4.4. Fold change of selected proteins that were commonly upregulated by the treatments SL42, SL48 and SL42+SL48 relative to control under salt stress.

	Protein	SL42	SL48	SL42+ SL48
1	argininosuccinate lyase, chloroplastic isoform X1	2		2
2	Cluster of alpha-amylase inhibitor/lipid transfer/seed storage family protein precursor		5.3	4
3	Cluster of clathrin heavy chain	1.3		1.3
4	Cluster of coatomer subunit delta	2.9	2.5	
5	Cluster of DEAD-box ATP-dependent RNA helicase 3, chloroplastic		1.8	2
6	Cluster of dihydrolipoyllysine-residue acetyltransferase component 4 of pyruvate dehydrogenase complex, chloroplastic isoform X2		2.3	2.4
7	Cluster of glyceraldehyde-3-phosphate dehydrogenase A subunit	1.3	1.4	1.3
8	Cluster of glycine dehydrogenase (decarboxylating), mitochondrial		1.2	1.3
9	Cluster of HSP90 superfamily protein isoform X1	1.4	1.4	1.3
10	Cluster of linoleate 13S-lipoxygenase 2-1, chloroplastic		1.8	1.8
11	Cluster of NADH dehydrogenase [ubiquinone] iron-sulfur protein 1, mitochondrial		1.6	1.2
12	Cluster of peroxisomal fatty acid beta-oxidation multifunctional protein AIM1	1.5	1.4	
13	Cluster of proline-rich protein precursor	10	7	5.7
14	Cluster of S-adenosylmethionine synthase		1.2	1.3
15	Cluster of SKP1-like protein 1A isoform X1		2.2	1.9
16	endoplasmin homolog isoform X1	1.4	1.4	1.3
17	photosystem I reaction center subunit psaK	2.3	2.7	3.2
18	PREDICTED: auxin-binding protein ABP19a-like	2.3	2.1	1.9
19	PREDICTED: peroxisomal citrate synthase isoform X1	4.2	4.5	
20	succinate dehydrogenase [ubiquinone] flavoprotein subunit 1, mitochondrial		1.6	1.7
21	topless-related protein 1 isoform X1		2.2	1.8
22	tripeptidyl-peptidase 2 isoform X1		2.2	2.4

Values represent fold change of quantitative spectra relative to control ($P \leq 0.05$; n=3).
SL42 – *Rhizobium* sp. SL42, SL48 – *Hydrogenophaga* sp. SL48

Table 4.5. Fold change of selected proteins that were commonly upregulated by the treatments Bj+SL42, Bj+SL48 and Bj+SL42+SL48 relative to Bj (control) under optimal condition.

	Protein	Bj+SL42	Bj+SL48	Bj+SL42 +SL48
1	ATPase ARSA1		1.9	1.8
2	Cluster of adenosylhomocysteinase-like		1.3	1.3
3	Cluster of bifunctional monothiol glutaredoxin-S16, chloroplastic		2	1.9
4	Cluster of catalase		1.2	1.3
5	Cluster of chlorophyll a-b binding protein		1.4	1.3
6	Cluster of glyceraldehyde-3-phosphate dehydrogenase A subunit	1.2	1.8	1.6
7	Cluster of glycine dehydrogenase (decarboxylating), mitochondrial	1.2	1.3	1.2
8	Cluster of isoflavone reductase homolog 2	3.1	3.5	3.6
9	Cluster of isopentenyl-diphosphate Delta-isomerase I	1.7	2	2.5
10	Cluster of kunitz-type trypsin inhibitor KTI1-like	1.6	1.8	
11	Cluster of linoleate 9S-lipoxygenase-4		1.2	1.2
12	Cluster of peptide methionine sulfoxide reductase B5	6.5	6.5	6.2
13	Cluster of PREDICTED: multicystatin	2.1	2.3	1.9
14	Cluster of proline-rich protein precursor		19	6.3
15	Cluster of S-adenosylmethionine synthase	1.2	1.4	1.3
16	Cluster of soyasapogenol B glucuronide galactosyltransferase-like	1.4	1.7	1.4
17	ferredoxin-A	2.1	2.9	3.7
18	glutamine synthetase precursor		1.2	1.2
19	ketol-acid reductoisomerase, chloroplastic	1.3	1.3	
20	KS-type dehydrin SLTI629		4.1	6
21	photosystem I reaction center subunit psaK	1.7	2.8	2.9
22	polyphenol oxidase A1, chloroplastic	2.4	2.5	2.4
23	PREDICTED: auxin-binding protein ABP19a-like	1.6	2.3	1.8
24	PREDICTED: UDP-glucose flavonoid 3-O-glucosyltransferase 7-like	1.7	1.9	1.6
25	protoporphyrinogen oxidase 1, chloroplastic		1.7	1.5
26	ribulose bisphosphate carboxylase small chain 1	1.3	1.4	1.3
27	soyasaponin III rhamnosyltransferase	1.4	1.5	
28	subtilisin-like protease Glyma18g48580 isoform X1	2.9	2.3	2.4

	Protein	Bj+SL42	Bj+SL48	Bj+SL42 +SL48
29	succinate dehydrogenase [ubiquinone] flavoprotein subunit 1, mitochondrial		1.8	1.8
30	superoxide dismutase [Cu-Zn], chloroplastic	2.5	2.3	2.4

Values represent fold change of quantitative spectra relative to control ($P \leq 0.05$; n=3). Bj – *Bradyrhizobium japonicum* 532C, SL42 – *Rhizobium* sp. SL42, SL48 – *Hydrogenophaga* sp. SL48

Table 4.6. Fold change of selected proteins that were commonly upregulated by the treatments Bj+SL42, Bj+SL48 and Bj+SL42+SL48 relative to Bj (control) under salt stress.

	Protein	Bj+SL42	Bj+SL48	Bj+SL42 +SL48
1	Cluster of 1-aminocyclopropane-1-carboxylate oxidase	1.6	1.7	
2	Cluster of 15-cis-phytoene desaturase, chloroplastic/chromoplastic	1.6	2.2	1.6
3	Cluster of 4-alpha-glucanotransferase DPE2		1.4	1.4
4	Cluster of aconitate hydratase, cytoplasmic	1.3	1.4	
5	Cluster of calvin cycle protein CP12-2		1.4	1.8
6	Cluster of carbamoyl-phosphate synthase large chain, chloroplastic	1.6	1.6	
7	Cluster of catalase	1.3	1.3	1.2
8	Cluster of DEAD-box ATP-dependent RNA helicase 56	1.5		1.5
9	Cluster of gibberellin-regulated protein 6 precursor		1.6	1.2
10	Cluster of glutamine synthetase precursor isoform X1		1.3	1.3
11	Cluster of glyceraldehyde-3-phosphate dehydrogenase A subunit	1.3	1.1	
12	Cluster of glycine dehydrogenase (decarboxylating), mitochondrial	1.2	1.1	1.2
13	Cluster of NADP-dependent malic enzyme	1.4	1.3	1.2
14	Cluster of probable 3-hydroxyisobutyrate dehydrogenase-like 1, mitochondrial	2.5	2	
15	Cluster of proline-rich protein precursor	3.3	2.6	1.8
16	Cluster of ribulose bisphosphate carboxylase/oxygenase activase	1.1	1.2	1.1
17	cucumisin	1.6	1.8	1.9
18	glucose-6-phosphate 1-dehydrogenase		1.7	1.5
19	heme-binding protein 2		1.3	1.6
20	MFP1 attachment factor 1	4.3	4.3	

	Protein	Bj+SL42	Bj+SL48	Bj+SL42 +SL48
21	NAD(P)H-quinone oxidoreductase subunit N	6	6.5	5
22	photosystem I reaction center subunit psaK	1.6	1.4	1.5
23	photosystem II protein H		1.3	1.9
24	polygalacturonase inhibitor 1-like protein precursor	3.5	4.5	2.9
25	PREDICTED: UDP-glucose flavonoid 3-O-glucosyltransferase 7-like	2.4	2.9	2.6
26	probable UDP-arabinopyranose mutase 1		1.5	1.4
27	protein TOPLESS		2.2	2.2
28	protein transport protein Sec24-like At4g32640		3.2	4.6
29	ribulose bisphosphate carboxylase small chain 4	1.4	1.5	1.2
30	ribulose-1,5-bisphosphate carboxylase/oxygenase large subunit	1.2	1.2	1.2
31	topless-related protein 3		4.3	3.3
32	topless-related protein 4 isoform X2		3.8	3
33	UDP-glycosyltransferase 84B2	3.4	3.2	3.2
34	UDP-sulfoquinovose synthase, chloroplastic	2		1.7

Values represent fold change of quantitative spectra relative to control ($P \leq 0.05$; n=3). Bj – *Bradyrhizobium japonicum* 532C, SL42 – *Rhizobium* sp. SL42, SL48 – *Hydrogenophaga* sp. SL48

Table 4.7. Proteins that were specifically upregulated by treatments SL42, SL48 and SL42+SL48 relative to control under optimal condition.

SL42	**SL42+SL48**
• Cluster of matrix metalloproteinase precursor • isoflavone reductase-like protein	• Cluster of aconitate hydratase 1 • Cluster of adenosylhomocysteinase • Cluster of catalase • Cluster of chlorophyll a-b binding protein P4, chloroplastic • Cluster of fumarate hydratase 1, mitochondrial • Cluster of glyceraldehyde-3-phosphate dehydrogenase A subunit • Cluster of glycine dehydrogenase (decarboxylating), mitochondrial • Cluster of linoleate 9S-lipoxygenase-4 • Cluster of peroxisomal (S)-2-hydroxy-acid oxidase GLO1-like • Cluster of phosphoenolpyruvate carboxylase • indole-3-glycerol phosphate synthase, chloroplastic • NAD(P)H-quinone oxidoreductase subunit N, chloroplastic • photosystem I reaction center subunit psaK, chloroplastic • protein PELPK1 • ribulose-1,5 bisphosphate carboxylase/oxygenase large subunit N-methyltransferase, chloroplastic • soyasapogenol B glucuronide galactosyltransferase-like
SL48	
• 26S proteasome regulatory subunit 4 homolog A • Cluster of clathrin heavy chain 2 • stress-induced protein SAM22 • UDP-glucuronic acid decarboxylase 2	

Fold change ≥ 1.2 ($P \leq 0.05$; n=3). SL42 – *Rhizobium* sp. SL42, SL48 – *Hydrogenophaga* sp. SL48

Table 4.8. Proteins that were specifically upregulated by treatments SL42, SL48 and SL42+SL48 relative to control under salt stress.

SL42	SL42+SL48
• 12-oxophytodienoate reductase 3 • Cluster of ABC transporter C family member 4 • Cluster of alpha-glucan water dikinase, chloroplastic isoform X1 • Cluster of calnexin homolog precursor • Cluster of chaperonin CPN60-2, mitochondrial • Cluster of citrate synthase, glyoxysomal • Cluster of IAA-amino acid hydrolase ILR1-like 4 • osmotin-like protein • PREDICTED: ferredoxin-A-like • protein ROOT HAIR DEFECTIVE 3 homolog 2	• aquaporin PIP2-7 • Cluster of aconitate hydratase, cytoplasmic • Cluster of carbamoyl-phosphate synthase large chain, chloroplastic • Cluster of chlorophyll a/b-binding protein • Cluster of diphosphomevalonate decarboxylase MVD2, peroxisomal • Cluster of magnesium-protoporphyrin IX monomethyl ester [oxidative] cyclase, chloroplastic • Cluster of plastidial pyruvate kinase 2 • Cluster of PREDICTED: zinc finger BED domain-containing protein DAYSLEEPER-like • Cluster of protochlorophyllide reductase, chloroplastic • Cluster of subtilisin-like protease SBT1.6 • D-3-phosphoglycerate dehydrogenase 2, chloroplastic • fatty acid hydroperoxide lyase, chloroplastic • heat shock 70 kDa protein 14 isoform X1 • KS-type dehydrin SLTI629 • NADH dehydrogenase subunit 7 (chloroplast) • pyruvate dehydrogenase E1 component subunit beta-3, chloroplastic • pyruvate kinase 1, cytosolic isoform X1 • ribulose-1,5-bisphosphate carboxylase/oxygenase large subunit (chloroplast) • soyasaponin III rhamnosyltransferase • succinate dehydrogenase [ubiquinone] iron-sulfur subunit 2, mitochondrial
SL48	
• ATP synthase CF1 beta subunit (chloroplast) • chlorophyll a-b binding protein 3, chloroplastic • Cluster of cytosolic chaperonin • Cluster of gamma carbonic anhydrase 1, mitochondrial • Cluster of heat shock 70 kDa protein 14 • Cluster of phosphoglucomutase, chloroplastic • nifU-like protein 4, mitochondrial • pullulanase 1, chloroplastic • succinate--CoA ligase [ADP-forming] subunit alpha, mitochondrial • xanthoxin dehydrogenase	

Fold change ≥ 1.2 ($P \leq 0.05$; n=3). SL42 – *Rhizobium* sp. SL42, SL48 – *Hydrogenophaga* sp. SL48

Table 4.9. Proteins that were specifically upregulated by treatments Bj+SL42, Bj+SL48 and Bj+SL42+SL48 relative to Bj (control) under optimal condition.

Bj+SL42	**Bj+ SL42+SL48**
• Cluster of isoamylase 3, chloroplastic isoform X1 • Cluster of ribosomal protein L11 family protein • Cluster of subtilisin-like protease Glyma18g48580 • kunitz family trypsin and protease inhibitor protein precursor • peptide methionine sulfoxide reductase B5 • PREDICTED: peptidyl-prolyl cis-trans isomerase 1-like • protein PELPK1 • succinate dehydrogenase [ubiquinone] iron-sulfur subunit 2, mitochondrial	• carbonic anhydrase 2 • chaperonin CPN60-like 2, mitochondrial • Cluster of carbamoyl-phosphate synthase large chain, chloroplastic • Cluster of PREDICTED: zinc finger BED domain-containing protein DAYSLEEPER-like • Cluster of pyrophosphate-energized vacuolar membrane proton pump • Cluster of transketolase, chloroplastic • glutathione S-transferase L3 • NAD(P)H-quinone oxidoreductase subunit N, chloroplastic • peroxisomal 3-ketoacyl-CoA thiolase • protochlorophyllide reductase, chloroplastic • putative plastocyanin • ribulose-1,5-bisphosphate carboxylase/oxygenase large subunit
Bj+SL48	
• 15-cis-phytoene desaturase, chloroplastic/chromoplastic • aquaporin PIP2-10 • Cluster of DEAD-box ATP-dependent RNA helicase 3, chloroplastic • Cluster of linoleate 13S-lipoxygenase 2-1, chloroplastic • Cluster of serine glyoxylate aminotransferase 3 isoform X1 • gamma-glutamyl hydrolase precursor • indole-3-glycerol phosphate synthase, chloroplastic • iron-superoxide dismutase • malonyl-CoA:isoflavone 7-O-glucoside-6"-O-malonyltransferase • probable carboxylesterase 2 • ribulose bisphosphate carboxylase/oxygenase activase • UDP-glucosyl transferase 73B2	

Fold change ≥ 1.2 ($P \leq 0.05$; n=3). Bj – *Bradyrhizobium japonicum* 532C, SL42 – *Rhizobium* sp. SL42, SL48 – *Hydrogenophaga* sp. SL48

Table 4.10. Proteins that were specifically upregulated by treatments Bj+SL42, Bj+SL48 and Bj+SL42+SL48 relative to Bj (control) under salt stress.

Bj+SL42	**Bj +SL48**
• 12-oxophytodienoate reductase 3 • abscisate beta-glucosyltransferase • caffeic acid 3-O-methyltransferase-like • Cluster of ferritin • Cluster of iron-superoxide dismutase • Cluster of pyrophosphate--fructose 6-phosphate 1-phosphotransferase subunit alpha • ferredoxin-A • harpin binding protein 1 • putative glucose-6-phosphate 1-epimerase • ruBisCO large subunit-binding protein subunit beta, chloroplastic • stress-induced protein SAM22 • superoxide dismutase [Fe], chloroplastic precursor	• alpha-amylase inhibitor/lipid transfer/seed storage family protein precursor • amidase 1 isoform X1 • Cluster of adenylosuccinate synthetase 2, chloroplastic • Cluster of peroxisomal glycolate oxidase isoform X1 • Cluster of pyruvate decarboxylase 2 • glutamate decarboxylase • lipoxygenase • peroxisomal (S)-2-hydroxy-acid oxidase GLO1-like • phi class glutathione S-transferase • phosphoenolpyruvate carboxylase 4 • PREDICTED: auxin-binding protein ABP19a-like • probable glutathione S-transferase • soyasapogenol B glucuronide galactosyltransferase • soyasaponin III rhamnosyltransferase • trifunctional UDP-glucose 4,6-dehydratase/UDP-4-keto-6-deoxy-D-glucose 3,5-epimerase/UDP-4-keto-L-rhamnose-reductase RHM1 • seed linoleate 9S-lipoxygenase
Bj+ SL42+SL48	
• carbamoyl-phosphate synthase small chain, chloroplastic • carbonic anhydrase 2 • Cluster of ATP synthase subunit b', chloroplastic • Cluster of gamma-tocopherol methyltransferase • Cluster of PREDICTED: phosphoglycerate kinase, cytosolic • Cluster of stromal 70 kDa heat shock-related protein, chloroplastic • granule bound starch synthase Ia • NADH dehydrogenase subunit 7 (chloroplast) • phosphoglycerate kinase, cytosolic • photosystem I subunit VII (chloroplast) • PREDICTED: thioredoxin H1 • thioredoxin M1, chloroplastic	

Fold change ≥ 1.2 ($P \leq 0.05$; n=3). Bj – *Bradyrhizobium japonicum* 532C, SL42 – *Rhizobium* sp. SL42, SL48 – *Hydrogenophaga* sp. SL48

Table 4.11. Quantitative spectra of specific proteins under optimal and salt-stressed conditions.

Treatments	Control	SL42	SL48	SL42+ SL48	Bj	Bj+ SL42	Bj+ SL48	Bj+SL42 +SL48
15-cis-phytoene desaturase, chloroplastic/chromoplastic								
Optimal	21.8	23.0	40.4	38.8	27.0	33.2	42.9	38.2
Salt	16.3	16.9	26.1	33.6	23.8	38.4	51.2	39.9
photosystem I reaction center subunit psaK								
Optimal	53.5	51.7	47.4	80.7	40.4	65.0	106.3	84.4
Salt	18.3	40.7	48.9	55.8	56.3	88.5	78.8	57.9
ATP synthase CF1 beta subunit, chloroplastic								
Optimal	1434.1	1316.2	1353.1	1442.6	1440.6	1431.7	1543.8	1516.1
Salt	1227.3	1299.0	1310.0	1271.5	1357.3	1420.6	1380.2	1368.0
ribulose-1,5-bisphosphate carboxylase/oxygenase large subunit								
Optimal	8297.4	8447.6	8247.2	8125.0	8100.2	8245.4	8056.2	8320.7
Salt	6077.1	4919.4	5781.0	6554.7	6368.6	7426.5	7382.3	7072.7
ribulose bisphosphate carboxylase small chain, chloroplastic								
Optimal	1256.8	1513.0	1435.1	1588.9	1254.0	1520.3	1611.2	1521.7
Salt	985.5	684.8	811.2	1005.9	989.5	1340.0	1463.2	1226.8
glyceraldehyde-3-phosphate dehydrogenase A subunit, chloroplastic								
Optimal	812.2	787.9	817.9	1016.7	695.4	806.5	1182.5	1028.4
Salt	552.4	710.8	773.1	675.3	748.1	955.6	842.1	730.4
granule-bound starch synthase 1, chloroplastic/amyloplastic								
Optimal	538.4	562.0	537.1	544.6	651.9	638.0	661.9	654.2
Salt	456.1	445.6	457.6	453.4	429.2	477.9	457.1	455.4
glutamine synthetase precursor isoform X1, chloroplastic								
Optimal	686.9	721.3	723.3	725.0	795.5	783.4	773.6	680.3
Salt	663.8	573.7	533.6	557.7	534.4	568.5	704.5	692.8

Treatments	Control	SL42	SL48	SL42+ SL48	Bj	Bj+ SL42	Bj+ SL48	Bj+SL42 +SL48
glutathione S-transferase GST 8								
Optimal	85.36	101.01	100.74	104.94	92.51	104.53	101.31	105.93
Salt	165.85	171.82	151.82	136.73	150.35	159.28	158.62	150.00
Catalase								
Optimal	398.12	428.15	411.16	452.44	424.40	429.27	478.38	455.12
Salt	423.50	423.99	426.91	426.68	389.42	481.33	508.19	478.04
Carbonic anhydrase								
Optimal	516.58	490.25	487.69	453.32	358.31	385.88	391.60	385.10
Salt	426.01	405.88	443.23	416.17	365.75	382.04	387.62	360.62
proline-rich protein precursor								
Optimal	9.96	7.94	17.12	65.87	6.16	11.95	111.38	37.23
Salt	2.98	30.81	20.95	16.72	13.59	45.39	36.46	25.24
1-aminocyclopropane-1-carboxylate oxidase								
Optimal	4.97	2.00	1.98	6.00	9.43	7.14	6.84	9.76
Salt	12.14	19.90	14.27	7.92	37.21	57.99	61.48	48.85
NADP-dependent malic enzyme								
Optimal	146.88	138.00	143.07	161.01	226.75	216.22	207.55	202.06
Salt	130.66	123.03	151.17	154.77	144.80	195.65	180.30	183.33
gibberellin-regulated protein 6 precursor								
Optimal	33.70	39.01	43.30	41.96	34.19	42.20	37.08	27.45
Salt	69.37	78.42	33.42	24.56	28.37	30.55	45.66	64.63
soyasaponin III rhamnosyltransferase								
Optimal	98.23	120.93	125.19	149.75	121.86	159.89	172.46	139.28
Salt	53.20	44.59	54.91	73.06	74.84	93.60	119.49	93.84
Bj – *Bradyrhizobium japonicum* 532C, SL42 – *Rhizobium* sp. SL42, SL48 – *Hydrogenophaga* sp. SL48								

4.4.2.2 Functional classification of proteins based on GO categories

Based on Blast2GO pro analysis, the enzymes classes distribution was studied (Figure 4.6). Some of the enzyme classes were increased under salt stress including oxidoreductases, transferases, hydrolases and translocases. Under optimal conditions, the difference between the treatments was not more or less than 10 protein sequences. Under salt stress, the oxidoreductases, transferases and hydrolases were higher in the bacterial treatments than in control. Lyases (17.4%) and ligases (23.3%) were increased, particularly with the treatment of SL42+SL48. When co-inoculated with *B. japonicum*, little difference was observed among treatments under optimal and salinity conditions. Although, treatment of *B. japonicum*+SL42 increased isomerases (14.5%) under optimal and ligases (21.5%) under salt stress compared to *B. japonicum*.

The GO categories distribution of proteins involved in biological processes, molecular functions and cellular components were analyzed and the number of proteins associated with almost all functions were increased under salt stress. The major functions (> 1000 protein sequences) related to cellular and metabolic processes, binding and catalytic activity, and cellular components including cytoplasm, organelles, membranes and intracellular structures were all highly upregulated by the bacterial treatments compared to control, but the differences were more prominent under salt stress (> 100 sequences) than under optimal conditions. The major GO function proteins were also predominantly upregulated in co-inoculation treatments with *B. japonicum* under optimal conditions (> 50 sequences). However, minimal differences (< 25 sequences) were observed between the co-inoculation treatments and *B. japonicum* under salt stress (Figure 4.7).

Similarly, other proteins (< 400 sequences) participating in the biological regulation, localization, response to stimulus, detoxification, development, signaling, multicellular organismal processes, interspecies interaction, and reproduction and molecular functions of cellular structures, transport, regulation, translation, and antioxidant activities, were increased by bacterial inoculation compared to the control treatment (Figures 4.8 & 4.9). The cellular components including cytosol, membrane-protein complex, catalytic complex, ribonucleoprotein, plastid (lumen, stroma and thylakoid) and mitochondrial proteins were higher in the bacterial treatments than the control (Figure 4.10).

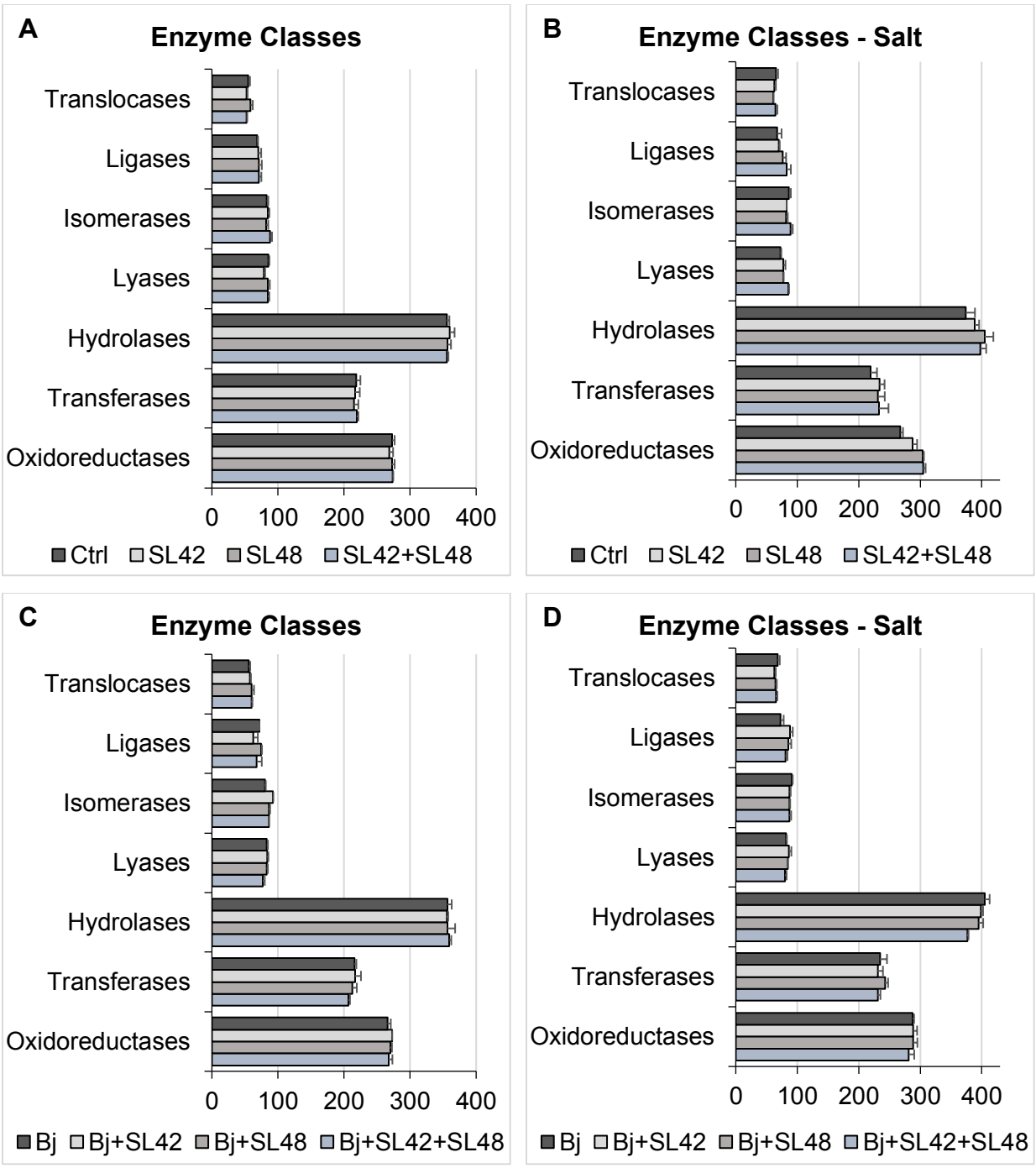

Figure 4.6. Number of sequences involved in the enzyme classes of the soybean leaf proteome. **(A)** The seeds were treated with 10 mM $MgSO_4$ or bacterized with the strains *Rhizobium* sp. SL42, *Hydrogenophaga* sp. SL48 or co-inoculated under optimal and **(B)** under salt stress **(C)** seeds were bacterized with *Bradyrhizobium japonicum* (Bj) as control or the strains were co-inoculated with Bj under optimal and **(D)** under salt stress conditions. Values represent mean ± SE (n=3).

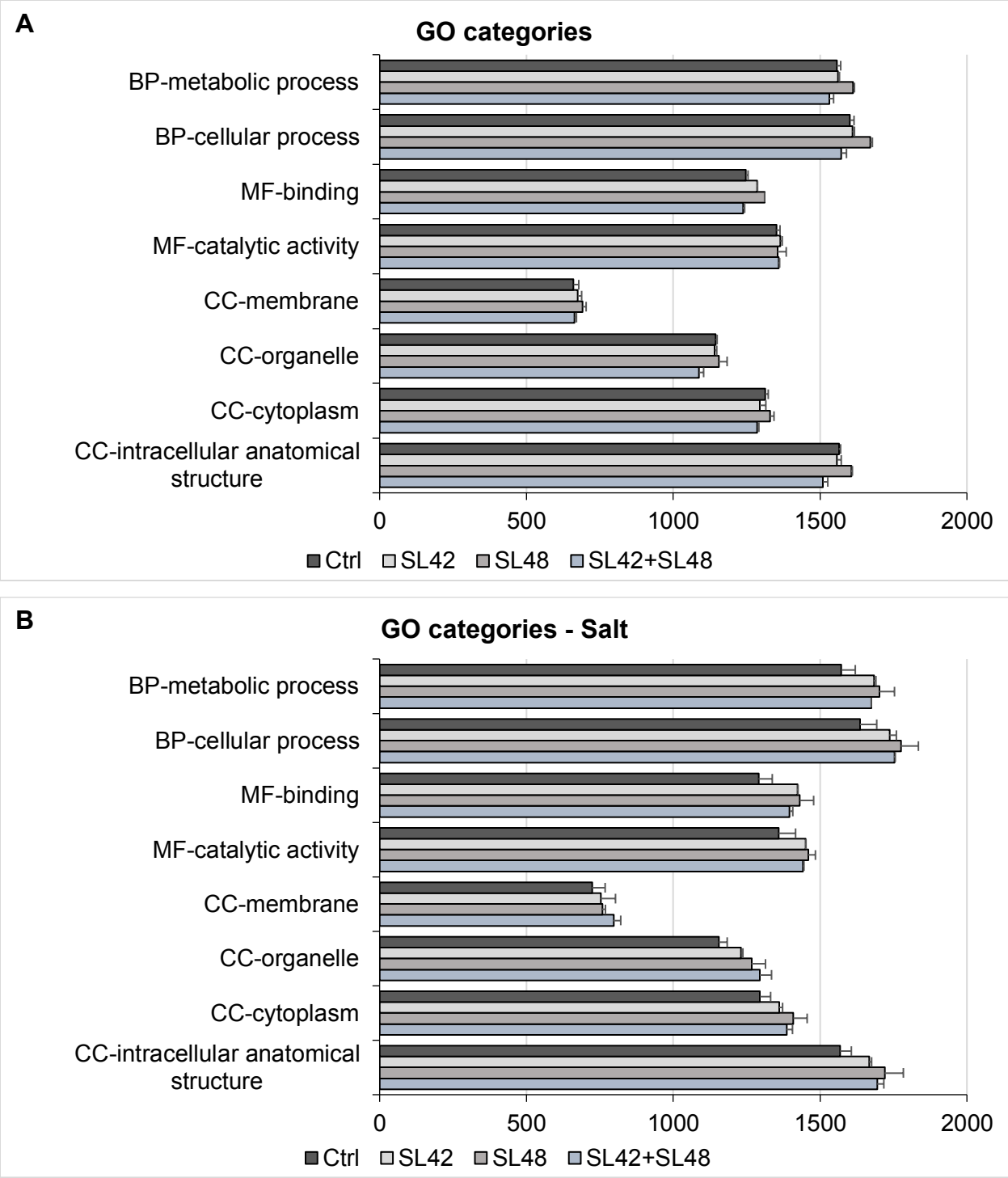

Figure 4.7. Number of sequences involved in the major GO categories of the soybean leaf proteome.
(A) The seeds were treated with 10 mM $MgSO_4$ or bacterized with the strains *Rhizobium* sp. SL42, *Hydrogenophaga* sp. SL48 or co-inoculated under optimal and **(B)** under salt stress conditions. Values represent mean ± SE (n=3).

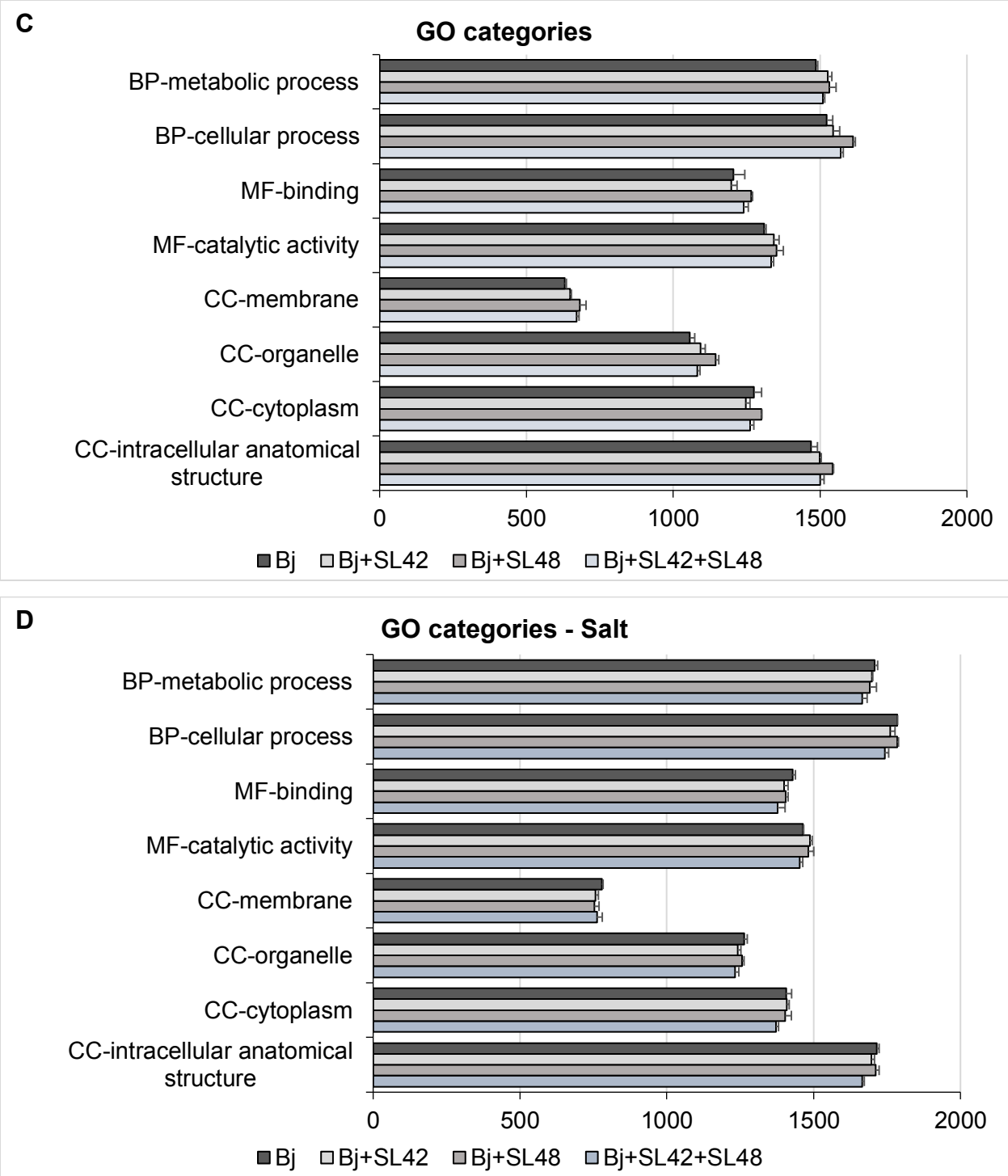

Figure 4.7. (cont.) Number of sequences involved in the major GO categories the soybean leaf proteome. **(C)** seeds were bacterized with *Bradyrhizobium japonicum* (Bj) as control or the strains *Rhizobium* sp. SL42, *Hydrogenophaga* sp. SL48 were co-inoculated with Bj under optimal and **(D)** under salt stress conditions. Values represent mean ± SE (n=3).

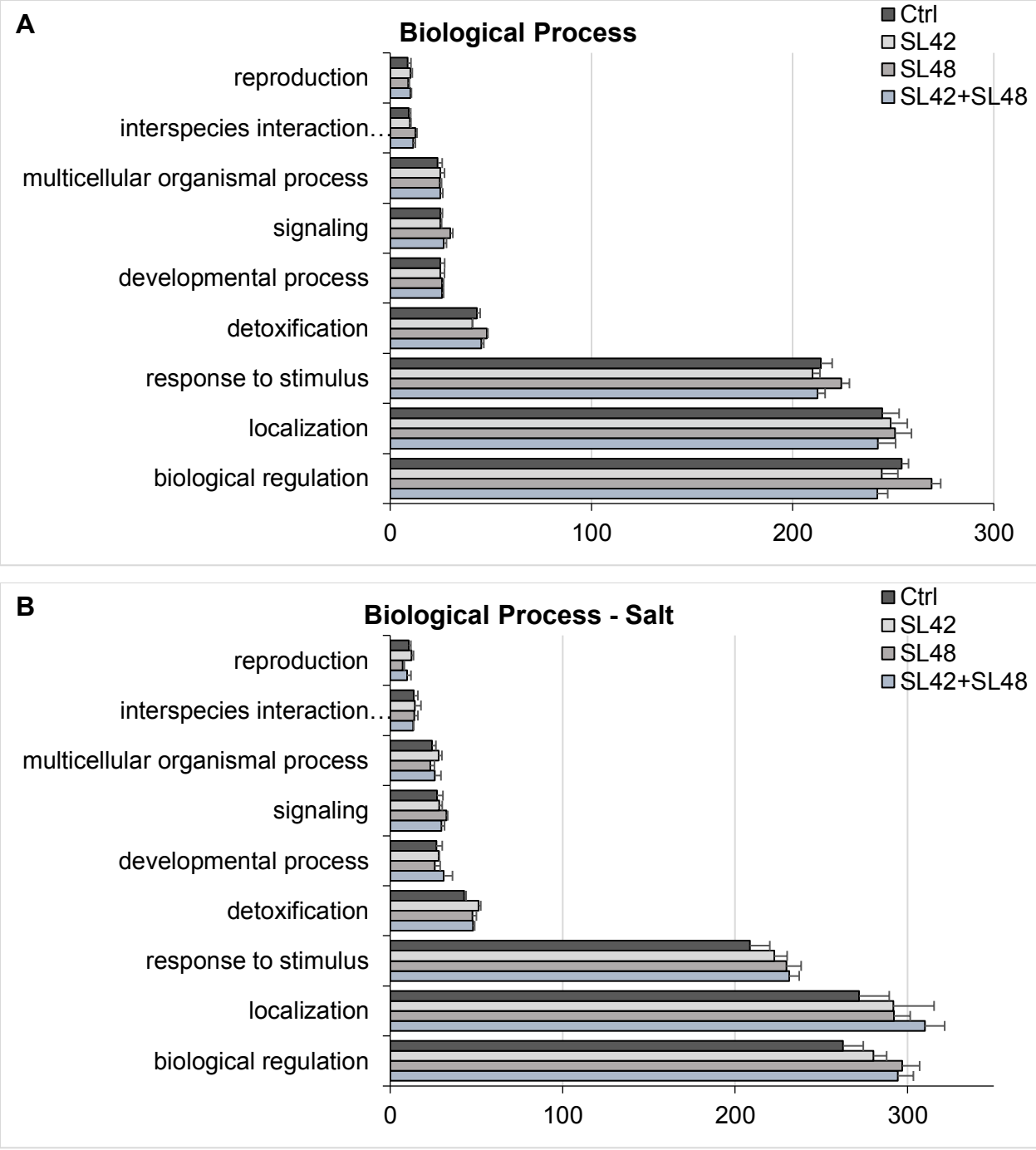

Figure 4.8. Number of sequences involved in the biological processes of the soybean leaf proteome.
(A) The seeds were treated with 10 mM $MgSO_4$ or bacterized with the strains *Rhizobium* sp. SL42, *Hydrogenophaga* sp. SL48 or co-inoculated under optimal and **(B)** under salt stress conditions. Values represent mean ± SE (n=3).

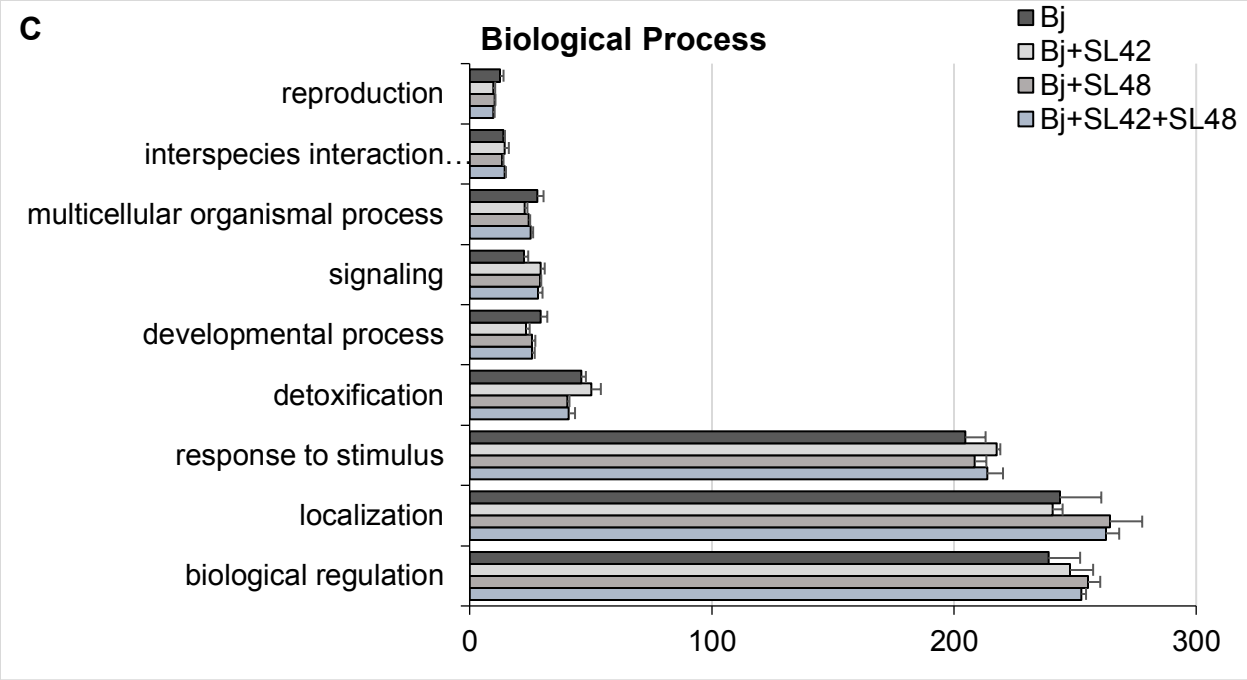

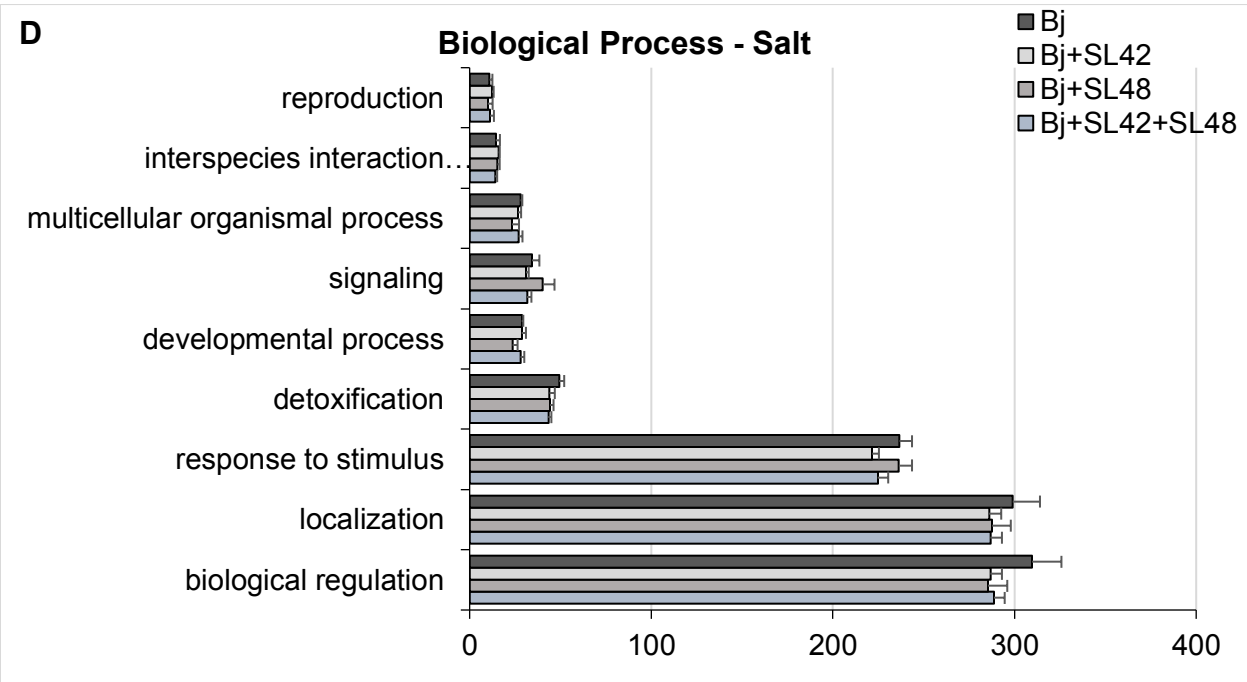

Figure 4.8. (cont.) Number of sequences involved in the biological processes of the soybean leaf proteome. **(C)** seeds were bacterized with *Bradyrhizobium japonicum* (Bj) as control or the strains *Rhizobium* sp. SL42, *Hydrogenophaga* sp. SL48 co-inoculated with Bj under optimal and **(D)** under salt stress conditions. Values represent mean ± SE (n=3).

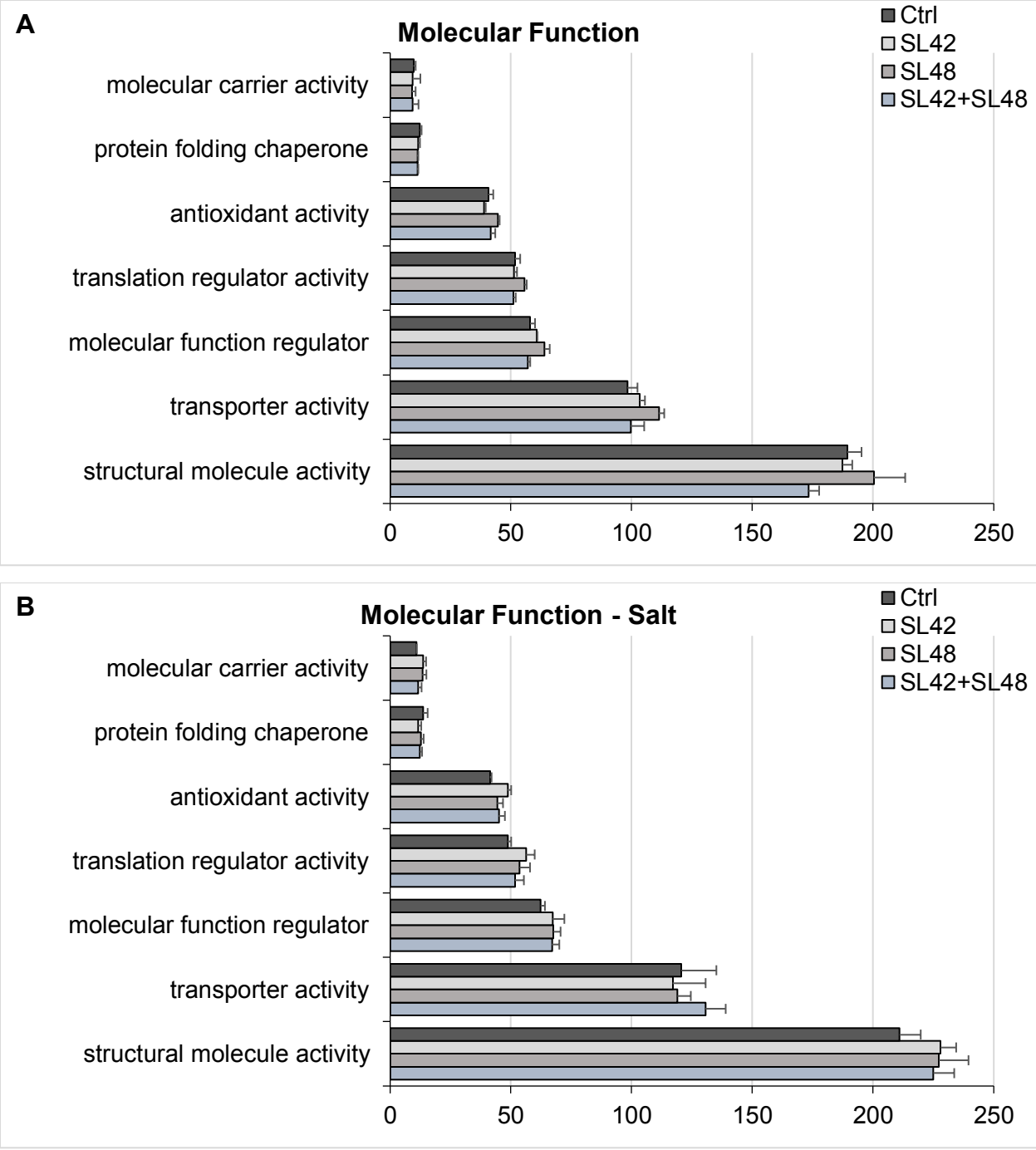

Figure 4.9. Number of sequences involved in the molecular functions of the soybean leaf proteome.
(A) The seeds were treated with 10 mM $MgSO_4$ or bacterized with the strains *Rhizobium* sp. SL42, *Hydrogenophaga* sp. SL48 or co-inoculated under optimal and **(B)** under salt stress conditions. Values represent mean ± SE (n=3).

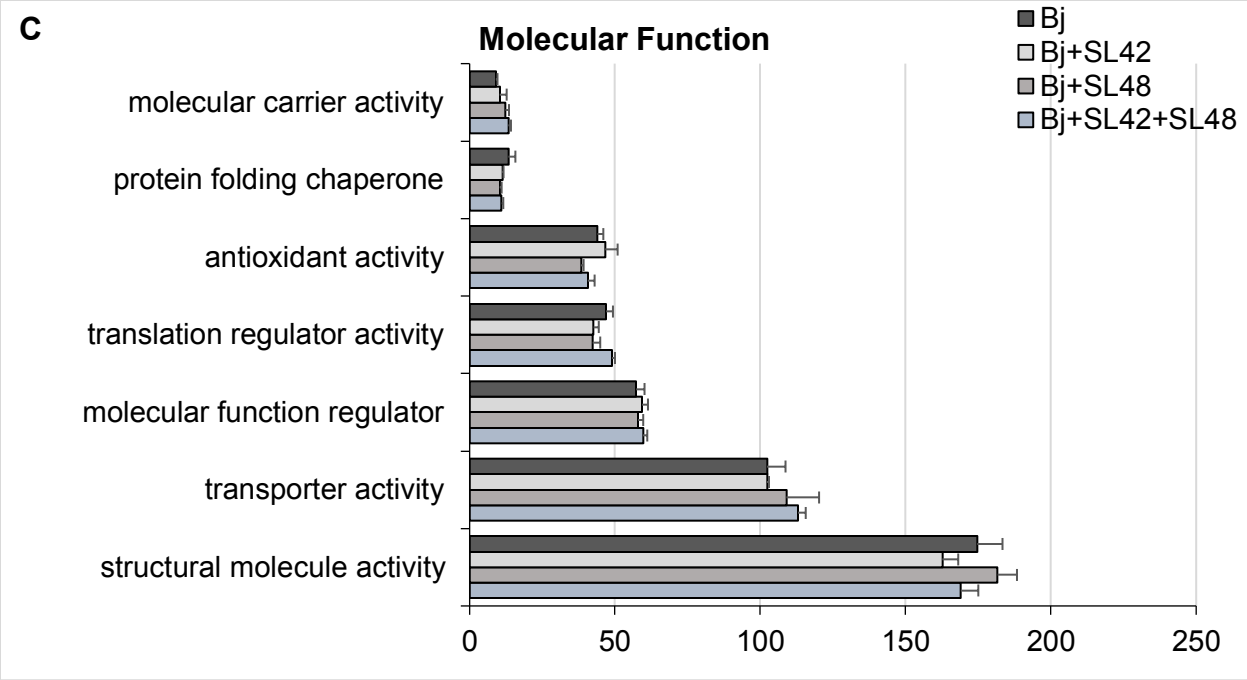

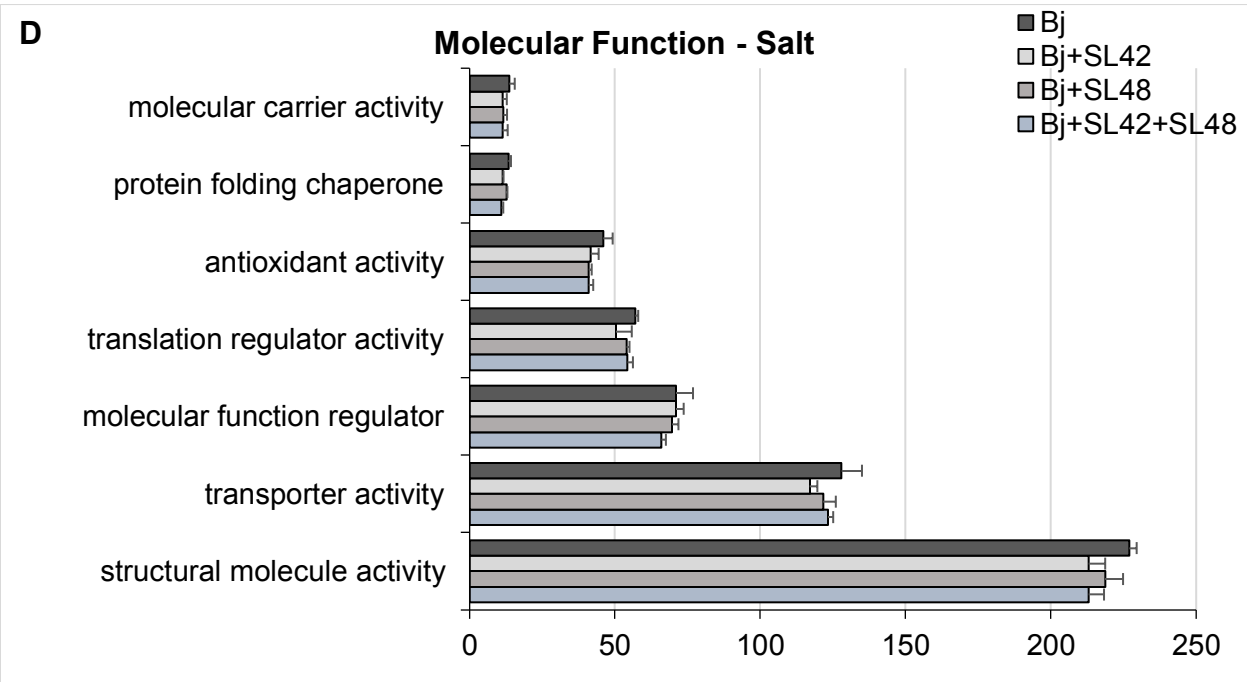

Figure 4.9. (cont.) Number of sequences involved in the molecular functions of the soybean leaf proteome. **(C)** seeds were bacterized with *Bradyrhizobium japonicum* (Bj) as control or the strains *Rhizobium* sp. SL42, *Hydrogenophaga* sp. SL48 were co-inoculated with Bj under optimal and **(D)** under salt stress conditions. Values represent mean ± SE (n=3).

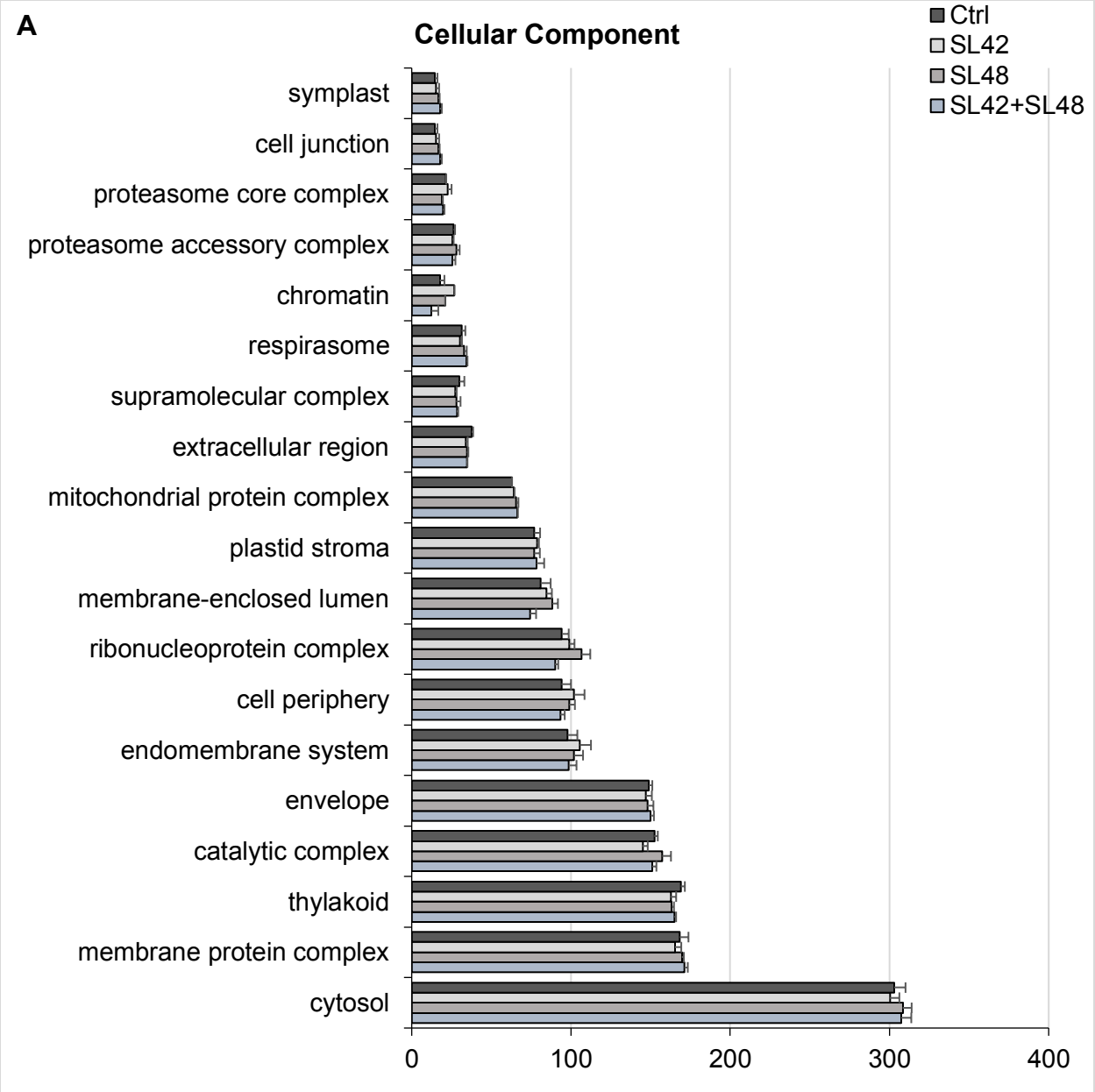

Figure 4.10. Number of sequences involved in the cellular components of the soybean leaf proteome.
(A) The seeds were treated with 10 mM $MgSO_4$ or bacterized with the strains *Rhizobium* sp. SL42, *Hydrogenophaga* sp. SL48 or co-inoculated under optimal conditions. Values represent mean ± SE (n=3).

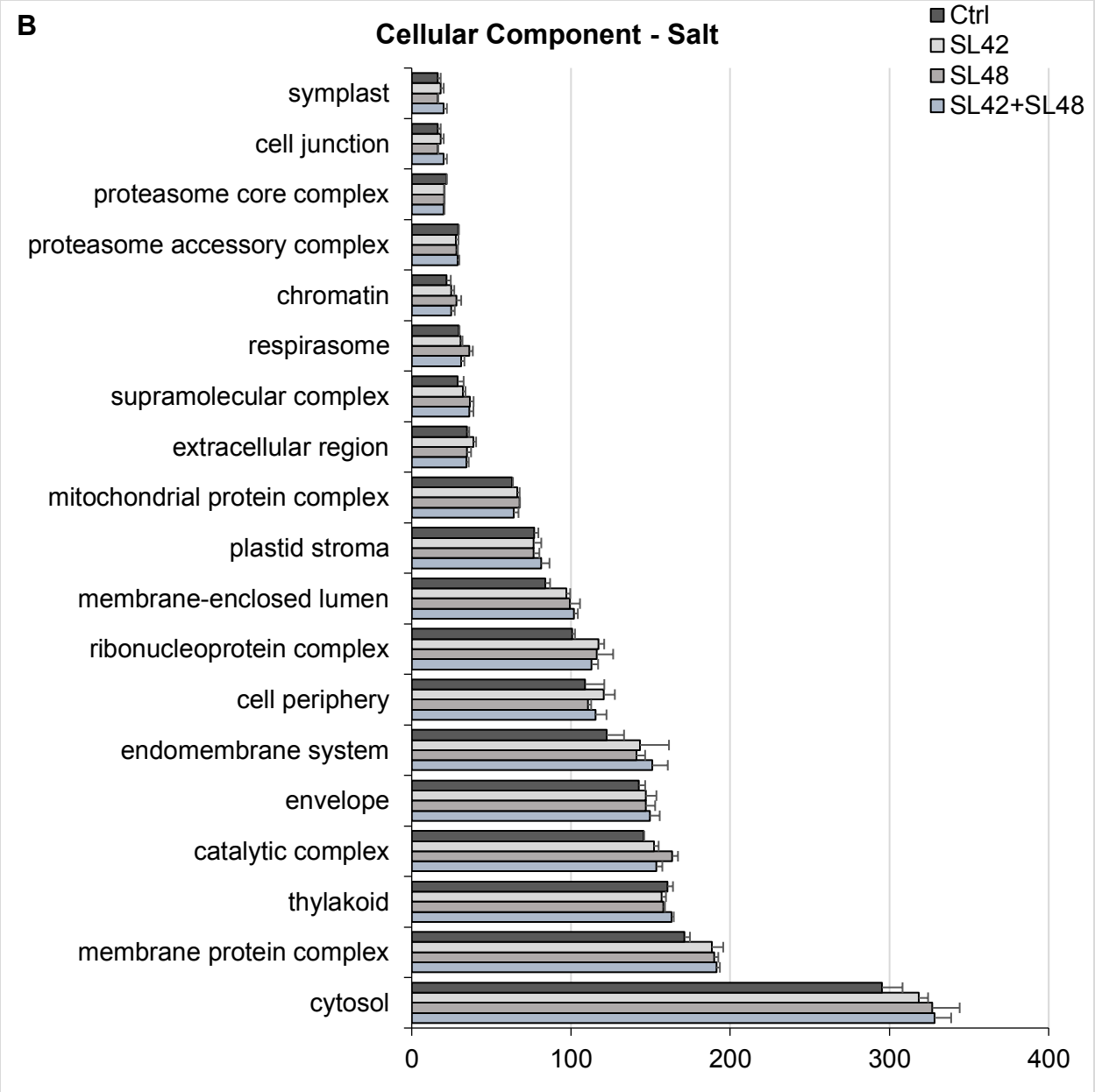

Figure 4.10. (cont.) Number of sequences involved in the cellular components of the soybean leaf proteome. **(B)** The seeds were treated with 10 mM $MgSO_4$ or bacterized with the strains *Rhizobium* sp. SL42, *Hydrogenophaga* sp. SL48 or co-inoculated under salt stress conditions. Values represent mean ± SE (n=3).

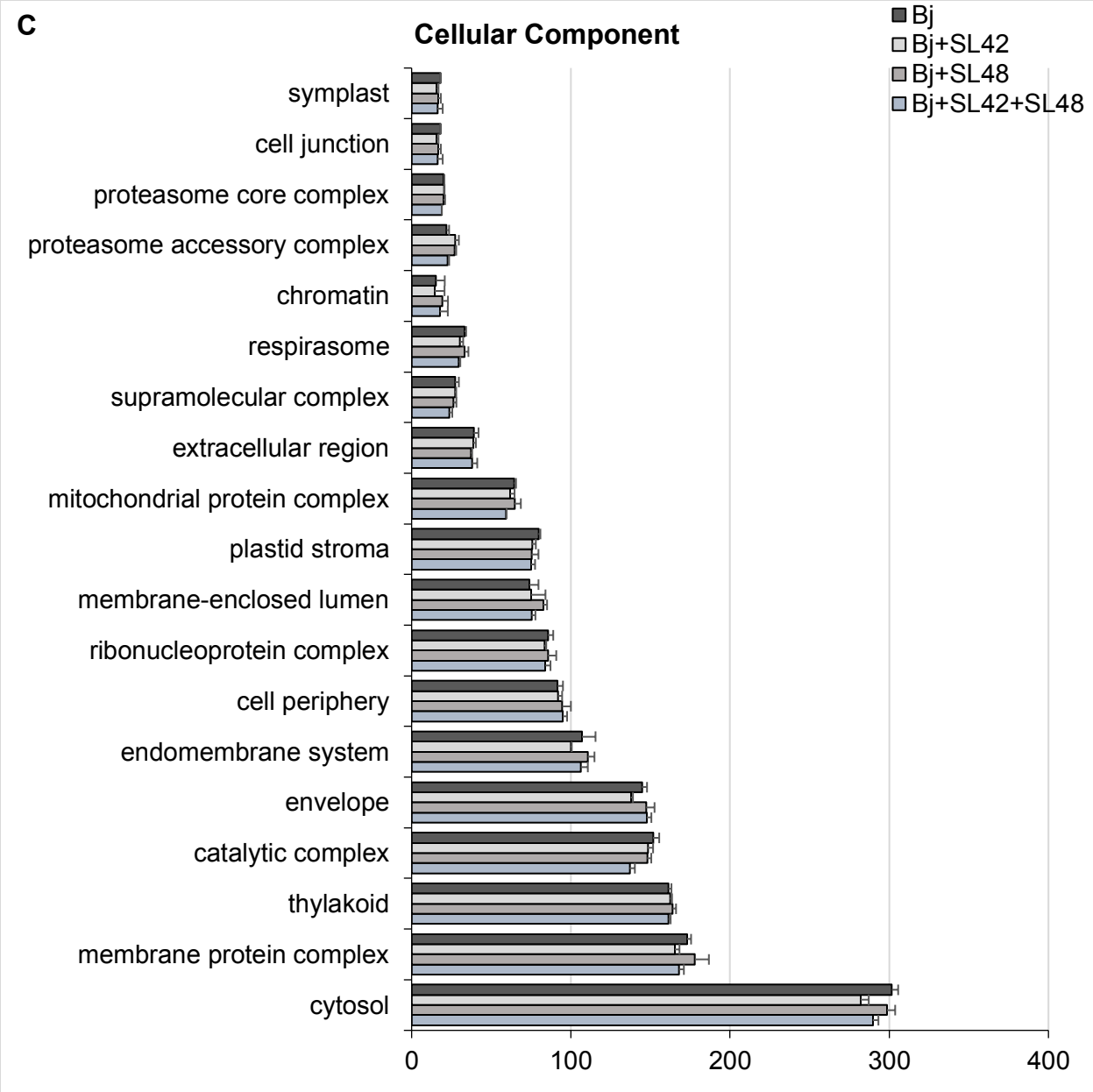

Figure 4.10. (cont.) Number of sequences involved in the cellular components of the soybean leaf proteome. **(C)** seeds were bacterized with *Bradyrhizobium japonicum* (Bj) as control or the strains *Rhizobium* sp. SL42, *Hydrogenophaga* sp. SL48 were co-inoculated with Bj under optimal conditions. Values represent mean ± SE (n=3).

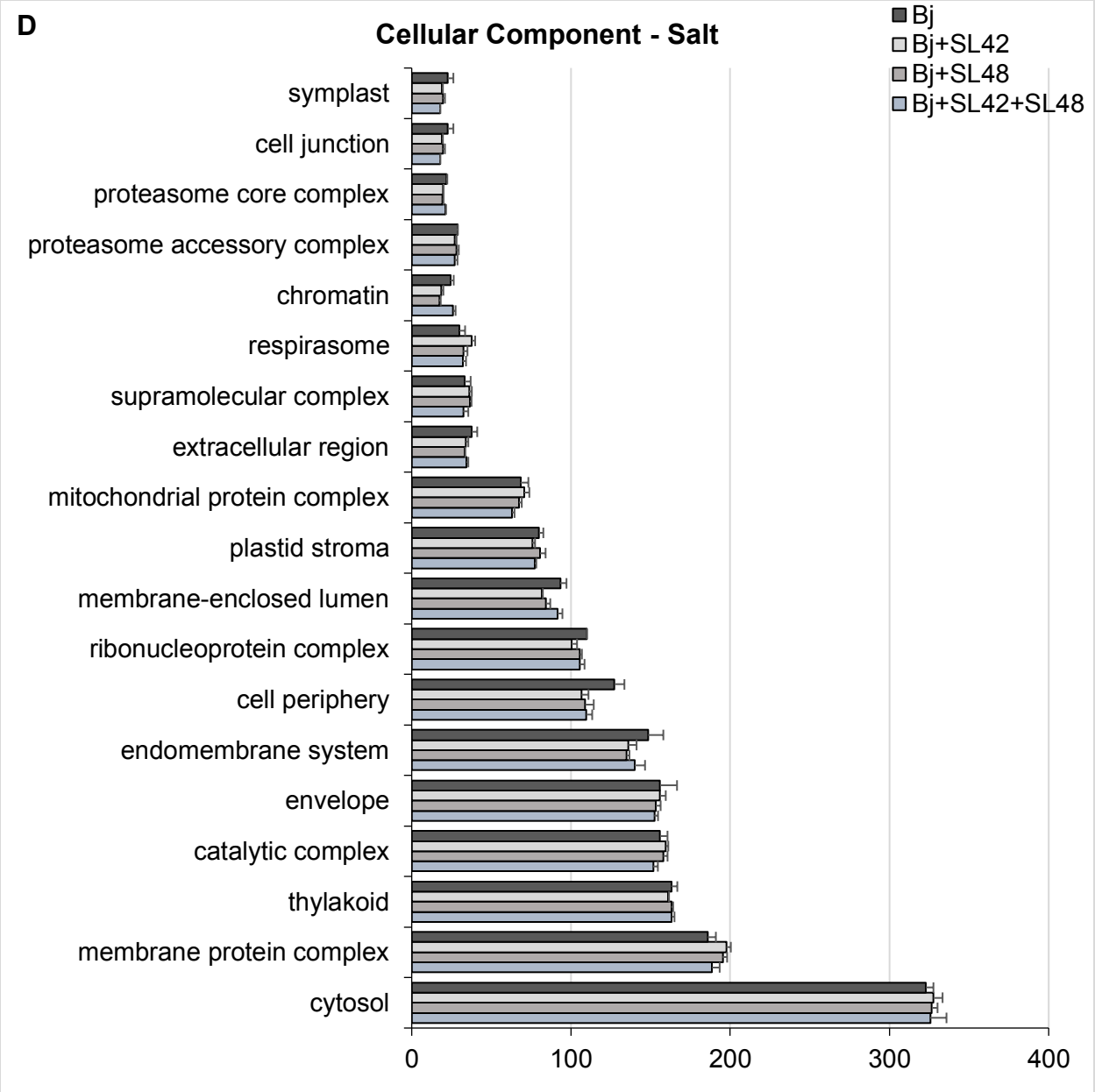

Figure 4.10. (cont.) Number of sequences involved in the cellular components of the soybean leaf proteome. **(D)** seeds were bacterized with *Bradyrhizobium japonicum* (Bj) as control or the strains *Rhizobium* sp. SL42, *Hydrogenophaga* sp. SL48 were co-inoculated with Bj under salt stress conditions. Values represent mean ± SE (n=3).

In the co-inoculation treatments with *B. japonicum*, most functions were upregulated compared to the *B. japonicum* control under optimal conditions. The proteins associated with biological regulation, localization, detoxification, molecular functions, endomembrane system, cell periphery and extracellular region were down-regulated while signaling, interspecies interaction, and reproduction and cellular components including cytosol, membrane-protein complex, catalytic complex, mitochondrion, respirasome, and supramolecular complex were upregulated in the co-inoculation treatments with *B. japonicum*, relative to *B. japonicum* alone under salt stress. The number of proteins related to other functions were more or less equal and the differences were seldom detectable among treatments. Moreover, when the number of protein sequences involved in a function was less than 20, the differences among treatments were marginal (± 3 sequences) (Appendix B, Supplementary Figures 4.1-4.4).

4.5 Discussion

The seedling development stage of soybean is more sensitive to salinity than the seed germination stage (Hosseini et al., 2002). This is because the young tissues are affected by osmotic stress due to the high salt concentration in the root zone. In our experiment, seedling emergence was decreased under salt stress and the cotyledons exhibited symptoms such as oxidative browning and wilting on some seedlings. The symptoms of salinity-induced osmotic stress overlap those of drought and cold stress (Zhu, 2002). Shoot growth is limited due to the osmotic imbalance, which affects stomatal conductance, cell expansion in meristems and growth of young leaves (Munns and Tester, 2008). The net photosynthetic rate is reduced and photosynthetic assimilates are utilized for maintenance and survival, rather than biomass accumulation (Munns and Gilliham, 2015). Plant growth was largely reduced by salt stress compared to plants grown under optimal conditions.

Yellowing and senescence of the first two true leaves were observed in salt-stressed soybean plants; this was caused by ionic toxicity and in turn reduced the leaf area (Munns and Gilliham, 2015). The influx of Na^+ ions affects the concentration of other cations in plant tissues. Salt-tolerant lines of soybean had increased capacity to sustain adequate levels of other nutrient elements required to conduct metabolic functions (Ning et al., 2018). The concentration of N, P and K were higher under salinity implying that the plants assimilated major nutrients to cope with the negative impacts of salt stress. The plants might have assimilated more K^+ to maintain ionic

homeostasis because of the high Na^+ content and low Ca_2^+ content (cytosolic flux). The tolerance mechanisms include Na^+ exclusion from the leaf tissues in addition to Na^+ compartmentalization in vacuoles. Accumulation of compatible solutes (osmolytes) and scavenging of reactive oxygen species (ROS) contribute to enhanced salinity tolerance (Flowers and Colmer, 2015).

Proteins related to important metabolic processes such as photosynthesis, respiration, photorespiration and production of starch, amino acids and secondary metabolites were upregulated in the treatments with SL42 and SL48. This showed that the PGPR strains modulated major plant functions under optimal and salt-stressed conditions. A number of proteins involved in seedling development, plant growth and stress responses were upregulated due to bacterial inoculation. Some of them are linked to phytohormone mediated pathways, suggesting that the bacteria influenced the signaling networks and modulated plant responses. A few key examples found in this study are discussed below.

4.5.1 Rhizobacteria upregulate proteins related to molecular functions, nutrient metabolism and photosynthesis

One of the important enzymes upregulated by SL42, SL48 and SL42+SL48 under optimal conditions and linked to increased plant growth was asparagine synthetase 2 (ASN2). The enzyme is involved in asparagine synthesis and is essential for the regulation of nitrogen assimilation and reallocation within the plant via the phloem companion cells. It is predominantly expressed during darkness in vegetative leaves. It is important for primary metabolism, chlorophyll content and biomass accumulation (Gaufichon et al., 2013). Hsp90 superfamily protein isoform X1 was upregulated in the treatments of SL42, SL48 and SL42+SL48 under salt stress. Hsp90 is a molecular chaperone family essential for protein folding in the chloroplasts that are synthesized *de novo* or imported into the chloroplast mediated by the Toc/Tic complexes and cooperates with other chaperones. It is required for chloroplast development, specifically thylakoid formation within chloroplasts. Malfunction of Hsp90 has been shown to be lethal in transgenic Arabidopsis seeds, therefore it is essential for chloroplast biogenesis and embryogenesis (Oh et al., 2014). Another upregulated protein under salt stress was clathrin heavy chain (CHC), which are subunits of clathrin, a major structural protein involved in coated pits and vesicles mediating endo- and exocytosis. One of the important functions of CHC is associated with stomatal movement linked to the expansion of guard cells. This in turn affects transpiration rate, gaseous exchange and cell metabolism. Arabidopsis *chc* mutants showed defects in stomatal function and plant growth under

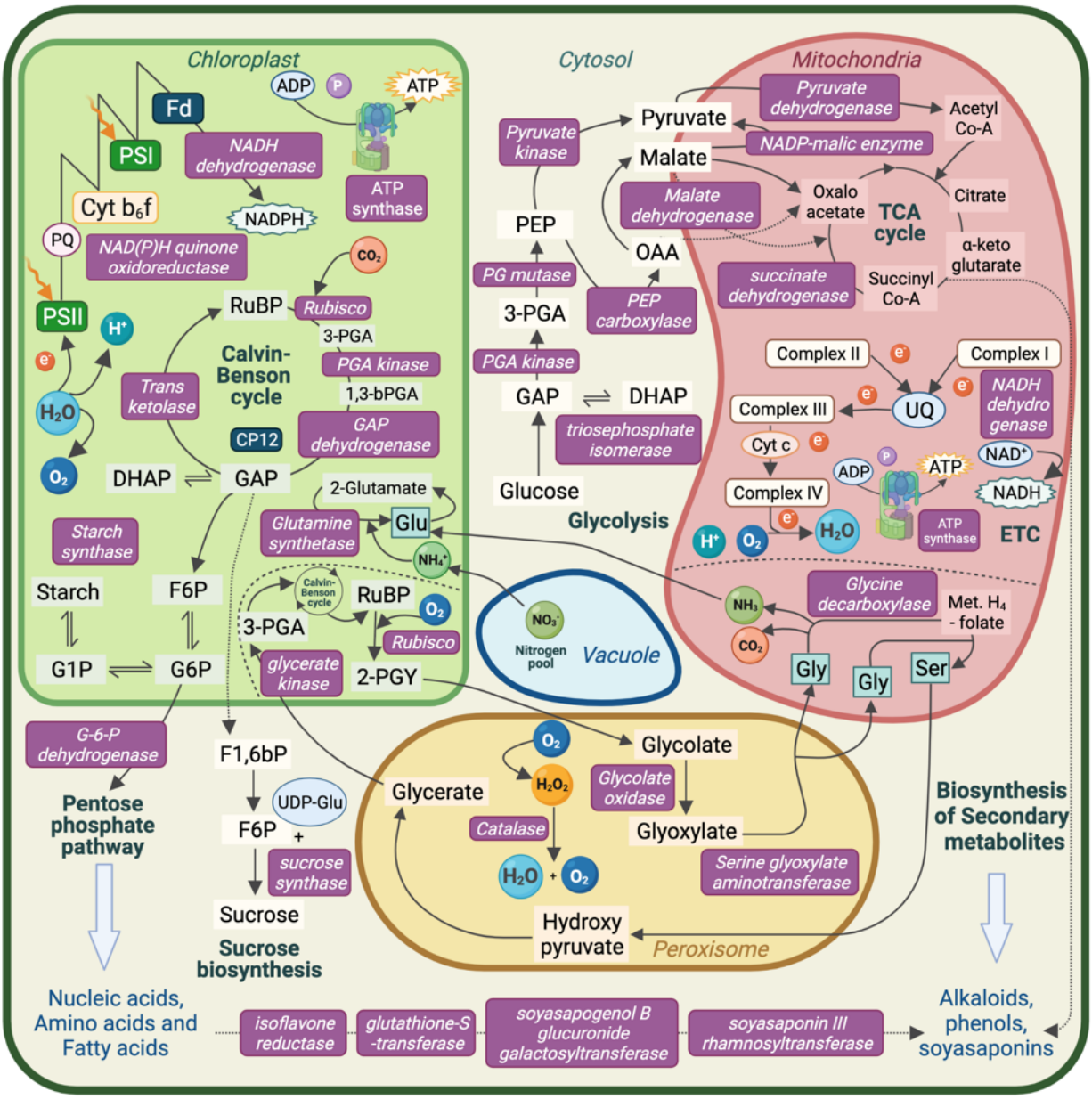

Figure 4.11. Schematic representation of the major metabolic pathways in a plant cell. Enzymes involved in photosynthesis, respiration, photorespiration, nutrient assimilation, and biosynthesis pathways that were upregulated in soybean leaf tissue by the bacterial inoculation treatments are indicated in purple text box.
PS – Photosystem, Cyt b_6f – Cytochrome, Fd – Ferredoxin, PQ – Plastoquinone, UQ – Ubiquinone, RuBP – Ribulose bisphosphate, PGA – phosphoglycerate, GAP – Glyceraldehyde-3-phosphate, DHAP – Dihydroxyacetone phosphate, F6P – Fructose-6-phosphate, G6P – Glucose-6-phosphate, PEP – phospho*enol*pyruvate, OAA – Oxaloacetate, Met. H4 -folate – Methylene H4 -folate, Gly – Glycine, Glu – Glutamine, Ser – Serine.

water deficit. Endocytosis is also crucial for the polarized localization of PIN proteins (auxin transporters) and provides directional gradients for auxin distribution within the plant (Larson et al., 2017).

Carbamoyl-phosphate synthase (CPS) is required for arginine biosynthesis, converting ornithine into citrulline. In higher plants, citrulline and arginine are essential for proper mesophyll development and reticulate venation in leaves. The enzyme is localized in the chloroplast and the large chain subunit was upregulated in the treatments SL42+SL48, Bj+SL42 and Bj+SL48 and small chain by Bj+SL42+SL48 under salt stress (Molla-Morales et al., 2011). Lipid transfer protein EARLI 1-like expressed only in the co-inoculation treatments of *B. japonicum* with SL42 and SL48. Upregulation of EARLI-1 improved seed germination, root elongation and reduced Na^+ accumulation in leaves under salt stress. It is induced in embryonic tissues and young seedlings suggesting that it has a positive role in seed germination and early seedling development under high salinity stress (Xu et al., 2011). Proline-rich proteins (PRP) are major constituents of cell wall structure organization. They were upregulated in all the bacterial treatments under salt stress and also in SL42+SL48, Bj+SL42+SL48 under optimal conditions. PRP accumulated in the cell wall soluble fraction of common bean (*Phaseolus vulgaris*) in response to water deficit. It also accumulated in developing seedlings, specifically in the phloem tissues. It plays a role in plant morphogenesis and cell wall modification induced by osmotic stress (Battaglia et al., 2007). In another study, the soybean *GmPRP* gene showed distinct expression patterns in different organs from 2-week-old seedlings and was upregulated in response to abiotic and biotic stresses (He et al., 2002).

Carbonic anhydrases (CA) are the second most abundant protein cluster next to Rubisco in C3 plant leaves and catalyzes reversible hydration of CO_2 to bicarbonate ion and proton. It is involved in CO_2 diffusion and is closely associated with Rubisco activity. Its function is important for photosynthesis in response to drought stress. It also modulates stomatal conductance to promote water use efficiency, thereby helping plants adapt to water-deficit (Wang et al., 2016). It was upregulated by treatment with Bj+SL42+SL48 under both conditions, supporting increased stress tolerance. Glutamine synthetase (GS) is a light-modulated enzyme targeted to leaf chloroplasts and mitochondria and upregulated by treatment with Bj+SL48 and Bj+SL42+SL48. It is primarily responsible for the reassimilation of ammonia generated by photorespiration in

mitochondria, which is highly cytotoxic, and converts it to nontoxic glutamate in chloroplasts, and therefore, linked to plant growth (Taira et al., 2004).

Lipoxygenases (LOX) are widely distributed in plants and catalyze hyperoxidation of polyunsaturated fatty acids containing a cis, cis-1,4-pentadiene structure to produce oxylipins. They play important physiological roles in seed germination, plant growth, nodule development, ripening, cell death, senescence, synthesis of ABA and jasmonic acid and responses to abiotic and biotic stresses. Soybean contains at least 4 distinct LOX isozymes in dry seeds and two isozymes in the hypocotyl/radicle region of the seedling stem. LOX act as vegetative storage proteins (VSPs), mobilize lipids and eliminate harmful ROS during rapid mobilization of nutrient reserves in germinating soybean seeds. LOXs were found in developing cotyledons, leaves and nodules. They also play crucial roles in abiotic stress responses by decreasing H_2O_2 accumulation and lipid peroxidation. Overexpression of *DkLOX3* (*Diospyros kaki* L. 'Fupingjianshi') in Arabidopsis was related to increased germination rate and upregulation of other stress-responsive genes under high drought and salinity stress conditions (Viswanath et al., 2020). The two major subfamilies, linoleate 13S-lipoxygenase and linoleate 9S-lipoxygenases, including seed linoleate 9S lipoxygenases, were upregulated by SL48 inoculation treatments under optimal and salt stress conditions.

4.5.2 Proteins involved in phytohormone mediated responses were influenced by rhizobacteria

Phytohormones are signaling molecules that regulate vital physiological processes and also control plant responses to abiotic and biotic stresses including salinity stress (Waśkiewicz et al., 2016). Auxin is a key regulator of cell division, expansion and differentiation in shoot and root meristems and plays crucial roles in plant development. Auxin binding protein abp19a-like (ABP19A) is an extracellular auxin receptor and binds to auxin. It is required for auxin responses in embryogenesis, and post-embryonic root growth and shoot development (Tromas et al., 2009). It was upregulated in all bacterial treatments, indicating that the bacteria play closely associated roles in auxin signaling, thereby promoting growth.

The enzyme 1-aminocyclopropane-1-carboxylate oxidase (ACO) is involved in ethylene biosynthesis. Ethylene mediates the reversion of ABA-induced inhibition of seed germination via endosperm cap rupture. It also confers salinity tolerance by enhancement of Na/K homeostasis and accumulation of ascorbic acid through ethylene-mediated pathways (Linkies et al., 2009; Jiang et

al., 2013). It was upregulated in the treatments of Bj+SL42 and Bj+SL48 under salt stress. Gibberellin-regulated protein 6 precursor (GASA6) is a small cysteine-rich peptide responsive to gibberellic acid (GA). It functions as an integrator in the downstream of GA signaling and regulates seed germination by promoting cell elongation at the embryonic axis. It takes part in redox reactions and decreases the accumulation of ROS in response to stress. It was also upregulated under salt stress by Bj+SL48 and Bj+SL42+SL48 treatments (Zhong et al., 2015).

NADP dependent malic enzyme (NADP-ME) was upregulated in plants under salt stress with SL42 and SL48 inoculation and co-inoculation with *B. japonicum* treatments. It catalyzes the oxidative decarboxylation of malate to generate pyruvate, CO_2 and NADPH. It plays functional roles in abscisic acid (ABA)-mediated signaling pathways related to seed development and osmotic stress. Treatment with ABA, NaCl and mannitol increased the accumulation of NADP-ME in Arabidopsis. The knockout *nadp-me1* mutants showed decreased seed viability, stomatal opening and root growth. Hence, the enzyme participates during both seed germination and seedling growth stages. It is also essential to enhance tolerance of drought and saline conditions (Arias et al., 2018). Other proteins involved in the phytohormone-mediated responses that were upregulated by specific bacterial treatments are given in Table 4.12.

4.6 Conclusion

The analysis of leaf proteomic profile provided a comprehensive insight into the growth and salinity tolerance mechanisms of soybean plants modulated by the influence of rhizobacteria. These mechanisms are regulated by the inter-organismal communication, an intricate network of signaling pathways (Smith et al., 2015). In conclusion, soybean plants inoculated with *Rhizobium* sp. SL42 and *Hydrogenophaga* sp. SL48 enhanced vigour and salinity tolerance under growth chamber conditions. The bacteria triggered multiple signaling pathways that regulated growth and stress tolerance mechanisms, which in turn is a result of beneficial plant-microbe interaction. Nevertheless, plants co-inoculated with *Bradyrhizobium japonicum* 532C and the strains SL42 and SL48 exhibited higher growth-promoting and stress-alleviating mechanisms, suggesting compatible co-inoculation between the symbiont and the rhizobacteria. This could ultimately lead to the crop improvement and salinity tolerance of soybean.

Table 4.12. Upregulated proteins involved in phytohormone-mediated responses.

Protein	Function	Treatment	Reference
Abscicate beta-glucosyltransferase	Glycosylation of ABA and upregulated by ABA or drought stress.	Bj+SL42 (S)	Xu et al. (2002)
Amidase 1 isoform X1	Involved in auxin biosynthesis. Converts indole-3-acetamide to indole-3-acetate.	Bj+SL48 (S)	Sanchez-Parra et al. (2014)
anthranilate synthase alpha subunit 1, chloroplastic	Part of a heterotetrameric complex that catalyzes the two-step biosynthesis of anthranilate, an intermediate in the biosynthesis of L-tryptophan. Plays an important regulatory role in auxin production via the tryptophan-dependent biosynthetic pathway.	SL42+SL48 (S)	Stepanova et al. (2005)
Aquaporin PIP2-7	Water channel required to facilitate the transport of water across cell membrane. Plays a predominant role in root water uptake process in conditions of reduced transpiration, and in osmotic fluid transport.	SL42+SL48 (S)	Pou et al. (2016)
gamma-tocopherol methyltransferase	Biosynthesis of tocopherol. Protect the photosynthetic apparatus against oxidative stress.	Bj +SL42 +SL48 (S)	Bergmuller et al. (2003)
haem oxygenase	Key enzyme in the synthesis of the chromophore of the phytochrome family of plant photoreceptors. Plays a role in salt acclimation signaling. May affect the plastid-to-nucleus signaling pathway by perturbing tetrapyrrole synthesis.	Bj +SL42 +SL48 (S)	Gisk et al. (2010)
IAA-amino acid hydrolase ILR1-like 4	Regulates amide-IAA hydrolysis and results in activation of auxin signaling.	SL42 (S)	Carranza et al. (2016)
peroxisomal 3-ketoacyl-CoA thiolase	Involved in long chain fatty-acid beta-oxidation prior to gluconeogenesis during germination and subsequent seedling growth.	Bj+SL42+SL48	Germain et al. (2001)

Protein	Function	Treatment	Reference
protein PELPK1	Positive regulator of germination and plant growth.	Bj+SL42, SL42+SL48	Rashid and Deyholos (2011)
serine glyoxylate aminotransferase 3 isoform X1	Photorespiratory enzyme that catalyzes transamination reactions. Functions in asparagine metabolism. Involved in root development during seedling establishment after seed germination.	Bj +SL48	Zhang et al. (2013)
Xanthoxin dehydrogenase	Generates abscisic aldehyde from xanthoxin, the last step of ABA biosynthetic pathway. Response to osmotic stress.	SL48 (S)	Gonzalez-Guzman et al. (2002)
* Functional description of proteins was adapted from UniProt database. (S) indicates treatments with salt stress.			

4.7 References

1. Abrol, I.P., Yadav, J.S.P., and Massoud, F.I. (1988). *Salt-Affected Soils and their Management* [Online]. Rome: Food and Agriculture Organization of the United Nations. Available online at: http://www.fao.org/3/x5871e/x5871e00.htm#Contents [accessed Apr 2017].
2. Arias, C.L., Pavlovic, T., Torcolese, G., Badia, M.B., Gismondi, M., Maurino, V.G., et al. (2018). NADP-Dependent Malic Enzyme 1 Participates in the Abscisic Acid Response in *Arabidopsis thaliana*. *Front. Plant Sci.* 9, 1637. doi: 10.3389/fpls.2018.01637
3. Battaglia, M., Solorzano, R.M., Hernandez, M., Cuellar-Ortiz, S., Garcia-Gomez, B., Marquez, J., et al. (2007). Proline-rich cell wall proteins accumulate in growing regions and phloem tissue in response to water deficit in common bean seedlings. *Planta* 225, 1121-1133. doi: 10.1007/s00425-006-0423-9
4. Bergmuller, E., Porfirova, S., and Dormann, P. (2003). Characterization of an Arabidopsis mutant deficient in gamma-tocopherol methyltransferase. *Plant Mol. Biol.* 52, 1181-1190. doi: 10.1023/b:plan.0000004307.62398.91
5. Carranza, A.P.S., Singh, A., Steinberger, K., Panigrahi, K., Palme, K., Dovzhenko, A., et al. (2016). Hydrolases of the ILR1-like family of Arabidopsis thaliana modulate auxin response by regulating auxin homeostasis in the endoplasmic reticulum. *Sci. Rep-Uk* 6, doi: 10.1038/srep24212
6. Chinnusamy, V., Zhu, J., and Zhu, J.K. (2006). Salt stress signaling and mechanisms of plant salt tolerance. *Genet. Eng.* (NY) 27, 141-177.
7. El-Esawi, M.A., Alaraidh, I.A., Alsahli, A.A., Alamri, S.A., Ali, H.M., and Alayafi, A.A. (2018). *Bacillus firmus* (SW5) augments salt tolerance in soybean (*Glycine max* L.) by modulating root system architecture, antioxidant defense systems and stress-responsive genes expression. *Plant Physiol. Biochem.* 132, 375-384. doi: 10.1016/j.plaphy.2018.09.026
8. Flowers, T.J., and Colmer, T.D. (2015). Plant salt tolerance: adaptations in halophytes. *Ann. Bot.* 115(3), 327-331. doi: 10.1093/aob/mcu267

9. Gaufichon, L., Masclaux-Daubresse, C., Tcherkez, G., Reisdorf-Cren, M., Sakakibara, Y., Hase, T., et al. (2013). *Arabidopsis thaliana* ASN2 encoding asparagine synthetase is involved in the control of nitrogen assimilation and export during vegetative growth. *Plant Cell Environ.* 36, 328-342. doi: 10.1111/j.1365-3040.2012.02576.x
10. Germain, V., Rylott, E.L., Larson, T.R., Sherson, S.M., Bechtold, N., Carde, J.P., et al. (2001). Requirement for 3-ketoacyl-CoA thiolase-2 in peroxisome development, fatty acid beta-oxidation and breakdown of triacylglycerol in lipid bodies of Arabidopsis seedlings. *Plant J.* 28a, 1-12. doi: 10.1046/j.1365-313X.2001.01095.x
11. Gisk, B., Yasui, Y., Kohchi, T., and Frankenberg-Dinkel, N. (2010). Characterization of the haem oxygenase protein family in *Arabidopsis thaliana* reveals a diversity of functions. *Biochem. J.* 425, 425-434. doi: 10.1042/Bj20090775
12. Gonzalez-Guzman, M., Apostolova, N., Belles, J.M., Barrero, J.M., Piqueras, P., Ponce, M.R., et al. (2002). The short-chain alcohol dehydrogenase ABA2 catalyzes the conversion of xanthoxin to abscisic aldehyde. *Plant Cell* 14, 1833-1846. doi: 10.1105/tpc.002477
13. Gray, E.J., and Smith, D.L. (2005). Intracellular and extracellular PGPR: commonalities and distinctions in the plant-bacterium signaling processes. *Soil Biol. Biochem.* 37, 395-412. doi: 10.1016/j.soilbio.2004.08.030
14. He, C.Y., Zhang, J.S., and Chen, S.Y. (2002). A soybean gene encoding a proline-rich protein is regulated by salicylic acid, an endogenous circadian rhythm and by various stresses. *Theor. Appl. Genet.* 104, 1125-1131. doi: 10.1007/s00122-001-0853-5
15. Hosseini, M.K., Powell, A.A., and Bingham, I.J. (2002). Comparison of the seed germination and early seedling growth of soybean in saline conditions. *Seed Sci. Res.* 12, 165-172. doi: 10.1079/Ssr2002108
16. Jiang, C.F., Belfield, E.J., Cao, Y., Smith, J.A.C., and Harberd, N.P. (2013). An Arabidopsis soil-salinity-tolerance mutation confers ethylene-mediated enhancement of sodium/potassium homeostasis. *Plant Cell* 25, 3535-3552. doi: 10.1105/tpc.113.115659
17. Kang, S.-M., Khan, A.L., Waqas, M., You, Y.-H., Kim, J.-H., Kim, J.-G., et al. (2014). Plant growth-promoting rhizobacteria reduce adverse effects of salinity and osmotic stress by regulating phytohormones and antioxidants in *Cucumis sativus*. *J. Plant Interact.* 9, 673-682. doi: 10.1080/17429145.2014.894587
18. Keller, A., Nesvizhskii, A.I., Kolker, E., and Aebersold, R. (2002). Empirical statistical model to estimate the accuracy of peptide identifications made by MS/MS and database search. *Anal. Chem.* 74, 5383-5392. doi: 10.1021/ac025747h
19. Khan, M.A., Asaf, S., Khan, A.L., Adhikari, A., Jan, R., Ali, S., et al. (2019a). Halotolerant rhizobacterial strains mitigate the adverse effects of NaCl stress in soybean seedlings. *Biomed. Res. Int.* 2019, doi: 10.1155/2019/9530963
20. Khan, M.A., Asaf, S., Khan, A.L., Jan, R., Kang, S.M., Kim, K.M., et al. (2019b). Rhizobacteria AK1 remediates the toxic effects of salinity stress via regulation of endogenous phytohormones and gene expression in soybean. *Biochem. J.* 476, 2393-2409. doi: 10.1042/Bcj20190435
21. Larson, E.R., Van Zelm, E., Roux, C., Marion-Poll, A., and Blatta, M.R. (2017). Clathrin heavy chain subunits coordinate endo- and exocytic traffic and affect stomatal movement. *Plant Physiol.* 175, 708-720. doi: 10.1104/pp.17.00970
22. Linkies, A., Muller, K., Morris, K., Tureckova, V., Wenk, M., Cadman, C.S.C., et al. (2009). Ethylene interacts with abscisic acid to regulate endosperm rupture during germination: a

comparative approach using *Lepidium sativum* and *Arabidopsis thaliana*. *Plant Cell* 21, 3803-3822. doi: 10.1105/tpc.109.070201
23. Marr, D.L., Devine, T.E., and Parker, M.A. (1997). Nodulation restrictive genotypes of *Glycine* and *Amphicarpaea*: A comparative analysis. *Plant Soil* 189, 181-188. doi: 10.1023/A:1004203018770
24. Martins, S.J., Rocha, G.A., de Melo, H.C., Georg, R.D., Ulhoa, C.J., Dianese, E.D., et al. (2018). Plant-associated bacteria mitigate drought stress in soybean. *Environ. Sci. Pollut. R.* 25, 13676-13686. doi:10.1007/s11356-018-1610-5
25. Molla-Morales, A., Sarmiento-Manus, R., Robles, P., Quesada, V., Perez-Perez, J.M., Gonzalez-Bayon, R., et al. (2011). Analysis of ven3 and ven6 reticulate mutants reveals the importance of arginine biosynthesis in Arabidopsis leaf development. *Plant J.* 65, 335-345. doi: 10.1111/j.1365-313X.2010.04425.x
26. Munns, R., and Gilliham, M. (2015). Salinity tolerance of crops - what is the cost? *New Phytol.* 208, 668-673. doi: 10.1111/nph.13519
27. Munns, R., and Tester, M. (2008). Mechanisms of salinity tolerance. *Annu. Rev. Plant Biol.* 59, 651-681. doi: 10.1146/annurev.arplant.59.032607.092911
28. Nesvizhskii, A.I., Keller, A., Kolker, E., and Aebersold, R. (2003). A statistical model for identifying proteins by tandem mass spectrometry. *Anal. Chem.* 75, 4646-4658. doi: 10.1021/ac0341261
29. Ning, L.H., Kan, G.Z., Shao, H.B., and Yu, D.Y. (2018). Physiological and transcriptional responses to salt stress in salt-tolerant and salt-sensitive soybean (*Glycine max* [L.] Merr.) seedlings. *Land Degrad. Dev.* 29, 2707-2719. doi: 10.1002/ldr.3005
30. Oh, S.E., Yeung, C., Babaei-Rad, R., and Zhao, R. (2014). Cosuppression of the chloroplast localized molecular chaperone HSP90.5 impairs plant development and chloroplast biogenesis in Arabidopsis. *BMC Res. Notes* 7, 643. doi: 10.1186/1756-0500-7-643
31. Phang, T.H., Shao, G.H., and Lam, H.M. (2008). Salt tolerance in soybean. *J. Integr. Plant Biol.* 50, 1196-1212. doi: 10.1111/j.1744-7909.2008.00760.x
32. Pou, A., Jeanguenin, L., Milhiet, T., Batoko, H., Chaumont, F., and Hachez, C. (2016). Salinity-mediated transcriptional and post-translational regulation of the Arabidopsis aquaporin PIP2;7. *Plant Mol. Biol.* 92, 731-744. doi: 10.1007/s11103-016-0542-z
33. Rashid, A., and Deyholos, M.K. (2011). PELPK1 (At5g09530) contains a unique pentapeptide repeat and is a positive regulator of germination in *Arabidopsis thaliana*. *Plant Cell Rep.* 30, 1735-1745. doi: 10.1007/s00299-011-1081-3
34. Sanchez-Parra, B., Frerigmann, H., Alonso, M.M., Loba, V.C., Jost, R., Hentrich, M., et al. (2014). Characterization of four bifunctional plant iam/pam-amidohydrolases capable of contributing to auxin biosynthesis. *Plants* (Basel) 3, 324-347. doi: 10.3390/plants3030324
35. Smith, D., Praslickova, D., and Ilangumaran, G. (2015). Inter-organismal signaling and management of the phytomicrobiome. *Front. Plant Sci.* 6, 722. doi: 10.3389/fpls.2015.00722
36. SoyStats (2020). *International: World Soybean Production* [Online]. The American Soybean Association. Available online at: http://soystats.com/international-world-soybean-production/ [accessed November 2020].
37. Stepanova, A.N., Hoyt, J.M., Hamilton, A.A., and Alonso, J.M. (2005). A link between ethylene and auxin uncovered by the characterization of two root-specific ethylene-insensitive mutants in Arabidopsis. *Plant Cell* 17, 2230-2242. doi: 10.1105/tpc.105.033365

38. Taira, M., Valtersson, U., Burkhardt, B., and Ludwig, R.A. (2004). *Arabidopsis thaliana* GLN2-encoded glutamine synthetase is dual targeted to leaf mitochondria and chloroplasts. *Plant Cell* 16, 2048-2058. doi: 10.1105/tpc.104.022046
39. Tromas, A., Braun, N., Muller, P., Khodus, T., Paponov, I.A., Palme, K., et al. (2009). The AUXIN BINDING PROTEIN 1 is required for differential auxin responses mediating root growth. *Plos One* 4, doi: 10.1371/journal.pone.0006648
40. Vaishnav, A., Kumari, S., Jain, S., Varma, A., and Choudhary, D.K. (2015). Putative bacterial volatile-mediated growth in soybean (*Glycine max* L. Merrill) and expression of induced proteins under salt stress. *J. Appl. Microbiol.* 119, 539-551. doi: 10.1111/jam.12866
41. Viswanath, K.K., Varakumar, P., Pamuru, R.R., Basha, S.J., Mehta, S., and Rao, A.D. (2020). Plant lipoxygenases and their role in plant physiology. *J. Plant. Biol.* 63, 83-95. doi: 10.1007/s12374-020-09241-x
42. Wang, L., Jin, X., Li, Q., Wang, X., Li, Z., and Wu, X. (2016). Comparative proteomics reveals that phosphorylation of beta carbonic anhydrase 1 might be important for adaptation to drought stress in *Brassica napus*. *Sci. Rep.* 6, 39024. doi: 10.1038/srep39024
43. Waśkiewicz, A., Gładysz, O., and Goliński, P. (2016). "Participation of phytohormones in adaptation to salt stress," in *Plant hormones under challenging environmental factors,* eds. G.J. Ahammed & J.-Q. Yu. (Dordrecht: Springer Netherlands), 75-115.
44. Xu, D., Huang, X., Xu, Z.Q., and Schlappi, M. (2011). The *HyPRP* gene EARLI1 has an auxiliary role for germinability and early seedling development under low temperature and salt stress conditions in *Arabidopsis thaliana*. *Planta* 234, 565-577. doi: 10.1007/s00425-011-1425-9
45. Xu, Z.J., Nakajima, M., Suzuki, Y., and Yamaguchi, I. (2002). Cloning and characterization of the abscisic acid-specific glucosyltransferase gene from adzuki bean seedlings. *Plant Physiol.* 129, 1285-1295. doi: 10.1104/pp.001784
46. Zhang, F.S., and Li, L. (2003). Using competitive and facilitative interactions in intercropping systems enhances crop productivity and nutrient-use efficiency. *Plant Soil* 248, 305-312. doi: 10.1023/A:1022352229863
47. Zhang, Q.Y., Lee, J., Pandurangan, S., Clarke, M., Pajak, A., and Marsolais, F. (2013). Characterization of Arabidopsis serine:glyoxylate aminotransferase, AGT1, as an asparagine aminotransferase. *Phytochem*. 85, 30-35. doi: 10.1016/j.phytochem.2012.09.017
48. Zhong, C.M., Xu, H., Ye, S.T., Wang, S.Y., Li, L.F., Zhang, S.C., et al. (2015). Gibberellic acid-stimulated Arabidopsis6 serves as an integrator of gibberellin, abscisic acid, and glucose signaling during seed germination in Arabidopsis. *Plant Physiol.* 169, 2288-2303. doi: 10.1104/pp.15.00858
49. Zhu, J.K. (2002). Salt and drought stress signal transduction in plants. *Annu. Rev. Plant Biol.* 53, 247-273. doi: 10.1146/annurev.arplant.53.091401.143329
50. Zorb, C., Geilfus, C.M., and Dietz, K.J. (2019). Salinity and crop yield. *Plant Biol.* 21, 31-38. doi: 10.1111/plb.12884

CONNECTING TEXT

In Chapters 3 and 4, the results showed that the plant growth and salinity tolerance of soybean were improved with the inoculation of *Rhizobium* sp. SL42 and *Hydrogenophaga* sp. SL48. Plant growth variables such as leaf area and shoot biomass were increased under optimal and salt-stressed conditions. They elicited mechanisms through regulating proteins related to growth and stress responses in the plant. These findings led to the understanding that these bacterial strains function as plant growth promoting rhizobacteria (PGPR). Many PGPR are known to secrete plant hormones and other compounds that serve as signaling molecules. This led to the research focused on determining the genomic characteristics of these bacteria, that contribute to their function and allow them to exert plant-beneficial activities. In Chapter 5, the genomes of *Rhizobium* sp. SL42 and *Hydrogenophaga* sp. SL48 were sequenced and analyzed to determine their genetic characteristics that facilitate their functional activity as PGPR.

5 Chapter 5 Complete Genome Sequences of *Rhizobium* sp. strain SL42 and *Hydrogenophaga* sp. strain SL48, Microsymbionts of *Amphicarpaea bracteata*

Authors: Gayathri Ilangumaran[1], Sowmyalakshmi Subramanian[1] and Donald Lawrence Smith[1]

Affiliations:

[1] Department of Plant Science, McGill University, Macdonald Campus, 21,111 Lakeshore Road, Sainte-Anne-de-Bellevue, QC, Canada.

This manuscript is in preparation for submission to Microbiological Resource Announcements.

5.1 Abstract

The genomes of rhizobacterial strains, *Rhizobium* sp. SL42 and *Hydrogenophaga* sp. SL48 were sequenced to determine their genetic characteristics. These strains were isolated from root nodules of *Amphicarpaea bracteata*, a native and undomesticated legume related to soybean. They were selected for sequencing as part of the isolation and characterization of beneficial rhizobacteria from native relatives of cultivated plants. Whole genome *de novo* sequencing was performed using Illumina and Nanopore sequencers and assembled in MaSuRCA. The genome of *Rhizobium* sp. SL42 consists of a 4.06 Mbp circular chromosome and two circular plasmids with a GC content of 60 %. The genome of *Hydrogenophaga* sp. SL48 consists of one 5.43 Mbp circular chromosome with a GC content of 65 %. Genes encoding for various metabolic functions, secretion systems, and biosynthetic gene clusters were present in their genomes. Whole genomic sequencing of SL42 and SL48 revealed functional properties of the genome related to the plant growth promoting characteristics exhibited by the bacteria. The root nodule bacteria in this project were selected on the basis of their ecological and agricultural importance relevant to plant-microbe interactions, plant growth promotion and enhancement of plant stress tolerance.

5.2 Introduction

Plants of the family Leguminosae engage in symbiotic relationships with nitrogen-fixing bacteria, collectively known as rhizobia, that dwell in the root nodules. Legume nodules are also known to contain bacteria other than the nitrogen-fixing symbiont and they presumably function as plant growth promoting rhizobacteria (PGPR) (Bai et al., 2002). *Amphicarpaea bracteata* (L.) is a wild legume indigenous to North America, native to Canada and the lower 48 states of the USA. It is usually found in the woody, shaded areas of wetlands but also occurs in similar areas

of non-wetlands in some regions. It is an herbaceous perennial that grows into a vine and produces flowers, pods, and seeds annually (PLANTS, 2017). The seeds and roots are edible, and the plant has been used by indigenous communities for both food and medicinal purposes (Moerman, 1998). It is the closest North American native relative to the cultivated soybean (*Glycine max* (L.) Merill) and their mutual symbiont belongs to the *Bradyrhizobium* genus, albeit with different genotypes. In the earlier study (Chapter 3), culturable members of the *A. bracteata* nodule phytomicrobiome were isolated and screened for beneficial effects on the growth and development of soybean plants. Two of the most promising isolates, *Rhizobium* sp. strain SL42 and *Hydrogenophaga* sp. SL48 improved salt tolerance and promoted the growth and maturity of soybean under greenhouse conditions.

Although the genus was identified using BLAST search of *16S rRNA* gene sequence, the species of strain SL42 and SL48 remain undetermined. Members of the Genus *Rhizobium* form nodules and benefit their legume host by fixing atmospheric nitrogen. *Rhizobium* sp. SL42 was isolated from the nodules of *A. bracteata*, also formed small nodules with soybean plants. However, the dominant symbiont of *A. bracteata* is the *Bradyrhizobium* genus (Sterner and Parker, 1999) and this is the first report of a *Rhizobium* species in this plant. *Rhizobium* sp. strain SL42 is closely related to the taxon *R. ipomoeae* shin9-1T (TaxID: 1210932) and the type strain was isolated from a water convolvulus field (Sheu et al., 2016). The Genus *Hydrogenophaga* consists of bacteria that utilize hydrogen as an energy source and oxidize it by the enzyme hydrogenase (Contzen et al., 2000). This is the first report of a *Hydrogenophaga* species associated with plant roots. The most closely related species to strain SL48 is *H. taeniospiralis* CCUG 15921T (TaxID: 1281780). The classification and other characteristics of the two strains are given in Table 5.1.

However, molecular functions related to their roles in plant growth and protection have to be explored. The aim of this study is to sequence the genome of SL42 and SL48 using high-throughput next-generation sequencing technology and analyze the whole genome sequence with available platforms to characterize the features of the genome that is relevant to the plant growth promoting characteristics of the bacteria.

Table 5.1. Taxonomic classification and general features of *Rhizobium* sp. *SL42* and *Hydrogenophaga* sp. SL48.

Property	**SL42**	**SL48**
Classification: Domain	Bacteria	Bacteria
Phylum	Proteobacteria	Proteobacteria
Class	Alphaproteobacteria	Betaproteobacteria
Order	Rhizobiales	Burkholderiales
Family	Rhizobiaceae	Comamonadaceae
Genus	*Rhizobium*	*Hydrogenophaga*
Species	unidentified	unidentified
Gram stain	Negative	Negative
Cell shape	Rod	Rod
Motility	Motile	Motile
Temperature range	Mesophile	Mesophile
Optimum temperature	25-30 °C (min. temp. 4 °C)	25-30 °C (min. temp. 4 °C)
pH range; Optimum	7.0	7.0
Carbon source	Mannitol	Mannitol
Habitat	Soil, root nodule on host	Soil, root nodule on host
Salinity	Up to 250 mM NaCl	Up to 100 mM NaCl
Oxygen requirement	Aerobic	Aerobic
Biotic relationship	Free-living/symbiont	Free-living/symbiont
Pathogenicity	Non-pathogenic	Non-pathogenic
Biosafety level	1	1
Isolation	Root nodule of *Amphicarpaea bracteata*	Root nodule of *Amphicarpaea bracteata*
Geographic location	Sainte-Anne-de-Bellevue, Canada	Sainte-Anne-de-Bellevue, Canada
Latitude	45. 404 °N	45. 404 °N
Longitude	73.934 °W	73.934 °W
Altitude	50 m	50 m
Sample collection	July 2017	July 2017

5.3 Materials and Methods

5.3.1 Growth conditions and Genomic DNA preparation

Rhizobium sp. SL42 and *Hydrogenophaga* sp. SL48 were streaked onto YEM agar plates and grown at 25 °C for 48 h to obtain well-developed colonies. A single colony was inoculated and sub-cultured in 25 mL YEM broth. The cultures were grown for 48 h in an orbital shaker (150 rpm) at 25 °C (OD_{600nm} of 1.0) and a pellet was obtained by centrifugation (5000 × g for 10 min, 25 °C). They were concentrated by discarding the excess broth and resuspending the pellets in 5 mL broth. Genomic DNA was isolated from 2 mL of cells using DNeasy Ultraclean Microbial Kit (QIAGEN). From the total DNA isolated, a concentration of 15 µg in 25 µl Tris buffer was dried using a vacuum-free evaporator (Centrifan PE, KD Scientific) in DNA stable (Biomatrica®) and shipped for *de novo* whole genome sequencing at Genotypic technology Ltd., Bangalore, India.

5.3.2 Quality control and Sanger sequencing

The concentration and purity of the genomic DNA were determined using the Nanodrop Spectrophotometer 2000 (Thermo Scientific) and Qubit dsDNA HS assay kit (Thermo Fisher Scientific). The integrity of the DNA was analyzed by agarose gel electrophoresis. PCR amplification was performed with 30-50 ng of the genomic DNA as the template using Takara ExTaq and 16S rRNA primers (27F' [AGAGTTTGATCCTGGCTCAG] and 1492R' [TACGGCTACCTTGTTACGACTT]) in a 25 µL reaction mixture. The PCR product was purified and used for Sanger sequencing.

5.3.3 Library preparation for Illumina sequencing

Library construction was carried out using the Nextera® XT DNA Library Preparation protocol (Illumina) for samples of SL42 and SL48. Briefly, 1 ng of Qubit quantified genomic DNA was tagmented (fragmented and adaptor tagged) using Amplicon Tagment Mix provided in the Nextera XT Kit. The adapter tagged DNA was subjected to 12 cycles of Indexing-PCR (72˚C for 3 min followed by denaturation at 95˚C for 30 sec, cycling (95˚C for 10 sec, 55˚C for 30 sec, 72˚C for 30 sec) and 72˚C for 5mins) to enrich the adapter-tagged fragments. The PCR products were purified using JetSeq Magnetic Beads (Bioline). The Illumina-compatible sequencing libraries were quantified by Qubit fluorometer (Thermo Fisher Scientific, MA, and USA) and their fragment size distribution was analyzed on Agilent TapeStation.

Adapter details:

Universal Adapter

5'AATGATACGGCGACCACCGAGATCTACACTCTTTCCCTACACGACGCTCTTCCGATCT

Adapter, Index

5'GATCGGAAGAGCACACGTCTGAACTCCAGTCAC **[INDEX]** ATCTCGTATGCCGTCTTCTGCTTG

5.3.3.1 Illumina sequencing

The libraries were sequenced on Illumina HiSeq X Ten sequencer (Illumina, San Diego, USA) using 150 bp paired-end chemistry. The data obtained from the sequencing run was de-multiplexed using Bcl2fastq software v2.20 and FastQ files were generated based on the unique dual barcode sequences (https://github.com/rrwick/Fast5-to-Fastq) The sequencing quality was assessed using FastQC v0.11.8 software. The adapter sequences were trimmed and bases above Q30 were considered, while low-quality bases were filtered off during read pre-processing and used for downstream analysis.

5.3.4 Library preparation for Nanopore sequencing

For nanopore sequencing, library preparation was performed as per instructions provided in the Native barcoding kit (EXP-NBD114) from Oxford Nanopore Technology (ONT). A total of 600 ng of purified genomic DNA from the samples was end-repaired (NEBnext ultra II end repair kit, New England Biolabs, MA, USA) and cleaned up with 1 x AmPure beads (Beckmann Coulter, USA). Native barcode ligation was performed with NEB blunt/ TA ligase (New England Biolabs, MA, USA) using EXP-NBD104 (ONT) and cleaned with 1 x AmPure beads.

Barcodes used for Nanopore sequencing:

Sample ID	Barcode name	Sequences
SL42_1	NB05	AAGGTTACACAAACCCTGGACAAG
SL48_1	NB06	GACTACTTTCTGCCTTTGCGAGAA

Qubit quantified, barcode ligated DNA sample was Adapter ligated for 15 minutes using NEB next Quick Ligation module (New England Biolabs, MA, USA). The library was cleaned up using 0.6X Ampure beads (Beckmann Coulter, USA) and the sequencing library was eluted in 15

µL of elution buffer and used for sequencing. The concentration and yield of the Nanopore library were optimal for sequencing on GridionX5.

5.3.4.1 Nanopore sequencing

Sequencing was performed on GridION X5 (Oxford Nanopore Technologies, Oxford, UK) using SpotON flow cell R9.4 (FLO-MIN106) in a 48 h sequencing protocol. Nanopore raw reads ('fast5' format) were base-called ('fastq5' format) and de-multiplexed using Guppy v2.3.4.

5.3.5 Genome assembly and annotation

The quality control report, trimming and part of the analyses were performed using Commander, the NGS analysis tool made by Genotypic Technology, Bangalore, India. The Illumina raw reads were processed using a standard tool named Trimgalore (https://www.bioinformatics.babraham.ac.uk/projects/trim_galore/) to remove bad quality reads and nanopore raw reads were processed using Porechop (https://github.com/rrwick/Porechop). The raw reads generated from both platforms were processed and good quality reads were retained. Raw reads from both Illumina and nanopore platforms were processed for quality and adaptor removal. Both Illumina paired-end and nanopore data were used for hybrid assembly using MaSuRCA v3.3.7 2 hybrid assembler (Zimin et al., 2013). The assembly resulted into 4 -5.5 Mbp genome for the 2 samples. The generated assembly was further used for gene prediction using PROKKA tool (Seemann, 2014). The predicted proteins were searched against the UniProt protein database using the DIAMOND BlastP program for the gene ontology and annotation (Buchfink et al., 2015). The predicted gene sequences were used for Pathway analysis using the Kyoto Encyclopedia of Genes and Genomes (KEGG) orthology (KO) database of molecular functions (Kanehisa et al., 2016). When the nucleotide/protein sequence is mapped, KO identifiers were assigned for each gene/protein and pathway maps are generated for the orthologs found in the sequence. The assembled genome was also used for SSR (Simple Sequence repeats) prediction. The SSR algorithm uses MISA (MIcro SAtellite identification tool) software (Beier et al., 2017). Microsatellites were segregated based on the number of repetitive nucleotides, from the input assembled sequence. The genome was also independently annotated by the NCBI Prokaryotic Genome Annotation Pipeline (PGAP) (Tatusova et al., 2016). The genome was analyzed using antiSMASH v. 5.0 to identify and annotate secondary metabolite biosynthesis gene clusters (Blin et al., 2019). Phylogenetic trees were constructed using BLAST pairwise alignment of the

sequences of *16S rRNA* and house-keeping genes *gyrB*, *recA* and *rpoD* retrieved from the whole genome sequence of SL42 and SL48.

5.4 Results

5.4.1 Quality control and Sanger sequencing

The samples passed quality assessment with optimal yield and concentration and were suitable for Illumina and Nanopore library preparation (Table 5.2 and Figure 5.1).

Table 5.2. DNA concentration and purity of samples estimated using Nanodrop spectrophotometer and Qubit fluorometer.

	Sample	SL42	SL48
Nanodrop	ng/μL	456.4	910.7
	260/280	1.89	1.93
	260/230	1.67	1.97
	Volume (μL)	25	25
	Yield (ng)	11410	22767.5
	Volume loaded on gel (ng/μL)	2 (1:4)	2 (1:7)
Qubit QC	Qubit conc. (ng/μL)	391.2	936.6
	Volume (μL)	25	25
	Yield (ng)	9780	23415
	QC purity	Optimal	Optimal
	QC Integrity	Intact	Intact

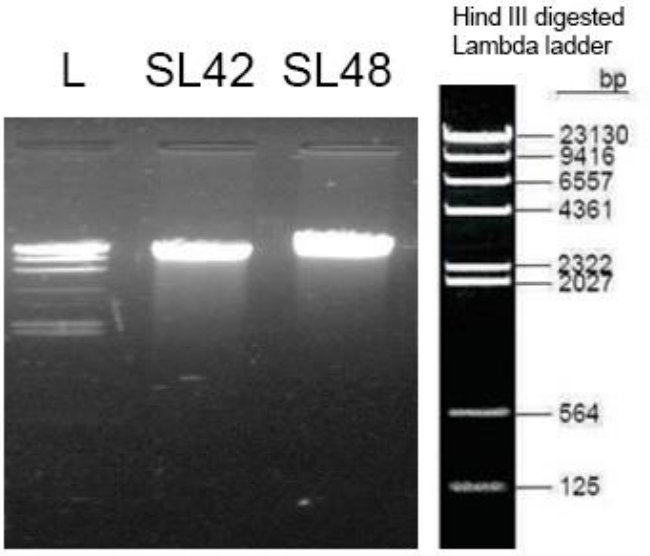

Figure 5.1. Agarose gel electrophoresis of DNA samples from SL42 and SL48.

Based on the BLAST similarity search of the 16S rRNA gene sequence, the strain SL42 was identified as *Rhizobium* sp. and the closely related species is *Rhizobium ipomoeae* strain NFB1 with 98% identity. The strain SL48 was identified as *Hydrogenophaga* sp. and the closely related species is *Hydrogenophaga taeniospiralis* CCUG 15921 strain NBRC 102512 with 99% identity. The ANI (Average Nucleotide Identity) was calculated with reference to the genomes of the type strains, and the values were 77.72% for SL42 and 83.39% for SL48, well below the threshold level of <95-96% (Yoon et al., 2017) for both the strains. Hence, they will be proposed as new species.

5.4.2 Library preparation and sequencing

The Illumina-compatible sequencing library for the samples showed an average fragment size of 580 bp as well as sufficient concentration for obtaining desired sequencing data.

5.4.2.1 Primary analysis

The pre-processing of data retained more than 2 million paired-end reads for SL42 and SL48. The sequencing quality was assessed using FastQC (Table 5.3). The number of reads retained after pre-processing, read statistics for the Nanopore data, and quality score per base for the processed Illumina reads are shown in Appendix C, Supplementary Tables 5.1-5.6 and Supplementary Figure 5.1.

5.4.3 Genome properties

The processed Illumina and nanopore reads were used for the hybrid assembly using MaSuRCA v3.3.7 2. The program uses both de Bruijn graph and Overlap-Layout-Consensus (OLC) approach to assemble short reads and long reads. The 2 bacterial samples were sequenced at ~170x coverage using Illumina HiSeq and ~120x coverage using nanopore sequencing (Table 5.4). The assemblies were 4 and 5.4 MB for SL42 and SL48 respectively (Table 5.5).

Table 5.3. FastQC output on raw sequence data.

Measure	SL42	SL48
File type	Conventional base calls	Conventional base calls
Encoding	Sanger/Illumina 1.9	Sanger/Illumina 1.9
Total sequences	2782606	3022451
Sequences flagged as poor quality	0	0
Sequence length (bp)	150	150
% GC	60	65

Table 5.4. Sequencing coverage.

Sample	SL42	SL48
Illumina	166.96	181.35
Nanopore	127.73	115.18

Table 5.5. Assembly statistics.

Assembly statistics	SL42	SL48
Contigs Generated	3	1
Maximum Contig Length	4063937	5433040
Minimum Contig Length	351829	5433040
Average Contig Length	1722001	5433040
Median Contig Length	750237.0	5433040.0
Total Contigs Length	5166003	5433040
Contigs >= 10 Kbp	3	1
Contigs >= 1 Mbp	1	1
N50 value	4063937	5433040

5.4.3.1 Gene prediction

The gene prediction and annotation are shown in Table 5.6 and complete gene ontology summary and protein predictions for SL42 and SL48 are shown in Figures 5.2 and 5.3.

Table 5.6. Annotation summary of predicted proteins.

Sample	Total proteins	Annotated proteins
SL42	4727	4642
SL48	5077	4937

5.4.4 Insights from the genome sequence

The predicted genes included gene clusters related to flagella, chemotaxis, homoserine lactone and multidrug resistance, in addition to genes associated with regulatory and transport proteins. In *Rhizobium* sp. SL42, genes encoding Type I and Type IV secretion systems were present. In *Hydrogenophaga* sp. SL48, genes encoding Type II and Type IV secretion systems and hydrogenase were present. Also, genes for photosystem I, nodulation, nitrogen fixation, heat shock and cold shock proteins, hypoxic response, iron chelation and carotenoid synthesis were found (Tables 5.7-5.8). The KEGG pathway mapping associated predicted proteins with functions related to bacterial motility proteins, secretion system proteins, bacterial chemotaxis, flagellar assembly, peptidoglycan biosynthesis and quorum sensing. However, there were unique proteins found in both strains. In SL42, photosynthesis, carbon fixation, and carotenoid biosynthesis pathway proteins were found. In SL48, proteins related to the biosynthesis of vancomycin group antibiotics

were present (Appendix C, Supplementary Tables 5.7-5.8). The phylogenetic analyses of the *16S rRNA* gene and house-keeping genes *gyrB*, *recA* and *rpoD* (Figures 5.4 and 5.5) demonstrated that the strains *Rhizobium* sp. SL42 and *Hydrogenophaga* sp. SL48 might represent novel species within their respective genera.

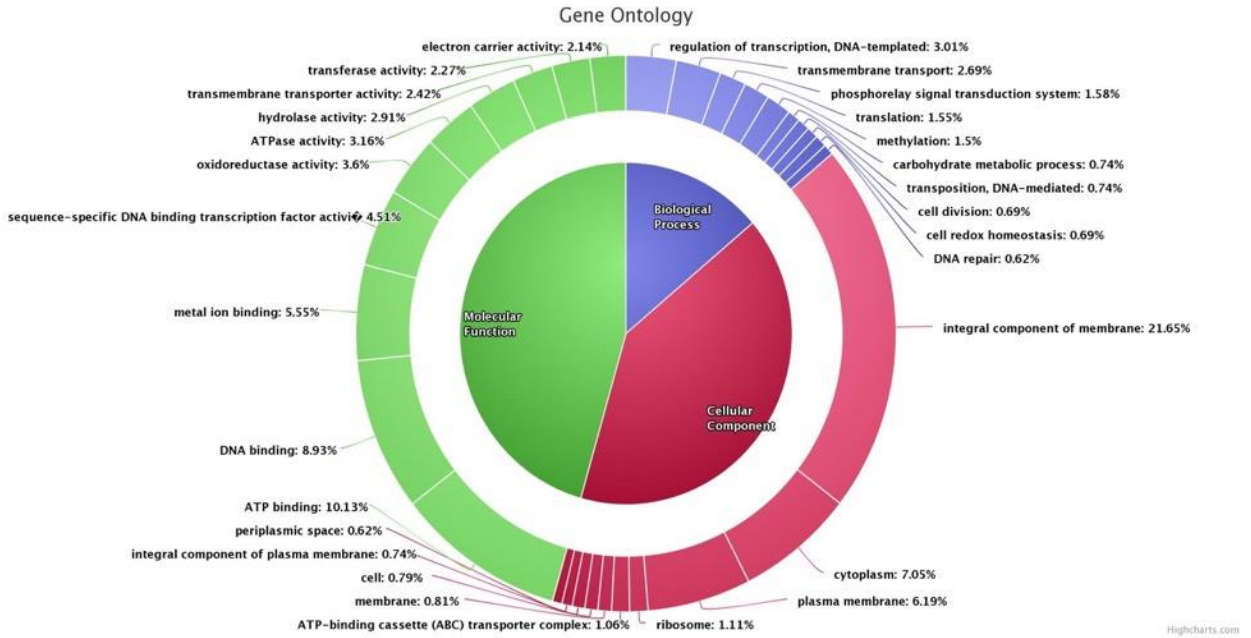

Figure 5.2. Gene Ontology distribution of annotated proteins in *Rhizobium* sp. SL42 genome.

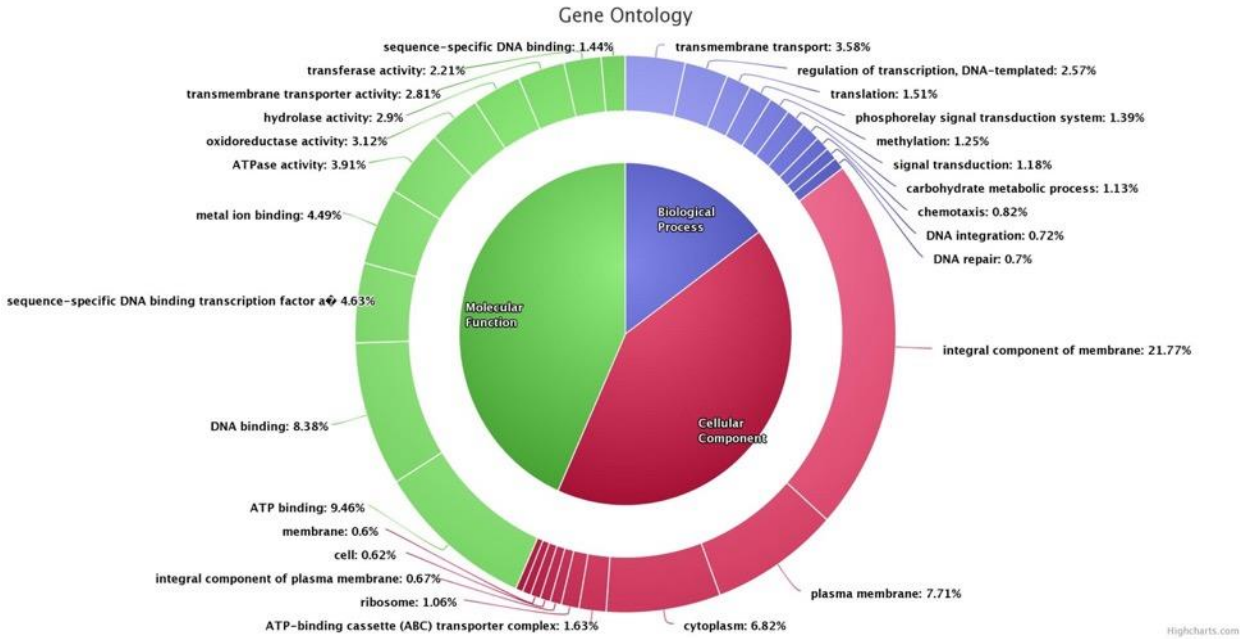

Figure 5.3. Gene Ontology distribution of annotated proteins in *Hydrogenophaga* sp. SL48 genome.

Table 5.7. Genes related to key functions in the genome of *Rhizobium* sp. SL42.

Gene	Function	# Genes encoding
bcr	Bicyclomycin resistance	3
bdlA; bigR	Biofilm	6
cspA; cspE; cspG	cold shock protein, cold shock-like protein	7
entS; fepC; fepD; fepG	Enterobactin	7
hspQ	heat shock protein	1
rhtB	homoserine lactone efflux protein	7
hrp1	hypoxic response protein	1
yfeA; hemH	Iron chelation	2
lptA; lptB; lptG; lapA; lapB	lipopolysaccharide assembly and export proteins	8
mdtA; mdtB; mdtC; mdtN; mdtK; mdtE	Multidrug resistance	24
mrpA; mrpB; mrpC; mrpD; mrpE; mrpG; mrpF	Na(+)/H(+) antiporter subunit	7
fixK	nitrogen fixation regulation	4
nodM, nolR	Nodulation	1
pleC	Non-motile and phage-resistance protein	3
envZ	Osmolarity sensor protein	1
hemF	Oxygen-dependent coproporphyrinogen-III oxidase	1
ycf3; regA	Photosynthesis	2
crtI; crtB; carA2	Phytoene	3
	Putative signaling	22
fpvA; fhuA; ftsY; chvE, cheD; fhuE;	Receptor	12
aroK; aroA; aroE; quiA	Shikimate pathway	5
chaA	Sodium-potassium/proton antiporter	1
potA; potB; potD	Spermidine/putrescine	25
gerE	Spore germination protein	1
soj	Sporulation initiation inhibitor	2
prsD; prsE;	Type I secretion system	15
virB4; virB9; virb10, virB11	Type IV secretion system	4
clcB	Voltage-gated ClC-type chloride channel	1

Table 5.8. Genes related to major functions in the genome of *Hydrogenophaga* sp. SL48.

Gene	Function	# Genes encoding
	Acid shock protein	1
ArpC	Antibiotic efflux pump outer membrane protein	1
bcr	Bicyclomycin resistance	2
icaR	Biofilm operon regulator	1
ble	Bleomycin resistance	1
KfoC	Chondroitin synthase	2
cspA; cspG	cold shock protein, cold shock-like protein	2
fas6	Cytokinin riboside 5'-monophosphate phosphoribohydrolase	1
entS	Enterobactin	1
fbpC	Fe(3+) ions import ATP-binding protein	1
hslR	heat shock protein	1
rhtB	homoserine lactone efflux protein	5
hypF; hypB; hypD	Hydrogenase maturation factor	3
hrp1	hypoxic response protein	1
hemH; sirB	Iron chelation	2
lptA; lptB; lptC; lptG; lptF; lapA; lapB	lipopolysaccharide assembly and export proteins	16
mdtB; mdtN; mdtE mdtA; mdtC; mexR; mexA; mdtD; mdtH; mdtG	Multidrug resistance	13
gerN; mrpA; mrpD; mrpE; mrpG; mrpF; mnhC1	Na(+)/H(+) antiporter subunit	7
hoxF; hoxU; hoxY; hoxH	NAD-reducing hydrogenase HoxS subunit	4
fixK	nitrogen fixation regulation	1
nifH; nifD; nifK	Nitrogenase iron protein	5
nifW	Nitrogenase-stabilizing/protective protein	1
nodD	Nodulation protein	4
envZ	Osmolarity sensor protein	2
osmY	Osmotically-inducible protein Y	3
hemF	Oxygen-dependent coproporphyrinogen-III oxidase	1
	Periplasmic [NiFeSe] hydrogenase subunit	2
kcsA	pH-gated potassium channel	1
regA	Photosynthesis	1

Gene	Function	# Genes encoding
crtB	Phytoene	1
	Putative signaling	1
cheD; cirA; aer; ftsY; fhuA; chvE; fucA; fhuE;	Receptor	8
cbbS1; cbbL; rlp2	Ribulose bisphosphate carboxylase	3
rubA; hrb	Rubredoxin	2
aroL; aroA; aroE; quiA; ydiB	Shikimate pathway	6
chaA	Sodium-potassium/proton antiporter	1
potA; potB; potD;	Spermidine/putrescine	12
spsA	Spore coat polysaccharide biosynthesis protein	1
srkA	stress response kinase A	1
iaaM	Tryptophan 2-monooxygenase	1
xpsD; gspE; gspF; epsE; epsF; hxcR; xcpQ; xcpV; xcpT; pulD;	Type II secretion system	13
virB1; virB4; virB8; virb10, virB1; ptlf	Type IV secretion system	7

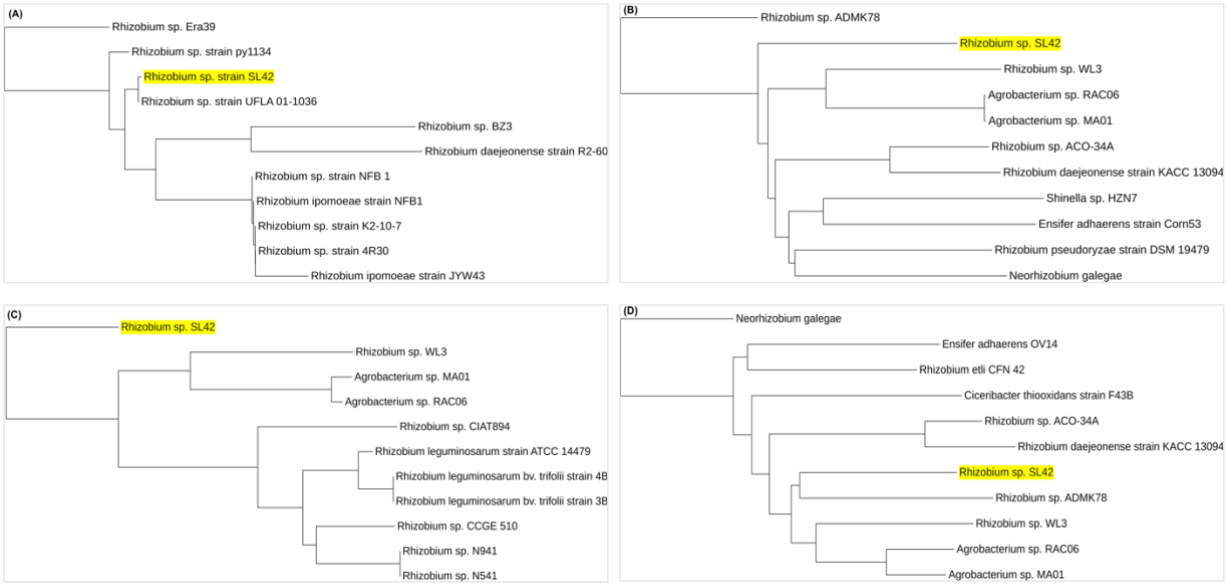

Figure 5.4. Phylogenetic trees of *Rhizobium* sp. SL42 and closely related strains using BLAST pairwise alignment.
Query gene sequences **(A)** *16S rRNA* **(B)** *gyrB* **(C)** *recA* and **(D)** *rpoD*.

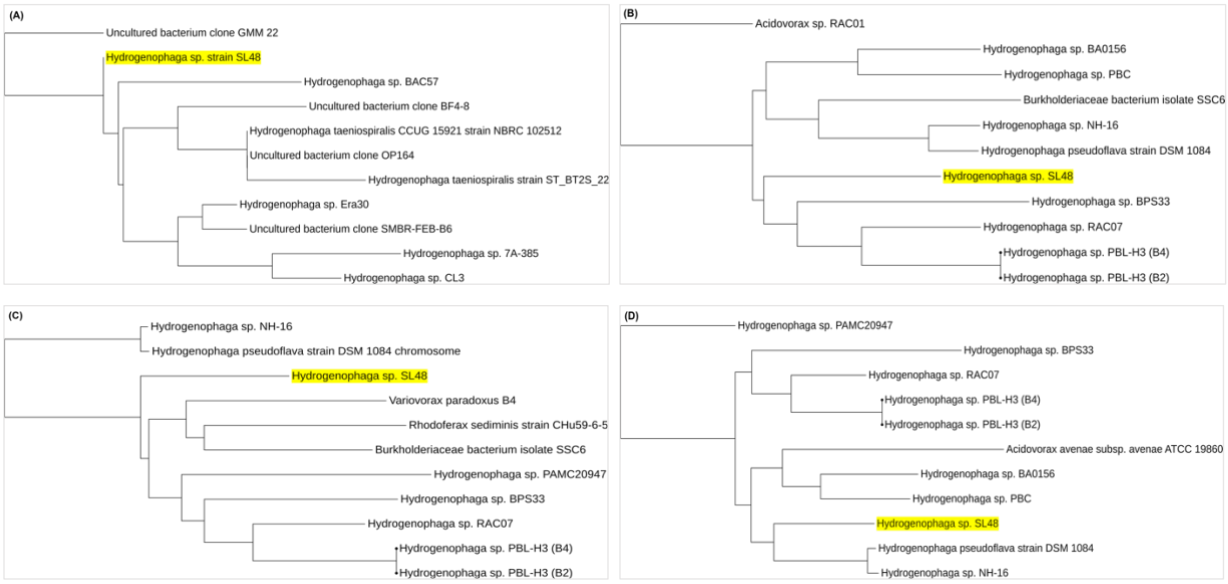

Figure 5.5. Phylogenetic trees of *Hydrogenophaga* sp. SL48 and closely related strains using BLAST pairwise alignment.
Query gene sequences **(A)** *16S rRNA* **(B)** *gyrB* **(C)** *recA* and **(D)** *rpoD*.

5.4.4.1 Finding secondary metabolites using Anti-SMASH

The AntiSMASH results indicated the presence of biosynthetic gene clusters encoding secondary metabolites, and some of them were unique to the strains *Rhizobium* sp. SL42 and *Hydrogenophaga* sp. SL48 (Tables 5.9 and 5.10; Figures 5.6 and 5.7).

Table 5.9. AntiSMASH results of secondary metabolite coding regions of *Rhizobium* sp. SL42.

Region	Type	From (bp)	To (bp)	Most similar known cluster	Similarity
Region 1.1	TfuA-related	850,531	872,449	-Not Identified	-Not Applicable
Region 1.2	Terpene	2,383,268	2,404,122		
Region 1.3	Hserlactone	2,965,914	2,986,555		
Region 1.4	Bacteriocin	3,703,712	3,714,620		
Region 2.1	NRPS, T1PKS	197,065	249,650		
Region 2.2	TfuA-related	546,474	568,488		
Region 3.1	Hserlactone	50,625	71,251		

Table 5.10. AntiSMASH results of secondary metabolite coding regions of *Hydrogenophaga* sp. SL48.

Region	Type	From (bp)	To (bp)	Most similar known cluster		Similarity
Region 1	Arylpolyene	1,139,130	1,192,715	Xanthomonadin I	Other	21%
Region 2	Terpene	1,251,962	1,275,723			
Region 3	T1PKS, NRPS-like, NRPS	1,868,166	1,929,593			
Region 4	Bacteriocin	3,079,772	3,090,659			
Region 5	Siderophore	3,327,234	3,339,111	Desferrioxamine E	Other	50%
Region 6	Betalactone	5,240,538	5,278,382	Mycosubtilin	NRP + Polyketide	20%

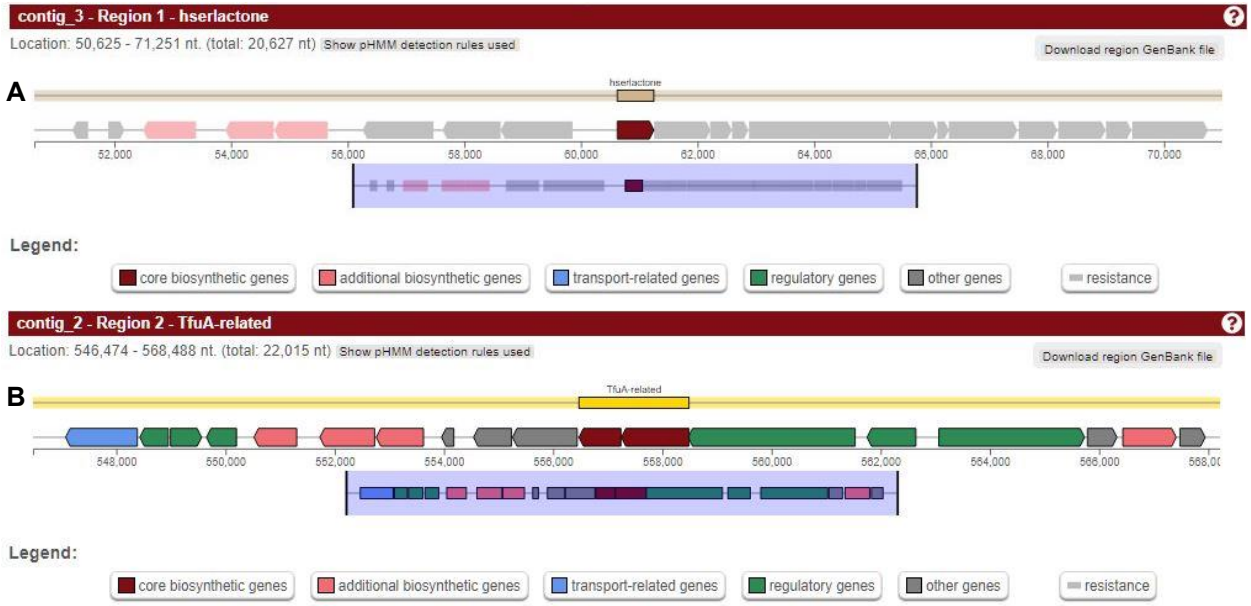

Figure 5.6. Coding regions of **(A)** homoserine lactone and **(B)** TfuA-related in *Rhizobium* sp. SL42 genome.

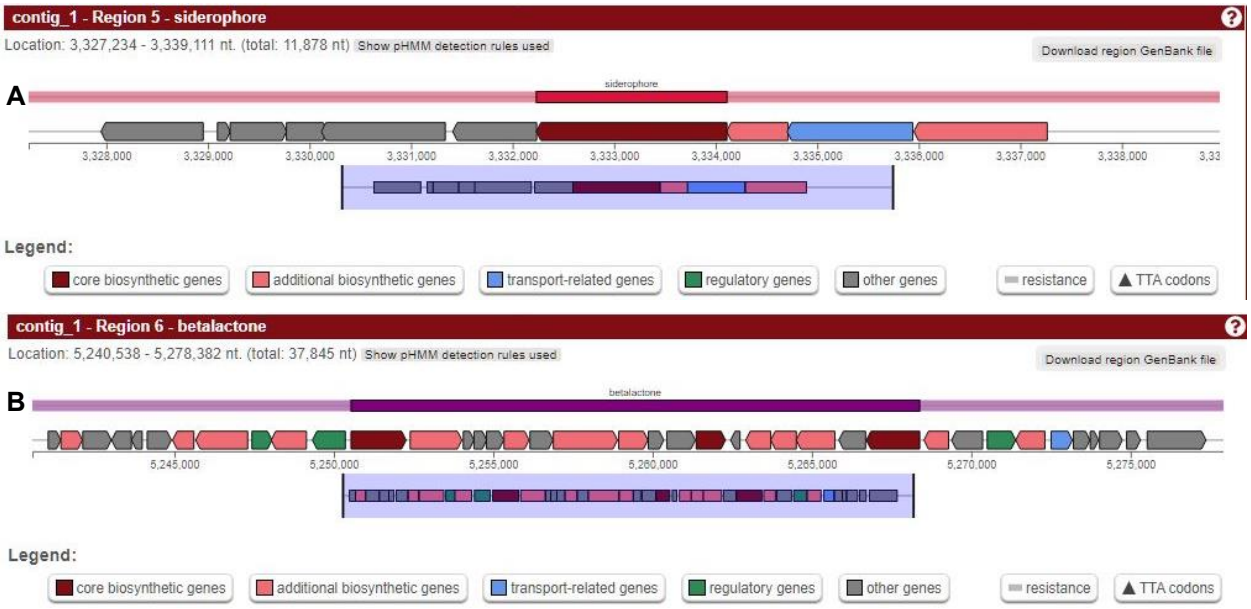

Figure 5.7. Coding regions of **(A)** siderophore and **(B)** betalactone in *Hydrogenophaga* sp. SL48 genome.

5.5 Discussion

Plant growth promoting rhizobacteria (PGPR) produce bioactive substances that improve plant growth and alleviate stress. Understanding the behaviour of PGPR when inoculated onto plants is important for their application in agriculture. Some of these compounds are also essential for plant root colonization (Bloemberg and Lugtenberg, 2001). The whole genome sequencing analysis revealed the genes harboured in the genomes of *Rhizobium* sp. SL42 and *Hydrogenophaga* sp. SL48 that might play key roles in their as PGPR. PGPR are known to produce auxins, gibberellins, cytokinins and ethylene and manipulate phytohormone balance in plants. PGPR stimulate root proliferation by excretion of indole-3-acetic acid (IAA) into the rhizosphere, thus enhancing uptake of water and nutrients (Sukumar et al., 2013). Several PGPR also secrete cytokinins that have been detected in cellfree medium (Garcia de Salamone et al., 2001). Genes encoding IAA and cytokinin biosynthesis (*iaaM* and *fas6*) were present in *Hydrogenophaga* sp. SL48. Volatile organic compounds (VOCs) produced by bacteria help in plant development and stress responses (Bailly and Weisskopf, 2012). Polyamines play important physiological and protective roles in plants. *Bacillus megaterium* BOFC15 secretes spermidine, a polyamine leading to enhanced cellular polyamine levels in Arabidopsis. Inoculation with the bacterium resulted in an increase in biomass, changed root architecture and elevated photosynthetic capacity. The plants also exhibited higher drought tolerance and abscisic acid content under water deficit (osmotic stress) (Zhou et al., 2016a). Both strains possess multiples genes that encode for spermidine/putrescine compounds.

Genes encoding the production of secondary metabolites found using Anti-SMASH showed that the PGPR produces antibiotics such as thiopeptides, polyketides and bacteriocins that suppress pathogens. Bacterial surface factors like flagellins and o-antigen of lipopolysaccharides induce systemic resistance (ISR) whereas, analogs of salicylic acid, jasmonic acid and ethylene elicit systemic acquired resistance (SAR) in plants (Ping and Boland, 2004; Lugtenberg and Kamilova, 2009; Pieterse et al., 2014). A bacteriocin, thuricin 17, isolated from the soybean endosymbiont *Bacillus thuriengenesis* NEB 17, when applied as foliar spray or root drench stimulated the growth of soybean and corn (Subramanian et al., 2016). Siderophores are iron chelators produced by some microorganisms and enhance plant growth under iron-depleted conditions where they are used as the method for accessing scarce iron and also act as biocontrol agents by reducing the availability of iron for pathogens (Saha et al., 2016).

Genes involved in the pathways of cell motility, chemotaxis, lipopolysaccharide synthesis and biofilm formation suggested that they might play important roles in rhizosphere colonization of SL42 and SL48. Plant beneficial bacteria present in the rhizosphere are in proximity to roots and many are known to form biofilms, which aid in the successful colonization of root surfaces and adjacent soil particles and thwart pathogenic bacteria. Biofilms are structured communities of bacterial cells living adherent to a surface embedded in an extracellular polysaccharide matrix. Biofilms of beneficial bacteria play a crucial role in plant growth promoting effects (Ramey et al., 2004). Plant roots exude signal compounds that regulate plant-bacteria interactions and trigger chemotaxis in bacteria, towards the rhizosphere (Fan et al., 2012). For example, flavonoids secreted by roots determine the legume-rhizobia symbiotic associations while malate and citrate are found to interact with *Bacillus* and *Pseudomonas* strains (Badri and Vivanco, 2009). There are genes related to the metabolism of these compounds in SL42 and SL48, suggesting that they possibly take part in plant-microbe interactions.

During colonization, PGPR assimilate substances released by the roots and in turn, produce bioactive compounds that promote plant growth or ameliorate stress (Xie et al., 2014). Recent advances in high-throughput strategies have led to detailed investigations of plant-microbe interactions and the differential effects of root exudates on mechanisms of rhizobacteria that are crucial to the beneficial effects observed. The differentially expressed genes or proteins were mainly those involved in nutrient utilization and transport, chemotaxis, secretion, quorum sensing, extracellular matrix, synthesis of volatile compounds, and antibiotic production (Fan et al., 2012; Beauregard et al., 2013; Kierul et al., 2015; Mwita et al., 2016; Zhou et al., 2016b). The presence of genes related to these functions indicates that SL42 and SL48 could potentially function as beneficial rhizobacteria. Understanding the dynamic function of bacterial cells and regulatory networks related to enzyme metabolism, transport and utilization of nutrients, signal transduction proteins and root colonization pattern is important in determining their potential applications in agriculture (Kierul et al., 2015; Zhang et al., 2015; Mwita et al., 2016; Zhou et al., 2016b).

5.6 Data availability statement

The genome project is deposited in the Genome database, NCBI (https://www.ncbi.nlm.nih.gov/genome/) and a high-quality permanent whole genome sequence for isolates SL42 and SL48 were submitted (Table 5.11).

Table 5.11. Whole genome sequencing project information.

	SL42	**SL48**
Name	*Rhizobium* sp. strain:SL42	*Hydrogenophaga* sp. strain:SL48
	Genome	Genome
Accession number	CP063397; CP063398; CP063399	CP063400
BioProject	PRJNA669345	PRJNA669344
BioSample	SAMN16451206	SAMN16451201
Locus Tag	IM739	IM738
Tax ID	1210932	1904254
Genome size	4.06 Mbp	5.43 Mbp
Assembly method	MaSuRCA 3.3.7	MaSuRCA 3.3.7
Assembly name	MGM_Rhim_1	MGM _Hyga_1
Reference Title	Genome sequence of *Rhizobium* sp. strain SL42	Genome sequence of *Hydrogenophaga* sp. strain SL48
Reference authors:	Ilangumaran, G., Subramanian, S., and Smith, D.	Ilangumaran, G., Subramanian, S., and Smith, D.

5.7 References

1. Badri, D.V., and Vivanco, J.M. (2009). Regulation and function of root exudates. *Plant Cell Environ.* 32, 666-681. doi: 10.1111/j.1365-3040.2009.01926.x
2. Bai, Y.M., D'Aoust, F., Smith, D.L., and Driscoll, B.T. (2002). Isolation of plant-growth-promoting *Bacillus* strains from soybean root nodules. *Can. J. Microbiol.* 48, 230-238. doi: 10.1139/W02-014
3. Bailly, A., and Weisskopf, L. (2012). The modulating effect of bacterial volatiles on plant growth: current knowledge and future challenges. *Plant Signal. Behav.* 7, 79-85. doi: 10.4161/psb.7.1.18418
4. Beauregard, P.B., Chai, Y.R., Vlamakis, H., Losick, R., and Kolter, R. (2013). *Bacillus subtilis* biofilm induction by plant polysaccharides. *P. Natl. Acad. Sci. USA* 110, E1621-E1630. doi: 10.1073/pnas.1218984110
5. Beier, S., Thiel, T., Munch, T., Scholz, U., and Mascher, M. (2017). MISA-web: a web server for microsatellite prediction. *Bioinformatics* 33, 2583-2585. doi: 10.1093/bioinformatics/btx198
6. Blin, K., Shaw, S., Steinke, K., Villebro, R., Ziemert, N., Lee, S.Y., et al. (2019). antiSMASH 5.0: updates to the secondary metabolite genome mining pipeline. *Nucleic Acids Res.* 47, W81-W87. doi: 10.1093/nar/gkz310

7. Bloemberg, G.V., and Lugtenberg, B.J.J. (2001). Molecular basis of plant growth promotion and biocontrol by rhizobacteria. *Curr. Opin. Plant Biol.* 4, 343-350. doi: 10.1016/S1369-5266(00)00183-7
8. Buchfink, B., Xie, C., and Huson, D.H. (2015). Fast and sensitive protein alignment using DIAMOND. *Nat. Methods* 12, 59-60. doi: 10.1038/nmeth.3176
9. Contzen, M., Moore, E.R.B., Blumel, S., Stolz, A., and Kampfer, P. (2000). *Hydrogenophaga intermedia* sp nov., a 4-aminobenzenesulfonate degrading organism. *Syst. Appl. Microbiol.* 23, 487-493. doi: 10.1016/S0723-2020(00)80022-3
10. Fan, B., Carvalhais, L.C., Becker, A., Fedoseyenko, D., von Wiren, N., and Borriss, R. (2012). Transcriptomic profiling of *Bacillus amyloliquefaciens* FZB42 in response to maize root exudates. *BMC Microbiol.* 12, doi: Artn 11610.1186/1471-2180-12-116
11. Garcia de Salamone, I.E., Hynes, R.K., and Nelson, L.M. (2001). Cytokinin production by plant growth promoting rhizobacteria and selected mutants. *Can. J. Microbiol.* 47, 404-411.
12. Kanehisa, M., Sato, Y., Kawashima, M., Furumichi, M., and Tanabe, M. (2016). KEGG as a reference resource for gene and protein annotation. *Nucleic Acids Res.* 44, D457-D462. doi: 10.1093/nar/gkv1070
13. Kierul, K., Voigt, B., Albrecht, D., Chen, X.H., Carvalhais, L.C., and Borriss, R. (2015). Influence of root exudates on the extracellular proteome of the plant growth-promoting bacterium *Bacillus amyloliquefaciens* FZB42. *Microbiology* 161, 131-147. doi: 10.1099/mic.0.083576-0
14. Lugtenberg, B., and Kamilova, F. (2009). Plant-Growth-Promoting Rhizobacteria. *Annu. Rev. Microbiol.* 63, 541-556. doi: 10.1146/annurev.micro.62.081307.162918
15. Moerman, D.E. (1998). Native American Ethnobotany Oregon: Timber Press. ISBN 0-88192-453-9
16. Mwita, L., Chan, W.Y., Pretorius, T., Lyantagaye, S.L., Lapa, S.V., Avdeeva, L.V., et al. (2016). Gene expression regulation in the plant growth promoting *Bacillus atrophaeus* UCMB-5137 stimulated by maize root exudates. *Gene* 590, 18-28. doi: 10.1016/j.gene.2016.05.045
17. Pieterse, C.M.J., Zamioudis, C., Berendsen, R.L., Weller, D.M., Van Wees, S.C.M., and Bakker, P.A.H.M. (2014). Induced Systemic Resistance by Beneficial Microbes. *Ann. Rev. Phytopathol.* 52, 347-375. doi: 10.1146/annurev-phyto-082712-102340
18. Ping, L.Y., and Boland, W. (2004). Signals from the underground: bacterial volatiles promote growth in Arabidopsis. *Trends Plant Sci.* 9, 263-266. doi: 10.1016/j.tplants.2004.04.008
19. PLANTS, U. (2017). *Amphicarpaea bracteata* (L.) Fernald American hogpeanut [Online]. Available online at: https://plants.usda.gov/core/profile?symbol=AMBR2 [accessed 12 Aug 2017].
20. Ramey, B.E., Koutsoudis, M., von Bodman, S.B., and Fuqua, C. (2004). Biofilm formation in plant-microbe associations. *Curr. Opin. Microbiol.* 7, 602-609. doi: 10.1016/j.mib.2004.10.014
21. Saha, M., Sarkar, S., Sarkar, B., Sharma, B.K., Bhattacharjee, S., and Tribedi, P. (2016). Microbial siderophores and their potential applications: a review. *Environ. Sci. Pollut. Res. Int.* 23, 3984-3999. doi: 10.1007/s11356-015-4294-0
22. Seemann, T. (2014). Prokka: rapid prokaryotic genome annotation. *Bioinformatics* 30, 2068-2069. doi: 10.1093/bioinformatics/btu153

23. Sheu, S.Y., Chen, Z.H., Young, C.C., and Chen, W.M. (2016). *Rhizobium ipomoeae* sp nov., isolated from a water convolvulus field. *Int. J. Syst. Evol. Microbiol.* 66, 1633-1640. doi: 10.1099/ijsem.0.000875
24. Sterner, J.P., and Parker, M.A. (1999). Diversity and relationships of *Bradyrhizohia* from *Amphicarpaea bracteata* based on partial nod and ribosomal sequences. *Syst. Appl. Microbiol.* 22, 387-392. doi: 10.1016/S0723-2020(99)80047-2
25. Subramanian, S., Souleimanov, A., and Smith, D.L. (2016). Proteomic studies on the effects of lipo-chitooligosaccharide and thuricin 17 under unstressed and salt stressed conditions in *Arabidopsis thaliana*. *Front. Plant Sci.* 7, 1314. doi: ARTN 131410.3389/fpls.2016.01314
26. Sukumar, P., Legue, V., Vayssieres, A., Martin, F., Tuskan, G.A., and Kalluri, U.C. (2013). Involvement of auxin pathways in modulating root architecture during beneficial plantmicroorganism interactions. *Plant Cell Environ.* 36, 909-919. doi: 10.1111/pce.12036
27. Tatusova, T., DiCuccio, M., Badretdin, A., Chetvernin, V., Nawrocki, E.P., Zaslavsky, L., et al. (2016). NCBI prokaryotic genome annotation pipeline. *Nucleic Acids Res.* 44, 6614-6624. doi: 10.1093/nar/gkw569
28. Xie, S.S., Wu, H.J., Zang, H.Y., Wu, L.M., Zhu, Q.Q., and Gao, X.W. (2014). Plant Growth Promotion by Spermidine-Producing *Bacillus subtilis* OKB105. *Mol. Plant-Microbe Interact.* 27, 655-663. doi: 10.1094/Mpmi-01-14-0010-R
29. Yoon, S.H., Ha, S.M., Lim, J., Kwon, S., and Chun, J. (2017). A large-scale evaluation of algorithms to calculate average nucleotide identity. *Anton. Leeuw. Int. J. G.* 110, 1281-1286. doi: 10.1007/s10482-017-0844-4
30. Zhang, N., Yang, D.Q., Wang, D.D., Miao, Y.Z., Shao, J.H., Zhou, X., et al. (2015). Whole transcriptomic analysis of the plant-beneficial rhizobacterium *Bacillus amyloliquefaciens* SQR9 during enhanced biofilm formation regulated by maize root exudates. *BMC Genomics* 16, doi: ARTN 68510.1186/s12864-015-1825-5
31. Zhou, C., Ma, Z., Zhu, L., Xiao, X., Xie, Y., Zhu, J., et al. (2016a). Rhizobacterial Strain *Bacillus megaterium* BOFC15 Induces Cellular Polyamine Changes that Improve Plant Growth and Drought Resistance. *Int. J. Mol. Sci.* 17, doi: 10.3390/ijms17060976
32. Zhou, D.M., Huang, X.F., Chaparro, J.M., Badri, D.V., Manter, D.K., Vivanco, J.M., et al. (2016b). Root and bacterial secretions regulate the interaction between plants and PGPR leading to distinct plant growth promotion effects. *Plant Soil* 401, 259-272. doi: 10.1007/s11104-015-2743-7
33. Zimin, A.V., Marcais, G., Puiu, D., Roberts, M., Salzberg, S.L., and Yorke, J.A. (2013). The MaSuRCA genome assembler. *Bioinformatics* 29, 2669-2677. doi: 10.1093/bioinformatics/btt476

6 Chapter 6 General Discussion

As soybean productivity is steadily on the rise in North America, technologies to enhance the crop's growth and salinity tolerance will be required. *Amphicarpaea bracteata* is a North American relative of soybean. The beneficial effects of rhizobacteria associated with this plant other than its nitrogen-fixing symbiont *Bradyrhizobium*, are very poorly understood. Hence, this study was focused on the concept that rhizobacteria of *A. bracteata* might also exert beneficial effects on soybean, along with its symbiont, *Bradyrhizobium japonicum*.

The results obtained from this study show that the bacteria *Rhizobium* sp. SL42 and *Hydrogenophaga* sp. SL48 isolated from root nodules of *Amphicarpaea bracteata* function as plant growth promoting rhizobacteria (PGPR) of soybean. The research conducted has facilitated the screening for potential PGPR strains under greenhouse conditions. Fifteen isolated strains were tested rigorously through a series of greenhouse trials, by measuring plant growth variables. In the screening experiments, soybean seeds were bacterized, and many isolates increased germination rate, seedling emergence, and shoot biomass, compared to the control, under optimal and salt stress conditions at 28 days after planting. Strains that significantly improved shoot and root growth variables were subjected to further screening. Four isolates were selected and inoculated onto soybean under a range of salt levels, from 0 to 200 mM NaCl. They increased shoot and root biomass relative to the control, but growth was constrained at higher salt concentrations. The experiment with salinity levels exhibited not only the tolerance threshold of soybean but also the influence of selected isolates on enhancing tolerance.

Variations were observed, in terms of the growth variables measured, between screening trials mainly because of the changes in the partially controlled greenhouse conditions, influenced by the external environment. The first trial was conducted during the summer when the temperatures were higher and the second trial in early autumn when the temperature and light levels were declining. In the final greenhouse trial, plant growth was substantially increased despite the application of low N fertilizer levels. This is most likely because of the biological nitrogen fixation performed by *B. japonicum* which added nitrogen content, which in turn boosted vegetative growth and biomass accumulation. Under salt stress, nitrogen accumulation was reduced, suggesting that root nodulation and biological nitrogen fixation were affected by salinity.

Soybean was grown to maturity and the impact of salinity stress has been assessed throughout its developmental stages by measuring growth and yield variables. Soybean growth

was strongly inhibited by salt stress at both vegetative and flowering stages, compared to the later stages. When seedlings develop, their roots are exposed to high salt concentration and absorption of saltwater leads to both osmotic imbalance and ionic toxicity in young plant tissues. At later stages, plants develop adaptation mechanisms such as compartmentalizing ions in older leaves and stems, which improves stress tolerance. This might also be because salt stress was applied only at the beginning of the experiment and not at later stages. The intensity of the stress was diluted by the continuous supply of water but, increased Na^+ accumulation in plant tissues indicated that the plants were constantly exposed to at least some level of stress. The ratio of K^+/Na^+ was higher with bacterial treatments, implying that the bacteria have assisted the plants to maintain ionic homeostasis by Na^+ compartmentalization or exclusion.

When co-inoculated with *B. japonicum*, the growth variables were not significantly different among the treatments under optimal and salt-stress conditions. However, growth variables were increased by the co-inoculation treatments of *B. japonicum*+SL42, *B. japonicum* +SL48 and *B. japonicum*+SL42+SL48, suggesting compatible co-inoculation and enhanced stress tolerance in soybean. An interesting observation was that the isolate SL42 also formed small (3-4 mm^2) functional nodules in soybean roots (observed by the dark-red cross-section – an indication of leghemoglobin). This suggests that the bacteria could have also performed biological nitrogen fixation in soybean nodules.

Salinity stress had a profound adverse effect on the growth and development of soybean. Under stress, the plants try to direct maximum effort to seed production and the progeny that will form the next generation and the shoot biomass is reduced, which explains the increase in harvest index of salt-stressed plants where seed weight to biomass ratio is higher. Plant growth and yield largely depend on the genetic potential and stress adaptation mechanisms of the plant throughout its developmental stages. They are also influenced by environmental conditions that are different between greenhouse and field, and that vary both spatially and temporally. Considering that the impact of inoculated microbes depends on all these factors, the strains exert substantial beneficial effects on soybean. The study also demonstrated that the two strains have co-inoculation compatibility with *B. japonicum* as there was growth improvement, which was significant at some instances, but often non-significant neutral effects.

Strategies to enhance plant growth and ameliorate stress are crucial to boost crop productivity. Soybean growth and development were enhanced by inoculation with strains SL42

and SL48 and inoculation technologies such as this are imperative from an agricultural point of view, to improve productivity and sustainability. Seed weight has increased by 8 % as a result of co-inoculation of *B. japonicum*+SL42+SL48 under optimal conditions. Soybean production in Canada could potentially be increased by the application of these two native strains. The utilization of PGPR to increase crop yield has been explored and numerous bacteria are successfully applied, as biofertilizers and biocontrol agents, in sustainable agriculture systems. However, their capability has to be determined through a course of multiple field trials. The application of beneficial bacteria has shown promising results in laboratory studies, under controlled conditions, but the results are often variable in the fields due to the influence of diverse environmental factors. The variation could be due to the myriad of genetic and environmental factors influencing the function of living organisms and the interactions among them. With regard to rhizosphere colonization, rhizosphere competent microorganisms have an advantage over other soil microbiota due to selective enrichment by the host plant.

Plant growth promotion and stress amelioration by the bacteria colonizing its rhizosphere are manipulated through intricate signaling pathways within the plant-microbe interaction. The knowledge of plant responses influenced by the phytomicrobiome are constantly evolving. Plant salinity tolerance is a complex trait and the advances in "omics" technologies help to elucidate tolerance mechanisms at the molecular level. In this study, soybean leaf proteome profile was analyzed to interpret the function of SL42 and SL48 in enhancing plant growth and mitigating stress. The proteomic analysis has brought an in-depth understanding of plant mechanisms and the mode of action by which the bacteria elicit these mechanisms. A number of proteins related to growth and stress responses were upregulated in the inoculated plants and also in the co-inoculated plants with *B. japonicum*. It was common to find proteins involved in drought and cold stresses were expressed since the plant tolerance mechanisms to drought, cold and salinity overlap during the osmotic phase.

Photosynthesis is the most significant activity that is inhibited during salinity stress, which in turn affects plant growth. Upregulation of proteins involved in photosynthesis processes in addition to Rubisco, glyceraldehyde-3-phosphate dehydrogenase and chlorophyll-binding proteins, suggest that inoculation with bacteria assist in the photosynthesis process and enhance growth under salinity stress. Other proteins involved in stomatal function, phytohormone signaling, chloroplast development, antioxidant activity and nutrient metabolism were also

upregulated in bacterial inoculated treatments. For example, proline function as an osmolyte is well established in plants exposed to environmental stresses. Accumulation of proline is positively correlated with increased osmotolerance. It is also synthesized in response to auxin signaling. The increase in proline-rich proteins suggests that the bacteria critically modulate plant salinity tolerance mechanisms.

The whole genome sequences of SL42 and SL48 revealed that the two strains carry genes related to abiotic stress tolerance and antibiotic resistance. Genes encoding plant hormones, nitrogen fixation, iron chelation, secondary metabolites, secretion systems and quorum sensing compounds were present, and are crucial to their beneficial roles as PGPR. Some of these compounds might also be essential for plant root colonization. However, detailed analysis of the genome sequences will further explain the functional properties of their genomes and bacterial regulatory networks related to plant growth promoting activities.

7 Chapter 7 Final Conclusion and Future Directions

Native relatives of cultivated plants may harbour beneficial microorganisms that could be harnessed for increasing plant growth and stress tolerance. Rhizobacteria were isolated from the nodules of *Amphicarpaea bracteata*, the closest relative to soybean in eastern North America, and screened for beneficial effects on plant growth and salinity stress tolerance of soybean under greenhouse conditions. Two of the most promising isolates, *Rhizobium* sp. SL42 and *Hydrogenophaga* sp. SL48 were co-inoculated with *Bradyrhizobium japonicum* 532C, the nitrogen-fixing symbiont of soybean under optimal and salt-stressed conditions. Plant growth was recorded at specific developmental stages of soybean until maturity. Co-inoculation with strains SL42 and SL48 resulted in improved plant growth in terms of biomass accumulation, nutrient assimilation and seed production of soybean.

The molecular basis of plant responses elicited by the inoculation of these two strains was elucidated using a proteomic approach. The analysis of leaf proteome showed that the bacteria modulate plant growth and development mechanisms through intricate signaling pathways within the plant-microbe interaction. Indeed, the interaction resulted in enhanced plant growth and salt stress tolerance, supported by the upregulation of proteins related to plant metabolism and function. Changes in the proteomic profile of soybean leaves under salt stress influenced by rhizobacteria provided key insights into the plant growth and stress response mechanisms that eventually lead to crop improvement and salinity tolerance of soybean.

Genomes of *Rhizobium* sp. SL42 and *Hydrogenophaga* sp. SL48 were sequenced and deposited in NCBI database. Whole genome sequencing provides an in-depth resolution of the genomic characteristics. Features of the genome related to metabolic functions such as secretion systems and production of secondary metabolites were identified. These elements contribute to their ecological, agricultural and biotechnological values, such as rhizosphere colonization and potentially novel biologically active metabolites that could aid in plant growth.

In this study, two strains isolated from a relative plant species of soybean showed potential for agricultural application to increase the growth and development of soybean. The mechanisms by which they influence plant growth and stress responses were determined using systems biology approaches. Overall, the study contributed to a comprehensive understanding of plant-microbe interactions between soybean, and its phytomicrobiome constituents including *Rhizobium* sp. SL42 and *Hydrogenophaga* sp. SL48 along with *Bradyrhizobium japonicum*. It seems that the microbes have profound effects upon plant growth and salt stress tolerance throughout the development of soybean. The active biomolecules released by the strains have elicited PGPR-mediated signaling pathways in soybean plants. These strains have significant potential application in sustainable crop production systems.

Soybean cultivation is expanding in North America, particularly in Canada. Reliable technologies must be developed not only to increase productivity but also to mitigate the detrimental effects of environmental stressors. The future directions of this project are to validate the beneficial effects of these strains under field conditions and to know if the strains can improve the growth and development of soybean and alleviate stress under the influence of various environmental factors. Their efficacy to improve growth and yield have to be determined by conducting multiple field trials. Introducing any organism will have an impact on the ecosystem, fortunately, these PGPR are native so they can be presumed safe. The strains have to be developed as an inoculum and seed treatment to be applied to soybean. Success at all these steps will ultimately lead to the commercialization of the strains. Further, they could be developed as bioinoculants to support soybean cultivation and adaptation relevant to Canadian agricultural scenarios.

Bibliography

1. Bai, Y.M., D'Aoust, F., Smith, D.L., and Driscoll, B.T. (2002). Isolation of plant-growth-promoting *Bacillus* strains from soybean root nodules. *Can. J. Microbiol.* 48, 230-238. doi: 10.1139/W02-014
2. Cloutier, J. (2017). *Soy Story: A Short History of Glycine max in Canada* [Online]. Statistics Canada: Statistics Canada. Available online at: https://www150.statcan.gc.ca/n1/pub/21-004-x/2017001/article/14779-eng.htm [accessed April 12 2020].
3. Dorff, E. (2007). *The soybean, agriculture's jack-of-all-trades, is gaining ground across Canada* [Online]. Statistics Canada. Available online at: https://www150.statcan.gc.ca/n1/en/pub/96-325-x/2007000/article/10369-eng.pdf?st=6wd-Sqjq [accessed April 12 2020].
4. Florinsky, I.V., Eilers, R.G., Wiebe, B.H., and Fitzgerald, M.M. (2009). Dynamics of soil salinity in the Canadian prairies: Application of singular spectrum analysis. *Environ. Model. Software* 24, 1182-1195. doi: 10.1016/j.envsoft.2009.03.011
5. Flowers, T.J. (2004). Improving crop salt tolerance. *J. Exp. Bot.* 55, 307-319. doi: 10.1093/jxb/erh003
6. Hasegawa, P.M., Bressan, R.A., Zhu, J.K., and Bohnert, H.J. (2000). Plant Cellular and Molecular Responses to High Salinity. *Annu. Rev. Plant Physiol. Plant Mol. Biol.* 51, 463-499. doi: 10.1146/annurev.arplant.51.1.463
7. Kloepper, J.W., and Schroth, M.N. (1979). Plant-growth promoting rhizobacteria - evidence that the mode of action involves root microflora interactions. *Phytopathol.* 69(9), 1034-1034.
8. Lee, K.D., Gray, E.J., Mabood, F., Jung, W.J., Charles, T., Clark, S.R.D., et al. (2009). The class IId bacteriocin thuricin-17 increases plant growth. *Planta* 229, 747-755. doi: 10.1007/s00425-008-0870-6
9. Loreau, M., Naeem, S., Inchausti, P., Bengtsson, J., Grime, J.P., Hector, A., et al. (2001). Ecology - Biodiversity and ecosystem functioning: Current knowledge and future challenges. *Science* 294, 804-808. doi: 10.1126/science.1064088
10. Moerman, D.E. (1998). Native American Ethnobotany Oregon: Timber Press. ISBN 0-88192-453-9
11. Munns, R., and Tester, M. (2008). Mechanisms of salinity tolerance. *Annu. Rev. Plant Biol.* 59, 651-681. doi:10.1146/annurev.arplant.59.032607.092911
12. NRCS (2002). *Salinity in Agriculture* [Online]. Natural Resources Conservation Service, United States Department of Agriculture. Available online at: https://www.nrcs.usda.gov/wps/portal/nrcs/detailfull/national/water/quality/tr/?cid=nrcs143_010914 [accessed April 12 2020].
13. Pitman, M.G., and Lauchli, A. (2002). "Global impact of salinity and Agricultural ecosystems," in Salinity: *Environment - Plants - Molecules,* eds. A. Lauchli & U. Luttage. (Netherlands: Kluwer Academic Publishers), 3-20.
14. PLANTS, U. (2017). *Amphicarpaea bracteata* (L.) Fernald American hogpeanut [Online]. Available online at: https://plants.usda.gov/core/profile?symbol=AMBR2 [accessed 12 Aug 2017].
15. Prithiviraj, B., Zhou, X., Souleimanov, A., Khan, W.M., and Smith, D.L. (2003). A host-specific bacteria-to-plant signal molecule (Nod factor) enhances germination and early growth of diverse crop plants. *Planta* 216, 890-890. doi: 10.1007/s00425-003-0990-y

16. Ragauskas, A.J., Williams, C.K., Davison, B.H., Britovsek, G., Cairney, J., Eckert, C.A., et al. (2006). The path forward for biofuels and biomaterials. *Science* 311, 484-489. doi: 10.1126/science.1114736
17. Smith, D.L., Gravel, V., and Yergeau, E. (2017). Signaling in the Phytomicrobiome. *Front. Plant Sci.* 8, 611. doi: 10.3389/fpls.2017.00611
18. Subramanian, S., Ricci, E., Souleimanov, A., and Smith, D.L. (2016). A proteomic approach to lipo-chitooligosaccharide and thuricin 17 effects on soybean germination unstressed and salt stress. *Plos One* 11, e0160660. doi: 10.1371/journal.pone.0160660
19. Tang, J., Bromfield, E.S.P., Rodrigue, N., Cloutier, S., and Tambong, J.T. (2012). Microevolution of symbiotic *Bradyrhizobium* populations associated with soybeans in east North America. *Ecol. Evol.* 2, 2943-2961. doi: 10.1002/ece3.404
20. Van Breusegem, F., and Dat, J.F. (2006). Reactive oxygen species in plant cell death. *Plant Physiol.* 141, 384-390. doi: 10.1104/pp.106.078295
21. Wiebe, B.H., Eilers, R.G., Eilers, W.D., and Brierley, J.A. (2007). Application of a risk indicator for assessing trends in dryland salinization risk on the Canadian Prairies. *Can. J. Soil Sci.* 87, 213-224.
22. Xie, S.S., Wu, H.J., Zang, H.Y., Wu, L.M., Zhu, Q.Q., and Gao, X.W. (2014). Plant Growth Promotion by Spermidine-Producing *Bacillus subtilis* OKB105. *Mol. Plant-Microbe Interact.* 27, 655-663. doi: 10.1094/Mpmi-01-14-0010-R
23. Zhu, J.-K. (2007). Plant Salt Stress. doi:10.1002/9780470015902.a0001300.pub2
24. Zhu, T., Shi, L., Doyle, J.J., and Keim, P. (1995). A single nuclear locus phylogeny of soybean based on DNA-sequence. *Theor. Appl. Genet.* 90, 991-999. doi: 10.1007/Bf00222912

APPENDIX A

Supplementary Figures and Tables – Chapter 3

Supplementary Table 3.1. Estimated area, yield and production of soybean in Canada.

Reference period	Seeded area (acres)	Harvested area (acres)	Average yield (kg per hectare)	Production (metric tonnes)
2016	5,607,397	5,514,700	3,000	6,596,500
2017	7,282,000	7,252,000	2,600	7,716,600
2018	6,320,100	6,275,500	2,900	7,416,600
2019	5,714,300	5,610,400	2,662	6,045,100
2020	5,070,300	4,910,700	3,088	6,137,100

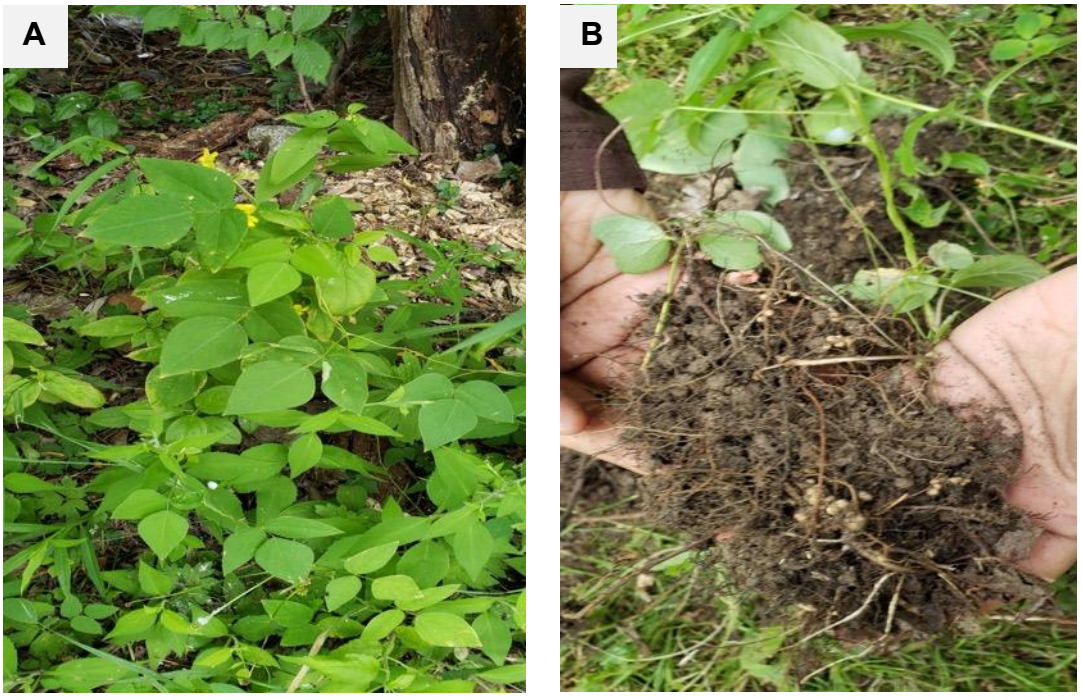

Supplementary Figure 3.1. **(A)** *Amphicarpaea bracteata* plant found on the shores of Lac St. Louis, Sainte-Anne-de-Bellevue, Canada. **(B)** The root system and the root nodules of *A. bracteata*.

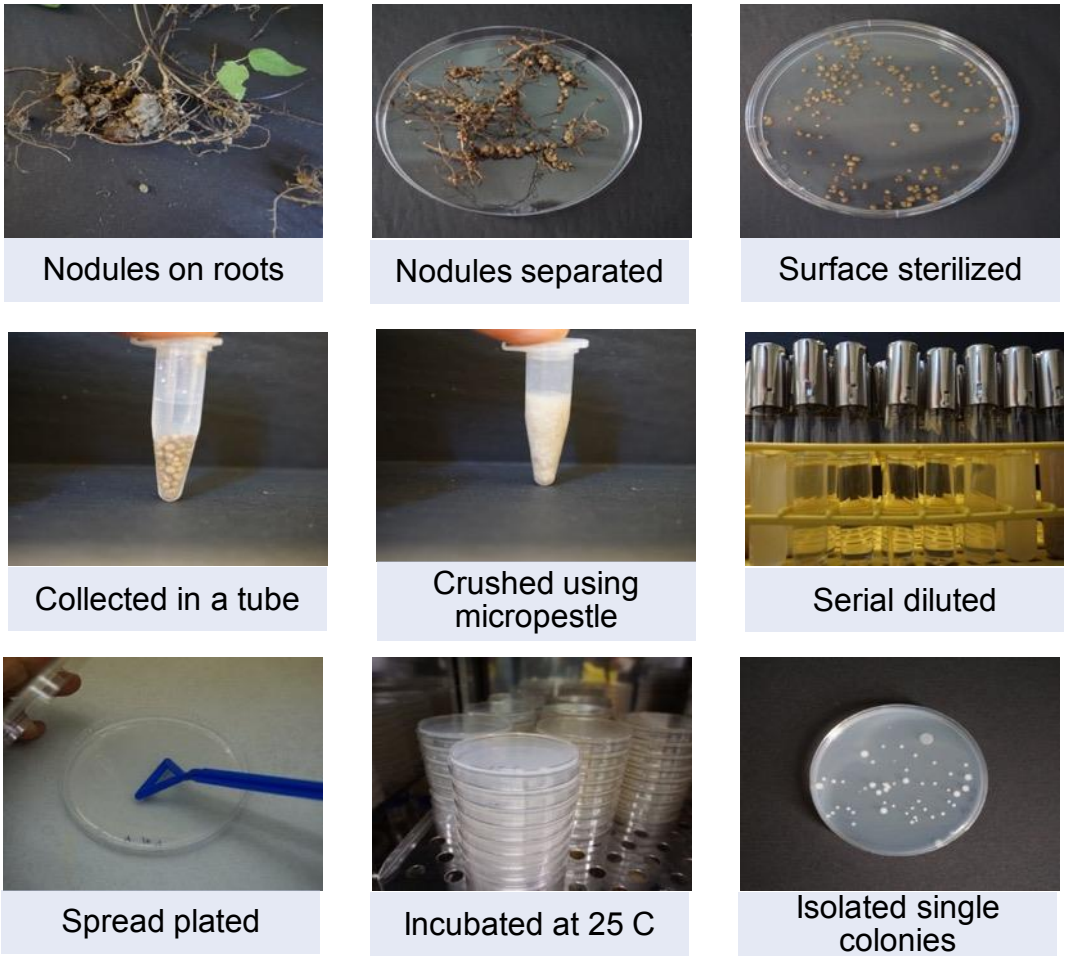

Supplementary Figure 3.2. Methodological procedure for the isolation of bacteria from the nodules of *Amphicarpea bracteata*.

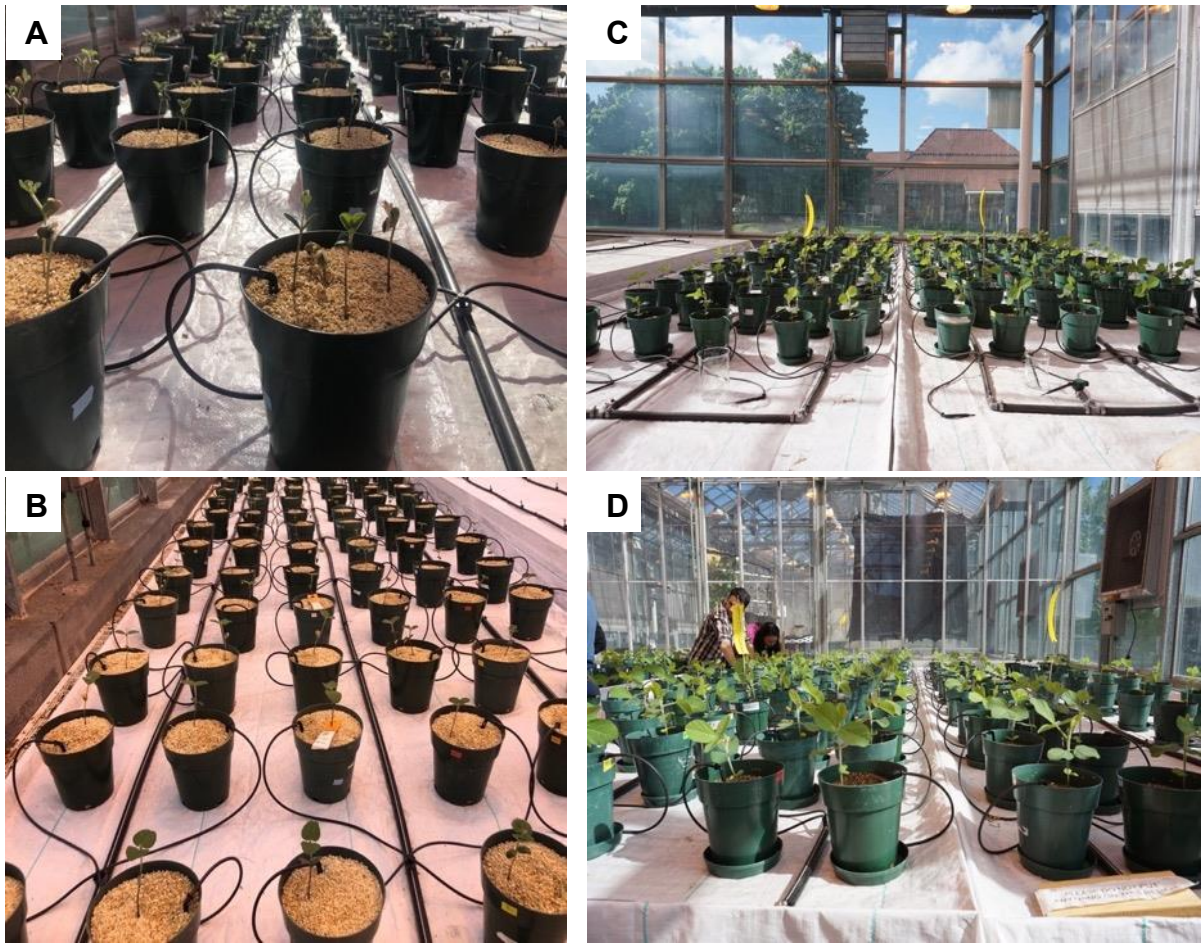

Supplementary Figure 3.3. Screening experiement setup in greenhouse **(A)** Soybean plants emerging at 5th DAP **(B)** Plants after thinned out on 8th DAP **(C)** Plants growing in the greenhouse at early vegetative stage and treatments were distributed randomly **(D)** Plants in the mid-vegetative stage and sampling of plants at 28th DAP.

Supplementary Figure 3.4. Growth and development of soybean **(A)** Soybean plants at the vegetative stage (14th DAP) **(B)** flowering stage (40th DAP) **(C)** pod-filling stage (80th DAP) **(D)** harvest stage (100th DAP).

Supplementary Figure 3.5. **(A)** Soybean seedlings at 8th DAP **(B)** Soybean flowers **(C)** Soybean at early-pod-filling stage **(D)** mature pods at harvest.

Supplementary Table 0.2. Organism identification and BLAST reference sequence similarity search results for the 16s rRNA gene query of the isolated strains of nodule bacteria.

	GenBank Accession	Strain	Organism	BLAST – related strains	Identity
1.	MT952563	SL31	*Pseudomonas mandelii*	*Pseudomonas mandelii* strain AB16	100%
2.	MT952564	SL33	*Hydrogenophaga sp.*	*Hydrogenophaga sp.* M4_20	99.78%
3.	MT952565	SL42	*Rhizobium sp.*	*Rhizobium sp.* strain py1134	99.56%
4.	MT952566	SL43	*Devosia sp.*	*Devosia sp.* strain 90	95.61%
5.	MT952567	SL44	*Flavobacterium sp.*	*Flavobacterium sp.* WB1.2-3	99.35%
6.	MT952568	SL45	*Gemmobacter sp.*	*Gemmobacter tilapiae* strain Ruye-53	98.80%
7.	MT952569	SL47	*Variovorax sp.*	*Variovorax sp.* Bca18	99.93%
8.	MT952570	SL48	*Hydrogenophaga sp.*	*Hydrogenophaga taeniospiralis* CCUG 15921 strain NBRC102512	99.50%
9.	MT952571	SL49	*Pseudomonas borealis*	*Pseudomonas borealis*	99.43%
10.	MT952572	SL50	*Pseudomonas fluorescens*	*Pseudomonas fluorescens* strain S2	99.85%
11.	MT952573	SL52	*Pseudomonas baetica*	*Pseudomonas baetica* strain S42_BP2TU	100%
12.	MT952574	SL54	*Bacillus subtilis*	*Bacillus subtilis* strain soilG2B	100%
13.	MT952575	SL55	*Variovorax sp.*	*Variovorax sp.* Bca18	99.71%
14.	MT952576	SL56	*Pseudomonas fluorescens*	*Pseudomonas fluorescens* strain S2	99.57%

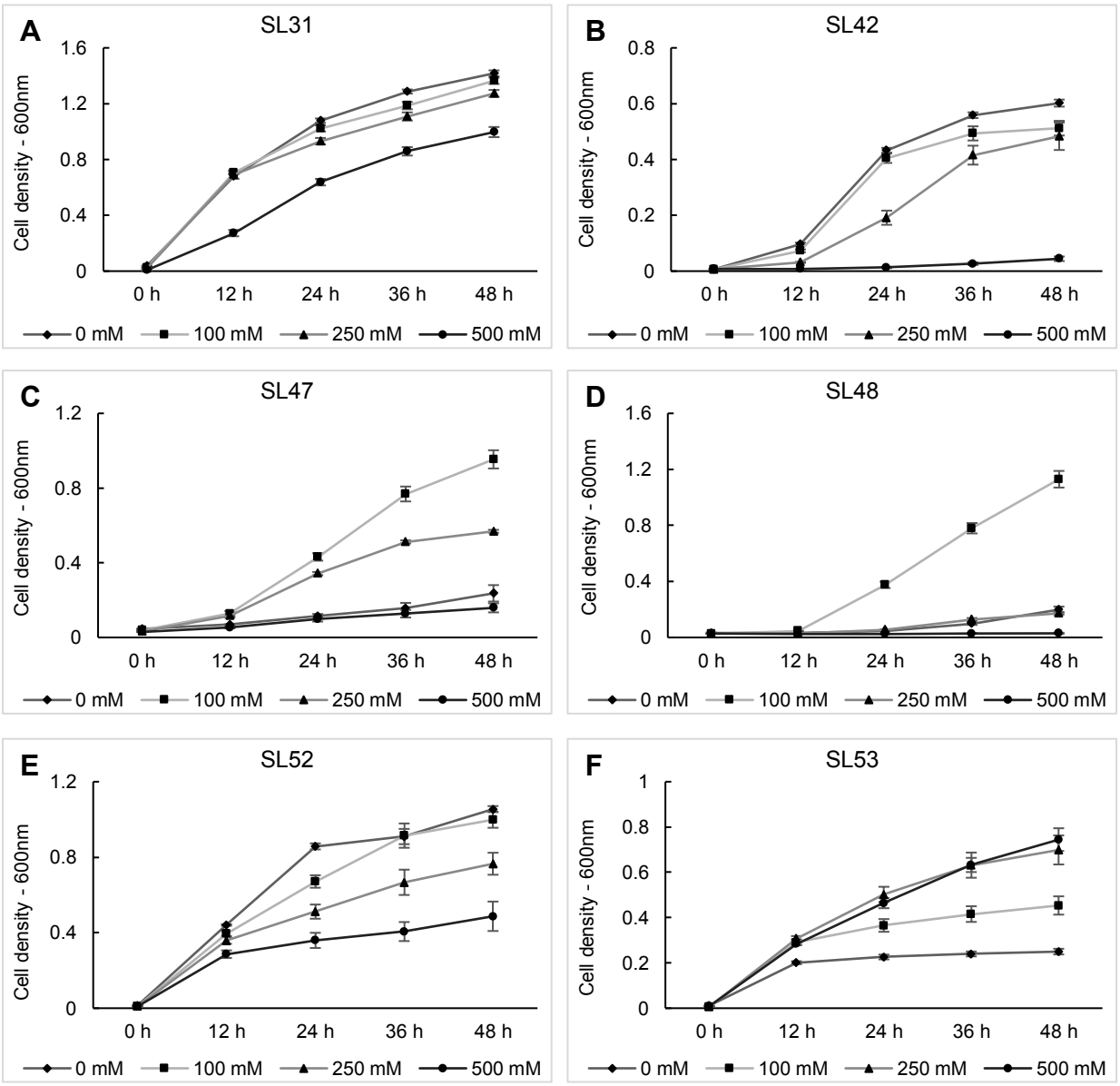

Supplementary Figure 3.6. Salt tolerance capacity of the nodule isolates.
(A) SL31, **(B)** SL42, **(C)** SL47, **(D)** SL48, **(E)** SL52, and **(F)** SL53. The bacteria were grown under 0, 100, 250 and 500 mM NaCl and growth was measured by increase in optical density at A_{600nm} with respect to blank, plotted every 12 h up to 48 h. Values represent mean ± SE (n=8).

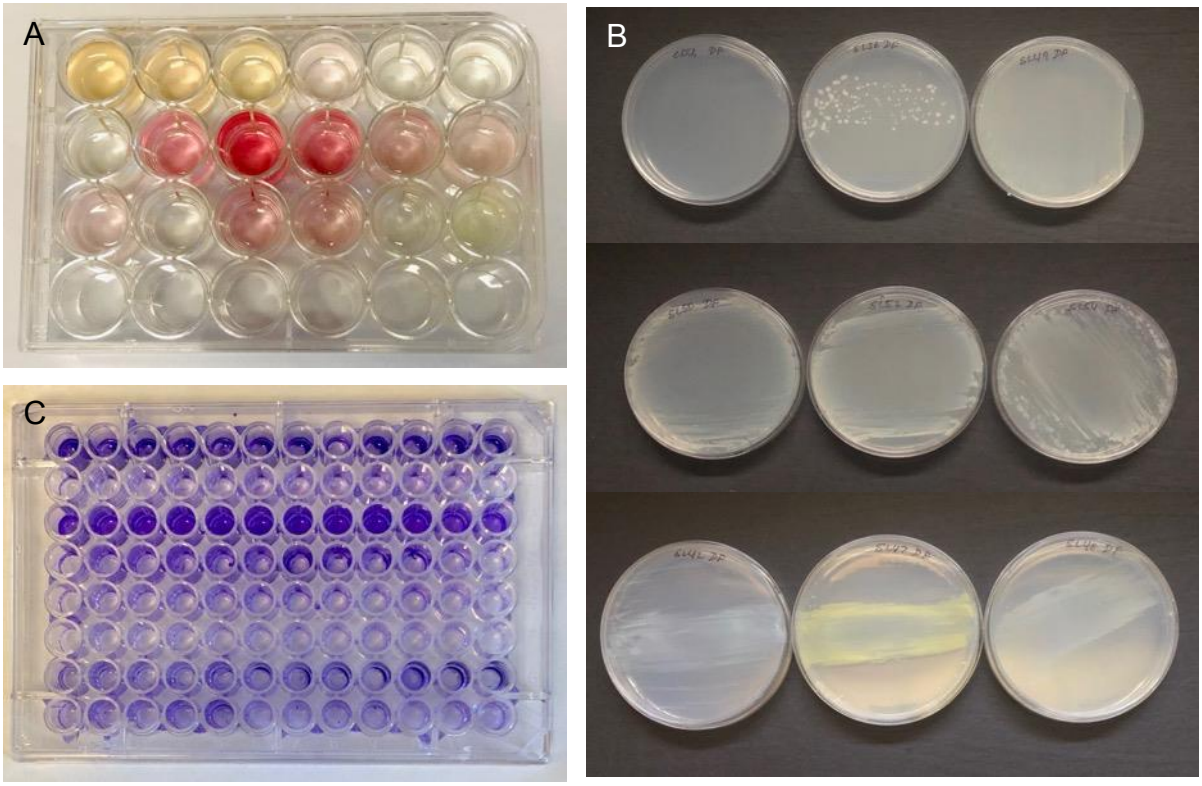

Supplementary Figure 3.7. PGPR characteristics of the isolated strains **(A)** Production IAA detected by adding Salkowski's reagent **(B)** Detection of ACC deaminase by using ACC as the sole carbon source **(C)** Biofilm stained with 0.1% (v/v) crystal violet.

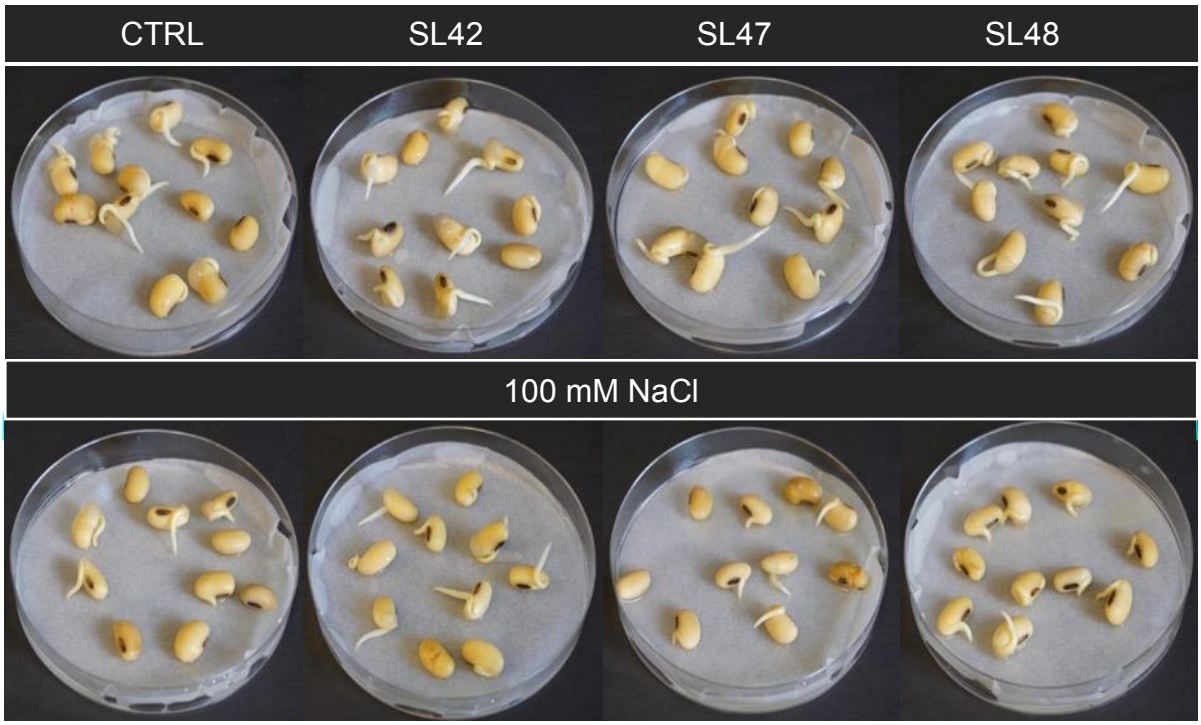

Supplementary Figure 3.8. Seeds germinating at 48 h under optimal conditions and salt stress. Ctrl is water, SL42, SL47 and SL48 are bacterial treatments that showed higher germination rate.

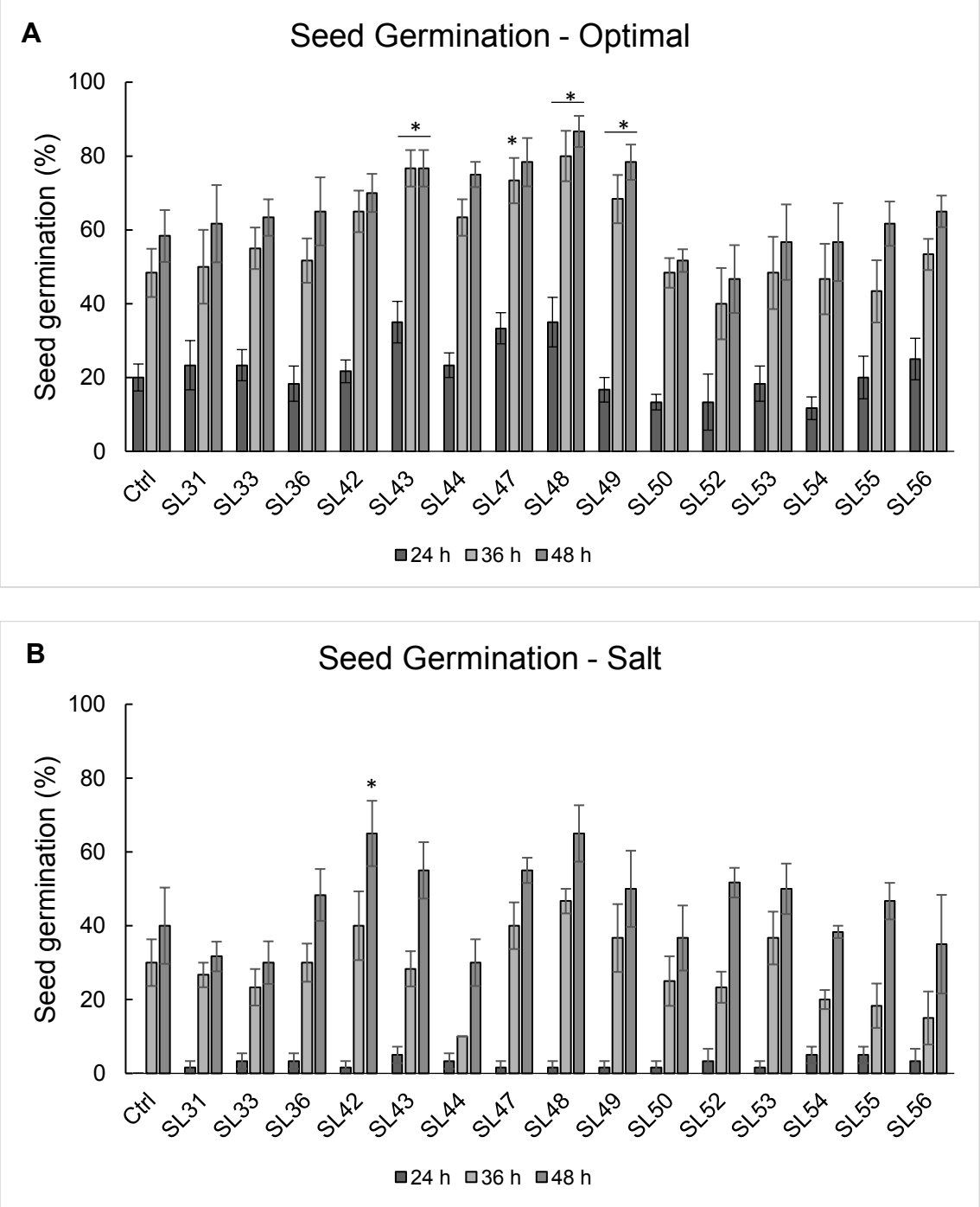

Supplementary Figure 3.9. Seed germination rate of soybean at 24, 36, and 48 h under **(A)** optimal (water) and **(B)** salt (100 mM NaCl) conditions. The seeds were treated with 10 mM $MgSO_4$ as control or bacterized with isolated strains. Values represent mean ± SE (n=6[10]). Significant differences (increase) between the bacterial treatments and the respective control treatments (optimal or salt) are indicated by an asterisk above the data points, * - $p \leq 0.05$ ($\alpha = 0.05$).

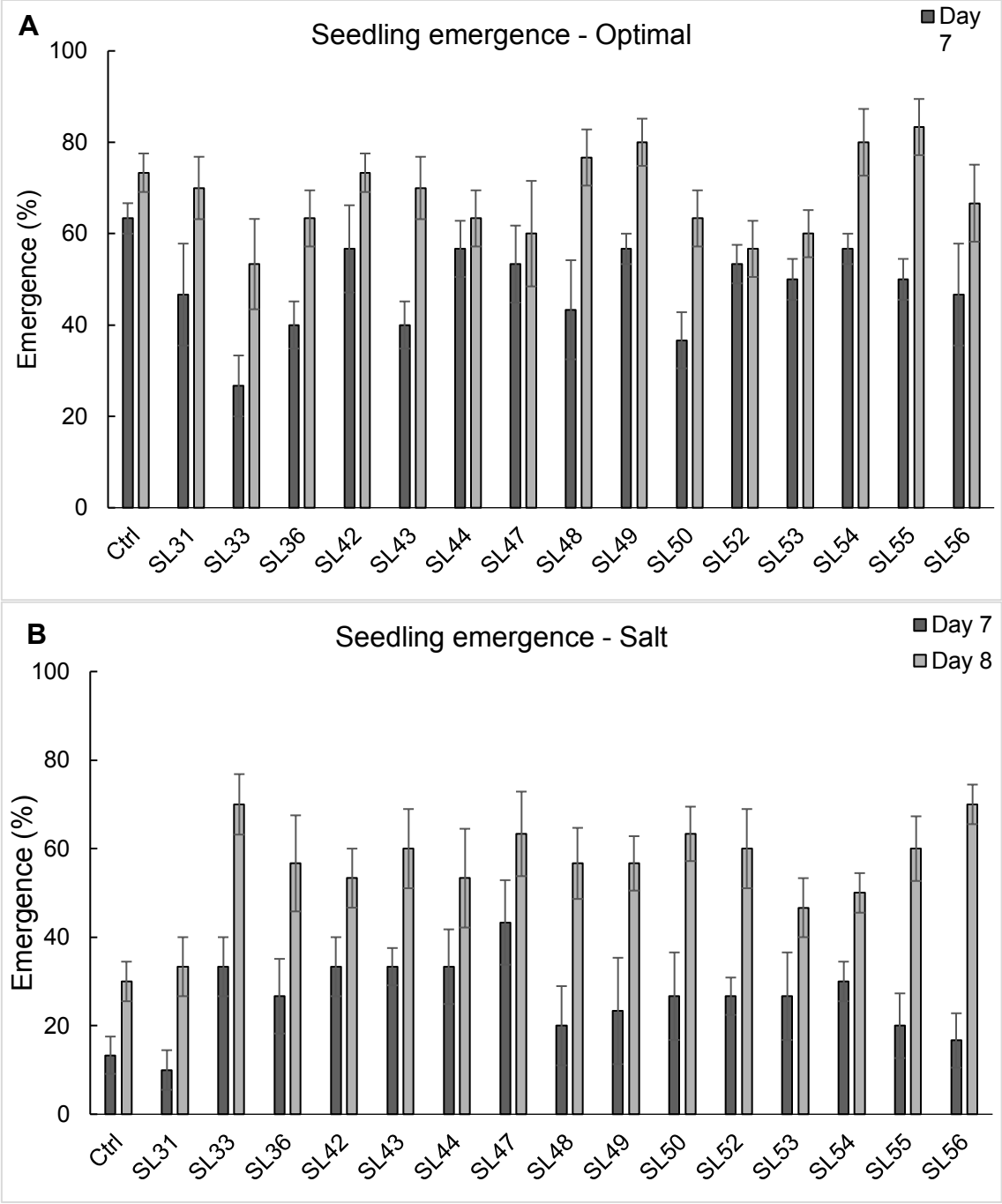

Supplementary Figure 3.10. Seedling emergence rate of soybean measured on 7th and 8th DAP under optimal or salt stress (100 mM NaCl) conditions. The seeds were treated with 10 mM $MgSO_4$ as control or bacterized with the isolated strains. Values represent mean ± SE (n=6[5]).

Supplementary Figure 3.11. Soybean plants at vegetative stage under optimal condition from treatments, control, and bacterial isolates, SL42, SL48 and SL49. Bacteria- treated plants show half-emerged third trifoliate leaves.

Supplementary Figure 3.11. (cont.) Soybean plants at vegetative stage under salt stress from treatments, control, and bacterial isolates, SL42, SL48 and SL49. Bacteria- treated plants show fully emerged second trifoliate leaves.

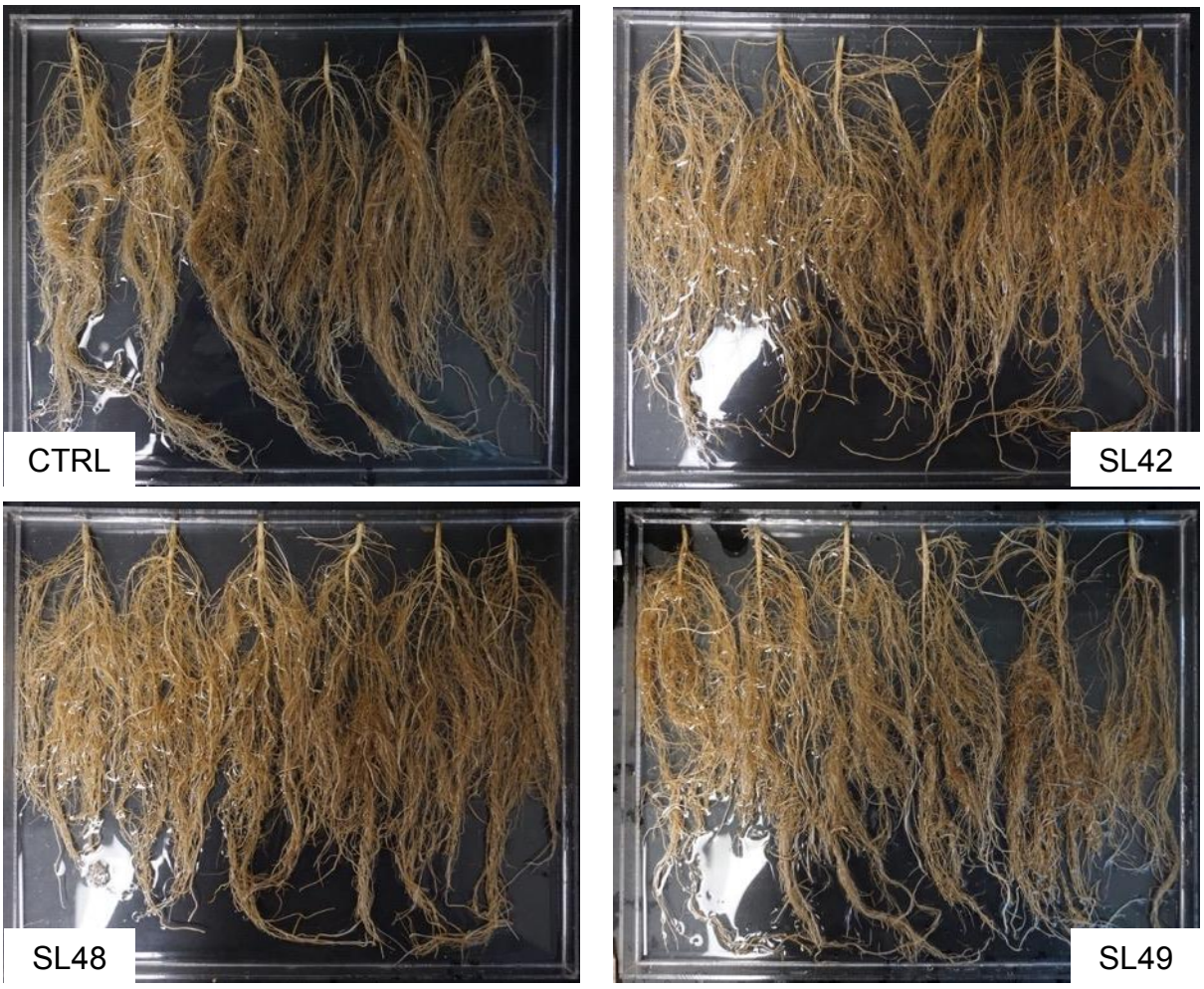

Supplementary Figure 3.11. (cont.) Soybean roots at vegetative stage under optimal condition from treatments, control, and bacterial isolates, SL42, SL48 and SL49.

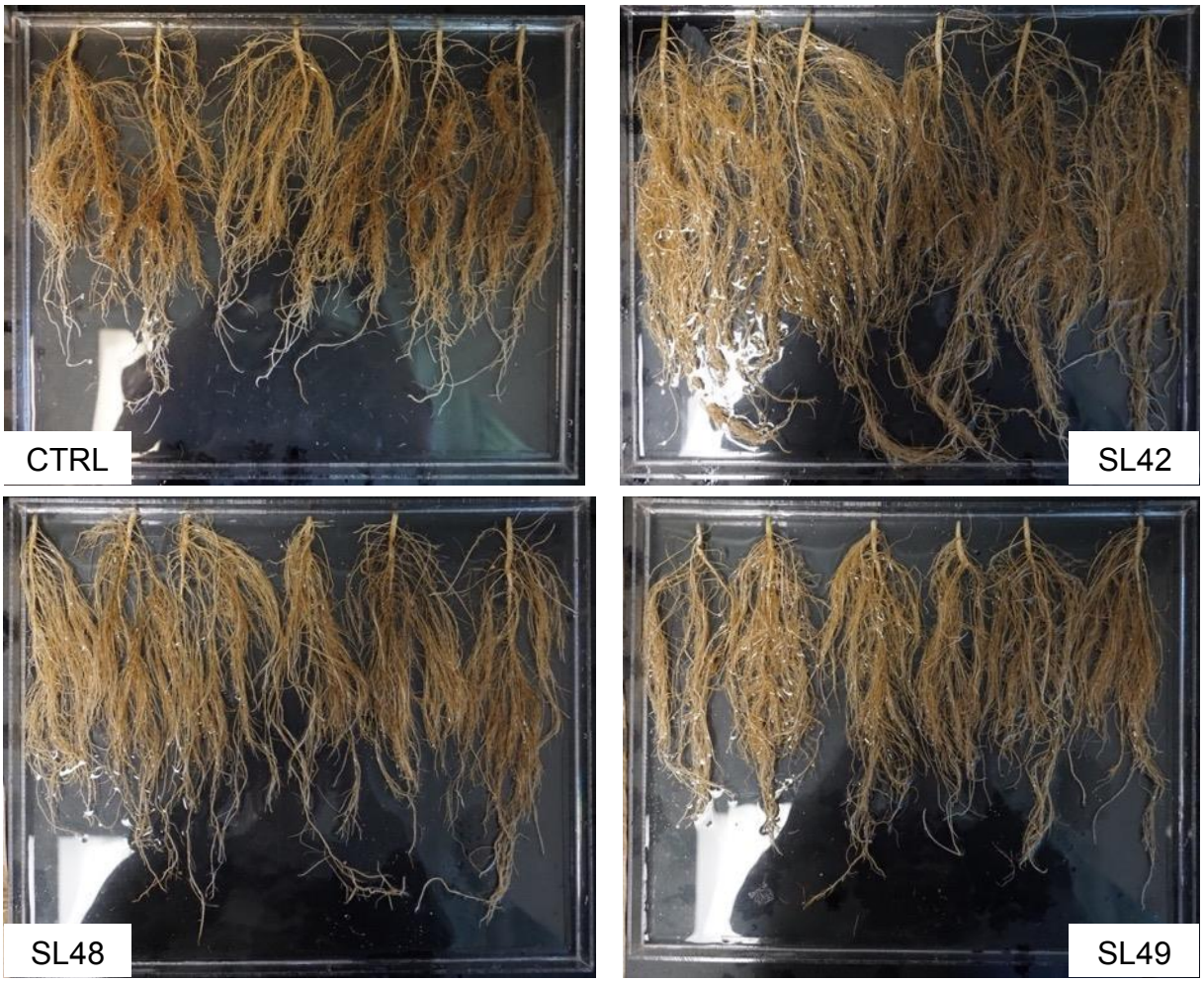

Supplementary Figure 3.11. (cont.) Soybean roots at vegetative stage under salt stress from treatments, control, and bacterial isolates, SL42, SL48 and SL49.

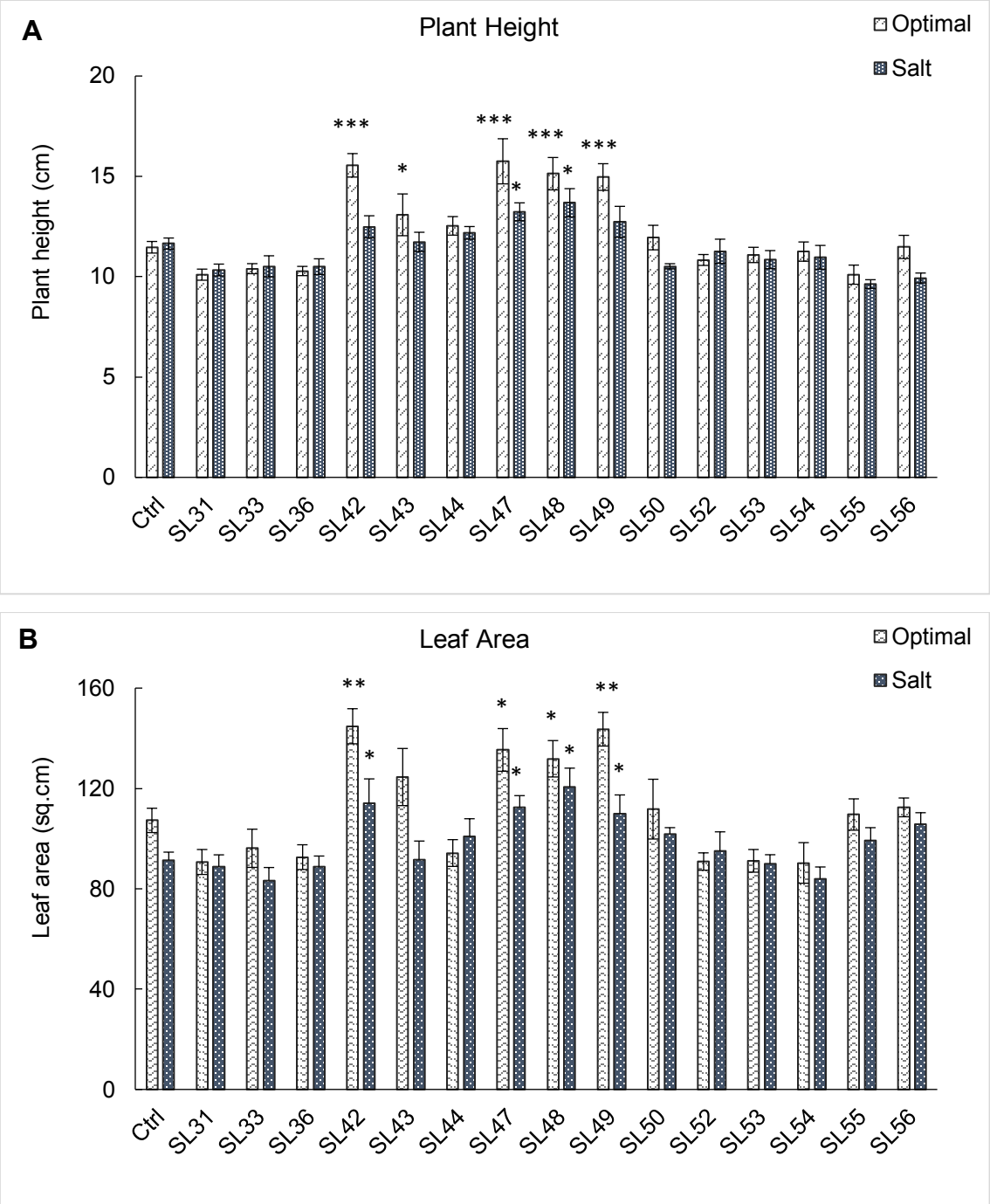

Supplementary Figure 3.12. Growth variables of soybean, **(A)** Plant height and **(B)** Leaf area measured at 28th DAP under optimal (water) and salt (100 mM NaCl) conditions. The seeds were treated with 10 mM $MgSO_4$ as control or bacterized with the isolated strains. Values represent mean ± SE (n=6). Significant differences (increase) between the bacterial treatments and the respective control treatments (optimal or salt) is indicated by an asterisk above the data points, * - $p \leq 0.05$, ** - $p \leq 0.001$, *** - $p \leq 0.0001$ ($\alpha = 0.05$).

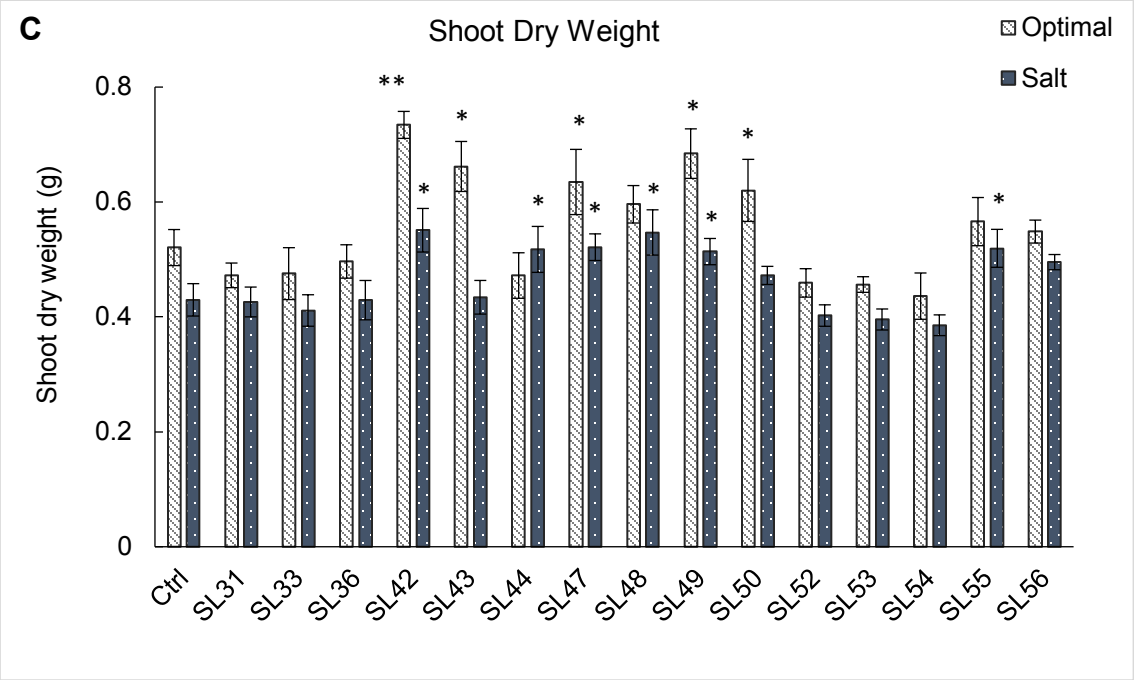

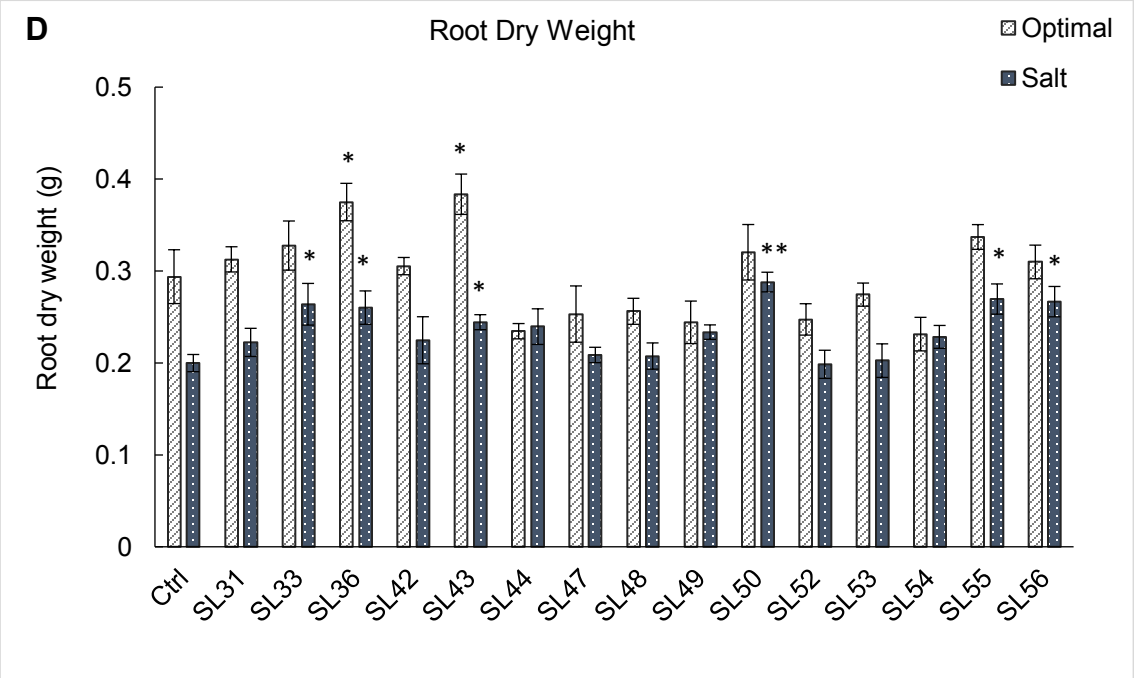

Supplementary Figure 3.12. (cont.) Growth variables of soybean, **(C)** Shoot dry weight and **(D)** Root dry weight measured at 28th DAP under optimal (water) and salt (100 mM NaCl) conditions. The seeds were treated with 10 mM $MgSO_4$ as control or bacterized with the isolated strains. Values represent mean ± SE (n=6). Significant differences (increase) between the bacterial treatments and the respective control treatments (optimal or salt) is indicated by an asterisk above the data points, * - $p \leq 0.05$, ** - $p \leq 0.001$ ($\alpha = 0.05$).

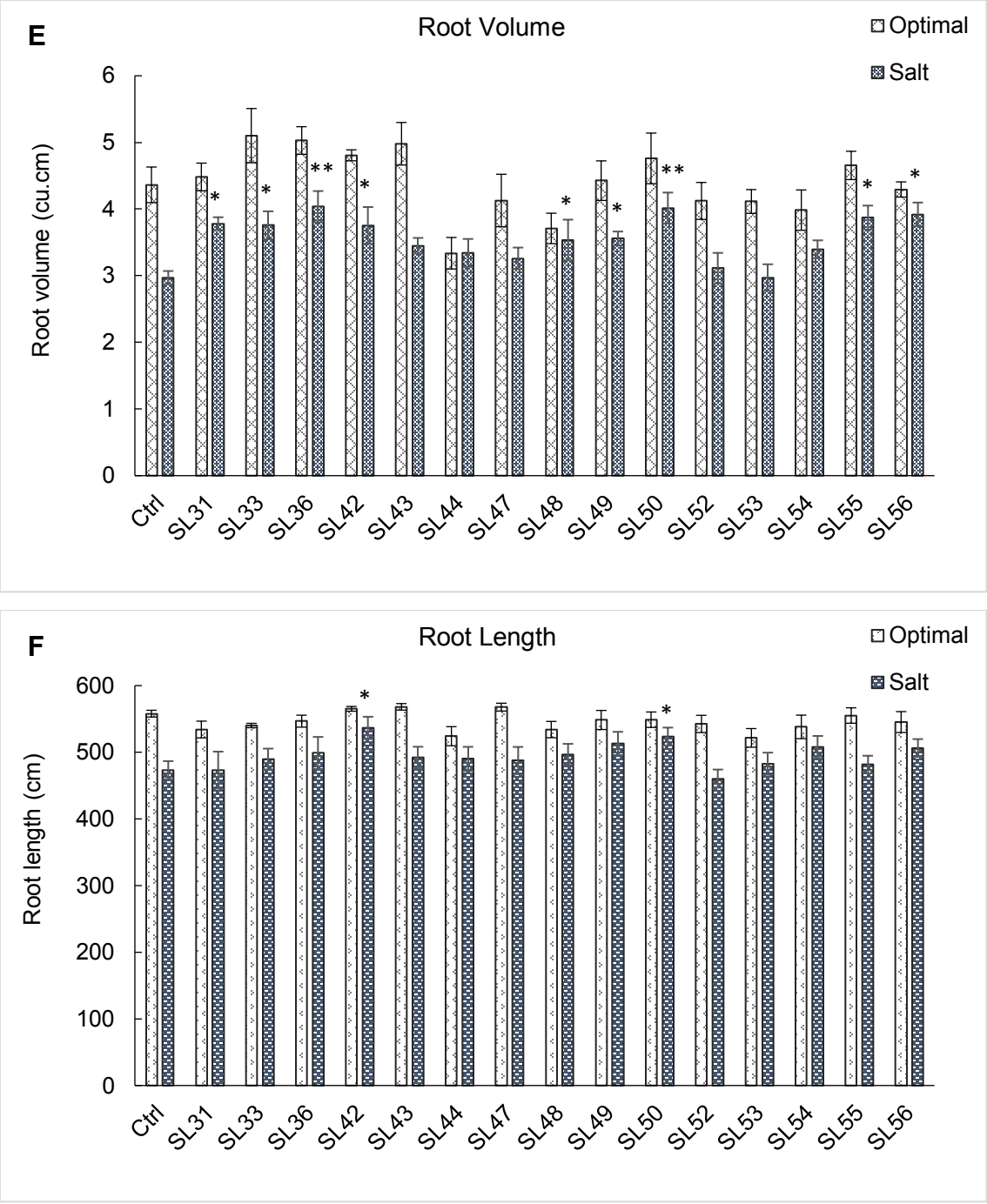

Supplementary Figure 3.12. (cont.) Growth variables of soybean, **(E)** Root volume and **(F)** Root length measured at 28th DAP under optimal (water) and salt (100 mM NaCl) conditions. The seeds were treated with 10 mM $MgSO_4$ as control or bacterized with the isolated strains. Values represent mean ± SE (n=6). Significant differences (increase) between the bacterial treatments and the respective control treatments (optimal or salt) is indicated by an asterisk above the data points, * - $p \leq 0.05$, ** - $p \leq 0.001$ ($\alpha = 0.05$).

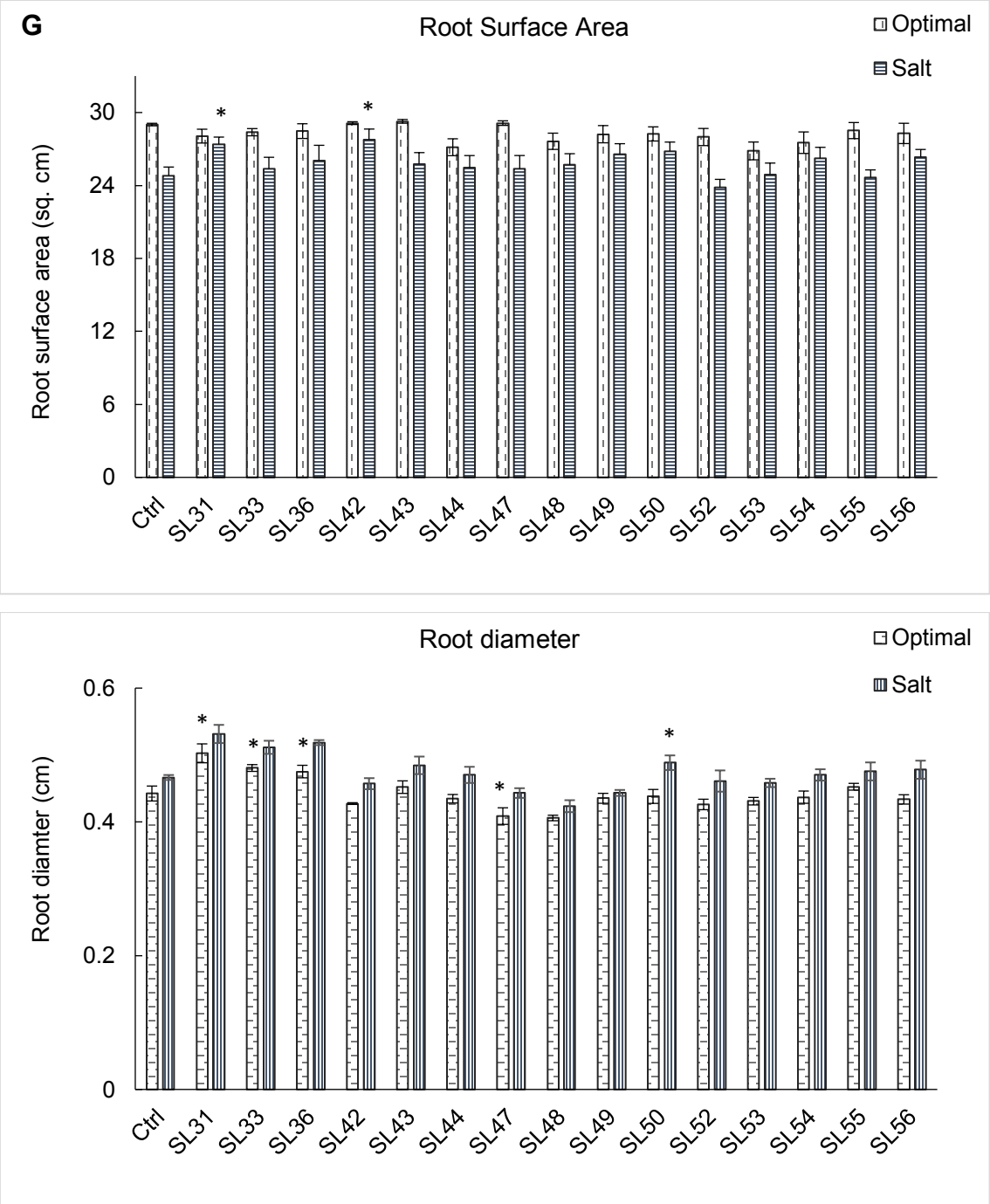

Supplementary Figure 3.12. (cont.) Growth variables of soybean, **(G)** Root surface area and **(F)** Root diametre measured at 28th DAP under optimal (water) and salt (100 mM NaCl) conditions. The seeds were treated with 10 mM $MgSO_4$ as control or bacterized with the isolated strains. Values represent mean ± SE (n=6). Significant differences (increase) between the bacterial treatments and the respective control treatments (optimal or salt) is indicated by an asterisk above the data points, * - $p \leq 0.05$ ($\alpha = 0.05$).

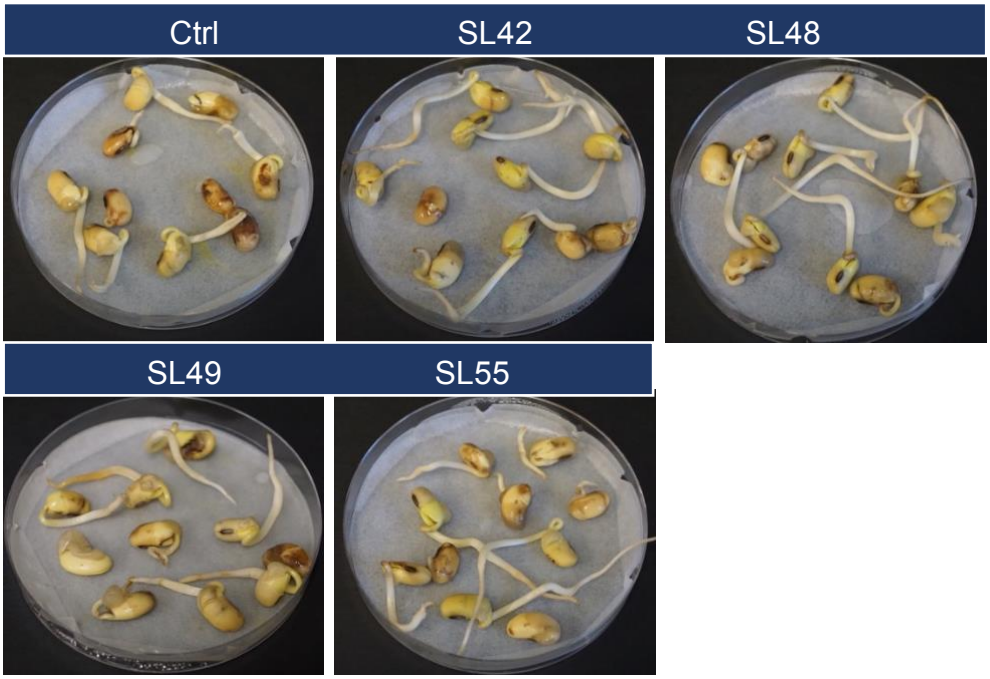

Supplementary Figure 3.13. Soybean seeds at 72 h under optimal conditions – 0 mM NaCl and treated with bacterial strains, SL42, SL48, SL49, and SL55 (1×10^8 cfu mL^{-1}).

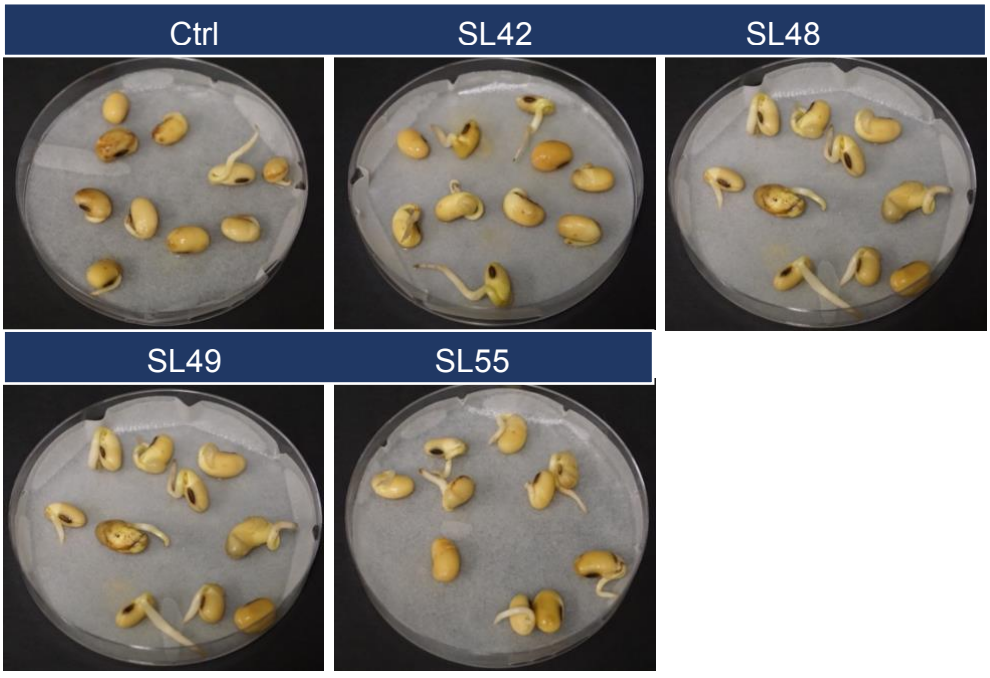

Supplementary Figure 3.13. (cont.) Soybean seeds at 72 h under optimal conditions – 100 mM NaCl and treated with bacterial strains, SL42, SL48, SL49, and SL55 (1×10^8 cfu mL^{-1}).

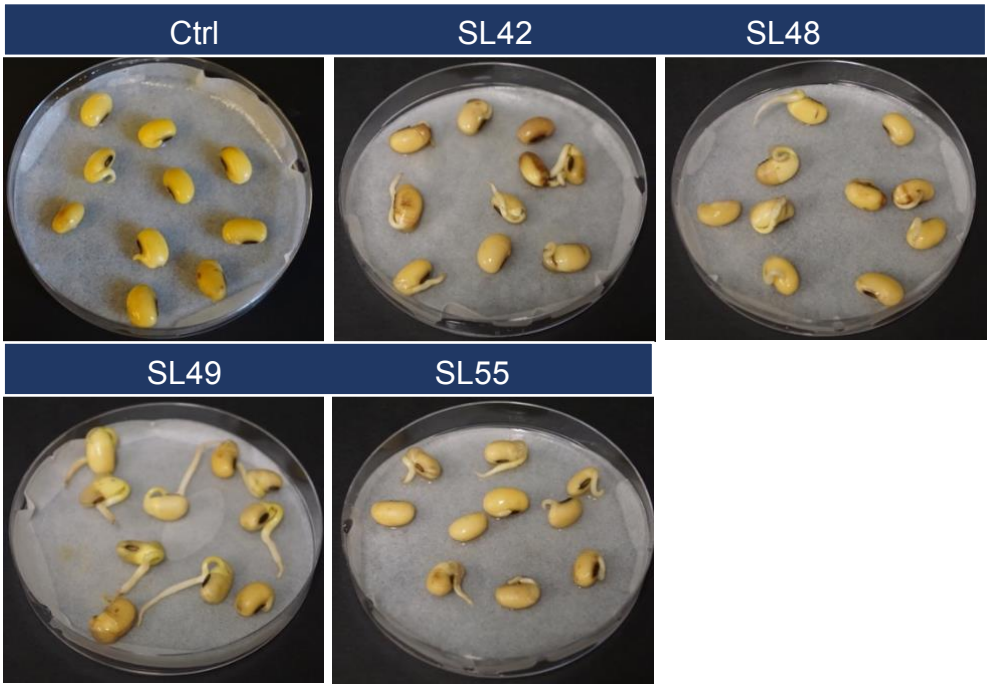

Supplementary Figure 3.13. (cont.) Soybean seeds at 72 h under optimal conditions – 150 mM NaCl and treated with bacterial strains, SL42, SL48, SL49, and SL55 (1×10^8 cfu mL^{-1}).

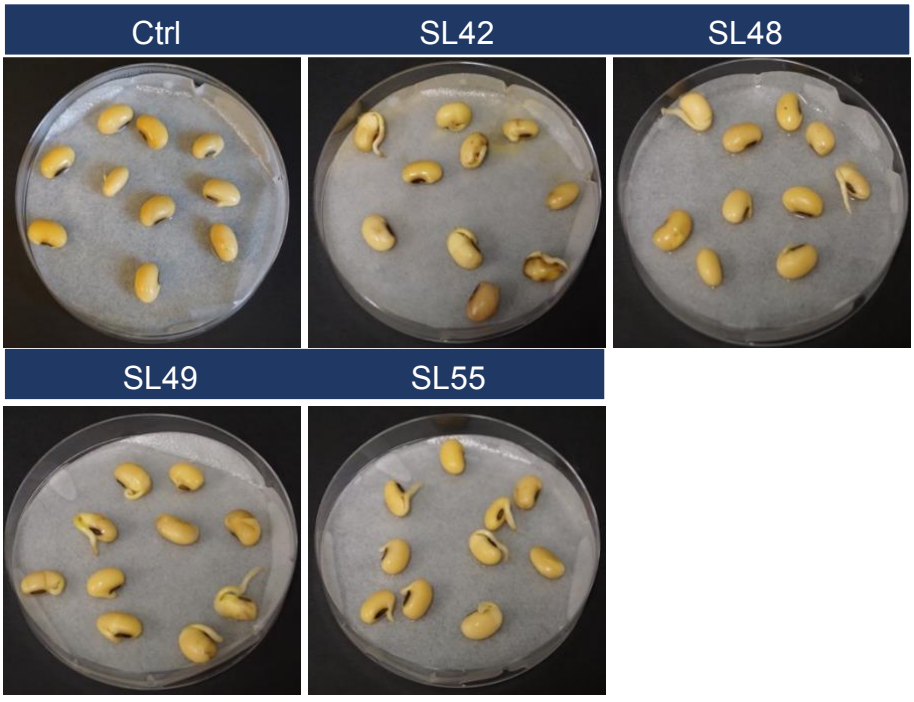

Supplementary Figure 3.13. (cont.) Soybean seeds at 72 h under optimal conditions – 200 mM NaCl and treated with bacterial strains, SL42, SL48, SL49, and SL55 (1×10^8 cfu mL^{-1}).

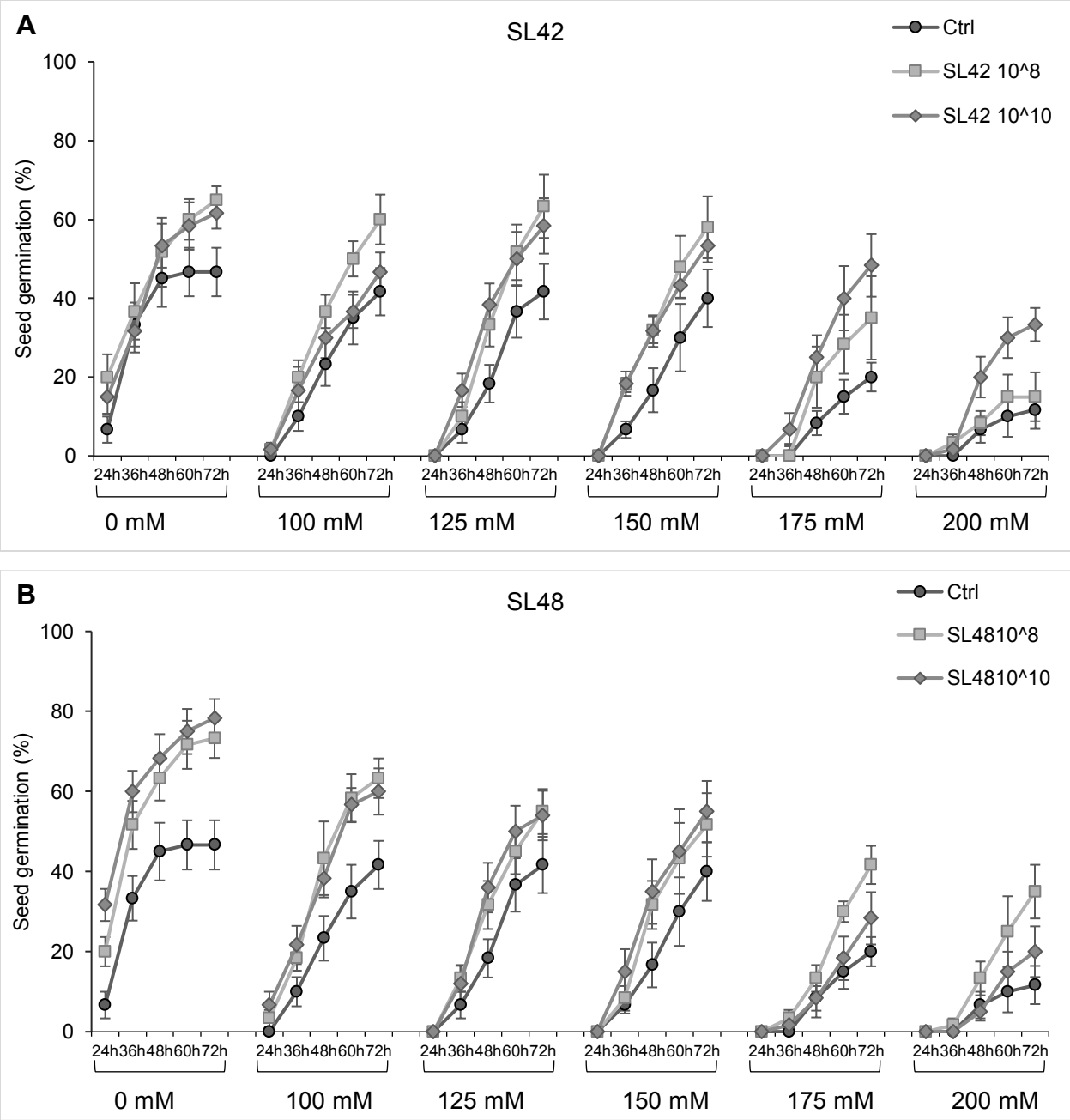

Supplementary Figure 3.14. Seed germination rate of soybean at 24, 36, 48, 60, and 72 h under increasing salt concentrations (0, 100, 125, 150, 175, and 200 mM NaCl) conditions. The seeds were treated with 10 mM $MgSO_4$ as control or bacterized with the strain **(A)** SL42 and **(B)** SL48 at 1×10^8 and 1×10^{10} cfu mL^{-1}. Values represent mean ± SE (n=6[10]).

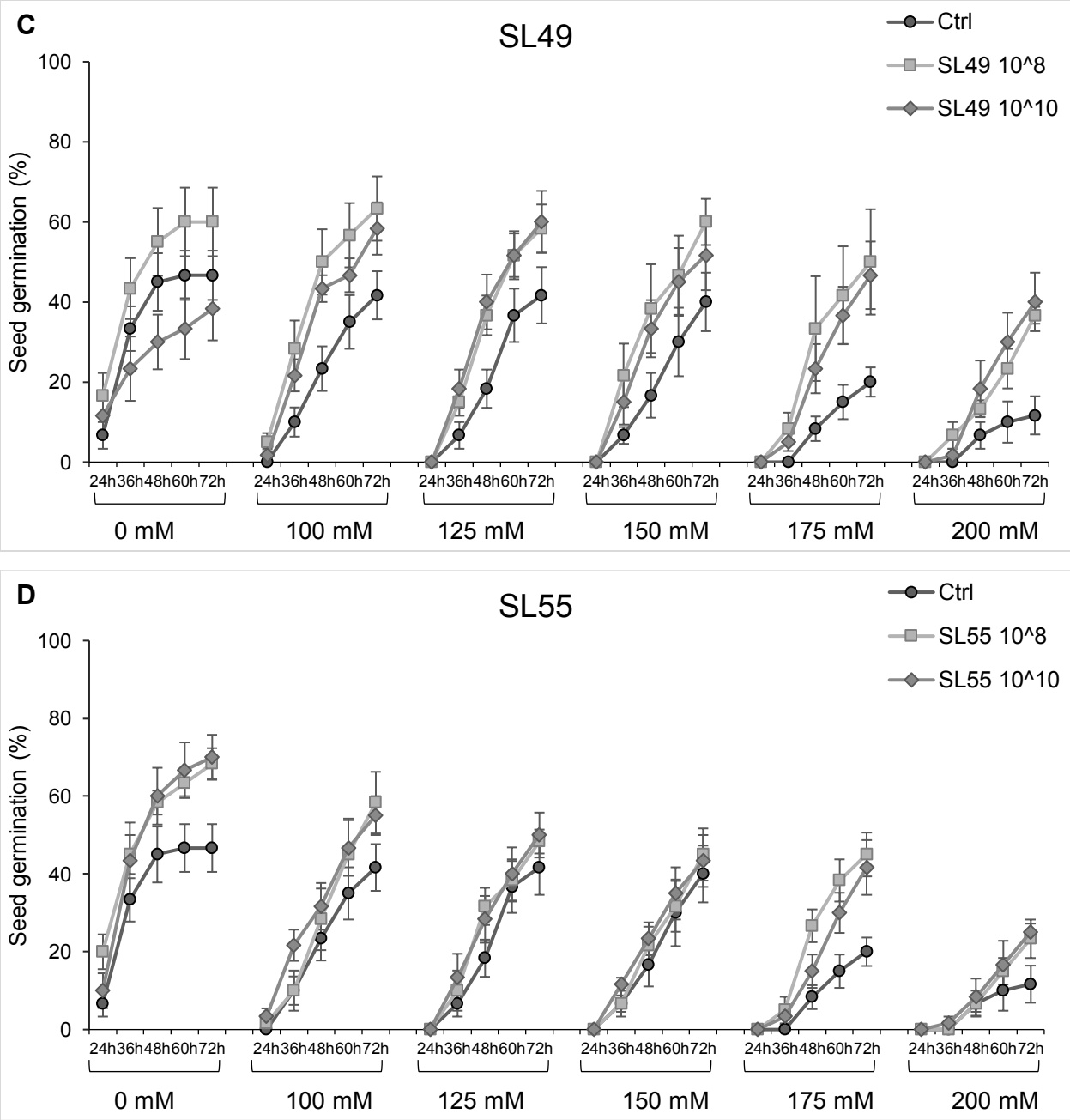

Supplementary Figure 3.14. Seed germination rate of soybean at 24, 36, 48, 60, and 72 h under increasing salt concentrations (0, 100, 125, 150, 175, and 200 mM NaCl) conditions. The seeds were treated with 10 mM $MgSO_4$ as control or bacterized with the strain **(C)** SL49 and **(D)** SL55 at 1×10^8 and 1×10^{10} cfu mL^{-1}. Values represent mean ± SE (n=6[10]).

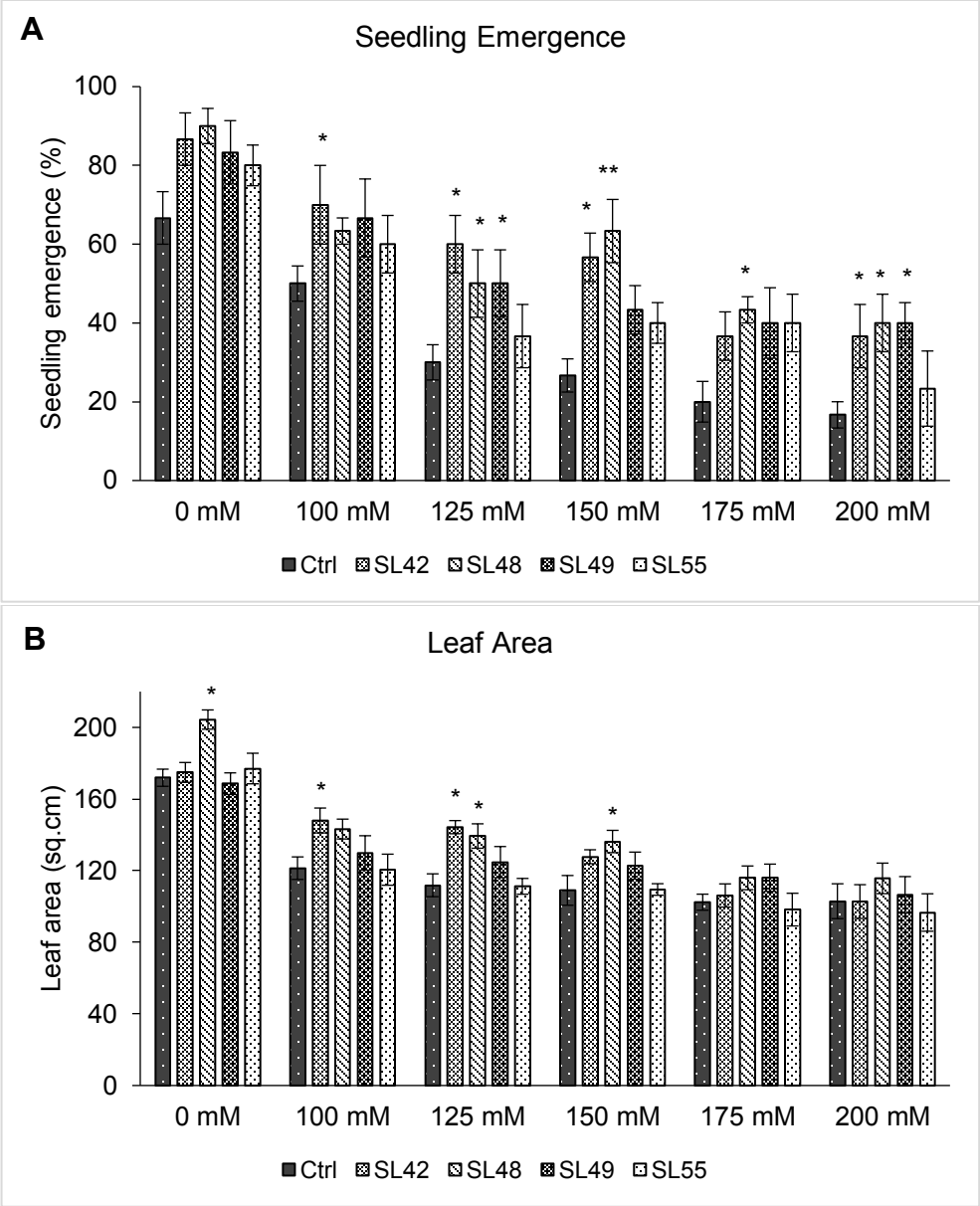

Supplementary Figure 3.15. Growth variables of soybean, **(A)** Seed emergence rate measured at 8th DAP and **(B)** Leaf area of soybean plants measured at 28th DAP under increasing salt concentrations (0, 100, 125, 150, 175, and 200 mM NaCl). The seeds were treated with 10 mM $MgSO_4$ as control or bacterized with strains SL42 and SL48. Values represent mean ± SE (n=6). Significant differences (increase) between the bacterial treatments and the respective control treatments of a particular salt concentration are indicated by an asterisk above the data points, * - $p \leq 0.05$, ** - $p \leq 0.001$ ($\alpha = 0.05$).

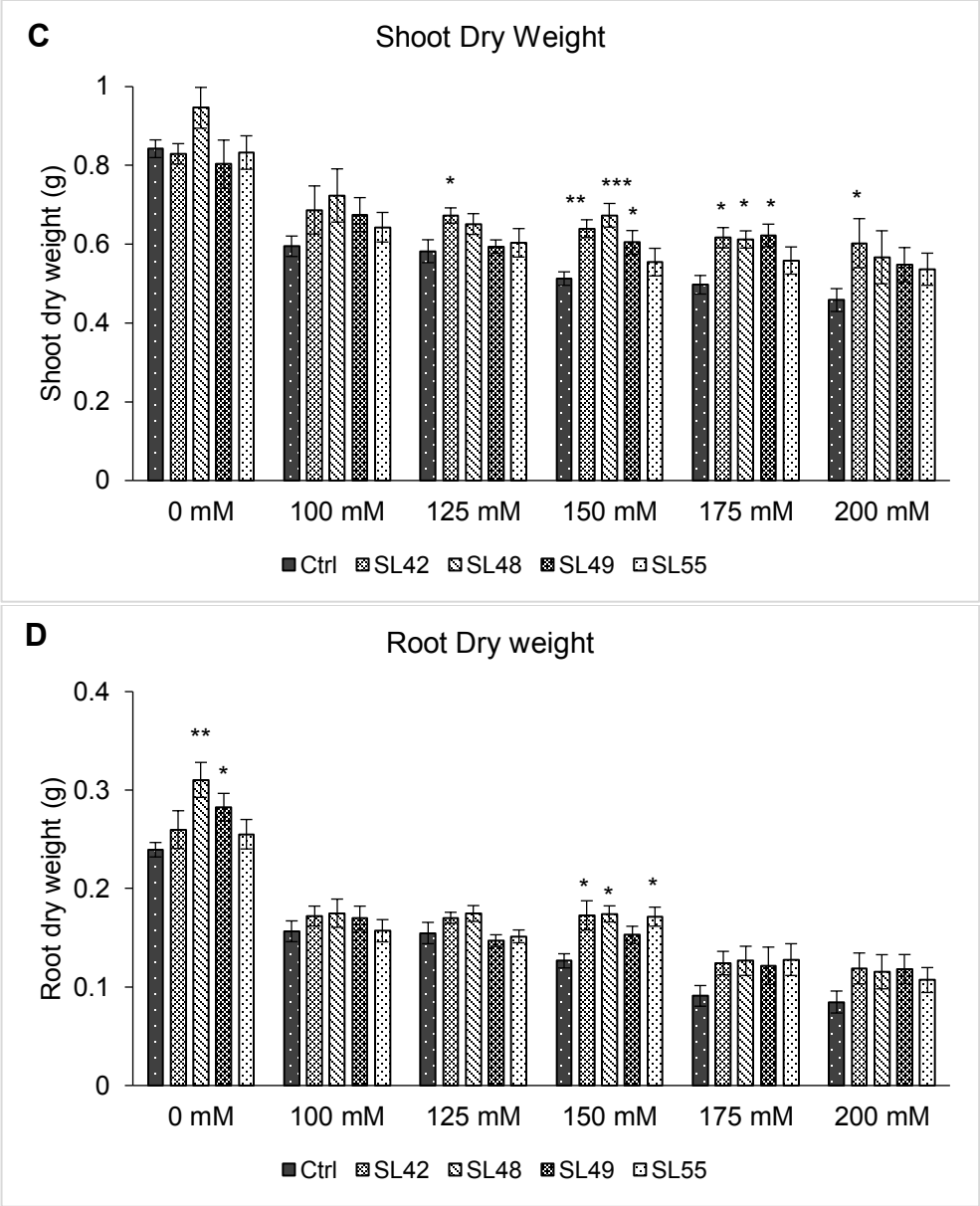

Supplementary Figure 3.15. (cont.) Growth variables of soybean, **(C)** Shoot dry weight and **(D)** Root dry weight of soybean plants measured at 28th DAP under increasing salt concentrations (0, 100, 125, 150, 175, and 200 mM NaCl). The seeds were treated with 10 mM $MgSO_4$ as control or bacterized with strains SL42 and SL48. Values represent mean ± SE (n=6). Significant differences (increase) between the bacterial treatments and the respective control treatments of a particular salt concentration are indicated by an asterisk above the data points, * - $p \leq 0.05$, ** - $p \leq 0.001$ ($\alpha = 0.05$).

Supplementary Table 3.4. Distribution of N in different plant tissues through the developmental stages

		Optimal		Salt	
Stages	Treatments	Mean	±SE	Mean	±SE
Vegetative					
Shoot	Bj	33.43	1.18	35.11	3.21
	Bj+SL42	38.31	0.35	31.79	5.63
	Bj+SL48	38.88	0.84	32.25	1.32
	Bj+SL42+SL48	35.50	1.54	29.64	1.58
Vegetative					
Root	Bj	19.18	0.85	21.32	0.77
	Bj+SL42	20.02	0.17	20.27	0.64
	Bj+SL48	19.21	0.76	19.86	1.23
	Bj+SL42+SL48	19.42	1.16	20.09	1.04
Flowering					
Leaves	Bj	41.01	1.99	41.19	1.30
	Bj+SL42	42.77	0.64	38.43	1.25
	Bj+SL48	42.22	1.53	39.26	3.34
	Bj+SL42+SL48	41.30	3.09	34.53	3.53
Flowering					
Shoot	Bj	19.31	0.95	25.19	2.26
	Bj+SL42	22.26	0.85	24.22	2.61
	Bj+SL48	20.68	0.38	22.24	2.37
	Bj+SL42+SL48	20.74	0.61	22.76	0.73
Flowering					
Root	Bj	18.46	0.59	17.73	0.62
	Bj+SL42	17.99	0.46	17.51	1.15
	Bj+SL48	17.48	0.64	16.87	1.52
	Bj+SL42+SL48	17.40	0.34	15.65	1.37
Pod-filling					
Leaves	Bj	33.43	1.26	29.77	2.39
	Bj+SL42	30.57	1.67	27.37	2.15
	Bj+SL48	34.91	1.01	30.50	1.99
	Bj+SL42+SL48	33.25	0.88	28.59	1.12

Supplementary Table 3.4. (cont.) Distribution of N in different plant tissues through the developmental stages

		Optimal		Salt	
Stages	Treatments	Mean	±SE	Mean	±SE
Pod-filling					
Shoot	Bj	18.38	2.29	15.71	1.27
	Bj+SL42	19.05	2.21	11.96	0.67
	Bj+SL48	18.21	0.62	14.39	1.43
	Bj+SL42+SL48	17.81	2.10	18.56	2.76
Pod-filling					
Pods	Bj	34.75	1.07	34.43	1.36
	Bj+SL42	35.52	1.34	34.34	2.78
	Bj+SL48	34.74	1.74	33.22	1.18
	Bj+SL42+SL48	35.42	0.65	32.96	3.29
Pod-filling					
Root	Bj	18.31	0.78	14.43	0.62
	Bj+SL42	16.35	0.79	15.73	1.36
	Bj+SL48	16.95	0.72	15.44	0.67
	Bj+SL42+SL48	16.65	0.38	15.22	2.04
Harvest					
Shoot	Bj	14.60	2.98	11.47	1.88
	Bj+SL42	14.48	1.89	11.14	1.60
	Bj+SL48	13.14	2.55	10.10	0.28
	Bj+SL42+SL48	16.30	1.67	11.18	1.91
Harvest					
Pods	Bj	7.63	0.52	5.10	0.20
	Bj+SL42	6.47	0.48	4.41	0.16
	Bj+SL48	6.12	0.19	4.43	0.32
	Bj+SL42+SL48	5.95	0.22	4.52	0.37
Harvest					
Root	Bj	16.02	1.05	16.85	1.38
	Bj+SL42	17.61	0.59	16.52	0.45
	Bj+SL48	15.20	0.19	16.44	1.79
	Bj+SL42+SL48	16.69	0.36	15.58	1.25

Supplementary Table 3.5. Distribution of P in different plant tissues through the developmental stages

		Optimal		Salt	
Stages	Treatments	Mean	±SE	Mean	±SE
Vegetative					
Shoot	Bj	4.84	0.37	4.84	1.08
	Bj+SL42	5.80	0.38	4.49	0.58
	Bj+SL48	4.98	0.36	3.89	1.39
	Bj+SL42+SL48	4.66	0.78	5.22	0.17
Vegetative					
Root	Bj	4.66	0.43	5.27	1.20
	Bj+SL42	4.62	0.90	4.45	0.23
	Bj+SL48	4.00	0.44	4.63	0.36
	Bj+SL42+SL48	4.29	0.92	5.08	0.24
Flowering					
Leaves	Bj	7.35	0.21	8.62	0.53
	Bj+SL42	6.66	0.52	9.04	0.83
	Bj+SL48	7.04	0.47	8.35	0.74
	Bj+SL42+SL48	7.02	0.37	8.06	0.88
Flowering					
Shoot	Bj	4.82	0.07	5.96	0.40
	Bj+SL42	4.71	0.32	6.02	0.32
	Bj+SL48	4.97	0.35	5.74	0.50
	Bj+SL42+SL48	5.37	0.31	5.53	0.51
Flowering					
Root	Bj	6.21	0.44	7.61	0.74
	Bj+SL42	6.52	0.99	7.96	0.25
	Bj+SL48	5.86	0.68	8.11	0.43
	Bj+SL42+SL48	6.88	0.62	6.81	0.78
Pod-filling					
Leaves	Bj	6.00	0.38	7.22	1.01
	Bj+SL42	5.59	0.66	5.90	0.99
	Bj+SL48	6.30	0.50	7.24	1.29
	Bj+SL42+SL48	5.32	0.27	6.14	0.28

Supplementary Table 3.5. (cont.) Distribution of P in different plant tissues through the developmental stages

		Optimal		Salt	
Stages	Treatments	Mean	±SE	Mean	±SE
Pod-filling					
Shoot	Bj	4.53	0.19	6.28	0.61
	Bj+SL42	4.89	0.24	4.87	0.47
	Bj+SL48	4.79	0.34	5.23	0.57
	Bj+SL42+SL48	4.85	0.27	5.08	0.16
Pod-filling					
Pods	Bj	3.74	0.16	4.07	0.18
	Bj+SL42	3.87	0.21	3.78	0.28
	Bj+SL48	3.84	0.15	3.74	0.18
	Bj+SL42+SL48	3.90	0.11	3.75	0.18
Pod-filling					
Root	Bj	6.18	0.30	7.54	0.46
	Bj+SL42	6.66	0.31	7.46	0.70
	Bj+SL48	6.36	0.68	7.74	0.98
	Bj+SL42+SL48	7.51	0.63	6.32	0.69
Harvest					
Shoot	Bj	5.64	0.06	6.21	0.99
	Bj+SL42	5.55	0.40	7.48	0.69
	Bj+SL48	6.31	0.28	7.75	1.58
	Bj+SL42+SL48	6.59	0.27	6.03	0.29
Harvest					
Pods	Bj	0.88	0.04	0.69	0.10
	Bj+SL42	0.64	0.05	0.76	0.12
	Bj+SL48	0.69	0.04	0.66	0.15
	Bj+SL42+SL48	0.61	0.05	0.60	0.09
Harvest					
Root	Bj	5.05	0.71	4.53	0.62
	Bj+SL42	4.88	0.14	3.88	0.42
	Bj+SL48	4.55	0.47	5.36	0.79
	Bj+SL42+SL48	5.17	0.36	5.12	0.32

Supplementary Table 3.6. Distribution of K in different plant tissues through the developmental stages

		Optimal		Salt	
Stages	Treatments	Mean	±SE	Mean	±SE
Vegetative					
Shoot	Bj	26.55	1.77	22.88	1.77
	Bj+SL42	30.82	2.98	25.43	1.73
	Bj+SL48	26.99	1.57	25.12	3.30
	Bj+SL42+SL48	24.51	4.18	24.31	1.38
Vegetative					
Root	Bj	17.24	0.76	16.76	1.70
	Bj+SL42	17.18	0.86	16.42	1.68
	Bj+SL48	17.55	0.26	18.99	0.62
	Bj+SL42+SL48	17.36	0.47	19.67	2.27
Flowering					
Leaves	Bj	21.49	1.00	24.34	0.58
	Bj+SL42	21.91	0.75	22.85	0.92
	Bj+SL48	22.37	1.11	22.33	2.36
	Bj+SL42+SL48	21.53	0.98	22.52	2.03
Flowering					
Shoot	Bj	35.64	5.16	36.92	2.28
	Bj+SL42	34.69	3.69	38.40	1.90
	Bj+SL48	35.44	3.65	37.57	4.30
	Bj+SL42+SL48	32.99	1.26	38.77	2.82
Flowering					
Root	Bj	17.74	0.62	15.54	0.17
	Bj+SL42	19.07	1.20	17.07	1.08
	Bj+SL48	16.69	0.89	15.89	0.55
	Bj+SL42+SL48	16.87	0.93	17.33	1.21
Pod-filling					
Leaves	Bj	15.27	0.85	14.40	1.19
	Bj+SL42	15.95	1.18	14.06	1.52
	Bj+SL48	16.85	0.52	14.67	1.30
	Bj+SL42+SL48	16.18	0.70	13.86	0.26

Supplementary Table 3.6. (cont.) Distribution of K in different plant tissues through the developmental stages

		Optimal		Salt	
Stages	Treatments	Mean	±SE	Mean	±SE
Pod-filling					
Shoot	Bj	16.72	1.09	22.30	1.15
	Bj+SL42	16.97	1.51	17.36	0.84
	Bj+SL48	17.60	1.16	16.79	0.32
	Bj+SL42+SL48	15.08	1.90	17.51	1.44
Pod-filling					
Pods	Bj	17.35	0.79	19.23	0.64
	Bj+SL42	16.82	0.73	18.47	0.54
	Bj+SL48	16.04	0.63	18.29	0.43
	Bj+SL42+SL48	17.29	0.68	17.77	0.33
Pod-filling					
Root	Bj	14.11	0.40	12.35	0.83
	Bj+SL42	12.78	0.43	12.41	0.45
	Bj+SL48	14.14	0.20	13.11	0.62
	Bj+SL42+SL48	16.63	1.37	10.85	0.15
Harvest					
Shoot	Bj	17.19	1.16	14.75	0.73
	Bj+SL42	17.56	0.61	13.87	1.87
	Bj+SL48	19.14	1.89	16.42	1.37
	Bj+SL42+SL48	20.49	1.02	17.05	1.75
Harvest					
Pods	Bj	18.22	1.19	19.93	0.59
	Bj+SL42	18.11	0.79	20.51	0.98
	Bj+SL48	20.16	0.52	21.51	0.87
	Bj+SL42+SL48	18.31	0.31	20.04	0.97
Harvest					
Root	Bj	7.74	0.62	3.33	0.47
	Bj+SL42	6.06	0.49	5.02	1.09
	Bj+SL48	6.76	0.88	2.83	0.47
	Bj+SL42+SL48	6.99	1.09	3.41	0.59

Supplementary Table 3.7. Distribution of Ca in different plant tissues through the developmental stages

		Optimal		Salt	
Stages	Treatments	Mean	±SE	Mean	±SE
Vegetative					
Shoot	Bj	8.58	0.70	7.55	0.43
	Bj+SL42	8.28	0.40	7.33	0.14
	Bj+SL48	8.25	0.29	5.54	1.81
	Bj+SL42+SL48	7.62	0.39	5.92	0.24
Vegetative					
Root	Bj	12.01	1.42	8.08	0.49
	Bj+SL42	9.22	1.52	9.59	1.76
	Bj+SL48	9.43	1.30	8.74	0.86
	Bj+SL42+SL48	10.43	2.68	8.88	1.48
Flowering					
Leaves	Bj	7.97	0.16	7.85	0.19
	Bj+SL42	7.82	0.26	7.58	0.21
	Bj+SL48	8.73	0.76	7.88	0.30
	Bj+SL42+SL48	7.51	0.13	7.10	0.55
Flowering					
Shoot	Bj	5.31	0.41	5.89	0.79
	Bj+SL42	4.91	0.17	5.59	0.30
	Bj+SL48	5.20	0.22	5.85	0.41
	Bj+SL42+SL48	5.72	0.55	5.84	0.50
Flowering					
Root	Bj	7.55	1.08	10.62	2.32
	Bj+SL42	9.51	1.74	10.54	0.28
	Bj+SL48	7.87	1.03	10.74	2.35
	Bj+SL42+SL48	7.77	1.14	10.69	2.06
Pod-filling					
Leaves	Bj	9.80	0.57	10.74	0.84
	Bj+SL42	10.40	0.40	11.67	1.07
	Bj+SL48	10.73	0.58	11.55	0.32
	Bj+SL42+SL48	9.71	0.13	11.22	0.49

Supplementary Table 3.7. (cont.) Distribution of Ca in different plant tissues through the developmental stages

		Optimal		Salt	
Stages	Treatments	Mean	±SE	Mean	±SE
Pod-filling					
Shoot	Bj	3.42	0.40	4.67	0.90
	Bj+SL42	3.58	0.15	4.86	1.01
	Bj+SL48	3.66	0.05	4.44	0.45
	Bj+SL42+SL48	3.21	0.63	4.80	0.29
Pod-filling					
Pods	Bj	3.07	0.20	3.30	0.12
	Bj+SL42	3.05	0.09	3.09	0.16
	Bj+SL48	3.00	0.12	3.09	0.06
	Bj+SL42+SL48	3.04	0.24	2.93	0.15
Pod-filling					
Root	Bj	7.41	1.29	9.07	1.79
	Bj+SL42	7.40	0.80	9.13	1.03
	Bj+SL48	6.63	1.26	7.88	0.73
	Bj+SL42+SL48	7.14	0.67	7.72	0.97
Harvest					
Shoot	Bj	3.86	0.09	3.91	0.29
	Bj+SL42	3.61	0.36	4.83	0.36
	Bj+SL48	4.07	0.29	4.40	0.38
	Bj+SL42+SL48	4.56	0.22	4.24	0.23
Harvest					
Pods	Bj	4.80	0.30	6.24	0.34
	Bj+SL42	4.87	0.53	5.24	0.26
	Bj+SL48	5.11	0.26	5.84	0.14
	Bj+SL42+SL48	4.73	0.23	5.54	0.28
Harvest					
Root	Bj	7.65	0.87	7.47	0.57
	Bj+SL42	7.15	0.49	7.61	0.59
	Bj+SL48	6.64	0.37	8.66	1.26
	Bj+SL42+SL48	7.77	0.58	7.80	0.74

Supplementary Table 3.8. Distribution of Na in different plant tissues through the developmental stages

		Optimal		Salt	
Stages	Treatments	Mean	±SE	Mean	±SE
Vegetative					
Shoot	Bj	0.12	0.03	0.53	0.09
	Bj+SL42	0.19	0.06	0.43	0.13
	Bj+SL48	0.19	0.03	0.67	0.21
	Bj+SL42+SL48	0.10	0.04	0.56	0.16
Vegetative					
Root	Bj	5.40	0.52	9.25	0.87
	Bj+SL42	5.38	0.15	9.91	0.43
	Bj+SL48	6.21	0.39	10.10	0.32
	Bj+SL42+SL48	5.61	0.27	10.73	1.19
Flowering					
Leaves	Bj	0.04	0.01	0.07	0.01
	Bj+SL42	0.05	0.02	0.08	0.02
	Bj+SL48	0.04	0.01	0.02	0.01
	Bj+SL42+SL48	0.03	0.02	0.09	0.03
Flowering					
Shoot	Bj	0.08	0.03	0.28	0.03
	Bj+SL42	0.05	0.01	0.24	0.05
	Bj+SL48	0.04	0.01	0.23	0.05
	Bj+SL42+SL48	0.03	0.02	0.21	0.06
Flowering					
Root	Bj	3.79	0.29	7.44	0.78
	Bj+SL42	4.20	0.11	7.68	0.63
	Bj+SL48	3.25	0.33	7.90	1.15
	Bj+SL42+SL48	3.11	0.30	8.10	1.21
Pod-filling					
Leaves	Bj	0.06	0.03	0.06	0.01
	Bj+SL42	0.05	0.01	0.03	0.01
	Bj+SL48	0.05	0.01	0.05	0.03
	Bj+SL42+SL48	0.01	0.01	0.05	0.03

Supplementary Table 3.8. (cont.) Distribution of Na in different plant tissues through the developmental stages

		Optimal		Salt	
Stages	Treatments	Mean	±SE	Mean	±SE
Pod-filling					
Shoot	Bj	0.01	0.01	0.34	0.09
	Bj+SL42	0.02	0.03	0.48	0.07
	Bj+SL48	0.04	0.02	0.26	0.04
	Bj+SL42+SL48	0.00	0.01	0.41	0.15
Pod-filling					
Pods	Bj	0.00	0.01	0.06	0.02
	Bj+SL42	0.01	0.01	0.03	0.01
	Bj+SL48	0.04	0.02	0.02	0.01
	Bj+SL42+SL48	0.03	0.01	0.03	0.01
Pod-filling					
Root	Bj	3.09	0.23	10.04	0.44
	Bj+SL42	3.27	0.30	8.86	0.61
	Bj+SL48	2.66	0.20	9.21	0.69
	Bj+SL42+SL48	3.00	0.31	9.32	0.75
Harvest					
Shoot	Bj	0.43	0.19	11.00	3.23
	Bj+SL42	0.30	0.09	13.28	2.48
	Bj+SL48	0.37	0.08	8.91	2.08
	Bj+SL42+SL48	0.34	0.07	8.03	1.19
Harvest					
Pods	Bj	0.09	0.04	0.36	0.06
	Bj+SL42	0.04	0.02	0.81	0.25
	Bj+SL48	0.06	0.01	0.28	0.05
	Bj+SL42+SL48	0.05	0.01	0.37	0.08
Harvest					
Root	Bj	3.00	0.16	6.35	1.11
	Bj+SL42	2.39	0.18	4.81	0.81
	Bj+SL48	2.61	0.28	5.70	0.62
	Bj+SL42+SL48	2.82	0.41	6.94	0.92

Supplementary Table 3.9. Seed nutrient composition (%) analysis

		Optimal		**Salt**	
Constituents	Treatments	Mean	±SE	Mean	±SE
Moisture	Bj	6.78	0.05	6.66	0.11
	Bj+SL42	6.87	0.04	6.60	0.09
	Bj+SL48	6.82	0.06	6.50	0.07
	Bj+SL42+SL48	6.91	0.10	6.50	0.04
		P = 0.5444		P = 0.6412	
Protein	Bj	37.69	0.24	34.78	0.84
	Bj+SL42	36.73	0.94	35.33	0.77
	Bj+SL48	36.77	0.42	34.69	0.50
	Bj+SL42+SL48	37.34	0.43	35.51	0.57
		P = 0.92		P = 0.1822	
Fat	Bj	18.48	0.09	20.49	0.33
	Bj+SL42	18.52	0.40	20.03	0.40
	Bj+SL48	18.71	0.18	20.27	0.44
	Bj+SL42+SL48	18.68	0.09	19.66	0.38
		P = 0.6497		P = 0.7405	
Fibre	Bj	12.72	1.02	11.07	0.24
	Bj+SL42	12.00	0.22	10.86	0.29
	Bj+SL48	12.69	0.31	11.32	0.18
	Bj+SL42+SL48	12.51	0.54	11.45	0.46
Ash	Bj	4.58	0.07	4.85	0.10
	Bj+SL42	4.26	0.26	4.63	0.16
	Bj+SL48	4.56	0.07	4.69	0.02
	Bj+SL42+SL48	4.22	0.25	4.50	0.07

Supplementary Table 3.9. (cont.) Seed nutrient composition (%) analysis

		Optimal		**Salt**	
Constituents	Treatments	Mean	±SE	Mean	±SE
		P = 0.0748		P = 0.1533	
Potassium	Bj	1.87	0.03	2.02	0.02
	Bj+SL42	1.78	0.05	1.96	0.01
	Bj+SL48	1.81	0.01	1.94	0.03
	Bj+SL42+SL48	1.85	0.02	2.00	0.02
		P = 0.2788		P = 0.4279	
Phosphorous	Bj	0.63	0.01	0.61	0.01
	Bj+SL42	0.60	0.01	0.61	0.01
	Bj+SL48	0.62	0.01	0.61	0.01
	Bj+SL42+SL48	0.61	0.01	0.63	0.01
		P = 0.7621		P = 0.8584	
Magnesium	Bj	0.28	0.01	0.26	0.01
	Bj+SL42	0.27	0.01	0.26	0.01
	Bj+SL48	0.27	0.01	0.27	0.00
	Bj+SL42+SL48	0.28	0.02	0.27	0.01
		P = 0.4648		P = 0.2025	
Calcium	Bj	0.16	0.00	0.14	0.01
	Bj+SL42	0.14	0.01	0.13	0.01
	Bj+SL48	0.16	0.01	0.15	0.01
	Bj+SL42+SL48	0.15	0.02	0.15	0.01
		P = 0.8004		P = 0.0079	
Sodium	Bj	0.03	0.00	0.03	0.00
	Bj+SL42	0.03	0.00	0.04	0.00
	Bj+SL48	0.03	0.01	0.04	0.01
	Bj+SL42+SL48	0.03	0.00	0.05	0.00

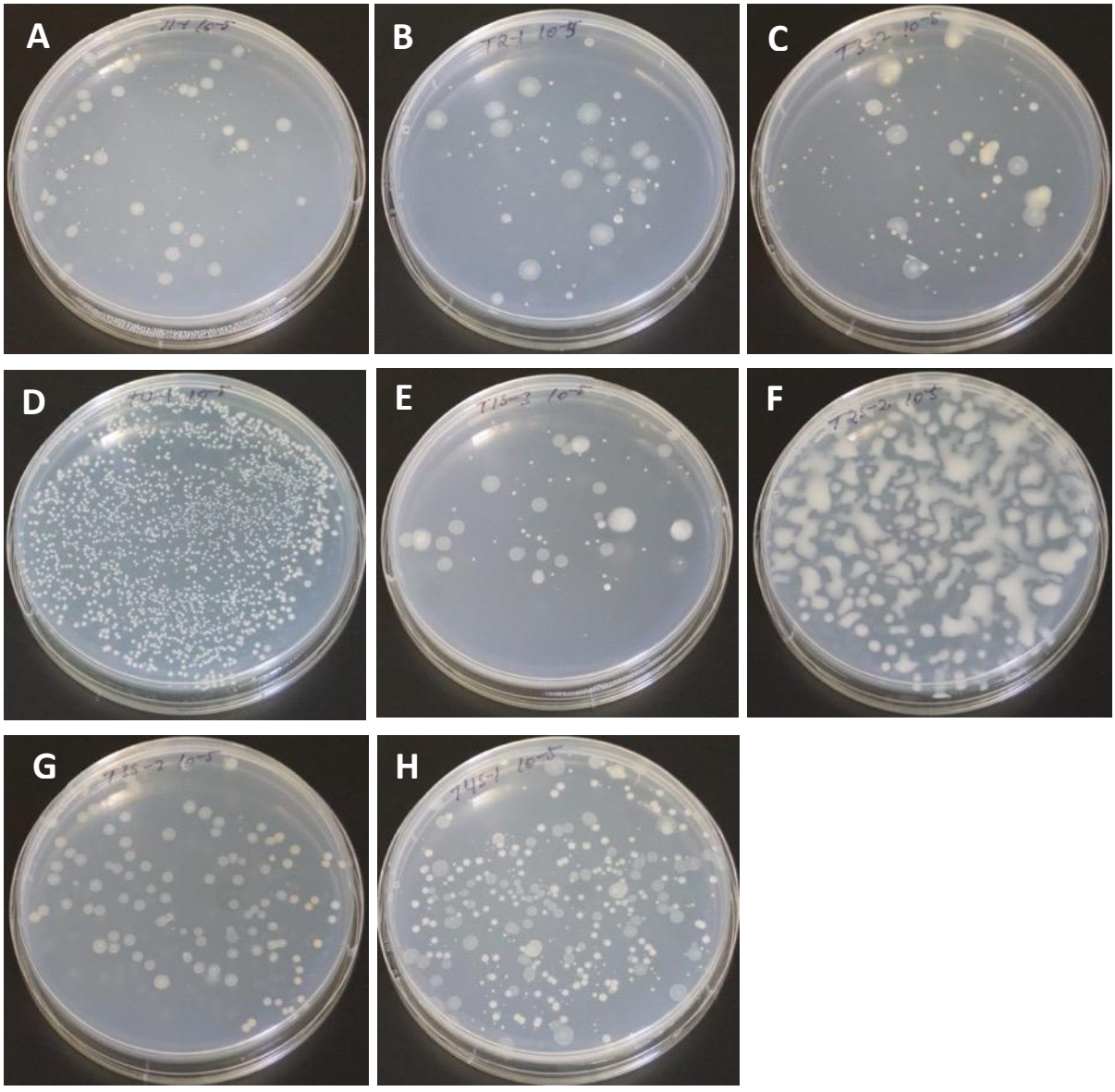

Supplementary Figure 3.15. Bacteria colonies isolated from soybean nodules at harvest stage from the treatments of **(A)** *Bradyrhizobium* (Bj), **(B)** Bj +SL42, **(C)** Bj +SL48 **(D)** Bj +SL42 +SL48 and under salt stress **(E)** Bj, **(F)** Bj +SL42, **(G)** Bj +SL48, and **(H)** Bj +SL42 +SL48 on YEM agr plates at 10^{-5} dilution after 48 h of incubation.

APPENDIX B

Supplementary Figures and Tables – Chapter 4

Quantitative spectra of Soybean leaf proteome profile

Fold change after normalization (> 1.0) and Fisher-exact test ($P < 0.05$) of proteins expressed in bacterial treatments relative to the control (n=3).

Supplementary Table 4.1. Fold change of proteins that were upregulated by treatment SL42, relative to the control under optimal conditions.

#	Identified Proteins (3076/3093)	Molecular Weight	Fisher's Exact Test	Fold Change	Control	SL42
2	ribulose bisphosphate carboxylase small chain 4, chloroplastic	20 kDa	< 0.00010	1.2	1,266	1,513
160	prolyl endopeptidase	86 kDa	0.0045	1.4	97	137
189	Cluster of PREDICTED: glutathione S-transferase GST 9 isoform X1	?	0.021	1.4	67	93
232	PREDICTED: thioredoxin H1	?	0.04	1.3	87	112
372	isoflavone reductase-like protein	34 kDa	0.039	1.4	51	71
412	31 kDa ribonucleoprotein, chloroplastic-like	32 kDa	0.0021	1.7	45	77
474	DNA-damage-repair/toleration protein DRT100-like precursor	40 kDa	0.03	1.6	25	41
845	aspartyl protease AED3	47 kDa	0.043	1.9	12	23
873	50S ribosomal protein L6, chloroplastic	25 kDa	0.031	1.8	18	32
895	Cluster of matrix metalloproteinase precursor	?	0.0087	2.1	15	32
1127	Cluster of asparagine synthetase 2	?	0.032	4.5	2	9
1307	long chain acyl-CoA synthetase 9, chloroplastic isoform X1	76 kDa	0.037	3	4	12
1366	Cluster of glucose-6-phosphate dehydrogenase	59 kDa	0.045	3.3	3	10
1482	UDP-glycosyltransferase 74G1	54 kDa	0.031	INF	0	5
1647	PREDICTED: patatin-like protein 3	?	0.019	5	2	10
1845	prolyl endopeptidase	82 kDa	0.0076	INF	0	7
2053	probable inactive purple acid phosphatase 1 isoform X1	69 kDa	0.031	INF	0	5
2055	Cluster of probable fructokinase-7 isoform X1	37 kDa	0.0076	INF	0	7

Supplementary Table 4.2. Fold change of proteins that were upregulated by treatment SL48, relative to the control under optimal conditions.

#	Identified Proteins (3076/3093)	Molecular Weight	Fisher's Exact Test	Fold Change	Control	SL48
2	ribulose bisphosphate carboxylase small chain 4, chloroplastic	20 kDa	0.00029	1.1	1,266	1,425
160	prolyl endopeptidase	86 kDa	0.00068	1.5	97	146
167	soyasaponin III rhamnosyltransferase	54 kDa	0.043	1.3	99	124
189	Cluster of PREDICTED: glutathione S-transferase GST 9 isoform X1	?	0.013	1.4	67	95
194	Cluster of clathrin heavy chain 2	193 kDa	0.0097	1.4	69	99
232	PREDICTED: thioredoxin H1	?	0.022	1.3	87	115
333	NADH dehydrogenase subunit 7 (chloroplast)	46 kDa	0.016	1.5	51	75
467	PREDICTED: UDP-glucose flavonoid 3-O-glucosyltransferase 7-like	?	0.01	1.7	33	55
639	15-cis-phytoene desaturase, chloroplastic/chromoplastic	63 kDa	0.013	1.8	22	40
652	Cluster of PREDICTED: multicystatin	?	0.00042	2.7	15	40
799	26S proteasome regulatory subunit 4 homolog A	50 kDa	0.043	1.8	16	28
911	Cluster of S-formylglutathione hydrolase	32 kDa	0.012	3.2	5	16
1127	Cluster of asparagine synthetase 2	?	< 0.00010	13	2	25
1307	long chain acyl-CoA synthetase 9, chloroplastic isoform X1	76 kDa	0.023	3.2	4	13
1330	40S ribosomal protein S9-2-like	23 kDa	0.01	9	1	9
1417	S-adenosyl-L-methionine:delta24-sterol-C-methyltransferase	?	0.03	INF	0	5
1482	UDP-glycosyltransferase 74G1	54 kDa	0.00022	INF	0	12
1516	probable splicing factor 3A subunit 1	89 kDa	0.01	5.5	2	11
1668	heterogeneous nuclear ribonucleoprotein 1	48 kDa	0.034	7	1	7
1739	stress-induced protein SAM22	17 kDa	0.00084	13	1	13
1783	Cluster of ubiquitin fusion degradation protein 1 homolog isoform X1	35 kDa	0.019	8	1	8
1845	prolyl endopeptidase	82 kDa	0.0074	INF	0	7
1912	probable inactive shikimate kinase like 2, chloroplastic	40 kDa	0.03	INF	0	5

1944	cinnamoyl-CoA reductase 1 isoform X1	35 kDa	0.0026	3.5	6	21
2038	UDP-glucuronic acid decarboxylase 2	44 kDa	0.05	2.1	8	17
2052	chlorophyll a-b binding protein, chloroplastic-like	29 kDa	0.015	INF	0	6
2053	probable inactive purple acid phosphatase 1 isoform X1	69 kDa	0.00022	INF	0	12

Supplementary Table 4.3. Fold change of proteins that were upregulated by treatment SL42+SL48, relative to the control under optimal conditions.

#	Identified Proteins (3076/3093)	Molecular Weight	Fisher's Exact Test	Fold Change	Control	SL42+ SL48
2	ribulose bisphosphate carboxylase small chain 4, chloroplastic	20 kDa	< 0.00010	1.3	1,266	1,591
5	Cluster of linoleate 9S-lipoxygenase-4	?	0.02	1.1	1,083	1,174
6	Cluster of glycine dehydrogenase (decarboxylating), mitochondrial	115 kDa	0.0058	1.1	910	1,015
9	Cluster of glyceraldehyde-3-phosphate dehydrogenase A subunit	?	< 0.00010	1.2	818	1,019
17	Cluster of peroxisomal (S)-2-hydroxy-acid oxidase GLO1-like	41 kDa	0.037	1.1	531	588
24	Cluster of catalase	57 kDa	0.033	1.1	401	453
38	Cluster of chlorophyll a-b binding protein P4, chloroplastic	28 kDa	0.033	1.1	371	421
85	Cluster of adenosylhomocysteinase	53 kDa	0.043	1.2	220	257
103	Cluster of phosphoenolpyruvate carboxylase	?	0.0033	1.3	159	211
160	prolyl endopeptidase	86 kDa	< 0.00010	1.8	97	173
167	soyasaponin III rhamnosyltransferase	54 kDa	0.00062	1.5	99	150
189	Cluster of PREDICTED: glutathione S-transferase GST 9 isoform X1	?	0.031	1.4	67	91
195	Cluster of aconitate hydratase, cytoplasmic	107 kDa	0.029	1.2	144	178
214	carotenoid 9,10(9',10')-cleavage dioxygenase 1	61 kDa	0.017	1.3	89	120
274	soyasapogenol B glucuronide galactosyltransferase-like	56 kDa	0.018	1.4	72	100
323	Cluster of aconitate hydratase 1	99 kDa	0.017	1.3	111	145
333	NADH dehydrogenase subunit 7 (chloroplast)	46 kDa	0.018	1.5	51	75
383	photosystem I reaction center subunit psaK, chloroplastic	13 kDa	0.011	1.5	54	81

412	31 kDa ribonucleoprotein, chloroplastic-like	32 kDa	0.047	1.4	45	63
467	PREDICTED: UDP-glucose flavonoid 3-O-glucosyltransferase 7-like	?	0.0017	1.9	33	62
474	DNA-damage-repair/toleration protein DRT100-like precursor	40 kDa	0.0013	2.1	25	52
639	15-cis-phytoene desaturase, chloroplastic/chromoplastic	63 kDa	0.019	1.8	22	39
646	NAD(P)H-quinone oxidoreductase subunit N, chloroplastic	26 kDa	0.0059	2.1	17	36
652	Cluster of PREDICTED: multicystatin	?	0.017	2	15	30
668	PREDICTED: 30S Ribosomal protein S1 isoform X1	?	0.025	1.8	19	34
812	Cluster of proline-rich protein precursor	13 kDa	< 0.00010	6.6	10	66
845	aspartyl protease AED3	47 kDa	0.022	2.1	12	25
911	Cluster of S-formylglutathione hydrolase	32 kDa	0.047	2.6	5	13
1033	Cluster of fumarate hydratase 1, mitochondrial	53 kDa	0.042	2.1	9	19
1127	Cluster of asparagine synthetase 2	?	0.0001	9.5	2	19
1215	indole-3-glycerol phosphate synthase, chloroplastic	43 kDa	0.01	4.3	3	13
1272	uridine 5'-monophosphate synthase-like	?	0.0081	3.4	5	17
1317	eukaryotic translation initiation factor 3 subunit M	46 kDa	0.038	2.5	6	15
1330	40S ribosomal protein S9-2-like	23 kDa	0.00088	13	1	13
1334	4-diphosphocytidyl-2-C-methyl-D-erythritol kinase, chloroplastic/chromoplastic	44 kDa	0.015	3.5	4	14
1366	Cluster of glucose-6-phosphate dehydrogenase	59 kDa	0.045	3.3	3	10
1379	protein PELPK1	39 kDa	0.047	2.6	5	13
1403	Cluster of ADP,ATP carrier protein 1, chloroplastic	68 kDa	0.032	4.5	2	9
1406	aspartyl protease AED3	49 kDa	0.028	2.1	11	23
1459	allene oxide synthase, chloroplastic-like	55 kDa	0.0063	6	2	12
1482	UDP-glycosyltransferase 74G1	54 kDa	0.0076	INF	0	7
1608	ribulose-1,5 bisphosphate carboxylase/oxygenase large subunit N-methyltransferase, chloroplastic	55 kDa	0.019	5	2	10
1717	acyl-coenzyme A oxidase 3, peroxisomal	76 kDa	0.034	7	1	7

1718	anthocyanidin 3-O-glucosyltransferase 7	50 kDa	0.01	9	1	9
1772	phenylalanine--tRNA ligase alpha subunit, cytoplasmic	56 kDa	0.015	INF	0	6
1842	aminopeptidase M1 isoform X1	102 kDa	0.0076	INF	0	7
1845	prolyl endopeptidase	82 kDa	0.00023	INF	0	12
1867	zinc transporter 4, chloroplastic isoform X1	51 kDa	0.031	INF	0	5
1882	dynamin-related protein 1E	69 kDa	0.031	INF	0	5
1944	cinnamoyl-CoA reductase 1 isoform X1	35 kDa	0.007	3.2	6	19
2003	putative leucine-rich repeat receptor-like protein kinase At2g19210-like precursor	101 kDa	0.031	INF	0	5
2052	chlorophyll a-b binding protein, chloroplastic-like	29 kDa	0.0076	INF	0	7
2053	probable inactive purple acid phosphatase 1 isoform X1	69 kDa	0.015	INF	0	6

Supplementary Table 4.4. Fold change of proteins that were upregulated by treatment SL42, relative to the control under salt-stressed conditions.

#	Identified Proteins (3518/3553)	Molecular Weight	Fisher's Exact Test	Fold Change	Control	SL42
9	Cluster of glyceraldehyde-3-phosphate dehydrogenase A subunit	?	< 0.00010	1.3	540	716
9.2	PREDICTED: glyceraldehyde-3-phosphate dehydrogenase A, chloroplastic	?	< 0.00010	1.4	482	660
31.2	elongation factor Tu, chloroplastic-like	52 kDa	0.044	1.2	325	382
31.3	PREDICTED: elongation factor Tu, chloroplastic	?	0.026	1.2	311	373
36.1	actin-7	42 kDa	0.042	1.2	225	272
36.4	actin	42 kDa	0.046	1.2	217	262
36.5	actin	42 kDa	0.028	1.2	206	255
36.6	actin	42 kDa	0.048	1.2	178	218
44	Cluster of leghemoglobin reductase-like	53 kDa	0.012	1.2	280	347
44.2	ferric leghemoglobin reductase-2 precursor	53 kDa	0.026	1.2	218	269
87	Cluster of cell division cycle protein 48 homolog	90 kDa	0.018	1.3	162	209
96	Cluster of clathrin heavy chain	193 kDa	0.026	1.3	130	169
152	Cluster of HSP90 superfamily protein isoform X1	93 kDa	0.0029	1.4	127	181
152.2	endoplasmin homolog isoform X1	94 kDa	0.0034	1.4	118	169

198	Cluster of 60S ribosomal protein L7a-1	29 kDa	0.017	1.4	89	124
209.2	PREDICTED: auxin-binding protein ABP19a-like	?	< 0.00010	2.3	57	132
232.1	PREDICTED: ras-related protein RABA5d-like	?	0.0087	INF	0	7
243	Cluster of chaperonin CPN60-2, mitochondrial	61 kDa	0.012	1.5	74	108
248	Cluster of 40S ribosomal protein S8 isoform X1	25 kDa	0.0041	1.5	74	114
253	Cluster of 60S ribosomal protein L8-3	28 kDa	0.01	1.5	69	103
273	Cluster of ribosomal protein L2 (chloroplast)	30 kDa	0.046	1.3	75	101
293	Cluster of importin subunit alpha-2	59 kDa	0.037	1.4	57	81
314	Cluster of peroxisomal fatty acid beta-oxidation multifunctional protein AIM1	78 kDa	0.017	1.5	60	89
320	Cluster of histone H1	20 kDa	0.00051	1.8	50	92
324.2	12-oxophytodienoate reductase 2	41 kDa	0.0044	INF	0	8
334	Cluster of alpha-glucan water dikinase, chloroplastic isoform X1	164 kDa	0.029	1.5	50	74
335	Cluster of patellin-3 isoform X1	70 kDa	0.026	1.4	93	126
339	Cluster of V-type proton ATPase subunit C	43 kDa	0.018	1.6	41	65
472	osmotin-like protein	26 kDa	0.012	1.7	38	63
478	patellin-3 isoform X1	65 kDa	0.026	1.4	76	106
483.2	beta-hexosaminidase 1	63 kDa	0.034	1.6	29	47
485	PREDICTED: ferredoxin-A-like	?	0.025	1.5	51	76
487.2	coatomer subunit gamma-2	99 kDa	0.034	1.8	19	34
522.1	PREDICTED: 12-oxophytodienoate reductase 3	?	0.042	1.5	37	56
522.2	12-oxophytodienoate reductase 3	44 kDa	0.04	1.6	28	45
524	Cluster of calnexin homolog precursor	62 kDa	0.044	1.4	47	68
567	photosystem I reaction center subunit psaK, chloroplastic	13 kDa	0.0027	2.3	18	41
596.2	GTP-binding protein SAR1A	22 kDa	0.0022	INF	0	9
624	Cluster of citrate synthase, glyoxysomal	56 kDa	0.036	1.6	30	48
624.2	PREDICTED: peroxisomal citrate synthase isoform X1	?	0.0044	4.2	4	17
718	aspartyl protease family protein At5g10770	52 kDa	0.024	1.5	59	86
725	Cluster of 26S proteasome non-ATPase regulatory subunit 13-like	44 kDa	0.021	1.9	17	33

772	Cluster of IAA-amino acid hydrolase ILR1-like 4	49 kDa	0.019	2	16	32
867	Cluster of coatomer subunit delta	58 kDa	0.0023	2.9	10	29
1057	Cluster of proline-rich protein precursor	13 kDa	< 0.00010	10	3	31
1061	argininosuccinate lyase, chloroplastic isoform X1	57 kDa	0.048	2	11	22
1164.3	asparagine synthetase	?	0.039	7	1	7
1199	GDP-mannose 4,6 dehydratase 1	41 kDa	0.021	2.8	6	17
1208.2	NADPH--cytochrome P450 reductase	77 kDa	0.017	INF	0	6
1279	Cluster of ABC transporter C family member 4	168 kDa	0.038	2.4	7	17
1298	Cluster of calreticulin-3	50 kDa	0.0044	6.5	2	13
1338	PREDICTED: cystathionine gamma-synthase 1, chloroplastic	?	0.0087	INF	0	7
1361.2	ubiquitin fusion degradation protein 1 homolog	35 kDa	0.034	INF	0	5
1522	eukaryotic translation initiation factor 3 subunit G	32 kDa	0.002	12	1	12
1545	probable glucan 1,3-alpha-glucosidase	104 kDa	0.013	5.5	2	11
1613	titin isoform X3	101 kDa	0.013	5.5	2	11
1682	Cluster of proteasome activator subunit 4	204 kDa	0.017	INF	0	6
1734	protein BOBBER 1	34 kDa	0.039	7	1	7
1749	probable acyl-activating enzyme 16, chloroplastic isoform X1	80 kDa	0.037	4.5	2	9
1751	protein ROOT HAIR DEFECTIVE 3 homolog 2	93 kDa	0.037	4.5	2	9
1829	probable histone H2A.5	15 kDa	0.037	4.5	2	9
1859	beta-ketoacyl-acyl carrier protein synthase III	42 kDa	0.0044	INF	0	8
1880	chaperone protein dnaJ A6, chloroplastic isoform X1	47 kDa	0.045	1.9	13	25
1945	linamarin synthase 1	55 kDa	0.022	8	1	8
2075	Cluster of probable inactive purple acid phosphatase 1 isoform X1	69 kDa	0.00029	INF	0	12
2087	protein HLB1	59 kDa	0.017	INF	0	6
2088	GDSL esterase/lipase EXL3	41 kDa	0.034	INF	0	5
2197	PREDICTED: probable S-sulfocysteine synthase, chloroplastic	?	0.0087	INF	0	7
2273	7-deoxyloganetin glucosyltransferase	54 kDa	0.017	INF	0	6

Supplementary Table 4.5. Fold change of proteins that were upregulated by treatment SL48, relative to the control under salt-stressed conditions.

#	Identified Proteins (3518/3553)	Molecular Weight	Fisher's Exact Test	Fold Change	Control	SL48
4	ATP synthase CF1 beta subunit (chloroplast)	54 kDa	0.046	1.1	1,197	1,308
8	Cluster of glycine dehydrogenase (decarboxylating), mitochondrial	115 kDa	0.00015	1.2	606	754
9	Cluster of glyceraldehyde-3-phosphate dehydrogenase A subunit	?	< 0.00010	1.4	540	773
9.2	PREDICTED: glyceraldehyde-3-phosphate dehydrogenase A, chloroplastic	?	< 0.00010	1.5	482	719
11.1	chlorophyll a/b-binding protein	?	0.037	1.1	444	510
11.3	chlorophyll a-b binding protein 3, chloroplastic	28 kDa	0.032	1.1	477	548
44	Cluster of leghemoglobin reductase-like	53 kDa	0.042	1.2	280	330
44.2	ferric leghemoglobin reductase-2 precursor	53 kDa	0.049	1.2	218	260
54	Cluster of S-adenosylmethionine synthase	43 kDa	0.016	1.2	241	297
75.4	enolase 1, chloroplastic	52 kDa	0.033	INF	0	5
93.2	ATP-dependent zinc metalloprotease FTSH, chloroplastic	74 kDa	0.047	1.2	157	193
96.5	clathrin heavy chain 1 isoform X1	193 kDa	< 0.00010	INF	0	20
118	Cluster of phosphoglucomutase, chloroplastic	68 kDa	0.028	1.3	159	200
144.3	NADP-dependent malic enzyme	71 kDa	0.0011	INF	0	10
152	Cluster of HSP90 superfamily protein isoform X1	93 kDa	0.0026	1.4	127	180
152.2	endoplasmin homolog isoform X1	94 kDa	0.0032	1.4	118	168
157	Cluster of methylenetetrahydrofolate reductase 2	67 kDa	0.027	1.3	96	128
209.2	PREDICTED: auxin-binding protein ABP19a-like	?	< 0.00010	2.1	57	119
217	Cluster of heat shock 70 kDa protein 14	95 kDa	0.018	1.4	74	105
220.3	alpha-1,4 glucan phosphorylase L-2 isozyme, chloroplastic/amyloplastic isoform X1	112 kDa	0.017	INF	0	6
226	Cluster of 2-oxoglutarate dehydrogenase, mitochondrial	116 kDa	0.019	1.4	72	102
266.5	14-3-3 protein SGF14p	30 kDa	0.0042	3	8	24
266.6	14-3-3 protein SGF14n	30 kDa	0.012	2.6	9	23

284	50S ribosomal protein L1, chloroplastic	38 kDa	0.0069	1.7	35	61
299	Cluster of guanosine nucleotide diphosphate dissociation inhibitor 2	50 kDa	0.029	1.5	49	72
299.2	rab GDP dissociation inhibitor alpha-like	50 kDa	0.039	1.4	47	68
314	Cluster of peroxisomal fatty acid beta-oxidation multifunctional protein AIM1	78 kDa	0.036	1.4	60	84
336	Cluster of DEAD-box ATP-dependent RNA helicase 56	48 kDa	0.03	1.4	54	78
415.2	60S ribosomal protein L13a-4	24 kDa	0.049	1.6	25	40
428	PREDICTED: alcohol dehydrogenase class-3	?	0.0025	1.8	38	69
442	Cluster of linoleate 13S-lipoxygenase 2-1, chloroplastic	104 kDa	0.0049	1.8	31	57
487.2	coatomer subunit gamma-2	99 kDa	0.041	1.7	19	33
487.3	coatomer subunit gamma-2	99 kDa	0.015	2.1	15	31
503	succinate dehydrogenase [ubiquinone] flavoprotein subunit 1, mitochondrial	69 kDa	0.039	1.6	29	46
529	Cluster of peroxisomal fatty acid beta-oxidation multifunctional protein MFP2	79 kDa	0.0054	1.8	32	58
533	Cluster of T-complex protein 1 subunit alpha	59 kDa	0.029	1.6	28	46
558	Cluster of eukaryotic translation initiation factor 3 subunit E	51 kDa	0.0073	1.9	24	46
558.1	eukaryotic translation initiation factor 3 subunit E	51 kDa	0.0097	1.9	24	45
558.2	eukaryotic translation initiation factor 3 subunit E	51 kDa	0.013	1.9	21	40
567	photosystem I reaction center subunit psaK, chloroplastic	13 kDa	0.00013	2.7	18	49
570	Cluster of PREDICTED: aspartate-semialdehyde dehydrogenase	?	0.035	1.8	17	31
571	Cluster of NADH dehydrogenase [ubiquinone] iron-sulfur protein 1, mitochondrial	81 kDa	0.046	1.6	24	39
596.2	GTP-binding protein SAR1A	22 kDa	0.0084	INF	0	7
624.2	PREDICTED: peroxisomal citrate synthase isoform X1	?	0.0025	4.5	4	18
633	Cluster of cytosolic chaperonin	?	0.024	1.8	22	39
633.1	cytosolic chaperonin	?	0.026	1.8	20	36
638	3-isopropylmalate dehydratase large subunit, chloroplastic	55 kDa	0.015	1.8	23	42

653	Cluster of DEAD-box ATP-dependent RNA helicase 3, chloroplastic	84 kDa	0.024	1.8	22	39
683	Cluster of SKP1-like protein 1A isoform X1	17 kDa	0.0033	2.2	20	43
690.1	topless-related protein 1 isoform X1	125 kDa	0.035	2.2	9	20
721	Cluster of probable aldo-keto reductase 1	?	0.015	1.8	23	42
748.2	epimerase family protein SDR39U1 homolog, chloroplastic isoform X1	38 kDa	0.023	3	5	15
759.3	carbonic anhydrase 2	28 kDa	0.035	1.8	20	35
770	Cluster of gamma carbonic anhydrase 1, mitochondrial	30 kDa	0.032	1.8	19	34
798.3	protein EXPORTIN 1A isoform X2	123 kDa	0.017	INF	0	6
803	Cluster of 60S ribosomal protein L37-3	11 kDa	0.0027	2.7	11	30
816	protein disulfide isomerase-like 1-4	65 kDa	0.037	1.7	21	36
853	Cluster of translocase of chloroplast 159, chloroplastic-like	133 kDa	0.029	1.9	15	29
867	Cluster of coatomer subunit delta	58 kDa	0.0098	2.5	10	25
881.2	succinate--CoA ligase [ADP-forming] subunit alpha, mitochondrial	34 kDa	0.026	1.9	17	32
948	tripeptidyl-peptidase 2 isoform X1	146 kDa	0.029	2.2	10	22
1013.2	cyclase-like protein 2	31 kDa	0.0021	INF	0	9
1029	Cluster of protein translocase subunit SecA, chloroplastic isoform X1	115 kDa	0.02	2.3	10	23
1057	Cluster of proline-rich protein precursor	13 kDa	0.00017	7	3	21
1105	Cluster of dihydrolipoyllysine-residue acetyltransferase component 4 of pyruvate dehydrogenase complex, chloroplastic isoform X2	49 kDa	0.0099	2.3	12	28
1141	PREDICTED: UBP1-associated protein 2B	?	0.012	4.3	3	13
1164.2	PREDICTED: asparagine synthetase, root [glutamine-hydrolyzing]	?	0.02	2.8	6	17
1170	probable methionine--tRNA ligase isoform X2	90 kDa	0.0084	3.2	6	19
1176	Cluster of THO complex subunit 4A	26 kDa	0.024	2.3	9	21
1179	histidine--tRNA ligase, chloroplastic/mitochondrial isoform X1	56 kDa	0.013	3	6	18

1199	GDP-mannose 4,6 dehydratase 1	41 kDa	0.0035	3.5	6	21
1208.2	NADPH--cytochrome P450 reductase	77 kDa	0.033	INF	0	5
1234.2	ubiquitin-conjugating enzyme E2 variant 1D	17 kDa	0.012	5.5	2	11
1234.3	ubiquitin-conjugating enzyme E2 variant 1D	17 kDa	0.0035	11	1	11
1267	cysteine desulfurase, mitochondrial	50 kDa	0.029	2.7	6	16
1286	probable endo-1,3(4)-beta-glucanase ARB_01444	73 kDa	0.035	2.8	5	14
1319	Cluster of alpha-amylase inhibitor/lipid transfer/seed storage family protein precursor	13 kDa	0.0025	5.3	3	16
1333	Cluster of vesicle-fusing ATPase	82 kDa	0.011	3.8	4	15
1338	PREDICTED: cystathionine gamma-synthase 1, chloroplastic	?	0.00055	INF	0	11
1361	Cluster of ubiquitin fusion degradation protein 1 homolog isoform X1	35 kDa	0.017	3.5	4	14
1503.2	gamma carbonic anhydrase 1, mitochondrial	29 kDa	0.0072	6	2	12
1508	pullulanase 1, chloroplastic	106 kDa	0.031	3.7	3	11
1514.2	malonate--CoA ligase	66 kDa	0.00055	INF	0	11
1522	eukaryotic translation initiation factor 3 subunit G	32 kDa	0.037	7	1	7
1561	Cluster of serine/threonine-protein phosphatase PP2A catalytic subunit isoform X2	36 kDa	0.031	3.7	3	11
1562.2	putative 50S ribosomal protein L21, chloroplastic	23 kDa	0.033	INF	0	5
1602	xanthoxin dehydrogenase	29 kDa	0.031	3.7	3	11
1603	nifU-like protein 4, mitochondrial	29 kDa	0.035	4.5	2	9
1613	titin isoform X3	101 kDa	0.012	5.5	2	11
1639.2	protein SGT1 homolog	40 kDa	0.033	INF	0	5
1682	Cluster of proteasome activator subunit 4	204 kDa	0.017	INF	0	6
1695	ribosomal protein S12 (chloroplast)	14 kDa	0.021	8	1	8
1748	actin-related protein 4	49 kDa	0.035	4.5	2	9
1772	glutamyl-tRNA(Gln) amidotransferase subunit A, chloroplastic/mitochondrial	58 kDa	0.0084	INF	0	7
1812	Cluster of PREDICTED: probable pectate lyase 8	?	0.033	INF	0	5
1824	4-diphosphocytidyl-2-C-methyl-D-erythritol kinase, chloroplastic/chromoplastic	44 kDa	0.037	7	1	7

1890	probable linoleate 9S-lipoxygenase 5	98 kDa	0.033	INF	0	5
1898	Cluster of phospholipase A-2-activating protein	84 kDa	0.021	5	2	10
1940	geraniol 8-hydroxylase	58 kDa	0.037	7	1	7
1985	integrin-linked protein kinase 1	48 kDa	0.033	INF	0	5
2055	calcium-dependent protein kinase 2	60 kDa	0.037	7	1	7
2075	Cluster of probable inactive purple acid phosphatase 1 isoform X1	69 kDa	< 0.00010	INF	0	16
2105.1	geranylgeranyl pyrophosphate synthase, chloroplastic	40 kDa	0.033	INF	0	5
2123	RNA recognition motif-containing protein	20 kDa	0.033	INF	0	5
2129	lysM domain-containing GPI-anchored protein 1	43 kDa	0.0011	INF	0	10
2134	protein TSS	203 kDa	0.017	INF	0	6
2182	probable carotenoid cleavage dioxygenase 4, chloroplastic	65 kDa	0.033	INF	0	5
2197	PREDICTED: probable S-sulfocysteine synthase, chloroplastic	?	0.0042	INF	0	8
2214	scopoletin glucosyltransferase	54 kDa	0.033	INF	0	5

Supplementary Table 4.6. Fold change of proteins that were upregulated by treatment SL42+SL48, relative to the control under salt-stressed conditions.

#	Identified Proteins (3518/3553)	Molecular Weight	Fisher's Exact Test	Fold Change	Control	SL42+ SL48
1	ribulose-1,5-bisphosphate carboxylase/oxygenase large subunit (chloroplast)	53 kDa	< 0.00010	1.1	5,949	6,659
8	Cluster of glycine dehydrogenase (decarboxylating), mitochondrial	115 kDa	0.00026	1.3	606	762
9	Cluster of glyceraldehyde-3-phosphate dehydrogenase A subunit	?	0.00022	1.3	540	688
9.2	PREDICTED: glyceraldehyde-3-phosphate dehydrogenase A, chloroplastic	?	< 0.00010	1.3	482	642
11	Cluster of chlorophyll a/b-binding protein	?	0.0063	1.2	650	773
15	Cluster of transketolase, chloroplastic	80 kDa	0.0096	1.2	549	655
29.3	ruBisCO large subunit-binding protein subunit beta, chloroplastic	66 kDa	0.018	INF	0	6
31.3	PREDICTED: elongation factor Tu, chloroplastic	?	0.047	1.2	311	369
54	Cluster of S-adenosylmethionine synthase	43 kDa	0.0047	1.3	241	314

60	Cluster of tubulin alpha-3 chain	50 kDa	0.026	1.2	234	290
87	Cluster of cell division cycle protein 48 homolog	90 kDa	0.016	1.3	162	212
96	Cluster of clathrin heavy chain	193 kDa	0.017	1.3	130	174
110	Cluster of 26S proteasome regulatory subunit 6A homolog	47 kDa	0.022	1.3	148	193
113	glycine--tRNA ligase, mitochondrial 1	81 kDa	0.016	1.3	128	172
115	chlorophyll a-b binding protein 6A, chloroplastic	27 kDa	0.033	1.3	145	186
136.2	lectin DB58	30 kDa	0.00031	INF	0	12
137	Cluster of PREDICTED: LOW QUALITY PROTEIN: UDP-D-apiose/UDP-D-xylose synthase 2	?	0.02	1.4	109	148
137.3	UDP-D-apiose/UDP-D-xylose synthase 2	43 kDa	0.028	1.4	69	98
144.3	NADP-dependent malic enzyme	71 kDa	0.0012	INF	0	10
150	adenosylhomocysteinase-like	53 kDa	0.039	1.2	215	264
152	Cluster of HSP90 superfamily protein isoform X1	93 kDa	0.02	1.3	127	169
152.2	endoplasmin homolog isoform X1	94 kDa	0.019	1.3	118	159
199.4	trifunctional UDP-glucose 4,6-dehydratase/UDP-4-keto-6-deoxy-D-glucose 3,5-epimerase/UDP-4-keto-L-rhamnose-reductase RHM1	74 kDa	0.018	INF	0	6
209.2	PREDICTED: auxin-binding protein ABP19a-like	?	< 0.00010	1.9	57	110
217.4	heat shock 70 kDa protein 14 isoform X1	94 kDa	0.04	1.7	23	39
226	Cluster of 2-oxoglutarate dehydrogenase, mitochondrial	116 kDa	0.042	1.4	72	99
235	Cluster of aconitate hydratase, cytoplasmic	107 kDa	0.035	1.3	117	153
255	Cluster of trigger factor-like protein TIG, Chloroplastic	61 kDa	0.011	1.5	64	97
256.2	aquaporin PIP2-7	31 kDa	0.038	1.6	33	52
266.5	14-3-3 protein SGF14p	30 kDa	0.033	2.4	8	19
272	Cluster of polyadenylate-binding protein RBP45 isoform X1	45 kDa	0.011	1.5	59	91
284	50S ribosomal protein L1, chloroplastic	38 kDa	< 0.00010	2.4	35	84
289	KS-type dehydrin SLTI629	?	0.0073	1.7	45	75
327	protoporphyrinogen oxidase 1, chloroplastic	59 kDa	0.041	1.4	61	86
335.3	patellin-3	63 kDa	0.033	2.4	8	19
335.4	patellin-3	62 kDa	0.019	2.7	7	19

353.2	UDP-glucose 6-dehydrogenase 4-like	?	0.016	2.2	12	27
370	Cluster of carbamoyl-phosphate synthase large chain, chloroplastic	127 kDa	0.044	1.8	18	32
379	soyasaponin III rhamnosyltransferase	54 kDa	0.049	1.4	52	74
394	Cluster of glutamate decarboxylase	56 kDa	0.018	1.5	62	92
415.2	60S ribosomal protein L13a-4	24 kDa	0.0044	2	25	50
431	Cluster of magnesium-protoporphyrin IX monomethyl ester [oxidative] cyclase, chloroplastic	49 kDa	0.038	1.5	37	57
442	Cluster of linoleate 13S-lipoxygenase 2-1, chloroplastic	104 kDa	0.0063	1.8	31	57
462	Cluster of protochlorophyllide reductase, chloroplastic	43 kDa	0.045	1.5	45	66
463	DNA-damage-repair/toleration protein DRT100-like precursor	40 kDa	0.04	1.6	34	53
487	Cluster of coatomer subunit gamma	99 kDa	0.011	1.8	26	48
503	succinate dehydrogenase [ubiquinone] flavoprotein subunit 1, mitochondrial	69 kDa	0.024	1.7	29	49
539	NADH dehydrogenase subunit 7 (chloroplast)	46 kDa	0.0013	2.1	27	57
567	photosystem I reaction center subunit psaK, chloroplastic	13 kDa	< 0.00010	3.2	18	57
570	Cluster of PREDICTED: aspartate-semialdehyde dehydrogenase	?	0.005	2.2	17	38
571	Cluster of NADH dehydrogenase [ubiquinone] iron-sulfur protein 1, mitochondrial	81 kDa	0.0016	2.2	24	52
596.2	GTP-binding protein SAR1A	22 kDa	0.009	INF	0	7
638	3-isopropylmalate dehydratase large subunit, chloroplastic	55 kDa	0.014	1.9	23	43
653	Cluster of DEAD-box ATP-dependent RNA helicase 3, chloroplastic	84 kDa	0.0097	2	22	43
656	fatty acid hydroperoxide lyase, chloroplastic	53 kDa	0.022	1.8	22	40
683	Cluster of SKP1-like protein 1A isoform X1	17 kDa	0.018	1.9	20	38
690	Cluster of topless-related protein 1 isoform X1	125 kDa	0.048	1.8	16	29
803	Cluster of 60S ribosomal protein L37-3	11 kDa	0.0047	2.6	11	29
825.2	importin subunit beta-1	96 kDa	0.037	1.7	22	38
853	Cluster of translocase of chloroplast 159, chloroplastic-like	133 kDa	0.018	2.1	15	31

859	15-cis-phytoene desaturase, chloroplastic/chromoplastic	63 kDa	0.011	2.1	16	34
864	probable bifunctional methylthioribulose-1-phosphate dehydratase/enolase-phosphatase E1	57 kDa	0.031	2.1	12	25
877	pyruvate dehydrogenase E1 component subunit beta-3, chloroplastic	44 kDa	0.044	1.8	18	32
926	Cluster of plastidial pyruvate kinase 2	64 kDa	0.029	2	14	28
937.2	40S ribosomal protein S17	16 kDa	0.0016	3.8	6	23
948	tripeptidyl-peptidase 2 isoform X1	146 kDa	0.016	2.4	10	24
970	Cluster of subtilisin-like protease SBT1.6	82 kDa	0.0063	2.8	9	25
979	Cluster of UDP-glucuronic acid decarboxylase 2	48 kDa	0.031	1.9	17	32
1018	D-3-phosphoglycerate dehydrogenase 2, chloroplastic	66 kDa	0.034	1.8	18	33
1032.2	anthranilate synthase alpha subunit 1, chloroplastic	65 kDa	0.0046	INF	0	8
1047	NAD-dependent malic enzyme 59 kDa isoform, mitochondrial	67 kDa	0.04	2.4	7	17
1057	Cluster of proline-rich protein precursor	13 kDa	0.0017	5.7	3	17
1061	argininosuccinate lyase, chloroplastic isoform X1	57 kDa	0.027	2.2	11	24
1063	Cluster of PREDICTED: zinc finger BED domain-containing protein DAYSLEEPER-like	?	0.028	2.3	9	21
1091.2	calcium-transporting ATPase 4, plasma membrane-type	114 kDa	0.046	3	4	12
1105	Cluster of dihydrolipoyllysine-residue acetyltransferase component 4 of pyruvate dehydrogenase complex, chloroplastic isoform X2	49 kDa	0.0082	2.4	12	29
1111	adenosylhomocysteinase	53 kDa	0.041	1.3	94	125
1141	PREDICTED: UBP1-associated protein 2B	?	0.021	4	3	12
1170	probable methionine--tRNA ligase isoform X2	90 kDa	0.048	2.5	6	15
1176	Cluster of THO complex subunit 4A	26 kDa	0.039	2.2	9	20
1179	histidine--tRNA ligase, chloroplastic/mitochondrial isoform X1	56 kDa	0.015	3	6	18
1208.2	NADPH--cytochrome P450 reductase	77 kDa	0.0023	INF	0	9

1226	photosystem I chlorophyll a/b-binding protein 5, chloroplastic	31 kDa	0.022	2.8	6	17
1243	succinate dehydrogenase [ubiquinone] iron-sulfur subunit 2, mitochondrial	31 kDa	0.04	2.4	7	17
1319	Cluster of alpha-amylase inhibitor/lipid transfer/seed storage family protein precursor	13 kDa	0.021	4	3	12
1338	PREDICTED: cystathionine gamma-synthase 1, chloroplastic	?	< 0.00010	INF	0	15
1361	Cluster of ubiquitin fusion degradation protein 1 homolog isoform X1	35 kDa	0.012	3.8	4	15
1373	Cluster of diphosphomevalonate decarboxylase MVD2, peroxisomal	46 kDa	0.011	3.4	5	17
1387	omega-3 fatty acid desaturase	51 kDa	0.012	3.8	4	15
1430	protein KINESIN LIGHT CHAIN-RELATED 1	63 kDa	0.021	4	3	12
1477	dihydrolipoyllysine-residue acetyltransferase component 1 of pyruvate dehydrogenase complex, mitochondrial	68 kDa	0.038	2.8	5	14
1527	Cluster of protein transport protein Sec24-like At4g32640	118 kDa	0.021	4	3	12
1561.1	serine/threonine-protein phosphatase PP2A catalytic subunit isoform X2	36 kDa	0.038	4.5	2	9
1616	KH domain-containing protein HEN4	58 kDa	0.03	3.2	4	13
1640	Cluster of aminoacyl tRNA synthase complex-interacting multifunctional protein 1	42 kDa	0.023	8	1	8
1640.1	aminoacyl tRNA synthase complex-interacting multifunctional protein 1	42 kDa	0.04	7	1	7
1682	Cluster of proteasome activator subunit 4	204 kDa	0.034	INF	0	5
1720	Cluster of dihydrolipoyllysine-residue acetyltransferase component 5 of pyruvate dehydrogenase complex, chloroplastic	48 kDa	0.048	2.5	6	15
1761	costars family protein	10 kDa	0.023	8	1	8
1777	mitochondrial Rho GTPase 1	72 kDa	0.007	10	1	10
1812	Cluster of PREDICTED: probable pectate lyase 8	?	0.034	INF	0	5
1824	4-diphosphocytidyl-2-C-methyl-D-erythritol kinase, chloroplastic/chromoplastic	44 kDa	0.04	7	1	7

1841	Cluster of magnesium chelatase subunit	?	0.023	8	1	8
1859	beta-ketoacyl-acyl carrier protein synthase III	42 kDa	0.034	INF	0	5
1890	probable linoleate 9S-lipoxygenase 5	98 kDa	0.034	INF	0	5
1900	Cluster of transcription initiation factor TFIID subunit 15b isoform X2	50 kDa	0.04	7	1	7
1917.2	phosphatidylinositol 3,4,5-trisphosphate 3-phosphatase and protein-tyrosine-phosphatase PTEN2A	69 kDa	0.034	INF	0	5
1934	pyruvate kinase 1, cytosolic isoform X1	58 kDa	0.047	1.9	13	25
2075	Cluster of probable inactive purple acid phosphatase 1 isoform X1	69 kDa	0.00016	INF	0	13
2120	multiprotein-bridging factor 1a	16 kDa	0.018	INF	0	6
2129	lysM domain-containing GPI-anchored protein 1	43 kDa	0.0012	INF	0	10
2197	PREDICTED: probable S-sulfocysteine synthase, chloroplastic	?	0.0046	INF	0	8
2256	chaperone protein dnaJ A6, chloroplastic	41 kDa	0.034	INF	0	5

Supplementary Table 4.7. Fold change of proteins that were upregulated by treatment Bj+SL42, relative to Bj (control) under optimal conditions.

#	Identified Proteins (3060/3077)	Molecular Weight	Fisher's Exact Test	Fold Change	Bj	Bj+ SL42
2	ribulose bisphosphate carboxylase small chain 1, chloroplastic	20 kDa	< 0.00010	1.3	1,203	1,512
7	Cluster of glycine dehydrogenase (decarboxylating), mitochondrial	115 kDa	0.013	1.2	728	845
9	Cluster of glyceraldehyde-3-phosphate dehydrogenase A subunit	?	0.0023	1.2	668	803
9.2	PREDICTED: glyceraldehyde-3-phosphate dehydrogenase A, chloroplastic	?	0.00081	1.2	596	735
36	Cluster of PREDICTED: triosephosphate isomerase, cytosolic	?	0.042	1.2	351	413
58	Cluster of S-adenosylmethionine synthase	43 kDa	0.026	1.2	213	265
83	Cluster of elongation factor 1-alpha	?	0.00019	1.5	145	220
97.2	ketol-acid reductoisomerase, chloroplastic	63 kDa	0.041	1.3	130	166

97.3	ketol-acid reductoisomerase, chloroplastic-like	?	0.034	1.3	126	163
117	Cluster of soyasapogenol B glucuronide galactosyltransferase-like	56 kDa	0.011	1.4	118	162
146	soyasaponin III rhamnosyltransferase	54 kDa	0.015	1.4	117	159
181	Cluster of isoflavone reductase homolog 2	34 kDa	< 0.00010	3.1	49	154
213.2	PREDICTED: auxin-binding protein ABP19a-like	?	0.0046	1.6	63	100
289	photosystem I reaction center subunit psaK, chloroplastic	13 kDa	0.011	1.7	39	65
291	50S ribosomal protein L1, chloroplastic	38 kDa	< 0.00010	3.3	15	49
339	PREDICTED: peptidyl-prolyl cis-trans isomerase 1-like	?	0.046	1.3	90	119
340	kunitz family trypsin and protease inhibitor protein precursor	24 kDa	0.013	1.6	49	77
357	Cluster of PREDICTED: multicystatin	?	0.0006	2.1	33	68
380	polyphenol oxidase A1, chloroplastic	70 kDa	0.00011	2.4	28	66
387	ferredoxin-A	15 kDa	0.002	2.1	24	51
389	40S ribosomal protein S3	26 kDa	0.04	1.6	31	49
390	PREDICTED: UDP-glucose flavonoid 3-O-glucosyltransferase 7-like	?	0.0065	1.7	38	66
408	Cluster of isopentenyl-diphosphate Delta-isomerase I	34 kDa	0.031	1.7	27	45
415	subtilisin-like protease Glyma18g48580 isoform X1	84 kDa	< 0.00010	2.9	18	53
423	Cluster of subtilisin-like protease Glyma18g48580	86 kDa	0.042	1.5	40	60
431	isoflavone reductase-like protein	34 kDa	0.027	1.6	39	61
449.2	PREDICTED: fumarylacetoacetase-like	?	0.023	1.9	20	37
516	Cluster of kunitz-type trypsin inhibitor KTI1-like	23 kDa	0.042	1.6	28	45
527	superoxide dismutase [Cu-Zn], chloroplastic	21 kDa	< 0.00010	2.5	28	70
693	Cluster of ribosomal protein L11 family protein	18 kDa	0.039	1.8	20	35
698.2	ectonucleotide pyrophosphatase/phosphodiesterase family member 3-like	?	0.017	INF	0	6
728	PREDICTED: acid phosphatase 1	?	0.0043	3.8	5	19
743	Cluster of 50S ribosomal protein L5, chloroplastic-like	29 kDa	0.026	2.2	11	24

808	Cluster of isoamylase 3, chloroplastic isoform X1	87 kDa	0.047	1.8	16	29
858	26S proteasome regulatory subunit 4 homolog A	50 kDa	0.046	2.2	8	18
915	Cluster of peptide methionine sulfoxide reductase B5	22 kDa	< 0.00010	6.5	4	26
915.1	peptide methionine sulfoxide reductase B5	22 kDa	0.00037	5.5	4	22
975.2	PREDICTED: lipid transfer protein EARLI 1-like	?	0.034	INF	0	5
990	succinate dehydrogenase [ubiquinone] iron-sulfur subunit 2, mitochondrial	31 kDa	0.046	2.2	8	18
1024	Cluster of 50S ribosomal protein L18, chloroplastic	18 kDa	0.00061	14	1	14
1075	PLAT domain-containing protein 3	21 kDa	0.012	2.9	7	20
1083	40S ribosomal protein S17	16 kDa	0.012	3.8	4	15
1125	Cluster of 50S ribosomal protein L4, chloroplastic	34 kDa	0.0011	13	1	13
1203	UDP-glycosyltransferase 79A6	52 kDa	0.0045	INF	0	8
1261	uridine 5'-monophosphate synthase-like	?	0.00047	8.5	2	17
1273	omega-amidase, chloroplastic	39 kDa	0.00015	INF	0	13
1350	stress-induced protein H4	17 kDa	0.0012	INF	0	10
1426	stress-induced protein SAM22	17 kDa	0.0088	INF	0	7
1442	Cluster of cationic peroxidase 1	34 kDa	0.00061	14	1	14
1475	PREDICTED: stellacyanin-like	?	0.022	8	1	8
1500	Cluster of 40S ribosomal protein S7	22 kDa	0.037	4.5	2	9
1503	UDP-glycosyltransferase 74G1	54 kDa	0.022	5	2	10
1579	protein PELPK1	39 kDa	0.033	3.7	3	11
1612	heparanase-like protein 3	59 kDa	0.022	8	1	8
1626	chaperone protein dnaJ A6, chloroplastic isoform X1	47 kDa	0.031	2.2	10	22
1656	calreticulin-3	50 kDa	0.034	INF	0	5
1702	phospholipase A1-Igamma2, chloroplastic isoform X1	56 kDa	0.034	INF	0	5
1743	chaperone protein dnaJ A6, chloroplastic	47 kDa	0.00019	7	3	21
1754	protein CHLORORESPIRATORY REDUCTION 7, chloroplastic	17 kDa	0.034	INF	0	5
1755	mitochondrial import inner membrane translocase subunit TIM10	10 kDa	0.034	INF	0	5
1827	probable splicing factor 3A subunit 1	89 kDa	0.0045	INF	0	8

2026	BSP domain-containing protien precursor	25 kDa	0.017	INF	0	6

Supplementary Table 4.8. Fold change of proteins that were upregulated by treatment Bj+SL48, relative to Bj (control) under optimal conditions.

#	Identified Proteins (3060/3077)	Molecular Weight	Fisher's Exact Test	Fold Change	Bj	Bj+ SL48
2	ribulose bisphosphate carboxylase small chain 1, chloroplastic	20 kDa	< 0.00010	1.4	1,203	1,654
3	Cluster of linoleate 9S-lipoxygenase-4	?	< 0.00010	1.2	1,298	1,616
4.1	ribulose bisphosphate carboxylase/oxygenase activase, chloroplastic-like	49 kDa	0.028	1.2	952	1,109
7	Cluster of glycine dehydrogenase (decarboxylating), mitochondrial	115 kDa	< 0.00010	1.3	728	943
9	Cluster of glyceraldehyde-3-phosphate dehydrogenase A subunit	?	< 0.00010	1.8	668	1,214
9.2	PREDICTED: glyceraldehyde-3-phosphate dehydrogenase A, chloroplastic	?	< 0.00010	1.9	596	1,156
10.2	glutamine synthetase precursor	?	0.035	1.2	397	481
23	Cluster of catalase	57 kDa	0.039	1.2	407	491
26	Cluster of PREDICTED: gamma-glutamyl hydrolase isoform X1	?	0.026	1.2	373	458
26.2	gamma-glutamyl hydrolase precursor	?	0.0053	1.3	287	376
36	Cluster of PREDICTED: triosephosphate isomerase, cytosolic	?	0.0078	1.3	351	447
36.2	triosephosphate isomerase isoform X1	27 kDa	0.048	1.2	284	348
37	Cluster of serine glyoxylate aminotransferase 3 isoform X1	44 kDa	0.032	1.2	284	353
58	Cluster of S-adenosylmethionine synthase	43 kDa	0.001	1.4	213	301
61.1	3'-hydroxy-N-methyl-(S)-coclaurine 4'-O-methyltransferase-like	42 kDa	0.035	1.3	183	235
75	Cluster of adenosylhomocysteinase-like	53 kDa	0.017	1.3	210	274
83	Cluster of elongation factor 1-alpha	?	< 0.00010	1.7	145	251
97.3	ketol-acid reductoisomerase, chloroplastic-like	?	0.049	1.3	126	165
116	Cluster of chlorophyll a-b binding protein, chloroplastic	29 kDa	0.011	1.4	149	205

117	Cluster of soyasapogenol B glucuronide galactosyltransferase-like	56 kDa	< 0.00010	1.7	118	196
124	lipoxygenase-9	?	0.027	1.3	239	303
146	soyasaponin III rhamnosyltransferase	54 kDa	0.002	1.5	117	177
181	Cluster of isoflavone reductase homolog 2	34 kDa	< 0.00010	3.5	49	172
213.2	PREDICTED: auxin-binding protein ABP19a-like	?	< 0.00010	2.3	63	148
282	protoporphyrinogen oxidase 1, chloroplastic	59 kDa	0.0058	1.7	54	90
283	Cluster of polyadenylate-binding protein RBP45 isoform X1	45 kDa	0.023	1.6	44	70
289	photosystem I reaction center subunit psaK, chloroplastic	13 kDa	< 0.00010	2.8	39	109
291	50S ribosomal protein L1, chloroplastic	38 kDa	< 0.00010	4.4	15	66
337	Cluster of linoleate 13S-lipoxygenase 2-1, chloroplastic	104 kDa	0.012	1.7	46	76
348.2	linoleate 9S-lipoxygenase	97 kDa	0.0013	1.9	47	87
357	Cluster of PREDICTED: multicystatin	?	0.00013	2.3	33	75
367	ribosomal protein S3 (chloroplast)	25 kDa	0.021	1.7	33	56
380	polyphenol oxidase A1, chloroplastic	70 kDa	< 0.00010	2.5	28	71
387	ferredoxin-A	15 kDa	< 0.00010	2.9	24	70
389	40S ribosomal protein S3	26 kDa	0.0014	2.1	31	64
390	PREDICTED: UDP-glucose flavonoid 3-O-glucosyltransferase 7-like	?	0.0024	1.9	38	72
408	Cluster of isopentenyl-diphosphate Delta-isomerase I	34 kDa	0.0045	2	27	54
415	subtilisin-like protease Glyma18g48580 isoform X1	84 kDa	0.003	2.3	18	42
419	KS-type dehydrin SLTI629	?	< 0.00010	4.1	9	37
449.2	PREDICTED: fumarylacetoacetase-like	?	0.05	1.8	20	35
482.2	iron-superoxide dismutase	?	0.034	1.9	16	31
486	probable carboxylesterase 2	43 kDa	0.049	1.7	26	43
506	hydroxyphenylpyruvate reductase-like	?	0.012	1.9	26	49
508	Cluster of proline-rich protein precursor	13 kDa	< 0.00010	19	6	114
516	Cluster of kunitz-type trypsin inhibitor KTI1-like	23 kDa	0.023	1.8	28	49
527	superoxide dismutase [Cu-Zn], chloroplastic	21 kDa	0.00027	2.3	28	65

536	Cluster of D-3-phosphoglycerate dehydrogenase 2, chloroplastic	66 kDa	0.038	1.6	32	52
558	15-cis-phytoene desaturase, chloroplastic/chromoplastic	63 kDa	0.039	1.7	26	44
599	Cluster of bifunctional monothiol glutaredoxin-S16, chloroplastic	32 kDa	0.03	2	15	30
605	succinate dehydrogenase [ubiquinone] flavoprotein subunit 1, mitochondrial	69 kDa	0.033	1.8	21	38
697	ATPase ARSA1	44 kDa	0.027	1.9	19	36
698.2	ectonucleotide pyrophosphatase/phosphodiesterase family member 3-like	?	0.0099	INF	0	7
728	PREDICTED: acid phosphatase 1	?	0.0034	4	5	20
743	Cluster of 50S ribosomal protein L5, chloroplastic-like	29 kDa	0.00018	3.5	11	38
768	Cluster of DEAD-box ATP-dependent RNA helicase 3, chloroplastic	84 kDa	0.042	2	13	26
806	UDP-glucosyl transferase 73B2	53 kDa	0.036	2	14	28
839	PREDICTED: 30S Ribosomal protein S1 isoform X1	?	0.028	2.3	10	23
858	26S proteasome regulatory subunit 4 homolog A	50 kDa	0.0012	3.5	8	28
877.3	probable aldo-keto reductase 1	?	0.0051	INF	0	8
897	linoleate 9S-lipoxygenase 1	98 kDa	0.0049	1.9	30	58
915	Cluster of peptide methionine sulfoxide reductase B5	22 kDa	< 0.00010	6.5	4	26
917	malonyl-CoA:isoflavone 7-O-glucoside-6"-O-malonyltransferase	52 kDa	0.038	2.2	10	22
975.2	PREDICTED: lipid transfer protein EARLI 1-like	?	< 0.00010	INF	0	29
1024	Cluster of 50S ribosomal protein L18, chloroplastic	18 kDa	< 0.00010	19	1	19
1038	multiple organellar RNA editing factor 9-like	25 kDa	0.039	2.4	8	19
1069	indole-3-glycerol phosphate synthase, chloroplastic	43 kDa	0.0083	3.6	5	18
1075	PLAT domain-containing protein 3	21 kDa	0.022	2.7	7	19
1080.2	membrane steroid-binding protein 1	24 kDa	0.034	3.2	4	13
1083	40S ribosomal protein S17	16 kDa	0.0022	4.8	4	19
1100	Cluster of PREDICTED: glucan endo-1,3-beta-glucosidase	?	0.037	2.7	6	16
1100.2	glucan endo-1,3-beta-glucosidase-like	37 kDa	0.037	INF	0	5
1125	Cluster of 50S ribosomal protein L4, chloroplastic	34 kDa	0.00012	17	1	17

1162	Cluster of PREDICTED: 1,2-dihydroxy-3-keto-5-methylthiopentene dioxygenase 2	?	0.0057	5	3	15
1203	UDP-glycosyltransferase 79A6	52 kDa	0.00036	INF	0	12
1261	uridine 5'-monophosphate synthase-like	?	0.0054	6.5	2	13
1273	omega-amidase, chloroplastic	39 kDa	< 0.00010	INF	0	15
1314	glutathione hydrolase 1	67 kDa	0.0093	4.7	3	14
1337	probable carotenoid cleavage dioxygenase 4, chloroplastic	65 kDa	0.029	3	5	15
1350	stress-induced protein H4	17 kDa	< 0.00010	INF	0	19
1425.3	polyphenol oxidase A1, chloroplastic	70 kDa	0.0099	INF	0	7
1426	stress-induced protein SAM22	17 kDa	< 0.00010	INF	0	21
1428	probable endo-1,3(4)-beta-glucanase ARB_01444	73 kDa	0.034	3.2	4	13
1442	Cluster of cationic peroxidase 1	34 kDa	0.0044	11	1	11
1445	beta-amyrin 24-hydroxylase	?	0.0091	6	2	12
1475	PREDICTED: stellacyanin-like	?	0.0079	10	1	10
1500	Cluster of 40S ribosomal protein S7	22 kDa	0.025	5	2	10
1503	UDP-glycosyltransferase 74G1	54 kDa	0.042	4.5	2	9
1517	Cluster of ATP-dependent Clp protease proteolytic subunit 3, chloroplastic	35 kDa	0.043	7	1	7
1517.2	ATP-dependent Clp protease proteolytic subunit 3, chloroplastic	35 kDa	0.0099	INF	0	7
1551	glutathione S-transferase GST 23	?	0.043	7	1	7
1624	probable aldehyde dehydrogenase isoform X1	61 kDa	0.0014	INF	0	10
1629	PREDICTED: syntaxin-112-like isoform X2	?	0.037	INF	0	5
1647	Cluster of ABC transporter F family member 1	66 kDa	0.025	8	1	8
1656	calreticulin-3	50 kDa	0.0051	INF	0	8
1674	probable glucan 1,3-alpha-glucosidase	104 kDa	0.043	7	1	7
1702	phospholipase A1-Igamma2, chloroplastic isoform X1	56 kDa	0.0099	INF	0	7
1725	chloroplastic import inner membrane translocase subunit TIM22-2	25 kDa	0.0099	INF	0	7
1740	50S ribosomal protein L22, chloroplastic	?	0.0051	INF	0	8
1743	chaperone protein dnaJ A6, chloroplastic	47 kDa	0.0021	5.7	3	17

1783	rhodanese-like domain-containing protein 11, chloroplastic	32 kDa	0.019	INF	0	6
1825	Cluster of 50S ribosomal protein L6, chloroplastic	25 kDa	0.0099	INF	0	7
1846	Cluster of glutamine--tRNA ligase	90 kDa	0.0051	INF	0	8
1846.2	LOW QUALITY PROTEIN: glutamine--tRNA ligase	90 kDa	0.0051	INF	0	8
1977	aquaporin PIP2-10	30 kDa	0.033	2.3	9	21
2026	BSP domain-containing protien precursor	25 kDa	0.0026	INF	0	9

Supplementary Table 4.9. Fold change of proteins that were upregulated by treatment Bj+SL42+SL48, relative to Bj (control) under optimal conditions.

#	Identified Proteins (3060/3077)	Molecular Weight	Fisher's Exact Test	Fold Change	Bj	Bj+ SL42+ SL48
1	ribulose-1,5-bisphosphate carboxylase/oxygenase large subunit (chloroplast)	53 kDa	0.037	1.1	7,771	8,484
2	ribulose bisphosphate carboxylase small chain 1, chloroplastic	20 kDa	< 0.00010	1.3	1,203	1,552
3	Cluster of linoleate 9S-lipoxygenase-4	?	0.003	1.2	1,298	1,530
7	Cluster of glycine dehydrogenase (decarboxylating), mitochondrial	115 kDa	0.011	1.2	728	868
9	Cluster of glyceraldehyde-3-phosphate dehydrogenase A subunit	?	< 0.00010	1.6	668	1,049
9.2	PREDICTED: glyceraldehyde-3-phosphate dehydrogenase A, chloroplastic	?	< 0.00010	1.7	596	999
10.2	glutamine synthetase precursor	?	0.03	1.2	397	480
12	Cluster of transketolase, chloroplastic	80 kDa	0.031	1.2	679	796
23.4	catalase-3	57 kDa	0.039	1.3	186	236
30.7	probable mediator of RNA polymerase II transcription subunit 37c isoform X2	69 kDa	0.00068	INF	0	11
36	Cluster of PREDICTED: triosephosphate isomerase, cytosolic	?	0.035	1.2	351	426
58	Cluster of S-adenosylmethionine synthase	43 kDa	0.036	1.3	213	268
61.1	3'-hydroxy-N-methyl-(S)-coclaurine 4'-O-methyltransferase-like	42 kDa	0.027	1.3	183	236
75	Cluster of adenosylhomocysteinase-like	53 kDa	0.038	1.3	210	264
83	Cluster of elongation factor 1-alpha	?	0.0014	1.5	145	213

116	Cluster of chlorophyll a-b binding protein, chloroplastic	29 kDa	0.048	1.3	149	191
117	Cluster of soyasapogenol B glucuronide galactosyltransferase-like	56 kDa	0.015	1.4	118	164
181	Cluster of isoflavone reductase homolog 2	34 kDa	< 0.00010	3.6	49	174
181.1	isoflavone reductase homolog 2	34 kDa	< 0.00010	3.6	49	174
187	Cluster of pyrophosphate-energized vacuolar membrane proton pump	80 kDa	0.04	1.4	85	117
209	cysteine proteinase 15A	40 kDa	0.021	1.5	51	79
213.2	PREDICTED: auxin-binding protein ABP19a-like	?	0.00057	1.8	63	112
271.2	protochlorophyllide reductase, chloroplastic	43 kDa	0.0019	3.8	6	23
282	protoporphyrinogen oxidase 1, chloroplastic	59 kDa	0.041	1.5	54	79
283	Cluster of polyadenylate-binding protein RBP45 isoform X1	45 kDa	0.0048	1.8	44	77
289	photosystem I reaction center subunit psaK, chloroplastic	13 kDa	< 0.00010	2.2	39	86
291	50S ribosomal protein L1, chloroplastic	38 kDa	< 0.00010	4.9	15	73
321	Cluster of carbamoyl-phosphate synthase large chain, chloroplastic	127 kDa	0.037	1.7	23	40
321.1	carbamoyl-phosphate synthase large chain, chloroplastic	127 kDa	0.027	1.8	22	40
348.2	linoleate 9S-lipoxygenase	97 kDa	0.003	1.8	47	83
357	Cluster of PREDICTED: multicystatin	?	0.0036	1.9	33	63
373	putative plastocyanin	17 kDa	0.029	1.4	98	135
380	polyphenol oxidase A1, chloroplastic	70 kDa	0.00013	2.4	28	67
387	ferredoxin-A	15 kDa	< 0.00010	3.7	24	89
389	40S ribosomal protein S3	26 kDa	0.00039	2.2	31	68
390	PREDICTED: UDP-glucose flavonoid 3-O-glucosyltransferase 7-like	?	0.041	1.6	38	59
408	Cluster of isopentenyl-diphosphate Delta-isomerase I	34 kDa	< 0.00010	2.5	27	68
408.1	isopentenyl-diphosphate Delta-isomerase I	34 kDa	< 0.00010	2.5	27	68
415	subtilisin-like protease Glyma18g48580 isoform X1	84 kDa	0.002	2.4	18	43
419	KS-type dehydrin SLTI629	?	< 0.00010	6	9	54
480.3	PREDICTED: probable S-sulfocysteine synthase, chloroplastic	?	< 0.00010	INF	0	14

506	hydroxyphenylpyruvate reductase-like	?	0.018	1.8	26	47
508	Cluster of proline-rich protein precursor	13 kDa	< 0.00010	6.3	6	38
527	superoxide dismutase [Cu-Zn], chloroplastic	21 kDa	0.00018	2.4	28	66
536.1	D-3-phosphoglycerate dehydrogenase 2, chloroplastic	66 kDa	0.039	1.6	30	49
599	Cluster of bifunctional monothiol glutaredoxin-S16, chloroplastic	32 kDa	0.038	1.9	15	29
599.2	PREDICTED: bifunctional monothiol glutaredoxin-S16, chloroplastic-like	?	0.031	2.2	11	24
601	ribonuclease 2	30 kDa	0.043	2.1	11	23
605	succinate dehydrogenase [ubiquinone] flavoprotein subunit 1, mitochondrial	69 kDa	0.031	1.8	21	38
607	PREDICTED: aspartate-semialdehyde dehydrogenase	?	0.011	2	21	42
697	ATPase ARSA1	44 kDa	0.034	1.8	19	35
722	glutathione S-transferase L3	27 kDa	0.047	1.8	20	35
728	PREDICTED: acid phosphatase 1	?	0.002	4.2	5	21
743	Cluster of 50S ribosomal protein L5, chloroplastic-like	29 kDa	0.0027	2.8	11	31
760	NAD(P)H-quinone oxidoreductase subunit N, chloroplastic	26 kDa	0.03	2.1	13	27
784	20 kDa chaperonin, chloroplastic	26 kDa	0.046	1.7	26	43
798	peroxisomal 3-ketoacyl-CoA thiolase	49 kDa	0.032	1.9	16	31
880	ATPase subunit 8 (mitochondrion)	18 kDa	0.042	2.8	5	14
915	Cluster of peptide methionine sulfoxide reductase B5	22 kDa	< 0.00010	6.2	4	25
948.3	carbonic anhydrase 2	28 kDa	0.029	2	15	30
975.2	PREDICTED: lipid transfer protein EARLI 1-like	?	0.00018	INF	0	13
985	Cluster of eukaryotic translation initiation factor	86 kDa	0.016	2.6	9	23
1024	Cluster of 50S ribosomal protein L18, chloroplastic	18 kDa	0.00072	14	1	14
1083	40S ribosomal protein S17	16 kDa	0.0033	4.5	4	18
1100	Cluster of PREDICTED: glucan endo-1,3-beta-glucosidase	?	0.025	2.8	6	17
1125	Cluster of 50S ribosomal protein L4, chloroplastic	34 kDa	0.0013	13	1	13
1162	Cluster of PREDICTED: 1,2-dihydroxy-3-keto-5-methylthiopentene dioxygenase 2	?	0.037	3.7	3	11

1203	UDP-glycosyltransferase 79A6	52 kDa	0.0096	INF	0	7
1231	protein disulfide isomerase-like 1-4	65 kDa	0.043	1.9	16	30
1248.2	peroxisomal and mitochondrial division factor 2	35 kDa	0.042	7	1	7
1261	uridine 5'-monophosphate synthase-like	?	0.025	5	2	10
1273	omega-amidase, chloroplastic	39 kDa	0.00018	INF	0	13
1309	Cluster of PREDICTED: zinc finger BED domain-containing protein DAYSLEEPER-like	?	0.042	2.8	5	14
1350	stress-induced protein H4	17 kDa	< 0.00010	INF	0	21
1355	methionine S-methyltransferase isoform X2	121 kDa	0.037	3.7	3	11
1369	anthocyanidin reductase	38 kDa	0.037	3.7	3	11
1425.3	polyphenol oxidase A1, chloroplastic	70 kDa	0.0096	INF	0	7
1426	stress-induced protein SAM22	17 kDa	< 0.00010	INF	0	18
1442	Cluster of cationic peroxidase 1	34 kDa	0.014	9	1	9
1461.1	heterogeneous nuclear ribonucleoprotein A3	39 kDa	0.042	2.8	5	14
1475	PREDICTED: stellacyanin-like	?	0.00072	14	1	14
1500	Cluster of 40S ribosomal protein S7	22 kDa	0.041	4.5	2	9
1551	glutathione S-transferase GST 23	?	0.042	7	1	7
1626	chaperone protein dnaJ A6, chloroplastic isoform X1	47 kDa	0.027	2.3	10	23
1655	chaperonin CPN60-like 2, mitochondrial	61 kDa	0.036	2.7	6	16
1702	phospholipase A1-Igamma2, chloroplastic isoform X1	56 kDa	0.0096	INF	0	7
1725	chloroplastic import inner membrane translocase subunit TIM22-2	25 kDa	0.019	INF	0	6
1740	50S ribosomal protein L22, chloroplastic	?	0.019	INF	0	6
1743	chaperone protein dnaJ A6, chloroplastic	47 kDa	< 0.00010	7.7	3	23
1749	subtilisin-like protease SBT1.6	82 kDa	0.0096	INF	0	7
1761	galactinol--sucrose galactosyltransferase	84 kDa	0.036	INF	0	5
1794	costars family protein	10 kDa	0.019	INF	0	6
1805	REF/SRPP-like protein At1g67360 isoform X2	26 kDa	0.0096	INF	0	7
1857	protein transport protein SEC23	84 kDa	0.042	7	1	7
1900	PREDICTED: beta-amyrin synthase isoform X1	?	0.036	INF	0	5
1963	SAL1 phosphatase	43 kDa	0.036	INF	0	5

1966	24 kDa seed coat protein precursor	25 kDa	0.036	INF	0	5
2035.2	UDP-glucuronic acid decarboxylase 1	48 kDa	0.036	INF	0	5

Supplementary Table 4.10. Fold change of proteins that were upregulated by treatment Bj+SL42, relative to Bj (control) under salt-stressed conditions.

#	Identified Proteins (3583/3610)	Molecular Weight	Fisher's Exact Test	Fold Change	Bj	Bj+ SL42
1	ribulose-1,5-bisphosphate carboxylase/oxygenase large subunit (chloroplast)	53 kDa	< 0.00010	1.2	6,327	7,552
3	ribulose bisphosphate carboxylase small chain 4, chloroplastic	20 kDa	< 0.00010	1.4	985	1,361
5	Cluster of ribulose bisphosphate carboxylase/oxygenase activase, chloroplastic-like	49 kDa	0.0087	1.1	1,153	1,300
8	Cluster of glycine dehydrogenase (decarboxylating), mitochondrial	115 kDa	0.00013	1.2	653	810
9	Cluster of glyceraldehyde-3-phosphate dehydrogenase A subunit	?	< 0.00010	1.3	747	972
9.2	PREDICTED: glyceraldehyde-3-phosphate dehydrogenase A, chloroplastic	?	< 0.00010	1.3	701	922
17	Cluster of catalase	57 kDa	0.00094	1.3	386	489
30.3	ruBisCO large subunit-binding protein subunit beta, chloroplastic	66 kDa	0.032	3.7	3	11
54.1	PREDICTED: triosephosphate isomerase, cytosolic	?	0.043	1.2	306	359
57	Cluster of tubulin alpha-3 chain	50 kDa	0.02	1.2	243	298
105	Cluster of NADP-dependent malic enzyme	65 kDa	0.0034	1.4	144	199
184	Cluster of aconitate hydratase, cytoplasmic	107 kDa	0.026	1.3	152	193
198	Cluster of iron-superoxide dismutase	?	0.002	1.6	71	113
198.1	iron-superoxide dismutase	?	0.005	1.6	61	96
198.2	superoxide dismutase [Fe], chloroplastic precursor	28 kDa	0.0028	1.8	39	70
238	harpin binding protein 1	28 kDa	0.048	1.3	87	114
299.2	caffeic acid 3-O-methyltransferase-like	40 kDa	0.023	1.5	51	76
322	photosystem I reaction center subunit psaK, chloroplastic	13 kDa	0.0061	1.6	57	90
332	Cluster of carbamoyl-phosphate synthase large chain, chloroplastic	127 kDa	0.042	1.6	26	42
350	Cluster of DEAD-box ATP-dependent RNA helicase 56	48 kDa	0.036	1.5	44	65

438	Cluster of 1-aminocyclopropane-1-carboxylate oxidase	36 kDa	0.021	1.6	37	59
470	Cluster of T-complex protein 1 subunit eta	60 kDa	0.046	1.5	36	54
532	Cluster of PREDICTED: 12-oxophytodienoate reductase 3	?	0.046	1.5	36	54
532.2	12-oxophytodienoate reductase 3	44 kDa	0.047	1.5	32	49
532.3	12-oxophytodienoate reductase 3	43 kDa	0.027	3.2	4	13
553	PREDICTED: UDP-glucose flavonoid 3-O-glucosyltransferase 7-like	?	0.00076	2.4	19	46
579	Cluster of 15-cis-phytoene desaturase, chloroplastic/chromoplastic	63 kDa	0.047	1.6	24	39
591	ferredoxin-A	15 kDa	< 0.00010	3.1	24	74
632	abscisate beta-glucosyltransferase	53 kDa	0.0064	2	20	41
641	Cluster of ferritin	?	0.018	1.5	63	92
680	Cluster of ferritin-4, chloroplastic	28 kDa	0.011	1.6	44	71
709	Cluster of pyrophosphate--fructose 6-phosphate 1-phosphotransferase subunit alpha	68 kDa	0.035	1.8	20	35
739	polygalacturonase inhibitor 1-like protein precursor	38 kDa	0.00017	3.5	10	35
756	Cluster of proline-rich protein precursor	13 kDa	< 0.00010	3.3	14	46
758	UDP-sulfoquinovose synthase, chloroplastic	53 kDa	0.012	2	18	36
770	Cluster of probable 3-hydroxyisobutyrate dehydrogenase-like 1, mitochondrial	35 kDa	0.0049	2.5	12	30
784	dihydropyrimidinase	57 kDa	0.042	1.7	19	33
803.2	PREDICTED: lipid transfer protein EARLI 1-like	?	0.00014	INF	0	13
824	PREDICTED: ferritin-2, chloroplastic	?	0.0012	1.8	50	88
906	UDP-glycosyltransferase 84B2	59 kDa	0.0098	3.4	5	17
979.2	putative glucose-6-phosphate 1-epimerase	36 kDa	0.0015	4.2	5	21
991	cucumisin	77 kDa	0.047	1.6	24	39
1091.2	MFP1 attachment factor 1	16 kDa	0.012	4.3	3	13
1168	glucose-6-phosphate 1-dehydrogenase, cytoplasmic isoform	59 kDa	0.023	2.1	13	27
1219	ectonucleotide pyrophosphatase/phosphodiesterase family member 3	51 kDa	0.039	1.8	18	32

1241	NAD(P)H-quinone oxidoreductase subunit N, chloroplastic	26 kDa	0.0073	6	2	12
1273	probable aldo-keto reductase 1	?	< 0.00010	2.8	18	50
1307	anthocyanidin 3-O-glucosyltransferase 7	50 kDa	0.0073	6	2	12
1428	malonyl-CoA:isoflavone 7-O-glucoside-6"-O-malonyltransferase	52 kDa	0.0024	7	2	14
1471.2	starch synthase IIa-1	85 kDa	0.0043	INF	0	8
1555	15-cis-phytoene desaturase, chloroplastic/chromoplastic	52 kDa	0.013	5.5	2	11
1631	probable aldehyde dehydrogenase isoform X1	61 kDa	0.021	8	1	8
1749	probable aldo-keto reductase 1	37 kDa	< 0.00010	7	4	28
2002	probable carboxylesterase 8	36 kDa	0.033	INF	0	5
2032	probable carotenoid cleavage dioxygenase 4, chloroplastic	65 kDa	0.0043	INF	0	8
2053.2	glutamate synthase [NADH], amyloplastic isoform X1	240 kDa	0.017	INF	0	6
2101	stress-induced protein SAM22	17 kDa	0.05	3.3	3	10
2335	BURP domain protein GmRD22 isoform X1	34 kDa	0.033	INF	0	5

Supplementary Table 4.11. Fold change of proteins that were upregulated by treatment Bj+SL48, relative to Bj (control) under salt-stressed conditions.

#	Identified Proteins (3583/3610)	Molecular Weight	Fisher's Exact Test	Fold Change	Bj	Bj+ SL48
1	ribulose-1,5-bisphosphate carboxylase/oxygenase large subunit (chloroplast)	53 kDa	< 0.00010	1.2	6,327	7,461
3	ribulose bisphosphate carboxylase small chain 4, chloroplastic	20 kDa	< 0.00010	1.5	985	1,482
5	Cluster of ribulose bisphosphate carboxylase/oxygenase activase, chloroplastic-like	49 kDa	0.00016	1.2	1,153	1,354
8	Cluster of glycine dehydrogenase (decarboxylating), mitochondrial	115 kDa	0.016	1.1	653	746
9	Cluster of glyceraldehyde-3-phosphate dehydrogenase A subunit	?	0.011	1.1	747	853
9.2	PREDICTED: glyceraldehyde-3-phosphate dehydrogenase A, chloroplastic	?	0.015	1.1	701	798
11	Cluster of glutamine synthetase precursor isoform X1	48 kDa	< 0.00010	1.3	529	712
17	Cluster of catalase	57 kDa	< 0.00010	1.3	386	514
18	Cluster of peroxisomal glycolate oxidase isoform X1	41 kDa	0.02	1.1	573	656

18.2	peroxisomal (S)-2-hydroxy-acid oxidase GLO1-like	41 kDa	0.038	1.1	464	529
18.3	peroxisomal (S)-2-hydroxy-acid oxidase GLO1-like isoform X2	41 kDa	0.047	1.1	453	514
22	lipoxygenase	96 kDa	0.012	1.1	643	739
33	Cluster of tubulin beta chain	50 kDa	0.034	1.2	405	467
57	Cluster of tubulin alpha-3 chain	50 kDa	0.0088	1.3	243	304
86.1	glutamate decarboxylase	56 kDa	0.035	1.3	91	120
87.9	plasma membrane ATPase	104 kDa	< 0.00010	INF	0	26
105	Cluster of NADP-dependent malic enzyme	65 kDa	0.029	1.3	144	182
123.2	phosphoenolpyruvate carboxylase 4	118 kDa	0.027	1.7	24	41
143	Cluster of alpha-xylosidase 1	103 kDa	0.046	1.3	113	143
145.2	protein disulfide-isomerase	56 kDa	0.039	1.3	96	125
146.2	heme-binding protein 2	26 kDa	0.028	1.3	94	125
157	seed linoleate 9S-lipoxygenase	97 kDa	0.012	1.2	278	340
161	PREDICTED: aldehyde dehydrogenase family 2 member B4, mitochondrial	?	0.022	1.3	115	151
171.2	PREDICTED: auxin-binding protein ABP19a-like	?	0.025	1.3	108	142
184.2	aconitate hydratase, cytoplasmic	107 kDa	0.03	1.4	78	106
204	photosystem II protein H (chloroplast)	8 kDa	0.031	1.3	92	122
209.4	trifunctional UDP-glucose 4,6-dehydratase/UDP-4-keto-6-deoxy-D-glucose 3,5-epimerase/UDP-4-keto-L-rhamnose-reductase RHM1	74 kDa	0.023	2.2	11	24
218.4	polyadenylate-binding protein RBP47	47 kDa	0.033	INF	0	5
222	soyasaponin III rhamnosyltransferase	54 kDa	0.00093	1.6	75	121
243	Cluster of 4-alpha-glucanotransferase DPE2	111 kDa	0.016	1.4	69	99
259.4	protein THYLAKOID FORMATION1, chloroplastic isoform X1	33 kDa	0.0021	INF	0	9
291	glucose-6-phosphate 1-dehydrogenase, chloroplastic	67 kDa	0.002	1.7	52	88
302.2	probable UDP-arabinopyranose mutase 1	42 kDa	0.011	1.5	55	84
322	photosystem I reaction center subunit psaK, chloroplastic	13 kDa	0.037	1.4	57	80
330	Cluster of calvin cycle protein CP12-2, chloroplastic	14 kDa	0.013	1.4	72	104
332	Cluster of carbamoyl-phosphate synthase large chain, chloroplastic	127 kDa	0.05	1.6	26	41

338.2	phi class glutathione S-transferase	25 kDa	0.037	1.5	33	51
339	9-divinyl ether synthase-like	54 kDa	0.047	1.4	48	68
435.1	probable glutathione S-transferase	26 kDa	0.047	1.4	48	68
438	Cluster of 1-aminocyclopropane-1-carboxylate oxidase	36 kDa	0.0096	1.7	37	62
537	Cluster of gibberellin-regulated protein 6 precursor	13 kDa	0.028	1.6	28	46
553	PREDICTED: UDP-glucose flavonoid 3-O-glucosyltransferase 7-like	?	< 0.00010	2.9	19	56
555	Cluster of adenylosuccinate synthetase 2, chloroplastic	53 kDa	0.05	1.6	26	41
579	Cluster of 15-cis-phytoene desaturase, chloroplastic/chromoplastic	63 kDa	0.0011	2.2	24	52
600	Cluster of ubiquitin-activating enzyme E1 1	124 kDa	0.034	1.8	17	31
638	Cluster of PREDICTED: topless-related protein 3-like isoform X1	?	0.0013	2.5	15	38
638.2	protein TOPLESS	125 kDa	0.041	2.2	8	18
638.3	topless-related protein 4 isoform X2	125 kDa	0.011	3.8	4	15
638.4	topless-related protein 3	124 kDa	0.012	4.3	3	13
716	membrane primary amine oxidase	28 kDa	0.023	1.6	32	52
739	polygalacturonase inhibitor 1-like protein precursor	38 kDa	< 0.00010	4.5	10	45
756	Cluster of proline-rich protein precursor	13 kDa	0.0011	2.6	14	37
770	Cluster of probable 3-hydroxyisobutyrate dehydrogenase-like 1, mitochondrial	35 kDa	0.036	2	12	24
803.2	PREDICTED: lipid transfer protein EARLI 1-like	?	< 0.00010	INF	0	22
803.3	alpha-amylase inhibitor/lipid transfer/seed storage family protein precursor	13 kDa	0.0011	3.4	8	27
836	soyasapogenol B glucuronide galactosyltransferase	?	0.024	1.6	37	58
906	UDP-glycosyltransferase 84B2	59 kDa	0.015	3.2	5	16
908.3	PREDICTED: ras-related protein RABA5d-like	?	0.0083	INF	0	7
918	amidase 1 isoform X1	46 kDa	0.045	1.9	14	26
991	cucumisin	77 kDa	0.016	1.8	24	43
1091.2	MFP1 attachment factor 1	16 kDa	0.012	4.3	3	13
1203	protein transport protein Sec24-like At4g32640	118 kDa	0.015	3.2	5	16
1234	UDP-glycosyltransferase 79A6	52 kDa	0.00053	5.2	4	21

1241	NAD(P)H-quinone oxidoreductase subunit N, chloroplastic	26 kDa	0.0041	6.5	2	13
1272	Cluster of pyruvate decarboxylase 2	65 kDa	0.02	2.5	8	20
1304	Cluster of mannose-1-phosphate guanyltransferase alpha isoform X2	46 kDa	0.023	3	5	15
1307	anthocyanidin 3-O-glucosyltransferase 7	50 kDa	< 0.00010	10	2	20
1323	outer envelope pore protein 37, chloroplastic	36 kDa	0.035	2.4	7	17
1428	malonyl-CoA:isoflavone 7-O-glucoside-6"-O-malonyltransferase	52 kDa	0.007	6	2	12
1471.2	starch synthase IIa-1	85 kDa	0.016	INF	0	6
1519	glutamyl-tRNA(Gln) amidotransferase subunit A, chloroplastic/mitochondrial	58 kDa	0.049	3.3	3	10
1555	15-cis-phytoene desaturase, chloroplastic/chromoplastic	52 kDa	0.035	4.5	2	9
1631	probable aldehyde dehydrogenase isoform X1	61 kDa	0.037	7	1	7
1663	Cluster of tryptophan--tRNA ligase, cytoplasmic	46 kDa	0.007	6	2	12
1666	uridine 5'-monophosphate synthase-like	?	0.049	3.3	3	10
1691	Cluster of probable splicing factor 3A subunit 1	89 kDa	0.0021	INF	0	9
1691.2	PREDICTED: probable splicing factor 3A subunit 1	?	0.0021	INF	0	9
1965.2	nudix hydrolase 20, chloroplastic isoform X1	41 kDa	0.016	INF	0	6
1970	50S ribosomal protein L6, chloroplastic	25 kDa	0.035	4.5	2	9
2002	probable carboxylesterase 8	36 kDa	0.033	INF	0	5
2020	PREDICTED: UDP-glycosyltransferase 73C6-like	?	0.033	INF	0	5
2247	protein RETICULATA-RELATED 4, chloroplastic isoform X1	47 kDa	0.0021	INF	0	9

Supplementary Table 4.12. Fold change of proteins that were upregulated by treatment Bj+SL42+SL48, relative to Bj (control) under salt-stressed conditions.

#	Identified Proteins (3583/3610)	Molecular Weight	Fisher's Exact Test	Fold Change	Bj	Bj+ SL42+ SL48
1	ribulose-1,5-bisphosphate carboxylase/oxygenase large subunit (chloroplast)	53 kDa	< 0.00010	1.1	6,327	6,923
3	ribulose bisphosphate carboxylase small chain 4, chloroplastic	20 kDa	< 0.00010	1.2	985	1,201
5	Cluster of ribulose bisphosphate carboxylase/oxygenase activase, chloroplastic-like	49 kDa	0.0046	1.1	1,153	1,264
8.3	glycine dehydrogenase (decarboxylating), mitochondrial	111 kDa	0.037	1.2	200	235
11	Cluster of glutamine synthetase precursor isoform X1	48 kDa	< 0.00010	1.3	529	678
13	Cluster of PREDICTED: phosphoglycerate kinase, cytosolic	?	0.0064	1.1	719	806
13.2	phosphoglycerate kinase, cytosolic	50 kDa	0.0039	1.1	618	706
17	Cluster of catalase	57 kDa	0.0014	1.2	386	468
21.3	granule bound starch synthase Ia	67 kDa	0.01	3	6	18
31	Cluster of stromal 70 kDa heat shock-related protein, chloroplastic	74 kDa	0.036	1.1	353	398
57	Cluster of tubulin alpha-3 chain	50 kDa	0.049	1.1	243	278
60	photosystem I subunit VII (chloroplast)	9 kDa	< 0.00010	1.5	249	382
72.2	seed linoleate 9S-lipoxygenase-2	?	< 0.00010	INF	0	28
79	Cluster of ATP synthase subunit b', chloroplastic	23 kDa	0.016	1.3	150	188
79.2	putative ATP synthase subunit b'	24 kDa	0.023	1.3	122	154
105	Cluster of NADP-dependent malic enzyme	65 kDa	0.019	1.2	144	180
131	Cluster of 50S ribosomal protein L12, chloroplastic	20 kDa	0.00042	1.4	146	207
138.4	glutathione S-transferase GST 6	?	0.00022	INF	0	12
146.2	heme-binding protein 2	26 kDa	0.035	1.3	94	120
161	PREDICTED: aldehyde dehydrogenase family 2 member B4, mitochondrial	?	0.047	1.2	115	141
204	photosystem II protein H (chloroplast)	8 kDa	< 0.00010	1.9	92	174
218.3	polyadenylate-binding protein RBP45	45 kDa	0.014	2.1	14	29
227.2	thioredoxin M1, chloroplastic	26 kDa	0.049	1.3	64	84
231	PREDICTED: thioredoxin H1	?	0.011	1.3	98	132

243	Cluster of 4-alpha-glucanotransferase DPE2	111 kDa	0.02	1.4	69	95
291	glucose-6-phosphate 1-dehydrogenase, chloroplastic	67 kDa	0.017	1.5	52	76
302.2	probable UDP-arabinopyranose mutase 1	42 kDa	0.04	1.4	55	75
330	Cluster of calvin cycle protein CP12-2, chloroplastic	14 kDa	< 0.00010	1.8	72	126
344	NADH dehydrogenase subunit 7 (chloroplast)	46 kDa	0.05	1.4	50	68
350.2	DEAD-box ATP-dependent RNA helicase 56	48 kDa	0.048	1.5	31	46
537	Cluster of gibberellin-regulated protein 6 precursor	13 kDa	0.00012	2.2	28	63
553	PREDICTED: UDP-glucose flavonoid 3-O-glucosyltransferase 7-like	?	< 0.00010	2.6	19	50
566	Cluster of gamma-tocopherol methyltransferase	39 kDa	0.013	2	16	32
579	Cluster of 15-cis-phytoene desaturase, chloroplastic/chromoplastic	63 kDa	0.034	1.6	24	39
638	Cluster of PREDICTED: topless-related protein 3-like isoform X1	?	0.022	1.9	15	29
638.2	protein TOPLESS	125 kDa	0.035	2.2	8	18
638.3	topless-related protein 4 isoform X2	125 kDa	0.036	3	4	12
638.4	topless-related protein 3	124 kDa	0.044	3.3	3	10
739	polygalacturonase inhibitor 1-like protein precursor	38 kDa	0.0015	2.9	10	29
756	Cluster of proline-rich protein precursor	13 kDa	0.049	1.8	14	25
758	UDP-sulfoquinovose synthase, chloroplastic	53 kDa	0.05	1.7	18	30
801	Cluster of polyadenylate-binding protein 2	71 kDa	0.037	1.4	46	65
803.2	PREDICTED: lipid transfer protein EARLI 1-like	?	0.0074	INF	0	7
906	UDP-glycosyltransferase 84B2	59 kDa	0.012	3.2	5	16
985.2	heme oxygenase 3	?	0.03	INF	0	5
991	cucumisin	77 kDa	0.0065	1.9	24	45
1001.3	carbonic anhydrase 2	28 kDa	0.03	1.9	15	28
1141	Cluster of polyadenylate-binding protein 2	72 kDa	0.0049	1.7	37	63
1203	protein transport protein Sec24-like At4g32640	118 kDa	0.0004	4.6	5	23
1241	NAD(P)H-quinone oxidoreductase subunit N, chloroplastic	26 kDa	0.018	5	2	10

1333	multiple organellar RNA editing factor 9-like	25 kDa	0.043	2.3	7	16
1484	7-hydroxymethyl chlorophyll a reductase, chloroplastic	50 kDa	0.036	3	4	12
1488	protein transport protein Sec24-like At3g07100 isoform X2	113 kDa	0.01	5.5	2	11
1533.2	carbamoyl-phosphate synthase small chain, chloroplastic	48 kDa	0.027	3.7	3	11
1691	Cluster of probable splicing factor 3A subunit 1	89 kDa	< 0.00010	INF	0	16
1691.2	PREDICTED: probable splicing factor 3A subunit 1	?	< 0.00010	INF	0	14
1749	probable aldo-keto reductase 1	37 kDa	0.036	3	4	12
1765	U1 small nuclear ribonucleoprotein C	22 kDa	0.044	3.3	3	10
1841	splicing factor 3B subunit 4	40 kDa	0.0055	10	1	10
2247	protein RETICULATA-RELATED 4, chloroplastic isoform X1	47 kDa	0.0018	INF	0	9

Functional classification of proteins based on GO categories

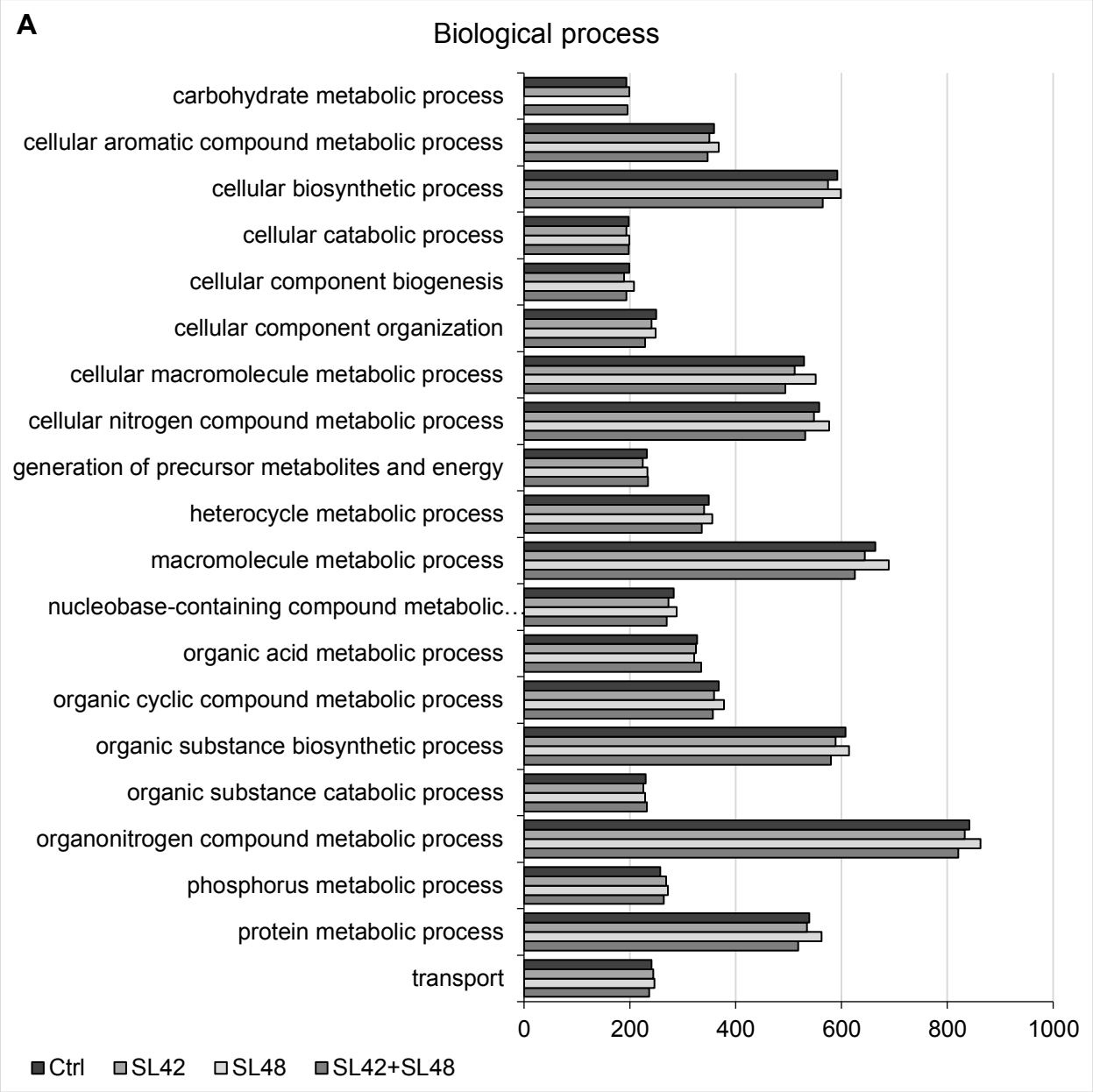

Supplementary Figure 4.1. Number of sequences involved in the cellular and metabolic processes of the soybean leaf proteome. **(A)** The seeds were treated with 10 mM $MgSO_4$ or bacterized with the strains *Rhizobium* sp. SL42, *Hydrogenophaga* sp. SL48 or co-inoculated under optimal conditions. Values represent mean ± SE (n=3).

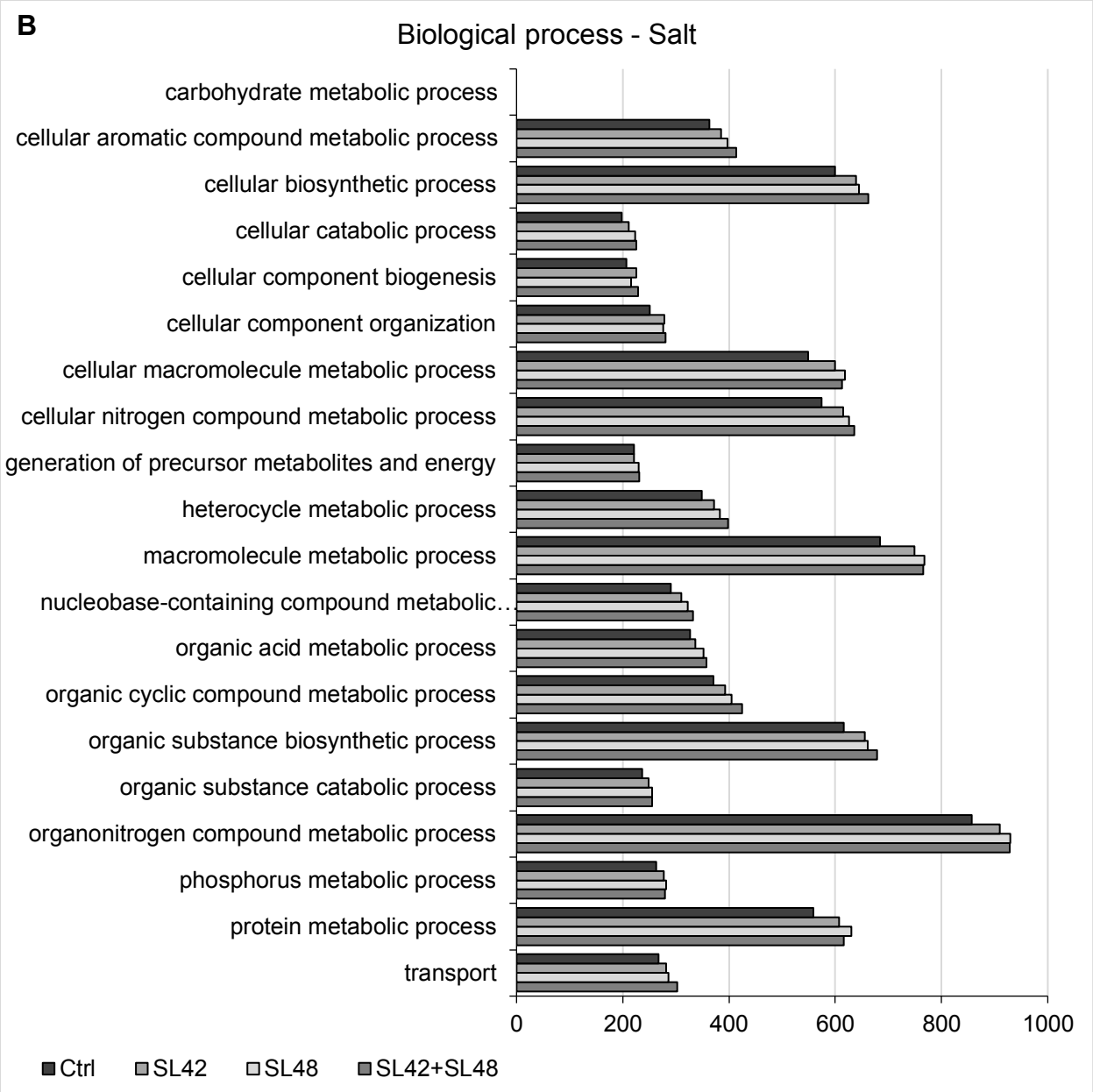

Supplementary Figure 4.1. (cont.) Number of sequences involved in the cellular and metabolic processes of the soybean leaf proteome. **(B)** The seeds were treated with 10 mM $MgSO_4$ or bacterized with the strains *Rhizobium* sp. SL42, *Hydrogenophaga* sp. SL48 or co-inoculated under salt stress. Values represent mean ± SE (n=3).

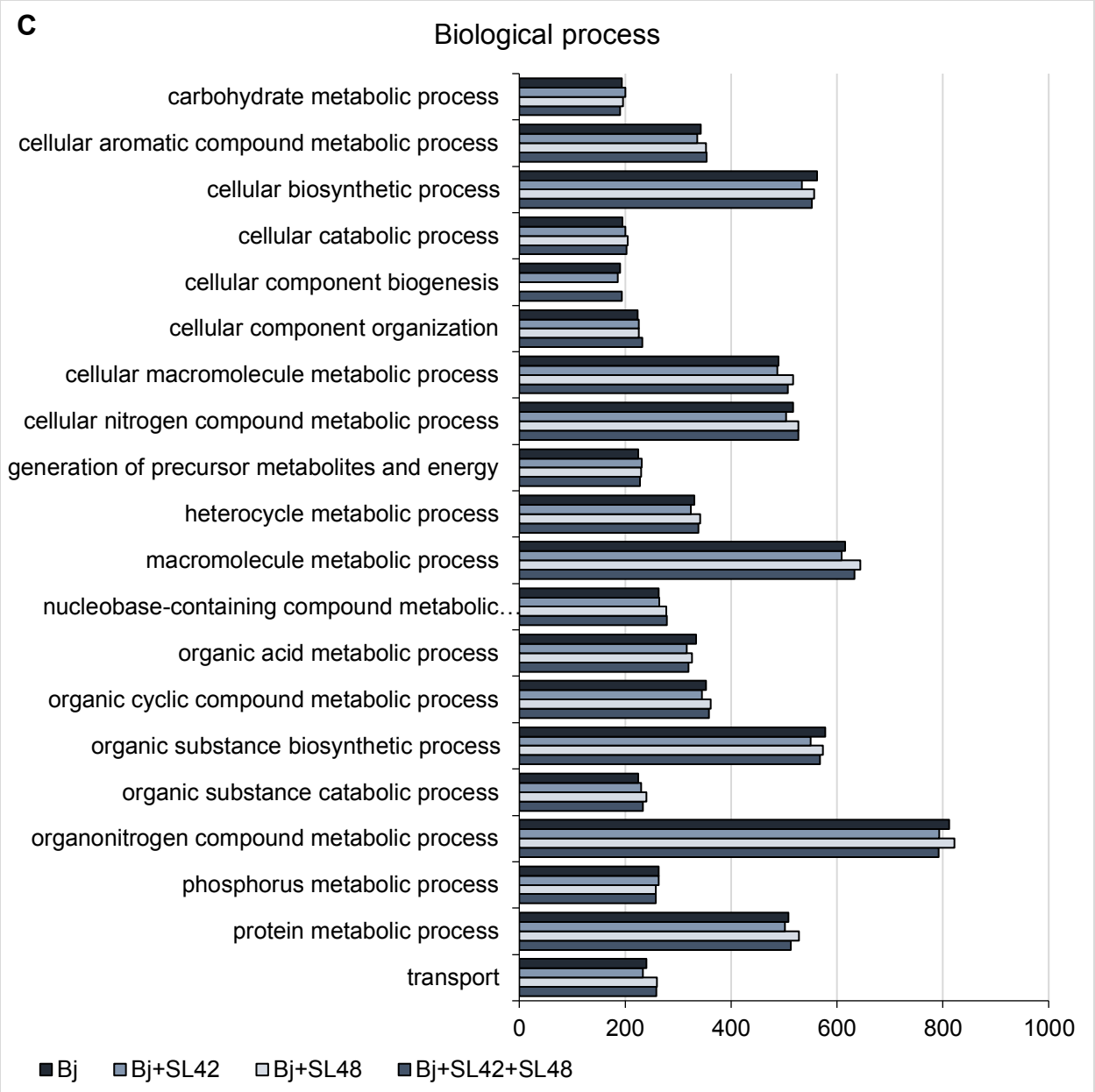

Supplementary Figure 4.1. (cont.) Number of sequences involved in the cellular and metabolic processes of the soybean leaf proteome. **(C)** The seeds were bacterized with *Bradyrhizobium japonicum* (Bj) as control or the strains *Rhizobium* sp. SL42, *Hydrogenophaga* sp. SL48 were co-inoculated with Bj under optimal conditions. Values represent mean ± SE (n=3).

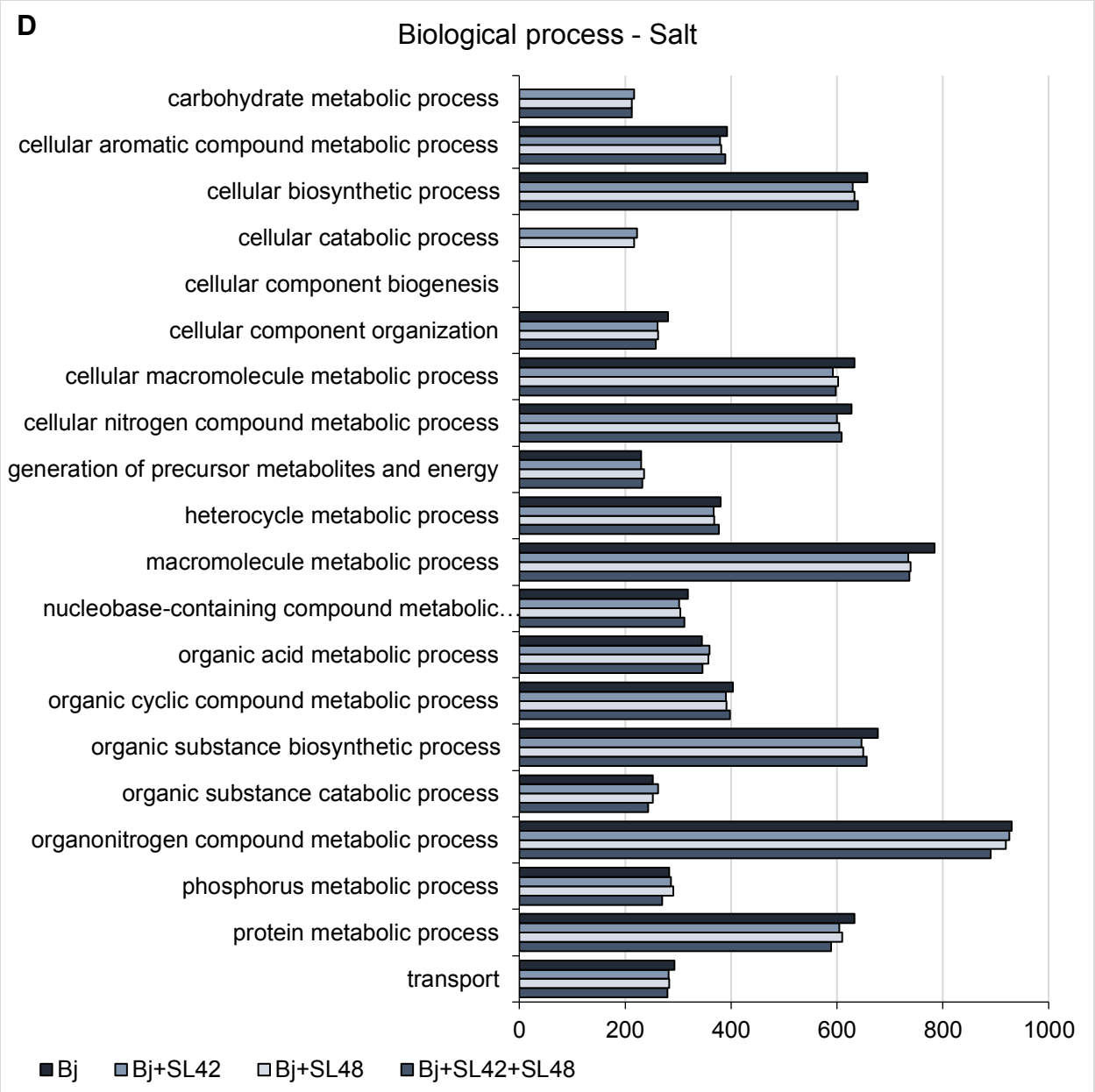

Supplementary Figure 4.1. (cont.) Number of sequences involved in the cellular and metabolic processes of the soybean leaf proteome. **(D)** The seeds were bacterized with *Bradyrhizobium japonicum* (Bj) as control or the strains *Rhizobium* sp. SL42, *Hydrogenophaga* sp. SL48 were co-inoculated with Bj under salt stress. Values represent mean ± SE (n=3).

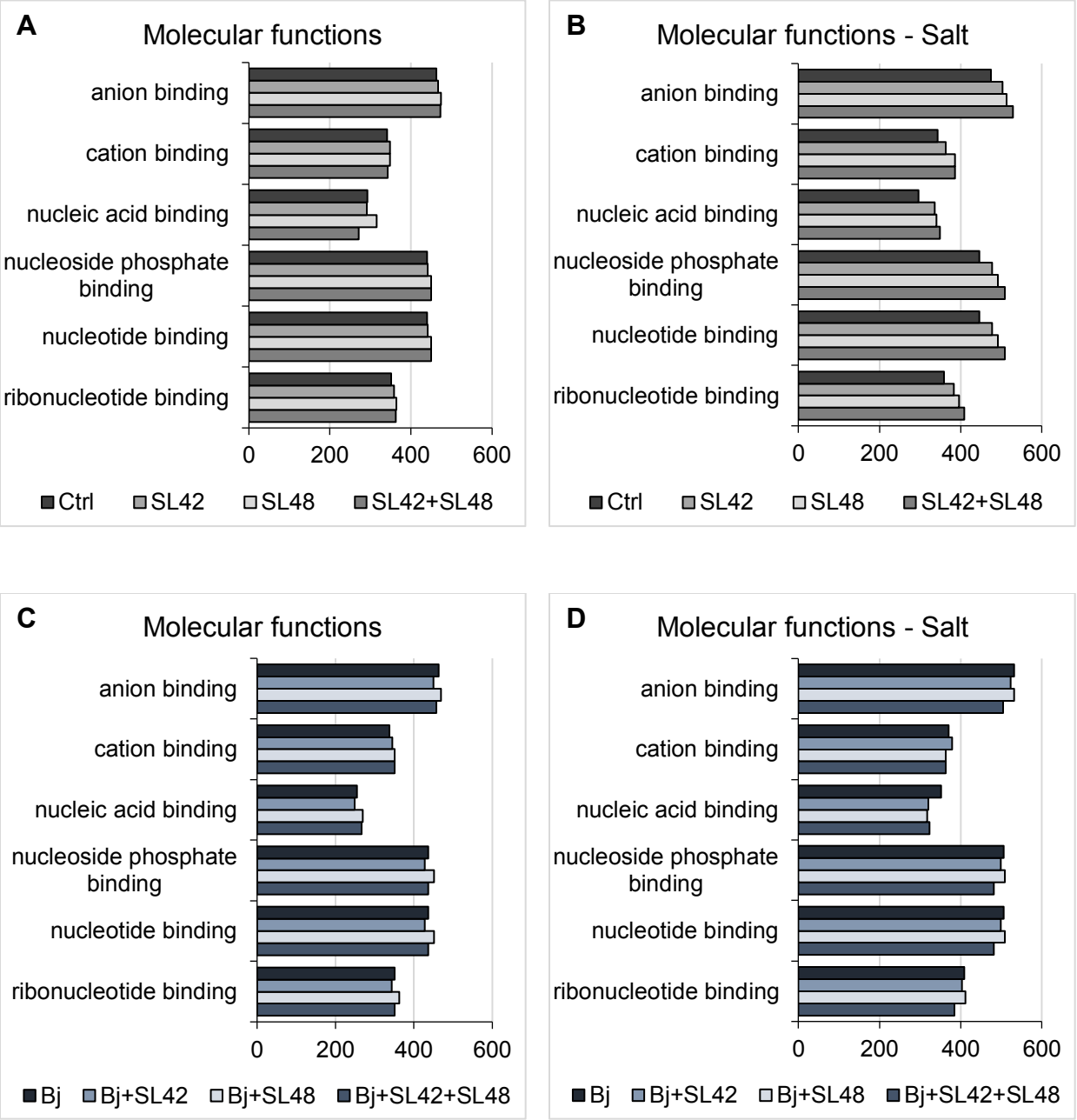

Supplementary Figure 4.2. Number of sequences involved in the molecular function - binding of the soybean leaf proteome. **(A)** The seeds were treated with 10 mM $MgSO_4$ or bacterized with the strains *Rhizobium* sp. SL42, *Hydrogenophaga* sp. SL48 or co-inoculated under optimal and **(B)** under salt stress or **(C)** the seeds were bacterized with *Bradyrhizobium japonicum* (Bj) as control or the strains were co-inoculated with Bj under optimal and **(D)** under salt stress conditions. Values represent mean ± SE (n=3).

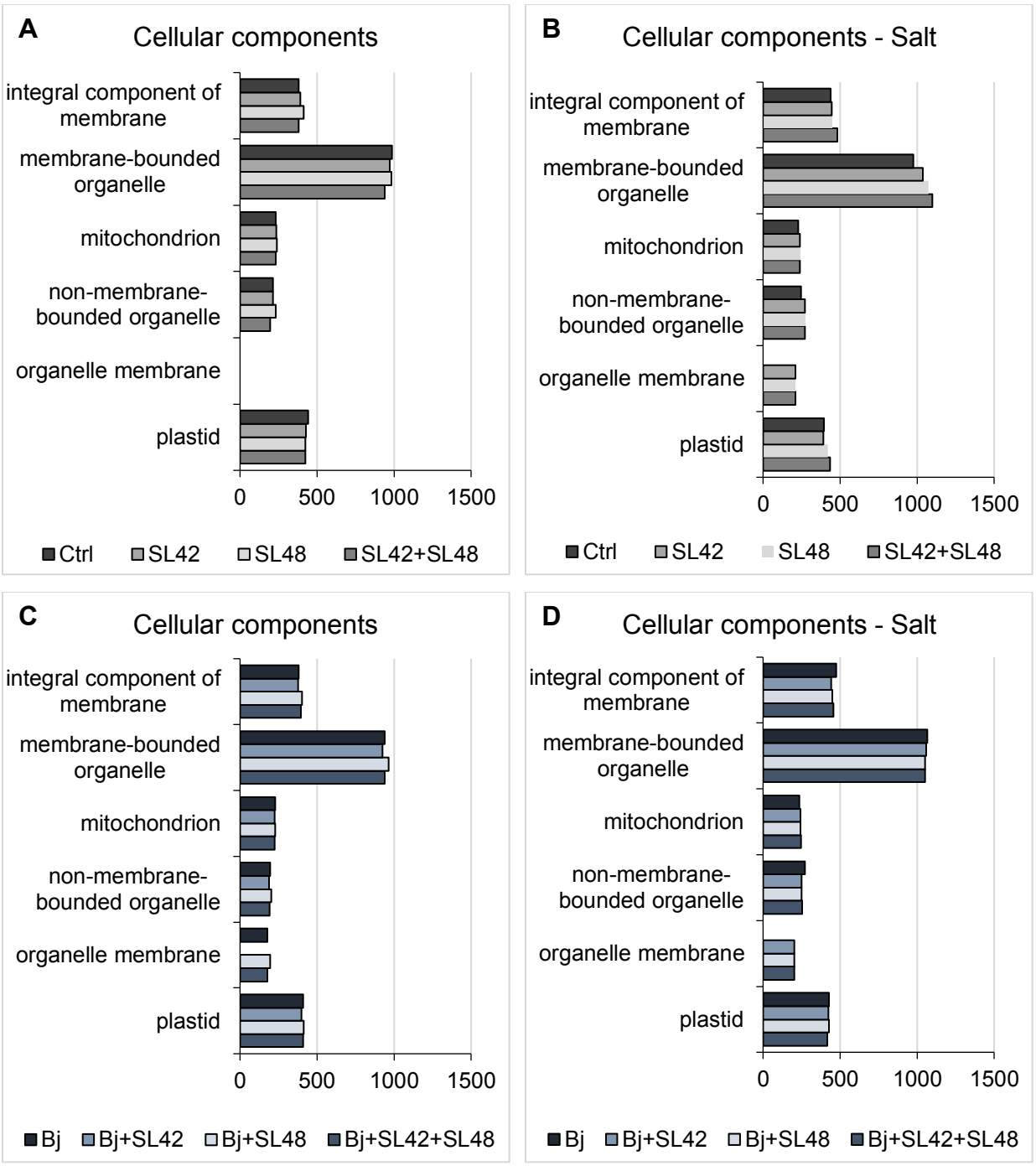

Supplementary Figure 4.3. Number of sequences involved in the cellular components – membranes and organelles of the soybean leaf proteome. **(A)** The seeds were treated with 10 mM $MgSO_4$ or bacterized with the strains *Rhizobium* sp. SL42, *Hydrogenophaga* sp. SL48 or co-inoculated under optimal and **(B)** under salt stress or **(C)** the seeds were bacterized with *Bradyrhizobium japonicum* (Bj) as control or the strains were co-inoculated with Bj under optimal and **(D)** under salt stress conditions. Values represent mean ± SE (n=3).

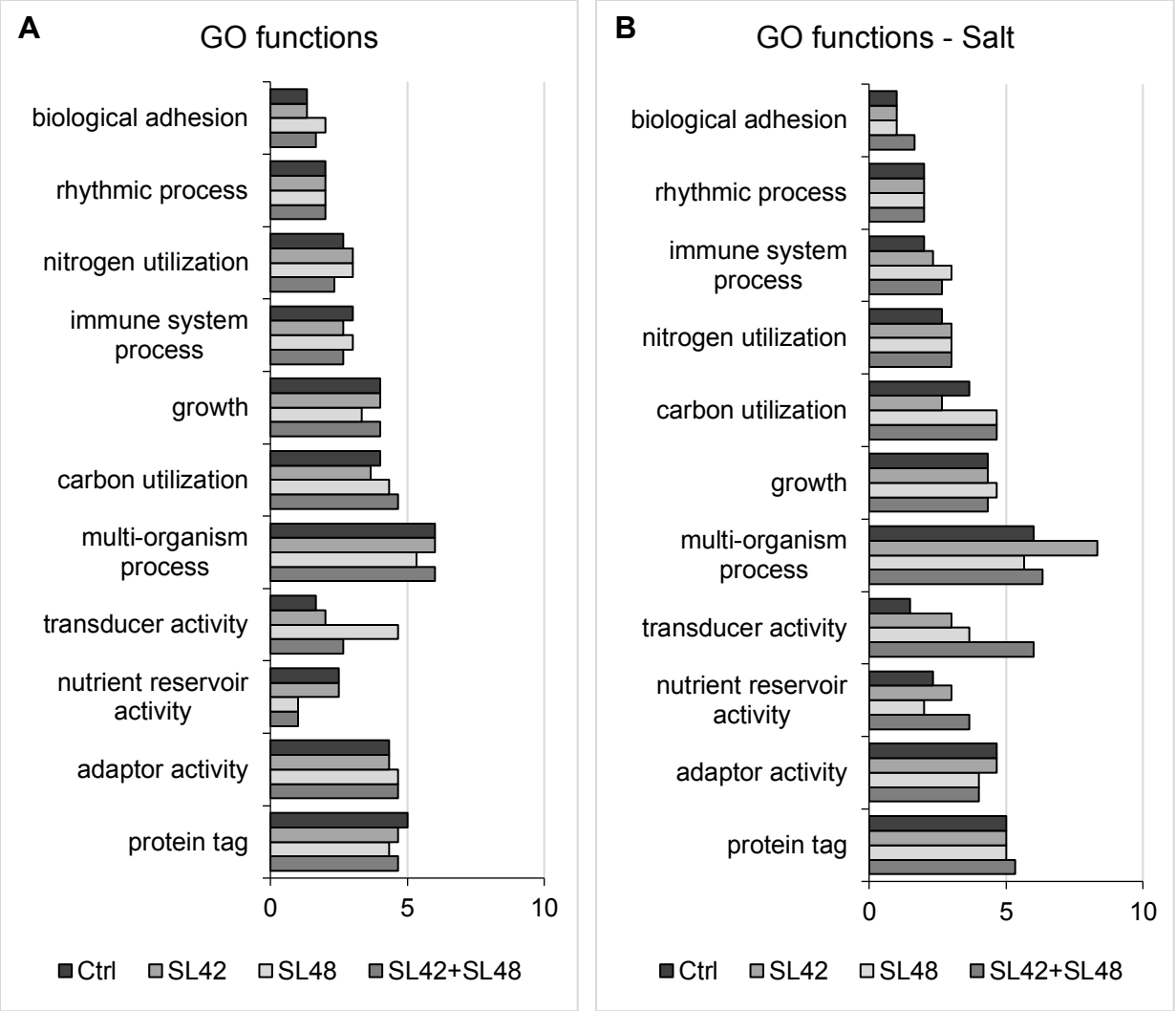

Supplementary Figure 4.4. Number of sequences (< 10) involved in the GO functions of the soybean leaf proteome. **(A)** The seeds were treated with 10 mM $MgSO_4$ or bacterized with the strains *Rhizobium* sp. SL42, *Hydrogenophaga* sp. SL48 or co-inoculated under optimal and **(B)** under salt stress conditions.

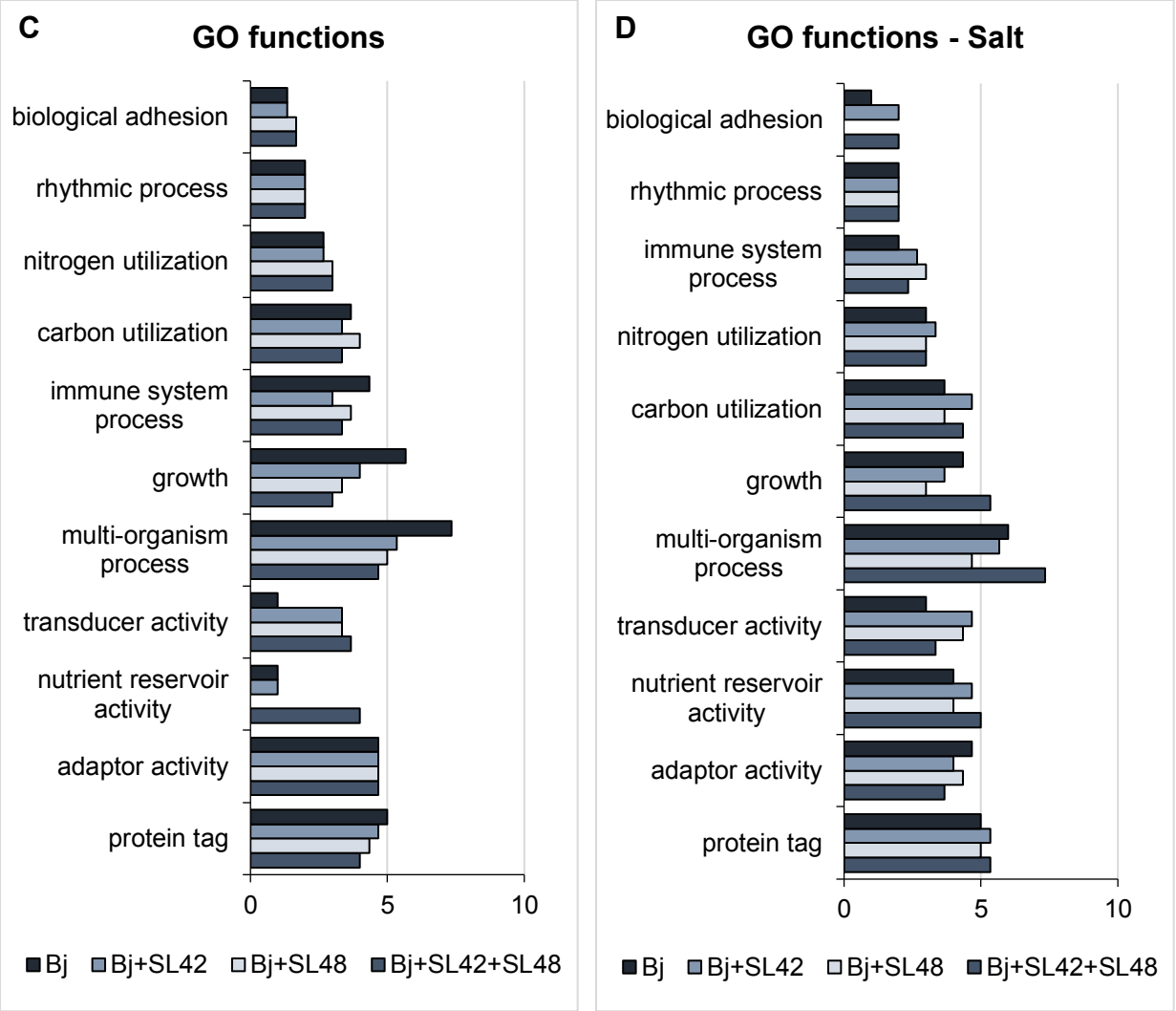

Supplementary Figure 4.4. (cont.) Number of sequences (< 10) involved in the GO functions of the soybean leaf proteome. **(C)** The seeds were bacterized with *Bradyrhizobium japonicum* (Bj) as control or the strains *Rhizobium* sp. SL42, *Hydrogenophaga* sp. SL48 were co-inoculated with Bj under optimal and **(D)** under salt stress conditions. Values represent mean ± SE (n=3).

APPENDIX C

Supplementary Figures and Tables – Chapter 5

Supplementary Table 5.1. Description of Illumina libraries.

Sample ID	SL42	SL48
Qubit Conc. (ng/µl))	25.2	37
Volume (µl)	10	10
Yield (ng)	252	370
Index 1	N704	N705
Index 1 Sequence	TCCTGAGC	GGACTCCT
Index 2	S502	S502
Index 2 Sequence	CTCTCTAT	CTCTCTAT

Supplementary Table 5.2. Tapestation Profile of the libraries.

	SL42	SL48
From (bp)	226	220
To (bp)	1192	1051
Average (bp)	574	591
Conc. ng/ml	28.9	31.1
Region Molarity nmol/l	86.7	91.9

Supplementary Table 5.3. Nanopore read statistics.

Statistics	SL42	SL48
Reads Generated	60262	44739
Maximum Read Length	71443	91232
Minimum Read Length	19	38
Average Read Length	6311.1	7323.4
Median Read Length	271.5	3762
Total Reads Length	380317539	327639793
Reads >= 100 bp	60213	44712
Reads >= 200 bp	58663	43957
Reads >= 500 bp	49279	40114
Reads >= 1 Kbp	44337	36607
Reads >= 10 Kbp	13605	11252
N50 value	11838	13578

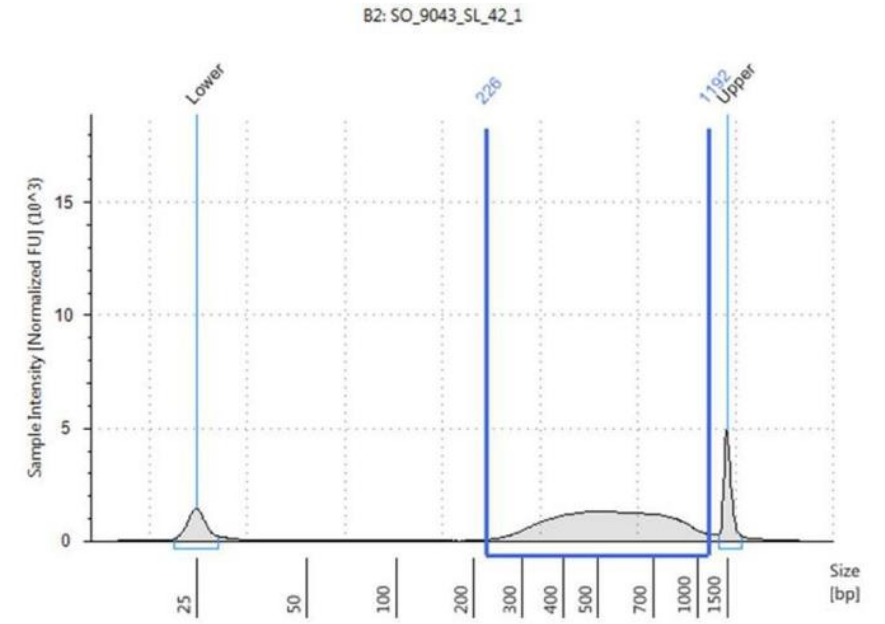

From [bp]	To [bp]	Average Size [bp]	Conc. [ng/µl]	Region Molarity [nmol/l]	% of Total
226	1192	574	28.9	86.7	95.27

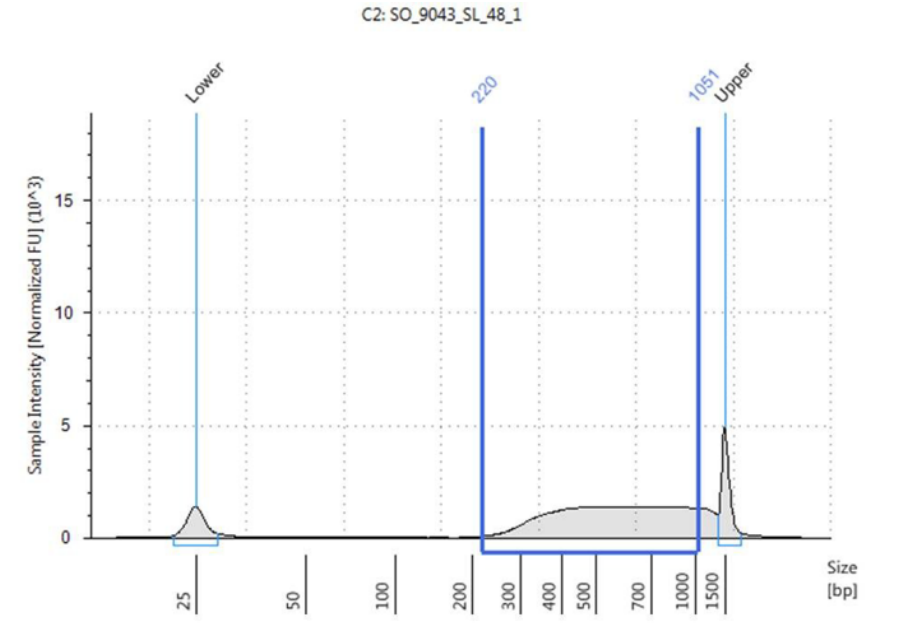

From [bp]	To [bp]	Average Size [bp]	Conc. [ng/µl]	Region Molarity [nmol/l]	% of Total
220	1051	591	31.1	91.9	88.33

Supplementary Figure 5.1. TapeStation Profiles of SL42 and SL48 DNA libraries.

Supplementary Table 5.4. Illumina read statistics.

Sample	Raw Read	Processed Reads	% Reads Retained
SL42	2782606	2533621	91.05
SL48	3022451	2780700	92.00

Supplementary Table 5.5. Read statistics combined.

	SL42_barcode05		SL48_barcode06	
Nanopore combined	**Raw**	**Processed**	**Raw**	**Processed**
Contigs Generated	110664	60262	82669	44739
Maximum Contig Length	71508	71443	91305	91232
Minimum Contig Length	117	19	121	38
Average Contig Length	5771.1	6311.1	6966.1	7323.4
Median Contig Length	672.5	271.5	3972	3762
Total Contigs Length	638654847	380317539	575884066	327639793
Total Number of Non-ATGC	0	0	0	0
% of Non-ATGC Characters	0	0	0	0
Contigs >= 100 bp	110664	60213	82669	44712
Contigs >= 200 bp	110218	58663	82354	43957
Contigs >= 500 bp	88956	49279	74407	40114
Contigs >= 1 Kbp	75713	44337	66310	36607
Contigs >= 10 Kbp	22414	13605	19423	11252
N50 value	11575	11838	13208	13578

Supplementary Table 5.6. Cut-offs and range of SSR in the genome assembly.

Statistics	SL42	SL48
Total number of sequences examined	3	1
Total size of examined sequences (bp)	5166003	5433040
Total number of identified SSRs	116	153
Number of SSR containing sequences	3	1
Number of compound SSRs	1	1
Mono nucleotide repeats p1 >= 10 bases	1	8
Di nucleotide repeats p2 >= 6 Pairs	4	26
Tri nucleotide repeats p3 >= 5 Sets	10	17
Tetra nucleotide repeats p4 >= 3 Sets	100	99
Penta nucleotide repeats p5 >= 5 Sets	1	1
Hexa nucleotide repeats p6 >= 5 Sets	3	2

Supplementary Table 5.7. KEGG pathway analysis of predicted proteins in SL42 genome.

Function	Pathway
BRITE hierarchy	
Genetic information processing	Transcription factors, Translation factors, Transcription machinery, tRNA biogenesis, mRNA biogenesis Mitochondrial biogenesis, Ribosome biogenesis, Ribosome proteins DNA replication proteins, DNA repair and recombination proteins Chromosome and associated proteins, Chaperones and folding catalysts, Membrane trafficking
Metabolism	Photosynthesis proteins Amino acid related enzymes, Protein kinases, Protein phosphatases and associated proteins, Peptidases and inhibitors Peptidoglycan biosynthesis and degradation proteins, Lipopolysaccharide biosynthesis, Lipid biosynthesis proteins Glycosyltransferases, Prenyltransferases
Signaling and cellular processes	Antimicrobial resistance genes, Prokaryotic defense system, Exosome Transporters, Two-component system, Cytoskeleton proteins Bacterial motility proteins, Bacterial toxins, Secretion system
Cellular processes	
Cell motility	Bacterial chemotaxis, Flagellar assembly
Cellular community	Quorum sensing
Environmental information processing	
Membrane transport	ABC transporters Phosphotransferase system (PTS) Bacterial secretion system
Signal transduction	Two-component system
Genetic Information Processing	
Folding, sorting and degradation	RNA degradation Protein export Sulfur relay system
Replication and repair	DNA replication, Homologous recombination Base excision repair, Nucleotide excision repair, Mismatch repair
Transcription	RNA polymerase
Translation	Aminoacyl-tRNA biosynthesis Ribosome proteins
Human diseases	
Anti-microbial drug resistance	Beta-lactam resistance Vancomycin resistance Cationic antimicrobial peptide (CAMP) resistance

Metabolism	
Amino acid	Arginine biosynthesis Alanine, aspartate and glutamate metabolism Glycine, serine and threonine metabolism Cysteine and methionine metabolism Valine, leucine and isoleucine degradation Valine, leucine and isoleucine biosynthesis Lysine biosynthesis, Lysine degradation Arginine and proline metabolism Histidine metabolism, Tyrosine metabolism Phenylalanine metabolism, Tyrosine metabolism Tryptophan biosynthesis
Secondary metabolites	Monobactam biosynthesis, Carbapenem biosynthesis Penicillin and cephalosporin biosynthesis, Prodigiosin biosynthesis Novobiocin biosynthesis, Streptomycin biosynthesis Neomycin, kanamycin and gentamicin biosynthesis
Carbohydrate metabolism	Glycolysis / Gluconeogenesis, TCA cycle Pentose phosphate pathway, Pentose and glucuronate interconversions Fructose and mannose metabolism, Galactose metabolism Ascorbate and aldarate metabolism Starch and sucrose metabolism Amino sugar and nucleotide sugar metabolism Inositol phosphate metabolism, Pyruvate metabolism Glyoxylate and dicarboxylate metabolism Propanoate metabolism, Butanoate metabolism, C5-Branched dibasic acid metabolism
Energy metabolism	Oxidative phosphorylation, Methane metabolism Carbon fixation in photosynthetic organisms Nitrogen metabolism, Sulfur metabolism
Glycan biosynthesis and metabolism	Lipopolysaccharide biosynthesis Peptidoglycan biosynthesis, Other glycan degradation
Lipid metabolism	Fatty acid biosynthesis, Fatty acid degradation, Biosynthesis of unsaturated fatty acids Glycerolipid metabolism, Glycerophospholipid metabolism Synthesis and degradation of ketone bodies
Metabolism of cofactors and vitamins	Ubiquinone and other terpenoid-quinone biosynthesis One carbon pool by folate metabolism, Folate biosynthesis Thiamine metabolism, Riboflavin metabolism, Vitamin B6 metabolism Nicotinate and nicotinamide metabolism, Biotin metabolism Pantothenate and CoA biosynthesis, Lipoic acid metabolism

	Porphyrin and chlorophyll metabolism
Metabolism of other amino acids	beta-Alanine metabolism, D-Alanine metabolism Taurine and hypotaurine metabolism, Phosphonate and phosphinate metabolism Selenocompound metabolism, Cyanoamino acid metabolism D-Glutamine and D-glutamate metabolism, Glutathione metabolism
Metabolism of terpenoids and polyketides	Geraniol degradation, Limonene and pinene degradation Terpenoid backbone biosynthesis Carotenoid biosynthesis Biosynthesis of type II polyketide products
Nucleotide metabolism	Purine metabolism Pyramidine metabolism
Xenobiotics biodegradation and metabolism	Chlorocyclohexane and chlorobenzene degradation Benzoate degradation, Fluorobenzoate degradation, Aminobenzoate degradation, Dioxin degradation, Xylene degradation Toluene degradation, Nitrotoluene degradation, Naphthalene degradation, Chloroalkane and chloroalkene degradation Polycyclic aromatic hydrocarbon degradation, Styrene, Atrazine, Caprolactam degradation

Supplementary Table 5.8. KEGG pathway analysis of predicted proteins in SL48 genome.

Function	**Pathway**
BRITE hierarchy	
Genetic information processing	Transcription factors, Translation factors, Transcription machinery, tRNA biogenesis, mRNA biogenesis Mitochondrial biogenesis, Ribosome biogenesis, Ribosome proteins DNA replication proteins, DNA repair and recombination proteins Chromosome and associated proteins, Chaperones and folding catalysts, Membrane trafficking
Metabolism	Photosynthesis proteins Amino acid related enzymes, Protein kinases, Protein phosphatases and associated proteins, Peptidases and inhibitors Peptidoglycan biosynthesis and degradation proteins, Lipopolysaccharide biosynthesis, Lipid biosynthesis Glycosyltransferases, Prenyltransferases
Signaling and cellular processes	Antimicrobial resistance genes, Prokaryotic defense system, Exosome Transporters, Two-component system, Cytoskeleton proteins Bacterial motility proteins, Bacterial toxins, Secretion system

Cellular processes	
Cell motility	Bacterial chemotaxis, Flagellar assembly
Cellular community	Quorum sensing
Environmental information processing	
Membrane transport	ABC transporters Bacterial secretion system
Signal transduction	Two-component system
Genetic Information Processing	
Folding, sorting and degradation	RNA degradation Protein export Sulfur relay system
Replication and repair	DNA replication, Homologous recombination Base excision repair, Nucleotide excision repair, Mismatch repair
Transcription	RNA polymerase
Translation	Aminoacyl-tRNA biosynthesis Ribosome proteins
Human diseases	
Anti-microbial drug resistance	Beta-lactam resistance Vancomycin Cationic antimicrobial peptide (CAMP) resistance
Metabolism	
Amino acid	Arginine biosynthesis Alanine, aspartate and glutamate metabolism Glycine, serine and threonine metabolism Cysteine and methionine metabolism Valine, leucine and isoleucine degradation Valine, leucine and isoleucine biosynthesis Lysine biosynthesis, Lysine degradation Arginine and proline metabolism Histidine metabolism, Tyrosine metabolism Phenylalanine, tyrosine and tryptophan biosynthesis
Secondary metabolites	Monobactam biosynthesis, Carbapenem biosynthesis Novobiocin biosynthesis, Phenazine biosynthesis Streptomycin biosynthesis Neomycin, kanamycin and gentamicin biosynthesis Acarbose and validamycin biosynthesis

Carbohydrate metabolism	Glycolysis / Gluconeogenesis, TCA cycle Pentose phosphate pathway, Pentose and glucuronate interconversions Fructose and mannose metabolism, Galactose metabolism Ascorbate and aldarate metabolism Starch and sucrose metabolism Amino sugar and nucleotide sugar metabolism Inositol phosphate metabolism, Pyruvate metabolism Glyoxylate and dicarboxylate metabolism Propanoate metabolism, Butanoate metabolism, C5-Branched dibasic acid metabolism
Energy metabolism	Oxidative phosphorylation, Methane metabolism, Nitrogen metabolism, Sulfur metabolism
Glycan biosynthesis and metabolism	Lipopolysaccharide biosynthesis Peptidoglycan biosynthesis
Lipid metabolism	Fatty acid biosynthesis, Glycerolipid metabolism
Metabolism of cofactors and vitamins	Ubiquinone and other terpenoid-quinone biosynthesis One carbon pool by folate metabolism, Folate biosynthesis Thiamine metabolism, Riboflavin metabolism, Vitamin B6 metabolism Nicotinate and nicotinamide metabolism, Biotin metabolism Pantothenate and CoA biosynthesis, Lipoic acid metabolism Porphyrin and chlorophyll metabolism
Metabolism of other amino acids	beta-Alanine metabolism, D-Alanine metabolism Selenocompound metabolism, Cyanoamino acid metabolism D-Glutamine and D-glutamate metabolism, Glutathione metabolism
Metabolism of terpenoids and polyketides	Polyketide sugar unit biosynthesis Terpenoid backbone biosynthesis Biosynthesis of ansamycins Biosynthesis of vancomycin group antibiotics
Nucleotide metabolism	Purine metabolism Pyramidine metabolism
Xenobiotics biodegradation and metabolism	Chlorocyclohexane and chlorobenzene degradation Fluorobenzoate degradation, Aminobenzoate degradation Toluene degradation, Nitrotoluene degradation, Naphthalene degradation, Chloroalkane and chloroalkene degradation